

**The impact of diabetes on cardiac remodelling after
myocardial infarction: potential role of thyroid hormone
signalling**

by

Christos Kalofoutis

A thesis submitted in partial fulfilment for the requirements of the
degree of Doctor of Philosophy at the University of Central
Lancashire

November 2012

**In collaboration with the Department of Pharmacology,
School of Medicine, University of Athens**

ABSTRACT

Diabetes (DM) increases mortality after myocardial infarction and deteriorates post-ischaemic cardiac remodelling. This study investigated possible implications of thyroid hormone (TH) signalling in either reducing or preventing this response. TH signalling has a regulatory role in metabolism, cardiac function, growth and ischaemic stress. Acute myocardial infarction (AMI) was induced in age-match healthy control rats (AMI-C) and in streptozotocin (STZ)-induced type I diabetic (DM) animals (DM+AMI) using 35 mg/kg body weight while sham operated animals served as controls (SHAM). The results show that AMI in tissue hypothyroidism caused significant down-regulation of TH receptors, TR α 1 and TR β 1, in the diabetic myocardium without changes in T3, T4 levels in plasma. This response was associated with increased expression of β -MHC and distinct changes in cardiac function and geometry. Ejection fractions (EF%) was decreased in DM-AMI as compared to DM+AMI animals. Systolic and diastolic chamber dimensions were increased without concomitant increase in wall thickness and thus, WTI (the ratio of LVIDd/2*Posterior Wall thickness), an index of wall stress, was significantly elevated. The absence of wall thickening in DM+AMI hearts was associated with changes in stretch-induced kinase hypertrophic signalling p38 MAPK. In contrast, ERK, p-ERK and p-p38 MAPK levels were not changed in DM+AMI as compared to non-infarcted hearts (DM+SHAM). TH administration after AMI prevented hypothyroidism and resulted in decreased β -MHC expression, increased wall thickening and normalized wall stress, while stretch-induced p38 MAPK activation was restored. The results show that diabetes can exacerbates post-ischaemic cardiac remodelling and tissue hypothyroidism and TH treatment can prevent this response and improve cardiac haemodynamics.

DECLARATION

I declare that while registered as a candidate for the research degree, I have not been a registered candidate or enrolled student for another award of the University or other academic or professional institution. No material contained in the thesis has been used in any other submission for an academic award and is solely my own work

.....

Signature

ACKNOWLEDGEMENTS

It is a pleasure to convey my sincere thanks to the many people who have made this thesis possible.

I cannot overstate my gratitude to Professor Costas Pantos and Professor Jaipaul Singh - PhD supervisors, friends, philosophers and guides. During my time at UCLAN and through our many travels, they have been a constant source of sound advice, great company and terrific ideas. Their mentorships have been paramount in providing a well rounded research experience and moreover, they have encouraged me to grow as an experimentalist and an independent thinker. For everything you have done for me Jai and Costas, I thank you. I am also extremely grateful to my wife, my two children and more so to my mother and father for their love and support.

Table of contents

	Page
Title Page	1
Abstract	2
Declaration	3
Acknowledgements	4
Table of contents	5
List of Tables and figures	10
Abbreviations	15
CHAPTER 1	22
GENERAL INTRODUCTION	
The mammalian heart	23
Extracellular matrix	25
Cardiomyocytes	26
Regulation of Ca ²⁺ in normal cardiac muscle	32
Heart and responses to stress - Cardiac structural remodelling	33
Molecular signature and Cardiac structural remodelling	35
Kinase signalling and Cardiac remodelling - MAPK	38
ERK 1/2	39
JNK	40
P-38	42
ERK5	43
Mitogen activated protein kinases in heart function and disease	45
ERK 1/2, Cardiac hypertrophy	46
1. Cardioprotection vs myocardial cell death	50

Cardiac remodelling	51
JNK and Cardiac hypertrophy	53
Cardioprotection vs myocardial cell death	55
Cardiac remodelling	56
2. p-38, Cardiac hypertrophy	58
3. Cardioprotection vs myocardial cell death	60
Cardiac remodelling	64
AKT Module	66
AKT and angiogenesis	67
AKT and cell death	68
AKT and Ca ²⁺ cycling proteins	69
AKT and metabolism	70
Exercise and AKT signalling in heart failure	71
Protein Kinase C	73
Protein Kinase C delta and epsilon	74
Protein Kinase C alpha	76
The diabetic heart	81
Diabetic cardiomyopathy	81
Changes in contractile proteins	81
Changes in metabolism	82
Apoptosis / Necrosis	82
STZ - induced type 1 diabetes rat model	83
Impact of diabetes on cardiac remodelling after myocardial infarction	84
New insights into cardiac remodelling: role of thyroid hormone	85
Thyroid hormone and cardiac remodelling	86
Thyroid hormone and embryonic development	87
Action of thyroid hormone (TH)	87

Thyroid hormone and the developing heart	89
Thyroid hormone responses in the myocardium to stress	90
Thyroid hormone and gene programming	91
AKT and Thyroid hormone in cardiac remodelling	92
Thyroid hormone and Cardiac preservation	92
Clinical Implications	93
Thyroid hormone in cardiac surgery	94
Thyroid hormone in myocardial infarction	95
Working hypothesis	95
Main aims	96
Specific aims	96
CHAPTER 2	97
MATERIALS AND METHODS	
Material and Methods	98
Methods - Animals	98
Induction of diabetes	99
Experimental model of myocardial infarction	99
Functional and structural assessment - Ecocardiography	102
Ecocardiograph analysis of myocardial deformation	104
Isolated heart preaparation	104
Measurement – Protein Expressions	107
Measurements of myosin heavy chain isoform content	108
Measurements of Thyroid hormones	108
Measurements of T3	108
Detection limit	109
Precision	109

Inter-precision assay	109
Linearity and Specificity	109
Measurements of T4	110
Detection limit, Precision T4	111
Specificity and Linearity	111
General experiments protocol in the study	112
Analysis of data and statistics	113
CHAPTER 3	114
RESULTS	
Preliminary studies - Establishment of experimental T1DM model	115
Contractile functions	117
General characteristics of all groups of rats	120
Physiological studies: Expression of isoform alpha and epsilon	121
Left ventricular function and heart rate	122
Systolic radial myocardial deformation	122
Thyroid hormones levels in plasma	124
Effects of TH administration on the response of the diabetic heart after AMI	136
Heart rate and functional indices after AMI in diabetic rats	136
Left ventricular deformation	136
Systolic radial myocardial infarction	136
Cardiac hypertrophy, wall tension and geometry	137
Molecular studies	148
Thyroid hormone nuclear receptor expression in the myocardium	148
Calcium cycling proteins and myosin isoform expression	148
Expression of isoform alpha and delta PKC	149
Activation of intracellular kinase signalling	149

Effect of thyroid hormone on the response of the diabetic heart after myocardial infarction	160
Thyroid hormone nuclear receptor expression in the myocardium	160
Calcium cycling proteins and myosin isoform expression	160
Expression of isoforms alpha and epsilon of Protein kinase C	161
Intracellular kinase signalling activation	161
CHAPTER 4	171
DISCUSSION	
Preview to Discussion	172
STZ-induced diabetes mellitus	172
General characteristics of the animals	174
Preliminary studies to establish baseline	175
Physiological and biomolecular methods involved with the project	175
Induction of myocardial infarction (AMI)	176
Isolated heart preparation	176
Echocardiography	177
Assessment of molecular changes	178
Baseline characteristics of unstressed diabetic myocardium	178
Diabetes-induced cardiomyopathy	178
Physiological studies	179
Thyroid hormone and its effect on the heart	181
Excitation-contraction coupling (ECC)	182
Calcium dysfunction in the diabetic heart	183
Diabetes and myocardial infarction	184
The diabetic heart, fibrosis and remodelling	186
Molecular mechanism of cardiac remodelling	187
TGFbeta1 in cardiac remodelling and failure	189

Molecular changes in the heart during failure	190
Role of thyroid hormone in DM, AMi and DM plus AMI	194
Thyroid hormone induced changes in the diabetic heart after AMI	196
Potential Mechanisms	198
CHAPTER 5 CONCLUSIONS	201
CHAPTER 6 SCOPE FOR FUTURE RESEARCH	204
REFERENCES	207
APPENDIX PRESENTATION AND PUBLICATIONS	256

List of Tables and figures

	Page
Chapter 1	
Figure 1.1 The mammalian heart	23
Figure 1.2 (A) cardiomyocytes and (B) internal structures of a myocyte	27
Figure 1.3 A diagram of the cardiac action potential showing the different phases	29
Figure 1.4 Processes involved in cardiac muscle contraction	30
Figure 1.5 A schematic diagram showing Ca ²⁺ cycling in the heart	32
Figure 1.6 Heart failure pathogenesis	35
Figure 1.7 Three different MAPK signaling pathways	72
Chapter 2	
Figure 2.1 Rat heart subjected to coronary artery ligation mounted on a Langendorff's apparatus	101
Figure 2.2 Long-axis view images	103
Figure 2.3 Isolated rat heart apparatus	105
Figure 2.4 Photograph (A) and traces (B) showing procedure for protein isolation using sodium dodecyl sulfate-protein polyacrylamide (SDS-PAGE) gel electrophoresis and immuno detection system	106
Figure 2.5 Standard assay curve for T3	110
Figure 2.6 Standard assay curve for T4	112
Chapter 3	
Table 3.1 Urine volume, urine glucose concentration and urine ketone concentration at base line and 4 days after STZ injection (ip) using 30 mg/bw	116
Table 3.2 Urine volume, urine glucose concentration and urine ketone concentration at base line and 4 days after STZ injection (ip) employing 60 mg/bw	117
Table 3.3 General characteristics of the experimental animals	120
Table 3.4 Left ventricular weight (LVW in mg), LVW to body weight ratio (LVW/BW, mg/g) and echocardiographic measurements of posterior wall thickness at diastolic phase (LVPW), wall tension index (WTI, LVIDd/2* LVPW) and sphericity index, left ventricular internal diameter at diastolic phase (LVIDd) and at systolic phase (LVIDs) and ejection fraction (EF%), in sham-operated rats (SHAM), sham-operated diabetic rats (DM-SHAM), post-infarcted rats (AMI) and post-infarcted diabetic rats (DM-AMI) after 2 weeks	123
Table 3.5 Thyroxine (T4) and triiodothyronine (T3) levels in plasma, heart rate (in beats per min) and the calculated area of the scar tissue and the weight of the scar in non-diabetic sham-operated rats (SHAM), sham-operated diabetic rats (DM-SHAM), post-infarcted diabetic rats (DM-AMI) and post-infarcted diabetic rats treated with thyroid hormone (DM-AMI+TH) after 2 weeks	124
Table 3.6 Regional Systolic radial strain at different segments of left ventricle	132
Table 3.7 Thyroxine (T4) and triiodothyronine (T3) levels in serum, heart rate (in beats per min) and the calculated areas of the scar tissues and the weights of the scar tissues in sham-operated diabetic rats (DM-SHAM), post-infarcted diabetic rats (DM-AMI) and post-infarcted diabetic rats treated with thyroid hormone (DM-AMI+TH) after 2 weeks	138

Table 3.8 Left ventricular weight (LVW in mg), LVW to body weight ratio (LVW/BW, mg/g) and echocardiographic measurements of posterior wall thickness at diastolic phase (LVPW), wall tension index (WTI, $LVIDd/2 * LVPW$) and sphericity index, left ventricular internal diameter at diastolic phase (LVIDd) and at systolic phase (LVIDs) and ejection fraction (EF%), in sham-operated diabetic rats (DM-SHAM), post-infarcted diabetic rats (DM-AMI) and post-infarcted diabetic rats treated with thyroid hormone (DM-AMI+TH) after 2 weeks	139
Table 3.9 Regional Systolic radial strain at different segments of left ventricle	145
Figure 3.1 Bar chart showing left ventricular developed pressure (LVDP in mmHg) was not significantly different between normal (NORM) and diabetic (DM) rat hearts	118
Figure 3.2 Bar Chart showing the rate of increase (+dp/dt) and decrease (-dp/dt) of left ventricular developed pressure (LVDP) in mmHg/sec were not significantly different between normal (NORM) and diabetic (DM) rat hearts	119
Figure 3.3 Bar chart showing ejection fraction (EF%) measured by echocardiography in sham-operated rats (SHAM), sham-operated diabetic rats (DM-SHAM), post-infarcted rats (AMI) and post-infarcted diabetic rats (DM-AMI) after 2 weeks	125
Figure 3.4 Bar chart showing regional systolic velocity of the posterior wall of the left ventricle (SVPW) measured by echocardiography is shown in sham-operated rats (SHAM), sham-operated diabetic rats (DM-SHAM), post-infarcted rats (AMI) and post-infarcted diabetic rats (DM-AMI) after 2 weeks	126
Figure 3.5 Left ventricular developed pressure (LVDP) (A) and the rate of increase and decrease of LVDP (+dp/dt and -dp/dt) (B) are shown in sham-operated rats (SHAM), sham-operated diabetic rats (DM-SHAM), post-infarcted rats (AMI) and post-infarcted diabetic rats (DM-AMI) after 2 weeks.	127
Figure 3.6(A) Wall tension index (defined as the ratio of LVIDd to 2 x LVPW) and (B) Sphericity Index (defined as the ratio of diastolic LV length to diastolic LV diameter) in sham-operated rats (SHAM), sham-operated diabetic rats (DM-SHAM), post-infarcted rats (AMI) and post-infarcted diabetic rats (DM-AMI) after 2 weeks	128
Figure 3.7(A) Left Ventricular Weight to Body weight (LVW/BW) and (B) Left Ventricular Wall Thickness (LVPW) are shown in sham-operated rats (SHAM), sham-operated diabetic rats (DM-SHAM), post-infarcted rats (AMI) and post-infarcted diabetic rats (DM-AMI) after 2 weeks	129
Figure 3.8 Left Ventricular Internal Diameter at (A) the end-diastole (LVIDd) and (B) at the end-systole (LVIDs) are presented in sham-operated rats (SHAM), sham-operated diabetic rats (DM-SHAM), post-infarcted rats (AMI) and post-infarcted diabetic rats (DM-AMI) after 2 weeks	130
Figure 3.9 Representative short axis imaging echocardiographic views at diastole and at systole from sham-operated rats (SHAM), post-infarcted rats (AMI) and post-infarcted diabetic rats (DM-AMI) after 2 weeks	131
Figure 3.10 Short-axis imaging view of the left ventricle at the level of the papillary muscles was used to evaluate systolic radial strain	132
Figure 3.11 Global systolic radial strain of the left ventricle (defined as the mean of the regional systolic radial strains of the different segments of the LV) is shown in sham-operated rats (SHAM), sham-operated diabetic rats (DM-SHAM), post-infarcted rats (AMI) and post-infarcted diabetic rats (DM-AMI) after 2 weeks.	133
Figure 3.12 Image showing representative analysis of systolic radial strain of the left ventricle in sham-operated rat heart (SHAM)	134
Figure 3.13 Images showing representative analysis of systolic radial strain of the left ventricle in (A) post-infarcted rat heart (AMI) and (B) diabetic post-infarcted rat heart (DM-AMI)	135

Figure 3.14 Left Ventricular Internal Diameter at (A) end-diastole (LVIDd) and at (B) end-systole (LVIDs) are presented in sham-operated diabetic rats (DM-SHAM), post-infarcted diabetic rats (DM-AMI) and post-infarcted diabetic rats with thyroid hormone treatment after 2 weeks	140
Figure 3.15 Ejection fraction (A) and (B) regional systolic velocity of the posterior wall of the left ventricle (SVPW) measured by echocardiography are shown in sham-operated diabetic rats (DM-SHAM), post-infarcted diabetic rats (DM-AMI) and post-infarcted diabetic rats with thyroid hormone treatment after 2 weeks.	141
Figure 3.16 Wall tension index (defined as the ratio of LVIDd to 2 x LVPW) and Sphericity Index (defined as the ratio of diastolic LV length to diastolic LV diameter) is shown in sham-operated diabetic rats (DM-SHAM), post-infarcted diabetic rats (DM-AMI) and post-infarcted diabetic rats with thyroid hormone treatment after 2 weeks.	142
Figure 3.17(A) Left Ventricular Weight to Body weight (LVW/BW) and (B) Left Ventricular Wall Thickness (LVPW) are shown in sham-operated diabetic rats (DM-SHAM), post-infarcted diabetic rats (DM-AMI) and post-infarcted diabetic rats with thyroid hormone treatment after 2 weeks.	143
Figure 3.18 Representative short axis imaging echocardiographic views at diastole and at systole from sham-operated rats (SHAM), post-infarcted rats (AMI) and post-infarcted diabetic rats (DM-AMI) after 2 weeks.	144
Figure 3.19 Global systolic radial strain of the left ventricle (defined as the mean of the regional systolic radial strains of the different segments of the LV) is shown in sham-operated diabetic rats (DM-SHAM), post-infarcted diabetic rats (DM-AMI) and post-infarcted diabetic rats with thyroid hormone treatment after 2 weeks	145
Figure 3.20 Images showing representative analysis of systolic radial strain of the left ventricle in diabetic post-infarcted rat heart (DM-AMI) and diabetic post-infarcted rat heart with thyroid hormone treatment (DM-AMI+TH).	146
Figure 3.21(A) Left ventricular developed pressure (LVDP) and (B) the rate of increase and decrease of LVDP (+dp/dt and -dp/dt) are shown in sham-operated diabetic rats (DM-SHAM), post-infarcted diabetic rats (DM-AMI) and post-infarcted diabetic rats with thyroid hormone treatment after 2 weeks.	147
Figure 3.22 (A) Densitometric assessment in arbitrary units and (B) representative western blots of thyroid hormone receptor $\alpha 1$ (TR $\alpha 1$) protein expression in sham-operated rats (SHAM), sham-operated diabetic rats (DM-SHAM), post-infarcted rats (AMI) and post-infarcted diabetic rats (DM-AMI) after 2 weeks	150
Figure 3.23(A) Densitometric assessment in arbitrary units and (B) representative western blots of thyroid hormone receptor $\beta 1$ (TR $\beta 1$) protein expression in sham-operated rats (SHAM), sham-operated diabetic rats (DM-SHAM), post-infarcted rats (AMI) and post-infarcted diabetic rats (DM-AMI) after 2 weeks.	151
Figure 3.24(A) Densitometric assessment in arbitrary units and (B) representative images of myosin heavy chain isoform expression in sham-operated rats (SHAM), sham-operated diabetic rats (DM-SHAM), post-infarcted operated rats (AMI) and post-infarcted diabetic rats (DM-AMI) after 2 weeks.	152
Figure 3.25(A) Densitometric assessment in arbitrary units and (B) representative western blots of SERCA and phospholamban (PLB) protein expression in sham-operated rats (SHAM), sham-operated diabetic rats (DM-SHAM), post-infarcted rats (AMI) and post-infarcted diabetic rats (DM-AMI) after 2 weeks.	153
Figure 3.26(A,B and D) Densitometric assessment in arbitrary units and (C and E) representative western blots of isoforms α , ϵ and δ of PKC in sham-operated rats (SHAM), sham-operated diabetic rats (DM-SHAM), post-infarcted rats (AMI) and post-infarcted diabetic rats (DM-AMI) after 2 weeks.	155
Figure 3.27(A) Densitometric assessment in arbitrary units and (B) representative western blots of phosphorylated levels of p38 MAP kinase in sham-operated rats (SHAM), sham-operated diabetic rats (DM-SHAM), post-infarcted rats (AMI) and post-infarcted diabetic rats (DM-AMI) after 2 weeks.	156

Figure 3.28(A) Densitometric assessment in arbitrary units and (B) representative western blots of phosphorylated levels of p54 JNK in sham-operated rats (SHAM), sham-operated diabetic rats (DM-SHAM), post-infarcted rats (AMI) and post-infarcted diabetic rats (DM-AMI) after 2 weeks.	157
Figure 3.29(A) Densitometric assessment in arbitrary units and (B) representative western blots of phosphorylated levels of Akt kinase in sham-operated rats (SHAM), sham-operated diabetic rats (DM-SHAM), post-infarcted rats (AMI) and post-infarcted diabetic rats (DM-AMI) after 2 weeks.	158
Figure 3.30(A) Densitometric assessment in arbitrary units and (B) representative western blots of phosphorylated levels of p44 and p42 ERKs in sham-operated rats (SHAM), sham-operated diabetic rats (DM-SHAM), post-infarcted rats (AMI) and post-infarcted diabetic rats (DM-AMI) after 2 weeks.	159
Figure 3.31(A and B) Densitometric assessment in arbitrary units and (C) representative western blots of thyroid hormone receptor $\alpha 1$ (TR $\alpha 1$) and $\beta 1$ (TR $\beta 1$) protein expression in are shown in sham-operated diabetic rats (DM-SHAM), post-infarcted diabetic rats (DM-AMI) and post-infarcted diabetic rats with thyroid hormone treatment after 2 weeks.	162
Figure 3.32 Densitometric assessment in arbitrary units and representative images of myosin heavy chain isoform expression shown in sham-operated diabetic rats (DM-SHAM), post-infarcted diabetic rats (DM-AMI) and post-infarcted diabetic rats with thyroid hormone treatment after 2 weeks.	163
Figure 3.33(A) Densitometric assessment in arbitrary units and (B) representative western blots of SERCA and phospholamban protein expression are shown in sham-operated diabetic rats (DM-SHAM), post-infarcted diabetic rats (DM-AMI) and post-infarcted diabetic rats with thyroid hormone treatment after 2 weeks.	164
Figure 3.34(A) Densitometric assessment in arbitrary units and (B) representative western blots of isoforms α , ϵ and δ of PKC are shown in sham-operated diabetic rats (DM-SHAM), post-infarcted diabetic rats (DM-AMI) and post-infarcted diabetic rats with thyroid hormone treatment after 2 weeks.	166
Figure 3.35(A) Densitometric assessment in arbitrary units and (B) representative western blots of phosphorylated levels of p38 MAP kinase are shown in sham-operated diabetic rats (DM-SHAM), post-infarcted diabetic rats (DM-AMI) and post-infarcted diabetic rats with thyroid hormone treatment after 2 weeks.	167
Figure 3.36(A) Densitometric assessment in arbitrary units and (B) representative western blots of phosphorylated levels of p54 JNK in sham-operated diabetic rats (DM-SHAM), post-infarcted diabetic rats (DM-AMI) and post-infarcted diabetic rats with thyroid hormone treatment after 2 weeks.	168
Figure 3.37 Densitometric assessment in arbitrary units and representative western blots of phosphorylated levels of Akt kinase are shown in sham-operated diabetic rats (DM-SHAM), post-infarcted diabetic rats (DM-AMI) and post-infarcted diabetic rats with thyroid hormone treatment after 2 weeks.	169
Figure 3.38(A) Densitometric assessment in arbitrary units and (B) representative western blots of phosphorylated levels of p44 and p42 ERKs in sham-operated diabetic rats (DM-SHAM), post-infarcted diabetic rats (DM-AMI) and post-infarcted diabetic rats with thyroid hormone treatment after 2 weeks.	170

Chapter 5

Figure 5.1 A schematic flow diagram showing the effect of myocardial infarction in the heart in the absence of TH (left) and in the presence of TH (right).	203
---	------------

ABBREVIATIONS

- ACh – Acetylcholine
- ADP – Adenosine diphosphate
- AIF – Apoptosis ionising factor
- Akt – Serine/threonine protein kinase
- Akt-p706K – Protein Kinase B
- AMI - Acute Myocardial Infarction
- AMI-C - Acute Myocardial Infarction- Control
- ANP-Atrial Natriuretic factor
- ATP - Adenosine triphosphate
- AU – Arbitrary units
- AV- Atrio ventricle
- AXC- Aortic cross clamp
- BNP – Brain Natriuretic factor
- BSA-Bovine serum albumin
- BW – Body weight
- Ca²⁺ - Calcium
- [Ca²⁺]_i – intracellular free calcium concentration
- CAMK – Calmodulin-Dependent Protein Kinase
- cAMP – Cyclic 3' 5'' adenosine monophosphate
- cfox – Cellular oncogene fox
- cGMP – Cyclic 3,5 guanosine monophosphate
- CH₃ – Carbonium ions
- CI – Cardiac Index
- CICR – Calcium- induced calcium release
- CMYC – Cellular oncogene myc

CRP – C- Reactive protein

CTGF-Cytokine transforming growth hormone

CV-Confidence variation

CTNI- Cardiac troponin –I

CTNT – Cardiac troponin - T

CytC – Cytochrome C

D1 – type 1 de-iodinase

D2 – type 2 de-iodinase

DG – Diacylglycerol

DHP – Dihydropyridine

DM - Diabetes Mellitus

DyM – Dystrophic Mice

DM+AMI - Diabetes Mellitus + Acute Myocardial Infarction

DM+AMI+TH – Diabetes Mellitus +Acute myocardial infarction +Thyroid hormone

DM-Sham – Non infarct Diabetic Mellitus Sham

DNA – Deoxyribonucleic acid

DOX – Doxorubicin

dp/dt – Rate of increase and decrease of LVDP

ECG – Electrocardiogram

ECM – Extracellular Matrix

ED – ERK Docking

EDTA-Ethylene diethyl tetra acetic acid

EF –Ejection fraction

EGF – Epidermal Growth Factor

EGTA-Ethylene glycerol tetra acetic acid

EF – Ejection Fraction

EMMPRIN – Extracellular Matrix Mellanoproteinase inducer

ENOS – Nitric oxide synthase

ERK – Extracellular Signal Regulated Kinase

FGF – Fibroblast Growth Factor

FOXO – Translocation of forkhead box O

GADD45 β – DNA damage inducible beta

GIK – Glucose insulin potassium

GKS – Growth kinase signal

GLUT – Glucose transporter

GPCRS – G-Protein coupled receptors

GRK – G-Protein coupled kinase

GSK – Glycogen synthase kinase

HF – Heart failure

HG – Hyperglycaemia

HMC – Hypotrophic cardiomyopathy

Hsp – Heat shock proteins

Hsp70 – Heat shock protein 70

IR-Insulin resistance

I – Inhibitor

IL-6 – Interleukin 6

IU – International Units

JIP – JNK Interacting protein

JLK – JNK associated zipper protein

JNK – Jan –N-terminal kinase

K+ - Potassium

KCl –Potassium Chloride

KG-Killogram

KO –Knock out

KSR – Kinase suppressor of Ras

LAD – LCK associated adaptor

LTCC – L- type calcium channel

LV- Left ventricle

LVAD – Left ventricle assisted device

LVDP – Left ventricular developed pressure

LVIDs- Left ventricle internal diameter at systole

LVIDd- Left ventricle internal diameter at diastole

LVPWT – Left ventricle posterior wall thickness

LVPW – Left ventricle pressure wall

LVW – Left Ventricular Weight

MAM-Mitochondrial autophagic marker

MAPK – Mitogen activated protein kinase

MI – Myocardial infarction

MLCK – Myosin light chain kinase

MMP-1 – Matrix metalloproteinase

MORG1 – MAPK Organiser 1

MPTP – Mitochondrial permeability transition pore

Mtor – Mammalian Target Rapamycin

NA – Noradrenaline

Na + - Sodium

NCX - Sodium calcium exchanger

NDM-AMI - Normal Diabetes Mellitus - Acute Myocardial Infarction

NFAT – Nuclear Factor Associated Transcriptor

NGF-Nerve growth factor

NORM – Normal

NO-Nitric oxide

NP – Naturetic peptide

OSM – Osmosensing scaffold for MEKKI

P38 – Tyrosine phosphorylated protein

P38-MAPK – P38 Mitogenic Activated Protein Kinase

PBI- Phox/berm-IP

PE – Phenylepinephrine

PI3K – Phosphatidylinositol 3 kinase

PKA – Protein Kinase A

PKC – Protein kinase C

Plb – Phospholamban

PMA- Phorbol -12 myrstate -13 acetate

POSH – Plenty of SH3

PP – Protein phosphatases

PP2C – Protein Serine/threonine phosphatases PCR

PPAR α – Proximine proliferator activated receptor alpha

PTP – Protein tyrosine phosphatase

PTP-SL – Phosphotyrosine specific phosphatases

PWT – Posterior Wall Thickness

RAAS- Renin-angiotensin system

RAGE – Advanced glycation- end products

RNA – Ribonucleic Acid

ROS – Reactive oxygen species

RTK - Receptor tyrosine kinase

RyR – Ryanodine receptor

SD- Standard deviation

SDS- Sodium dodecyl sulphate

SDS-PAGE – Sodium dodecyl sulphate protein polyacrylamide

SEM – Systemic errors of the means

SERCA – Sarcoplasmicreticular calcium -ATPase pump

SHAM – Sham-operated animals

SI – Sphericity index

SR – Sarcoplasmic reticulum

ST – Scar tissue

STEM – ST- elevation myocardial infarction

STP – Serine/Threonine phosphatases

STZ - Streptozotocin

SVPW – Systolic velocity of posterior wall radial displacement

SVPW – Systolic ventricle pressure wall

TIMPS-Tissue inhibitor metalloproteinases

T1DM – Type 1 diabetes mellitus

T2DM- type 2 diabetes mellitus

T3 - Thyroxine 3

T4 - Thyroxine 4

TG – Transgenic

TGF – Transforming growth factor

TGF- β 1 – Tumour growth factor β 1

TH - Thyroid hormone

THR – Thyroid hormone receptor

TM – Tropomyosin

TnC – Troponin C

TNF-2 – Tumour necrotic factor

TnI – Troponin I

TNR – Thyroid nuclear receptor

TnT – Troponin T

TR – Thyroid hormone receptor
TR α 1 - Thyroid Hormone Alpha receptors
TR β 1- Thyroid Hormone Beta receptors
TSH – Thyroid stimulating hormone
TV – Tricuspid valve
UVR – Ultra violet radiation
VCAM-I – Cell adhesion molecule
VEGF – Vascular endothelial growth factor
VO₂ – Oxygen Consumption
WT- Wall thickness
WTI – Wall tension index
 α -MHC – Alpha Myosin Heavy Chain
 α SKA - Adult isoforms of sarcomeric gene
 β AR – Beta adrenergic receptor
 β -MHC – Beta Myosin Heavy Chain

CHAPTER 1

GENERAL INTRODUCTION

The Mammalian Heart

The mammalian heart is a four-chambered muscular organ situated in the anterior mediastinum, immediately posterior to the sternum and encapsulated by the pericardium (figure 1.1). Its pumping ability is central to the functioning of the circulatory system wherein blood is pumped through a network of blood vessels namely arteries, veins, arterioles, venules and capillaries. These blood vessels can be subdivided into a pulmonary circuit carrying blood to and from gas exchange surfaces of the lungs and a systemic circuit through which blood is transported to and from the rest of the body (Sherwood, 2008).

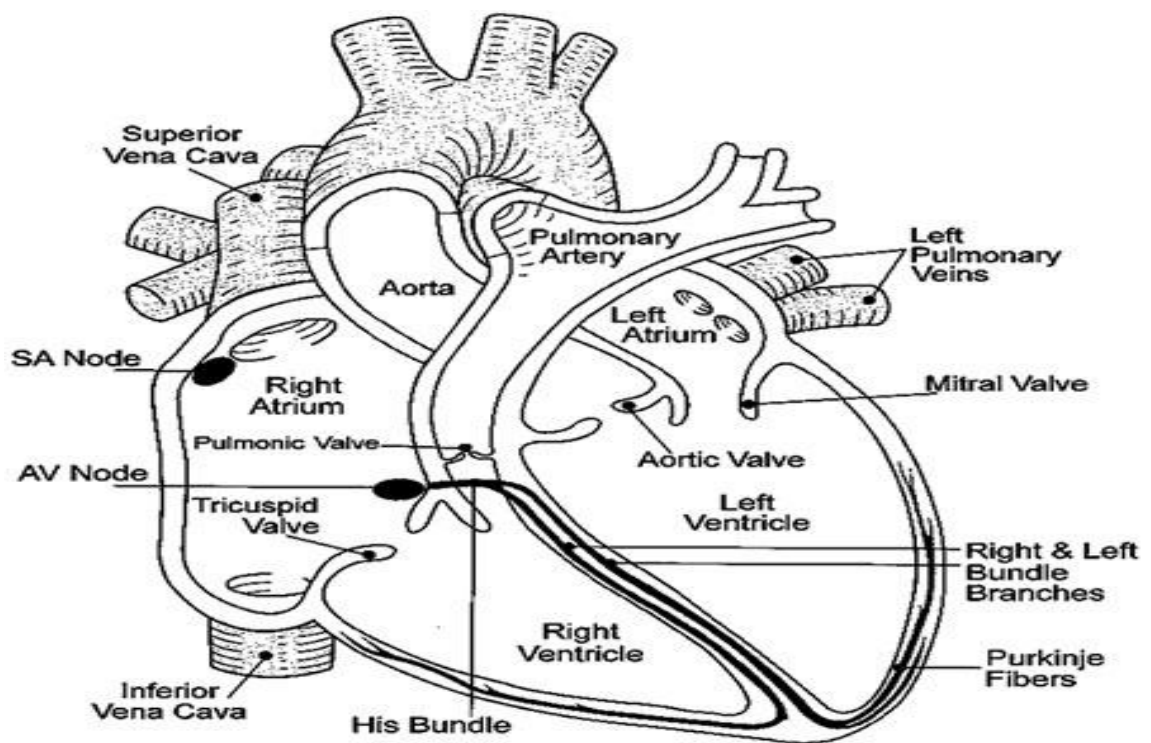


Figure 1.1 The mammalian heart. Components are described in the text (Image courtesy www.beyondbiology.org)

As shown in figure 1.1, the right and left atria and the right and left ventricles make up the four chambers of the mammalian heart. Two chambers of the heart may be associated with each circuit; the right atrium receives blood from the systemic circuit through the superior vena cava and the inferior vena cava and allows inflow into the right ventricle passing through the right atrio-ventricular (AV) or tricuspid valve. Blood is then pumped into the pulmonary circuit eventually being collected by the left atrium

and emptied into the LV through the left AV or bicuspid valve. Semi-lunar valves are situated between the ventricles and the major blood vessels of the heart and open and close passively due to pressure gradients. Blood pumped from the right atrium into the pulmonary trunk passes through the pulmonary valve and blood leaves the left ventricle through the aortic valve into the ascending aorta. The atria are separated by the inter-atrial septum and the ventricles by a much thicker inter-ventricular septum that houses electrical conduction tissue. Innervation of the heart is by both vagal and sympathetic fibres. The SA node and the atria are predominantly innervated by the right vagus whereas the left vagus nerve supplies the AV node and the bundle of His (Vander *et al.*, 2007). The ventricles of the myocardium are only sparsely innervated by vagal efferents. Although rhythmic contraction of the heart is initiated in the SA node, cardiac function is mediated by neural activation. The release of noradrenaline (NA) by sympathetic nerves and the subsequent activation of beta adrenergic receptors result in positive chronotropy, inotropy and dromotropy as well as enhanced metabolism. In contrast, parasympathetic nerves (vagus) release acetylcholine (ACh) that acts on muscarinic receptors in the heart leading to negative dromotropic, inotropic and chronotropic effects. The cardiac action potential that initiates contraction is generated in the sino-atrial (SA) node and spreads through the atria before converging upon the AV node for distribution to the ventricles by the specialised Bundle of His, right and left bundle branches and Purkinje fibre network.

The walls of the atria are thinner than those of the ventricles, particularly the LV whose wall is 3-4 times thicker than the right ventricle at a corresponding position (Vander *et al.*, 2007). The wall of the heart is typically described to be made up of 3 layers; the outer epicardium (visceral pericardium) is a serous membrane consisting of an exposed mesothelium and a layer of smooth connective tissue that is attached to the myocardium. The inner surfaces of the heart (including the valves) are lined by the endocardium that consists of squamous epithelial cells continuous with the endothelium of blood vessels. The myocardium is the middle muscular wall of the heart that forms both atria and ventricles. This layer encompasses several types of cells including atrial and ventricular contractile 'working' myocytes that comprise muscle fibres, nodal cells, Purkinje fibres, smooth muscle cells and fibroblasts (Levy *et al.*, 2006). Cardiac myocytes account for 70% to 75% of the myocardium by cell volume but only 25% to 30% by cell number (Miner and Miller, 2006). Cardiac fibroblasts that synthesize proteins of the ECM are the most abundant cell type of the myocardium.

The Extracellular Matrix (ECM)

The muscle fibre array of the myocardium is surrounded and interspersed by the ECM, a fibrillar, highly differentiated structure consisting of an organised hierarchy of connective tissue that provides structural support and functional integrity to the heart. The ECM is broadly differentiated into an epimysium encircling the endo- and epicardium, a perimysium that groups myofibrils into bundles and an endomysium that surrounds individual myocytes and provides connection to the vasculature (Fedak *et al.*, 2005). It comprises of a complex network of structural proteins (collagen and elastic fibres) and adhesive proteins (fibronectin, laminin) within a hydrated proteoglycan and glycosaminoglycan-rich milieu (Horn *et al.*, 2008). Coiled fibres of the ECM act to store energy produced during systole, and hence re-lengthening of cardiac myocytes during diastole (Miner and Miller, 2006). Apart from the provision of a structural network that translates developed force in individual myocyte into regular synchronous contraction and passive stiffness, the ECM also functions to prevent myocyte slippage, overstretch and interstitial oedema. Once considered an inert physical scaffolding, ongoing research has established diverse roles of the ECM in trans-membrane signalling, MAPK activation, growth factor mediation, cytoskeletal rearrangement, modulation of cell phenotype and among other, regulatory roles in hypertrophy and ontogenic development (Fedak *et al.*, 2005; Horn *et al.*, 2008; Bowers *et al.*, 2010; Hutchinson *et al* 2010). ECM trans-membrane mechanoreceptors known as integrins constitute another important feature that transduces mechanical forces and changes in ECM structure, through signals from the extracellular compartment to the cytoskeleton and vice versa. Integrins consist of two different chains, α (120±150 kDa) and β (110±190 kDa), linked by non covalent bounds. They modulate signals instigated by ionic channels, hormone receptors and growth factors, and participate in various transduction processes including those concerned with cell motility, division, differentiation and programmed death (Spinale, 2007; Horn *et al.*, 2008; Bowers *et al.*, 2010).

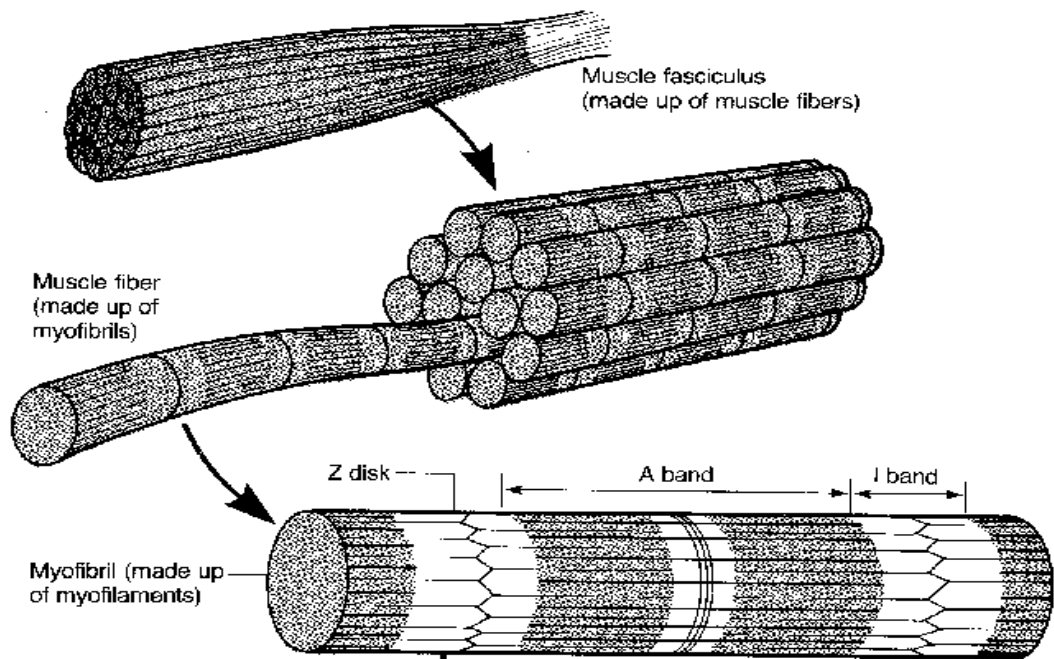
The ECM is a dynamic entity and component proteins are maintained by a finely controlled homeostatic balance between deposition and degradation. Different families of MMPs that favour or inhibit matrix degradation, regulate the ECM in both normal and pathological conditions. Collagenases or matrix metalloproteinases (MMP-1) cleave

collagens in fragments which in turn constitute the substrate of proteases including the gelatinases (MMP-2, MMP9) that are responsible for the degradation of type IV collagen and fibronectin (Bowers *et al.*, 2010). These zinc-dependent enzymes are regulated by a class of proteins called tissue inhibitor metalloproteinases (TIMPs). The ability to synthesize ECM components differs among cells in the heart and varies depending upon the inciting stimulus. For example, myocytes produce type IV and VI collagens including laminin and proteoglycans. Collagen type I and III and fibronectin, as well as MMPs are synthesised by the surrounding fibroblasts (Banerjee *et al.* 2006; 2007). Integrin activation also induces the synthesis of collagens and gelatinases, which regulate the synthesis and type of ECM proteins (Spinale, 2007). Modulation of these various components regulates mechanical, chemical and electrical signalling between cells (Miner and Miller, 2006).

The Cardiomyocyte

A ventricular myocyte is an elongated cell containing contractile myofibrils that give it a striated appearance (figure 1.2A). Ventricular myocytes are typically uni-nucleated, have a variable branching morphology, extensive capillary supply and are connected to adjacent cardiomyocytes at blunt ends by specialised intercalated discs. The intercalated discs of neighbouring cells are physically connected by types of cell junction i.e. gap junctions and desmosomes that together orchestrate and integrate cardiac electro-mechanical activity. As a result, the entire myocardium functions as a single unit known as a 'syncytium' with a single contraction of the atria followed by a single contraction of the ventricles (Vander *et al.*, 2007).

A.



B.

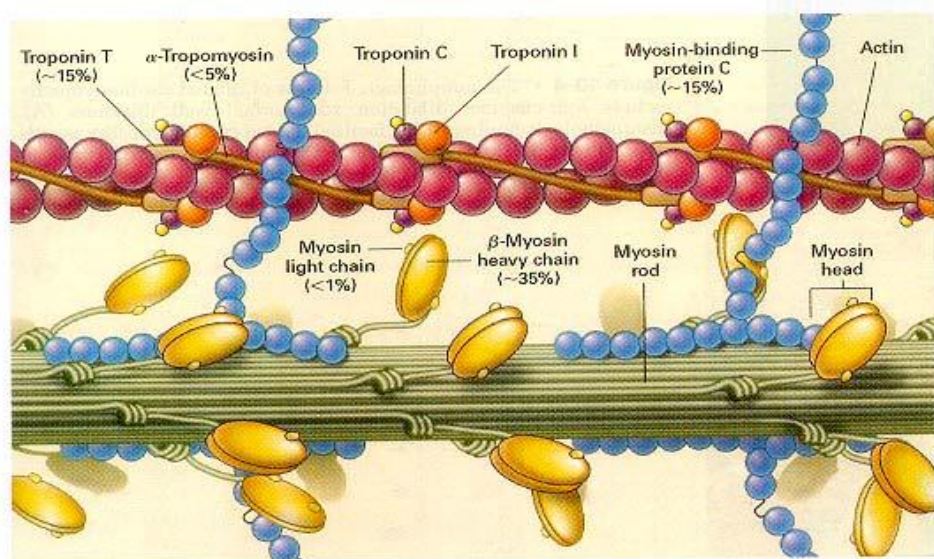


Figure 1.2: Diagrams showing typical (A) cardiacmyocytes and (B) internal structures of a myocyte (Taken from Vander et al, 2007)

An exquisitely specialised cardiac microanatomy coordinates the processes of orderly spread of action potentials, contraction of cardiac chambers and the pumping action of

the heart. Similar in many respects to skeletal muscle cells, the fundamental contractile unit within the myocyte is the sarcomere containing inter-digitating thick and thin filaments of the contractile apparatus, namely the proteins actin, myosin, the troponin complex and tropomyosin (Tm). Three proteins, Troponin T, I and C (TnT, TnI, TnC) make up the thin filament complex and together mediate the extent of crossbridge formation whilst contributing to the structural integrity of the sarcomere (figure 2.1B, Sherwood, 2008). Within the cardiomyocyte, each myofibril is surrounded by the sarcoplasmic reticulum (SR), a highly organised Ca^{2+} handling organelle made up of membranous tubules that regulate cytosolic Ca^{2+} flux in conjunction with key sarcoplasmic proteins namely SERCA), the regulatory protein of SERCA, phospholamban (Plb), and the Ca^{2+} release channels (figure 1.2B). Another specialised component of the cardiomyocyte is the sarcolemma, a lipid bilayer combination of the plasma membrane and the basement membrane that contains membrane receptors, pumps and channels that regulate contractility. The sarcolemma forms the intercalated disks and penetrates deep into the cell to form the Transverse 'T' tubular system that bring in close proximity ion channels and the SR calcium handling proteins, thus playing a pivotal role in cell contractility (Vander *et al.*, 2007) (figure 1.2). Although not given in the figure, integrins are interwoven throughout the sarcolemma and form an important collagen-integrin-cytoskeletal relation.

A more complete appreciation of the functional anatomy (contraction and relaxation) of myocyte ultra-structure perhaps comes from studies on ventricular myocyte. An over simplified process of contraction and relaxation of the heart is described below.

At the resting membrane potential (corresponding to phase 4 of the action potential (figure 1.3), the sarcolemma is only permeable to K^+ , a condition maintained by the combined activities of the inward K^+ rectifier, Na^+/K^+ ATPase and the $\text{Na}^+/\text{Ca}^{2+}$ exchanger operating in forward mode (figure 1.4). Depolarisation of the plasma membrane beyond an inherent threshold voltage results in the activation of voltage gated Na^+ and Ca^{2+} channels. Opening of fast Na^+ channels results in the rapid upstroke characteristic of phase 0 of the action potential whereas the subsequent inward current that maintains the plateau of the action potential is primarily due to Ca^{2+} influx via L-type Ca^{2+} channels, with $\text{Na}^+/\text{Ca}^{2+}$ exchanger playing a minor role. Rapid inactivation of the fast Na^+ channels (2-10 ms) and a transient net outward current of K^+ along the

electrochemical gradient contributes to an early, brief repolarisation (notch) during phase 1 of the action potential (figure 1.3). The small influx of Ca^{2+} that enters the cell after initial depolarisation triggers Ca^{2+} release from the SR by activating SR Ca^{2+} release channels culminating in a transient rise in cytosolic free calcium concentration to micro-molar concentrations (10 $\mu\text{mole/litre}$) from a resting (diastolic) nanomolar concentration (100 nano-moles/L). A central feature of ECC is the gating of the SR Ca^{2+} release channels by ryanodine receptors (RyR) located within terminal cisternae of the SR. This 'calcium-induced calcium release', activates the contractile machinery and initiates contraction in the myocyte by a mechanism termed Excitation-Contraction Coupling (EC coupling) (Bers, 1991a/b; Vander *et al.*, 2007).

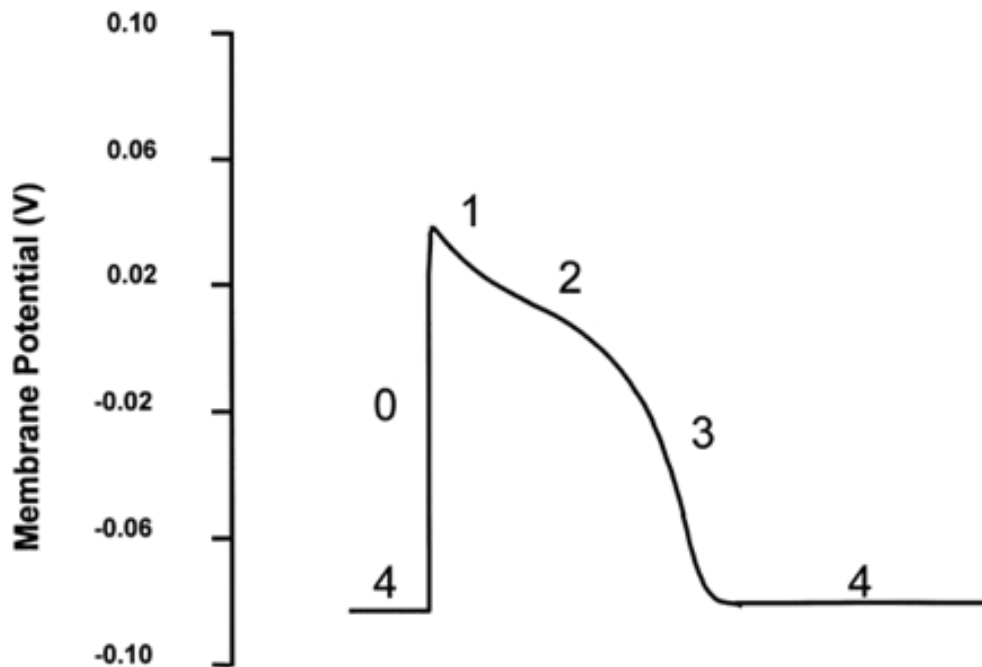


Figure 1.3: A diagram of the cardiac action potential showing the different phases. Phase 0, the upstroke, corresponds to rapid depolarization. The upstroke is followed by phase 1, a brief early repolarization, phase 2 or plateau, phase 3 or rapid repolarization, and phase 4, which corresponds to the resting membrane potential. (Taken from Vander *et al.*, 2007).

Under resting conditions, lower intracellular Ca^{2+} favours the shift of the Tn-Tm complex towards the outer grooves of the actin filament and thereby blocks actin-myosin interaction. Rise in Ca^{2+} concentrations during the action potential and subsequent binding to TnC strengthens TnC-TnI interaction and detaches TnI from the actin molecule by a conformational shift of the Tn-Tm complex, enabling crossbridge formation (figure 1.4). The available literature suggests that thin filament activation is achieved by the movement of Tm over the surface of actin and this motion permits force generation and shortening. After crossbridge formation, i.e. the attachment of the myosin head of the thick filament to the actin molecules of the thin filament, the myosin head changes confirmation ‘pivoting’ towards the M-line, with concomitant ATP hydrolysis to ADP that generates force causing the thin filament to slide over the thick filament and the sarcomere to shorten, altogether resulting in contraction. Binding of adenosine triphosphate (ATP) to the myosin head causes detachment of cross-bridges and (re)exposure of active sites making possible interaction with another cross-bridge (figure 1.4).

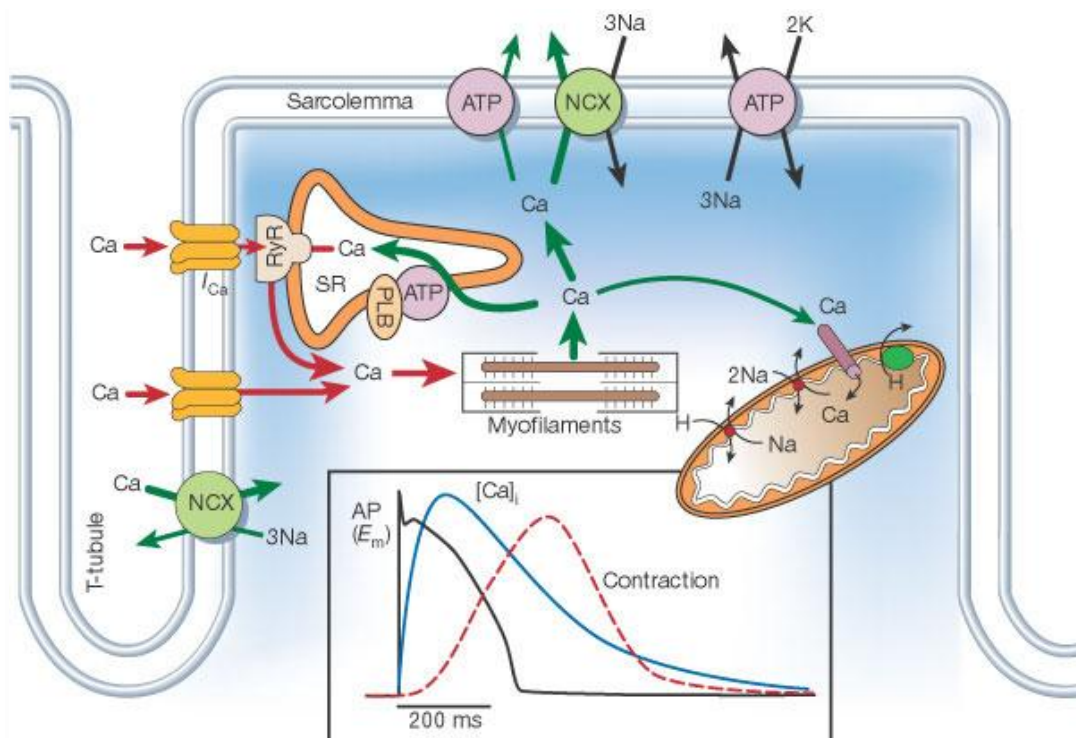


Figure 1.4: Diagram showing the processes involved in cardiac muscle contraction (sliding filament) (Taken Bers, 1991b).

This highly dynamic phenomenon termed the 'sliding filament theory' moves the filaments approximately 10nm with an average velocity of 0.98 $\mu\text{m/s}$ (Levy *et al.*, 2006). Factors such as SR Ca^{2+} release, sensitivity of the myo-filaments to Ca^{2+} , number of crossbridges formed, duration of the action potential and ATP stores appear to decisively affect cardiomyocyte contraction. Following contraction, relaxation and is achieved by the removal of Ca^{2+} (that activates myofilaments) from the cytosol by cellular Ca^{2+} transport systems. This phase corresponds to repolarisation or phase 3 of the action potential, wherein decay of the calcium transient occurs due to the reuptake of Ca^{2+} into the SR by SERCA and the extrusion of Ca^{2+} from the myocyte, primarily by the $\text{Na}^+/\text{Ca}^{2+}$ exchanger (figure 1.5). This phase is characterised by the closure of sarcolemmal Ca^{2+} channels and increased K^+ conductance through the (slow and rapid) delayed rectifier K^+ currents corresponding to a negative change in membrane potential. When membrane potential is restored to -80 to -85 mV, conductance is limited to the inward rectifier K^+ channels that together set the resting membrane potential (phase 4) (Bers, 1991a/b; Walker and Spinale 1999; Vander *et al* 2007).

Within the cardiomyocyte, membrane depolarization by an action potential activates voltage-dependent L-type Ca^{2+} channels that initiate Ca^{2+} influx (Barry and Bridge, 1993). This further triggers a transient rise of $[\text{Ca}^{2+}]_i$ (typically from a basal level of 100 nm to a peak of 1-2 μm 20-40 ms following depolarisation (Beuckelmann and Weir, 1988) via Ca^{2+} release channels of the sarcoplasmic reticulum (SR) through a Ca^{2+} -induced Ca^{2+} release mechanism (figure 1.4). Cardiac force development and/or contraction results from diffusion of Ca^{2+} through the cytosolic space to reach contractile proteins, binding to troponin C, the cessation of the inhibition produced by troponin I and initiation of the sliding action of thin and thick filaments. The decay of the Ca^{2+} transient is brought about mainly by activation of the SR Ca^{2+} pump (SERCA2a), the sarcolemmal $\text{Na}^+/\text{Ca}^{2+}$ exchanger, and the sarcolemmal Ca^{2+} ATPase resulting in $[\text{Ca}^{2+}]_i$ to return to diastolic levels (Bers, 1991; 2002; Boudina and Abel, 2007).

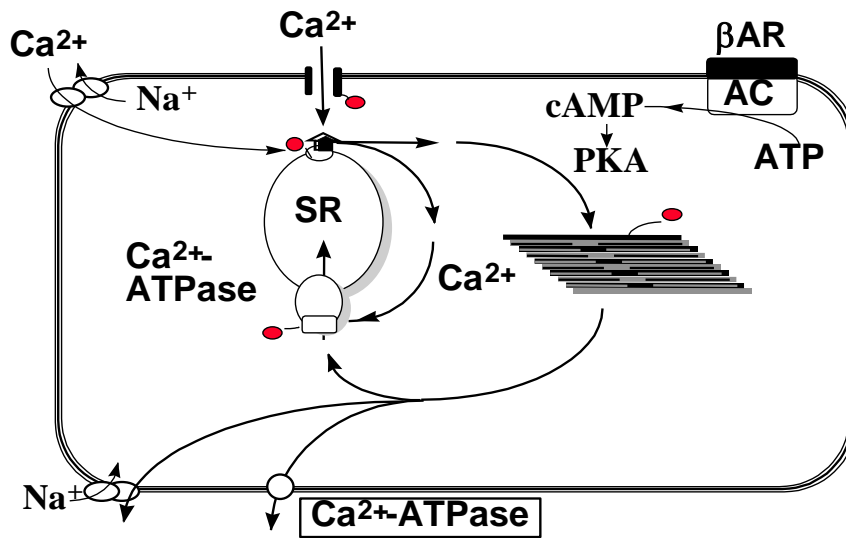


Figure 1.5: A schematic diagram showing Ca^{2+} cycling in the heart. Schematic illustration of the main pathways involved in Ca^{2+} cycling and the site of protein phosphorylation (solid circle) during β -adrenergic receptor (βAR) stimulation. Ca^{2+} enters the cell through L-type Ca^{2+} channels (and possibly reverse $\text{Na}^+:\text{Ca}^{2+}$ exchange) to trigger calcium –induced calcium release (CICR) from the SR. Ca^{2+} released from the SR then binds to troponin C to produce cell shorting. Relaxation occurs because cytosolic Ca^{2+} is lowered by uptake into the SR and also by extrusion across the sarcolemma (Diagram drawn for power point presentation)

Regulation of Ca^{2+} in normal cardiac muscle.

Normal EC coupling depolarization of the sarcolemmal membrane results in contraction of the cell. A key event in the excitation-contraction coupling process is the opening of the dihydropyridine-(DHP) sensitive L-type Ca^{2+} channels, which permit an influx of a small amount of Ca^{2+} into the cell. This Ca^{2+} entry, measured as the slow inward Ca^{2+} current, is an essential trigger for the release of Ca^{2+} from the sarcoplasmic reticulum (SR) (Bracken, *et al.*, 2003). Ca^{2+} released from the SR then binds to troponin C on the myofilaments to produce contraction of the cell. Relaxation is achieved after free $[\text{Ca}^{2+}]_i$ is lowered by a combination of reuptake into the SR and extrusion across the sarcolemmal membrane by the $\text{Na}^+:\text{Ca}^{2+}$ exchanger and the $\text{Na}^+ \text{K}^+ \text{-ATPase}$ pump (see figure 1.5).

Heart and response to stress - Cardiac Structural Remodelling

Structural and functional integrity of the heart is orchestrated by a fine balance between several neuro-hormonal and haemodynamic influences. Disruptions in this ‘fine tuning’ (e.g. in duress or injury) activate a complex, progressive process of diverse adaptive responses at transcriptional, molecular, cellular and functional levels that allow the heart to adjust to new working conditions and can be collectively termed ‘remodelling’ (Pantos et al 2007). For the intents and purposes of this work, cardiac remodelling may be broadly defined as alterations in cardiac structure resulting from altered hemodynamic load and/or cardiac injury. While remodelling may be physiological or pathological and by extension adaptive or maladaptive, in the present context the above definition excludes all aspects gestational or developmental as well as favourable remodelling that follows intensive exercise and is restricted to acquired structural rearrangement in the left myocardium (Pantos, 2007).

Cardiac remodelling is a common denominator in the aetiology of several primary cardiovascular diseases notably DM, coronary atherosclerosis, hypertension, cardiomyopathy, myocarditis (Swynghedauw, 1999). As shown in figure 1.6, HF may be viewed as a progressive disorder that is initiated in response to an index event (that may be acute i.e. MI, chronic i.e. DM or hereditary) that results in a loss/damage of functioning myocytes or alternatively produces a decline in the ability of the heart to function as a pump. Irrespective of the inciting event, several neurohormonal and inflammatory pathways are activated, including the renin–angiotensin–aldosterone system (RAAS), adrenergic system, inflammatory cytokine systems, and a host of other autocrine and paracrine mechanisms as compensatory mechanisms to maintain stroke volume at a reduced ejection fraction (Packer, 1992; Fedak *et al.*, 2005).

Thus far, a multitude of proteins, hormones, neurotransmitters and other mediators including norepinephrine, angiotensin II, endothelin, aldosterone, TGF β 1, tumor necrosis factor (TNF) have been implicated in to disease progression of the failing heart (Maytin and Colucci, 2002; Fedak *et al.*, 2005; Swynghedauw *et al.*, 2010). These processes are initially compensatory and beneficial, and in most instances, patients remain asymptomatic or minimally symptomatic following the initial decline in pumping capacity of the heart, or will develop symptoms only after the dysfunction has been present for some time (Maytin and Colucci, 2002). As such, the index event

produces remodelling of the LV frequently along one of two patterns: hypertrophy or dilation.

Myocardial hypertrophy associated remodelling results in increased LV mass without any effects on LV volume in a process termed ‘concentric remodelling’ that is associated with preserved function as the ventricle is capable of generating greater force and higher pressure. The onset of LV dilation is characterised by ‘eccentric remodelling’ and substantial increases in intra-ventricular volume with comparable increases in LV mass that represents a compensatory response to augment cardiac output in the face of diminished contractile function. Eventually, functional demands override physiological compensatory mechanisms. It follows that the hypertrophic reserve of the myocardium is met; LV dilation progresses without appreciable increases in LV mass and in accordance with the Law of Laplace induces excessive wall stresses known to be typically antecedent to overt HF (Swynghedauw, 1999) (figure 1.5). Self-sustaining neuro-hormonal and cytokine input becomes deleterious in the long term and the overexpression of the portfolio of bioactive molecules are known to contribute to disease progression independently of haemodynamic status by exerting direct cardiotoxic effects. Targeting neuro-hormonal input is therefore the basis of current HF treatment.

Altogether, the triggers that stimulate the development of HF and varied and diverse and sustained LV remodelling are associated with a poor prognosis, gradual myocardial deterioration and a critical step towards transition to decompensation. However, it is important to appreciate that cardiac remodelling is a biological adaptive processes triggered by environmental stress, and the onset of HF represents the limits of said adaptation.

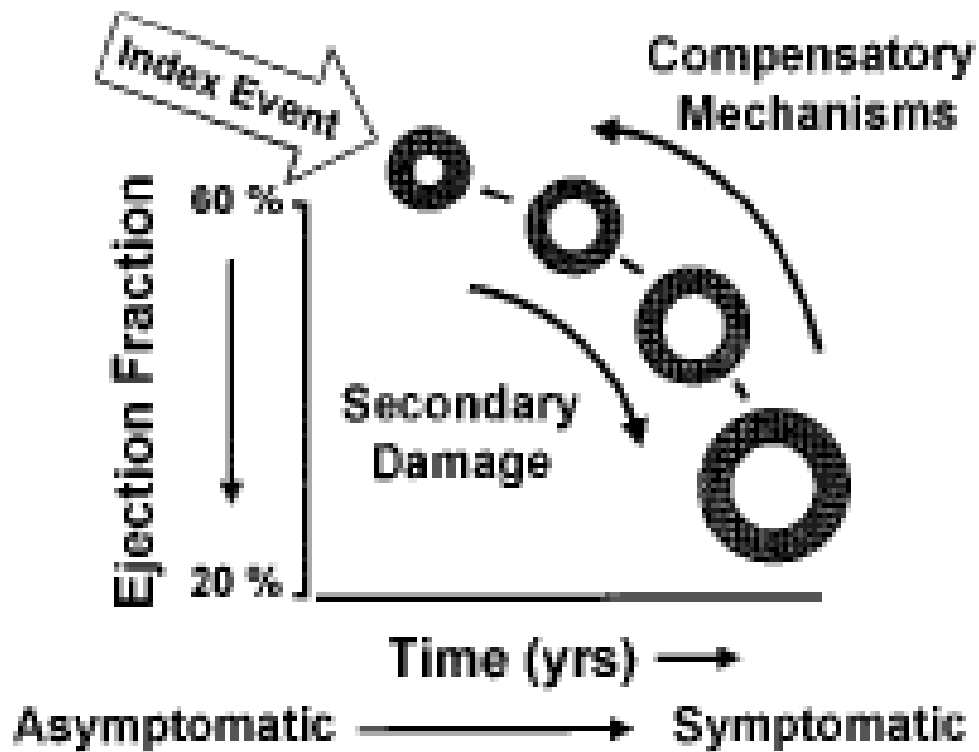


Figure 1.6: Heart failure pathogenesis. Currently accepted scheme of HF development and progression states that HF begins in response to an index event that produces an initial decline in pumping capacity of the heart following which a variety of compensatory mechanisms are activated to restore homeostatic CV function, including the adrenergic nervous system, the renin-angiotensin system and the cytokine system. Although beneficial in the short term, sustained activation of these systems can lead to worsening LV remodelling and cardiac decompensation that underscores the transition to symptomatic HF. (Image taken from Mann *et al.*, 2009)

Molecular signature of cardiac structural remodelling

Cardiac remodelling occurs in response to cues generated by mechano-sensors (Connexins, integrins) that couple cellular signalling pathways to altered or mechanical stress/ injury. Where the nature and extent of signals that are transiently activated are far from fully understood, it is accepted that the myocardial response to injury or altered mechanical load involves profound alterations in gene expression including the activation of those that are normally involved in embryogenesis, also known as the foetal gene program (Swynghedauw, 1999). In the context of MI-induced cardiac remodelling alone, genome-wide analyses have revealed significant co-ordinated

changes in over 1400 genes early and 125 genes late in the infarct zone, and nearly 600 genes early and 100 genes late in the non-infarct zone (La-Framboise *et al.*, 2005).

Fetal gene reprogramming, characteristic of pathological remodelling frequently involves an up-regulation of fetal isoforms of genes whose products regulate cardiac contractility and Ca^{2+} handling and paralleled by a down-regulation of their adult isoforms (i.e., up-regulation of β -MHC vs. down-regulation of α -MHC) and often includes decreased SERCA2a and increased NCX (sodium calcium exchanger) expression (Hilfiker-Kleiner *et al.*, 2006). Another important feature of the foetal gene phenotype markedly expressed in the remodelled myocardium is that of the natriuretic peptides, ANP and BNP, often detectable in the circulation where they are used as an indirect marker for myocardial injury/overload (Kapoun *et al.*, 2004). These transcriptional changes culminate in several molecular and cellular alterations that characterise myocardial remodelling. For the purposes of this work, they are broadly categorised into those that occur in the myocyte and changes that occur in the volume and composition of the ECM.

Within the myocyte, in addition to the functional changes described in the previous section, the remodelling process is invariably associated with sarcomeric reorganisation; Dilation of the heart is associated with myocyte re-lengthening, mediated by the generation of new sarcomeres in series and an enhancement of the length-to width ratio whereas a hypertrophic phenotype is the result parallel addition of new sarcomeres. At the molecular levels, hypertrophy appears to be characterized by increased expression of adult isoforms of sarcomeric genes (i.e., α MHC, cardiac α SKA) and is often concomitant with increased natriuretic peptide synthesis (Hilfiker-Kleiner *et al.*, 2006). Furthermore, biomechanical stretch signalling, altered redox states and pathological stimuli including HG and TGF β 1 may induce the activation of the phosphatidylinositol 3-kinase (PI3-K)/protein kinase B (Akt)-p70S6K, and/or activation of extracellular signal-regulated kinases (ERK) which co-ordinate the hypertrophic response (Selvetella *et al.*, 2004, Wu and Derynck, 2009)

Much experimental evidence suggests that the gradual loss of myocytes through necrotic and apoptotic cell death contributes to progressive and LV remodelling and cardiac dysfunction in the failing heart (Sabbah 2000; Wenker *et al.*, 2003; Foo *et al.*, 2005). Particularly in relation to apoptosis, this point of view has received increasing support with the recognition that DNA damage characteristic of apoptotic cell death

occurs in myocytes from failing hearts (Sabbah, 2000). Apoptotic events are characterised by the activation of caspase-8 and subsequently procaspase-3, an event initiated by the activation of cell surface death receptors (e.g., Fas/FasL). On activation, caspase-3 activates downstream pro-apoptotic effector proteins such as Bax and Bad and subsequently the release of cytochrome *c* (cyt *c*) and other apoptogens from mitochondria (Hilfiker-Kleiner *et al.*, 2006). Additionally, caspases may also cleave myocardial contractile proteins and promote systolic dysfunction. Therefore, treatment with caspase inhibitors after myocardial infarction has been shown to preserve myocardial contractile proteins, reduce systolic dysfunction and attenuate adverse ventricular remodelling and reduce infarct size after MI (Chandrashekar *et al.*, 2004).

Despite the undeniable intrinsic appeal of programmed cell death as a potentially important mechanism for disease progression in the failing heart, a definitive role for cell death has not been established on account of several considerations; (1). As catecholamines can provoke apoptosis, there is the possible over-stimulation of myocyte apoptosis frequency assessed in explanted hearts obtained from patients awaiting cardiac transplantation, many of whom receive inotropic support (Narula *et al.*, 1996; Olivetti *et al.*, 1997). (2). Data concerning myocyte cell death in mild to moderate HF is not forthcoming, casting doubt over whether apoptosis contributes to failure or whether it is a phenomenon that is observed only in end-stage HF. (3) Lastly there is considerable disparity in the published literature over estimates of apoptotic processes, ranging from 0.003%/year to clinically unrealistic estimates of '5% to 35% (estimated myocyte loss > 100%/year) (Mann, 1999). Thus, it is difficult to definitively ascertain whether myocyte cell loss is an important contributor to HF pathogenesis, occurs early and continually in HF or, instead, only in end-stage hearts.

Outside changes in the myocyte, structural remodelling in the myocardium is associated with alterations in the structure and function of the ECM. Indeed, ECM deposition is a widely recognized alteration in the failing heart and the notion that progressive fibrosis underlies LV dilatation and HF progression has been engendered by several experimental and clinical studies (Cohn, 1995; Mann, 1999; Maytin and Colucci, 2002; Fedak *et al.*, 2005, Miner and Miller, 2006; Bowers *et al.*, 2010). In pathological conditions, the ECM can be temporarily remodelled, reversibly remodelled or fully

adapt to the changes in biomechanical load. However, prolonged overload results in detrimental collagen deposition that can render the heart electrically and structurally heterogenous, result in excessive diastolic stiffness (Van Heerebeek, 2008) and/or induce LV dilatation altogether resulting in overt HF. Particular emphasis is given to the collagenolytic MMPs and their inhibitors, the TIMPs in underlying LV dilatation. The balance of proteolytic and anti-proteolytic activity appears to be an important determinant of the rate of ventricular enlargement. The general view is that disruption of this balance results in progressive MMP activation leading to degradation of the ECM, myocyte slippage, thinning of the ventricular wall, and ventricular dilation that occurs in end stage HF (Swynghedauw, 1999; Maytin and Colucci, 2006; Yan *et al.*, 2009).

In support of this premise, pharmacologic MMP inhibition in a pacing-induced animal model of heart failure improved LV dimensions and performance when administered early in the remodelling process (Spinale *et al.*, 1999). Chronic pharmacologic inhibition of MMP activity in rats with HF of hypertensive origin resulted in an attenuation of ventricular dilation and dysfunction that was sustained throughout the 4 months of therapy (Peterson *et al.*, 1999). Similarly, targeted deletion of MMPs has been shown to limit maladaptive remodelling in experimental models (Yan *et al.*, 2000) altogether indicating the potential therapeutic relevance of MMP inhibition which may be exploited in the near future. Studies employing transgenic mice clearly show the role of MMPs and TIMPs in mediating the preservation of normal cardiac geometry and function, and are consistent with less deleterious cardiac remodelling in animal models treated with pharmacological MMP inhibitors (Graham and Trafford, 2007).

KINASE SIGNALLING AND CARDIAC REMODELING

Structure and function of MAPKs

There are four classic MAPK subfamilies (see figure 1.7). Each of these family members has been studied extensively in a multitude of cellular settings and has been reviewed in great detail by others (Barr and Bogoyevitch, 2001; diwan and Dorn, 2007; Kyriakis and Avruch, 2001; Pearson *et al.*, 2001; Pentassuglia and Sawyer, 2009; Ramos, 2008; Roux and Blenis, 2004).

A. ERK1/2

First discovered in the early 1980s for its ability to phosphorylate microtubule-associated protein-2 (MAP-2) in 3T3-L1 adipocytes in response to insulin stimulation (Avruch, 2007), extracellular signal-regulated kinases (ERKs) are now one of the most widely studied signalling pathways in cellular biology. ERK1 and ERK2 are 83% identical, share most of the same signalling activities, and, as a result, are usually referred to simply as ERK1/2. However, these two proteins are not completely functionally redundant as demonstrated by gene knockout experiments. ERK1 null mice have, in general, a normal phenotype (Gerits *et al*, 2007; Pages *et al*, 1999), but ERK2 null mice are embryonic lethal between E6.5 and E8.5 (Gerits *et al*, 2007; Hatano *et al*, 2003; Saga-EI-Leill *et al*, 2003; Yao *et al*, 2003). ERK1/2 is ubiquitously expressed and has many diverse cellular and physiological functions. At the cellular level, ERK1/2 regulates cell cycle progression, proliferation, cytokinesis, transcription, differentiation, senescence, cell death, migration, GAP junction formation, actin and microtubule networks, and cell adhesion (Ramos, 2008). ERK1/2's role in cellular biology translates it into a prominent player in physiological settings, influencing the immune system and heart development and contributing to the response of many hormones, growth factors, and insulin. Furthermore, because of its role in so many biological processes, ERK1/2 has likewise been shown to play a significant part in various pathologies including cancer, diabetes, and cardiovascular disease. This extensive and diverse functional ability is the result of ERK1/2's ability to phosphorylate over 100 possible substrates (Yoon and Seger, 2006).

ERK1/2 is activated via a canonical three-tiered kinase cascade by both extracellular and intracellular stimuli). Growth factors, serum, and phorbol esters strongly activate the pathway, but it can also be activated by G protein-coupled receptors, cytokines, microtubule disorganization, and other stimuli. Prototypically, growth factor (such as fibroblast growth factor, FGF) binding to their respective receptor tyrosine kinase (RTK) activates Ras which recruits and activates Raf (MAP3K) at the plasma membrane. Once activated, Raf phosphorylates and activates MEK1/2 (MAP2K). MEK1/2 in turn activates ERK1/2 by phosphorylation of the Thr and Tyr residues in the conserved Thr-Glu-Tyr motif within its regulatory loop. Activated ERK1/2 can

phosphorylate downstream proteins in the cytoplasm or nucleus, including many transcription factors.

MAPK signalling is subject to many mechanisms of modulation that determine the specificity and magnitude of the signalling outcome. Interactions with scaffold proteins are one of these mechanisms. ERK has a number of known scaffold proteins including kinase suppressor of Ras (KSR), MEK partner 1 (MP1), MAPK organizer 1 (MORG1), and β -arrestin (Dhanasekaran et al, 2007). Structural studies also reveal specific docking site motifs that help direct the specificity of ERK1/2 signalling, including the ERK docking (ED) motif, the docking site for ERK and FXFG (DEF) motif, and the common docking (CD) motif (Raman *et al*, 2007). Protein phosphatases are a third mechanism that contributes to MAPK regulation. ERK signalling has been shown to be regulated by various phosphatases including dual-specificity MAPK phosphatases (MKP1, -2, -3, and -4), protein serine/threonine phosphatases (PP2A, PPM1 α), and protein tyrosine phosphatases (SHP-2 PTP, hematopoietic PTP, STEP, PTP- ϵ) (Juntilla *et al*, 2008). The final way that MAPK activity is regulated is by positive and negative feedback regulation from other components of the MAPK signalling network. This includes negative regulation of ERK by other MAPKs such as JNK and p38 (Juntilla *et al*, 2008).

B. JNK

In the early 1990s, 10 years after the discovery of ERK, JNK was discovered as a second subfamily of MAPKs for its ability to phosphorylate microtubule-associated protein 2 in rat liver following cycloheximide injection. It was further detailed for its ability to phosphorylate the transcription factor c-jun at two sites following UV radiation (Hibi et al, 1993; Kyriakis and Avruch, 1990; Kyriakis *et al*, 1991). JNK1, JNK2, and JNK3 are encoded by three separate genes, and alternative splicing can produce 10 different protein sequences that share >80% homology (Barr and Bogoyevitch, 2001). JNK1 and JNK2 are ubiquitously expressed, while JNK3 is predominantly found in the brain, heart, and testis (Davis, 2000). While there is some redundancy in the functions of the three isoforms, gene knockout studies have shown specific roles for different JNK isoforms in vivo (Bogoyevitch, 2006; Gerits *et al*, 2007). Like ERK, JNK plays a role in a number of different biological processes

including cell proliferation, differentiation, apoptosis, cell survival, actin reorganization, cell mobility, metabolism, and cytokine production (Bogoyevitsch and Kobe, 2006; Davis, 2000; Raman *et al*, 2007). This translates into JNK's physiological role in insulin signalling, the immune response and inflammation, and its pathological role in neurological disorders, arthritis, obesity, diabetes, atherosclerosis, cardiac disease, liver disease, and cancer (Bogoyevitsch, 2006).

Activation of the JNK pathway occurs in response to a number of different stimuli. As a stress-activated protein kinase, JNK responds most robustly to inflammatory cytokines and cellular stresses such as heat shock, hyperosmolarity, ischemia-reperfusion, UV radiation, oxidant stress, DNA damage, and ER stress (Bogoyevitsch, 2006; Raman *et al*, 2007). However, they are also activated to a lesser extent by growth factors, G protein-coupled receptors, and noncanonical Wnt pathway signalling (Pandur *et al*, 2002). Once stimulated, JNK is activated by the previously described three-tiered kinase cascade. After the cell is stimulated, signaling occurs which eventually leads to the activation of the first tier. The MAP3Ks that can activate JNKs are MEKK1, MEKK2, and MEKK3, as well as mixed lineage kinase 2 and 3 (MLK2 and MLK3) and others (Raman *et al*, 2007). These kinases then activate the MAP2Ks involved in the JNK cascade, MKK4 and MKK7. MKK4/7 then activates JNK by phosphorylation on a conserved Thr-Pro-Tyr motif. It has been shown that MKK4 has a preference for Tyr phosphorylation while MKK7 has a preference for Thr in the TPY motif, allowing these two kinases to work synergistically in JNK activation (Lawler *et al*, 1998). Activated JNK has a large number of downstream substrates, including nuclear and cytoplasmic proteins. Similar to the other MAPKs, JNK has the ability to shuttle between the cytoplasm and the nucleus to exert its effects depending on the specific cellular stimuli. The diversity of JNK signalling can be conferred by signalling via more than 25 nuclear substrates and more than 25 nonnuclear substrates for any specific stimulus (Bogoyevitsch and Kobe, 2006).

JNKs, like all MAPKs, utilize the same mechanisms to impart specificity and degree of magnitude to its signalling. Interaction with scaffold proteins such as JNK-interacting proteins (JIP1, JIP2), JNK/stress-activated protein kinase-associated protein 1 (JSAP1/JIP3), JNK-associated leucine-zipper protein (JLP), and plenty of SH3 (POSH) help direct the specificity of this pathway (Dhanasekaran *et al*, 2007). The specificity of

JNK's interaction with these scaffold proteins and its up and downstream partners is also mediated, in part, through specific docking sites, including D motifs, MAPK-docking sites, and others (Raman *et al*, 2007). Like all protein kinases, JNK activity is also counterregulated by phosphatases including dual specific phosphatases MKP1, -2, -5, and -7.

C. p38

p38 was originally isolated as a tyrosine phosphorylated protein found in LPS-stimulated macrophages (Han *et al*, 1994; Han *et al*, 1993). At the same time, it was also reported as a molecule that binds pyridinyl imidazoles which inhibit the production of proinflammatory cytokines (Lee *et al*, 1994). Since then, four different p38 isoforms have been identified, including the prototypic p38 α (often referred to as simply p38), p38 β (Jiang *et al*, 1996), p38 γ (Li *et al*, 1996), and p38 δ (Lechner *et al*, 1996). p38 and p38 β are ubiquitously expressed, while p38 γ is expressed primarily in skeletal muscle and p38 δ is found in lung, kidney, testis, pancreas, and small intestine (Ono and Han, 2000). The four isoforms share structural similarities (>60% homology within the group and even higher in their kinase domains) and substrate similarities as well. However, it is unclear *in vivo* if activity towards a given substrate can vary between isoforms and if each isoform also has its own set of specific substrates. This is demonstrated by gene knockout experiments in which deletion of the p38 α gene leads to embryonic lethality due to placental and erythroid differentiation defects (Mudgett *et al*, 2000; Tamura *et al*, 2000), but mice carrying deletion of any of the other three isoforms are phenotypically normal (Gerits *et al*, 2007). Like other MAPK subfamilies, p38 kinases also play numerous biological roles. Most prominently, p38 signalling is involved in the immune response, promoting expression of proinflammatory cytokines [interleukin (IL)-1 β , tumor necrosis factor (TNF)- α , and IL-6], cell adhesion molecules (VCAM-1), and other inflammatory related molecules and regulating the proliferation, differentiation, and function of immune cells (Kyriakis and Avruch, 2001; Rincón and Davis, 2009). p38 also plays a role in many other biological functions, namely, apoptosis, cell survival, cell cycle regulation, differentiation, senescence, and cell growth and migration (Thornton and Rincón, 2008; Zarubin and Han, 2005). Physiologically, this translates into a role for p38 in chronic inflammatory diseases (rheumatoid arthritis,

Crohn's disease, psoriasis, and chronic asthma), tumorigenesis, cardiovascular disease, and Alzheimer's disease (Cuenda and Rousseau, 2007).

As a stress-activated kinase, p38 responds to most of the same stimuli as JNK as well as others that are specific to p38. p38 can be activated by such stimuli as UV radiation, heat, osmotic shock, pathogens, inflammatory cytokines, growth factors, and others. Making this pathway complicated, p38 can respond to over 60 different extracellular stimuli in a cell-specific manner, making it challenging to elucidate its exact functional role in vivo (Ono and Han, 2000). Regardless of the exact stimuli, the canonical pathway of p38 activation is the same as for ERK and JNK. A number of upstream kinases are implicated in the phosphorylation cascades leading to the activation of p38, including MEKK1–4, TAK1, and ASK1 at the MAP3K level and MKK3, -6, and, possibly, -4 at the MAP2K level. These MAP2Ks activate p38 by phosphorylation of its conserved Thr-Gly-Tyr motif. Of interesting note, p38 can be activated in noncanonical ways as well. One way is TAB-1-mediated autophosphorylation (Geet *et al*, 2002; Tanno *et al*, 2003), and another is T-cell receptor-induced activation of p38 through ZAP70 (Salvador *et al*, 2005). Once activated, p38 can function in the cytoplasm or translocate to the nucleus. Substrates for p38 include transcription factors, other nuclear proteins, and cytoplasmic proteins (Ono and Han, 2000).

The magnitude of the signal and the specificity of the p38 pathway are determined by similar mechanisms as both ERK and JNK. While scaffold proteins have been shown to be important in p38 signalling, there have only been three such proteins identified so far: osmosensing scaffold for MEKK1 (OSM), JIP2, and JLP (Dhanasekaran *et al*, 2007). p38 also utilizes specific domains, such as CD motifs, ED motifs, and D motifs to facilitate its interaction with other proteins (Raman *et al*, 2008). Finally, protein phosphatases are yet another form of p38 regulation, including dual specific MKPs (MKP1, -2, -5, -7) and protein Ser/Thr phosphatases (PP2C) (Juntilla *et al*, 2008).

D. ERK5

ERK5 is the final classic MAPK subfamily and the least studied among the four. Discovered in the mid 1990s by two groups simultaneously, many questions remain to be answered, although progress is rapidly being made on many fronts. The first group

identified ERK5 using a yeast two-hybrid screen with the upstream activator MEK5 as the bait (Bao *et al*, 1995), while the second group used a degenerate PCR strategy to clone novel MAPKs (Lee *et al*, 1995). The most distinguishing feature of this MAPK is its size, 816 amino acids, making it more than twice the size of the other MAPK family members (thus the alternative name big MAPK or BMK). This increased size is due to a large 396-amino acid COOH-terminal extension. While only one ERK5 gene has been identified, it undergoes alternative splicing to produce four different protein species: ERK5a, ERK5b, ERK5c, and ERK-T. ERK5a is the most prominently expressed, and the other three appear to function as negative regulators of ERK5a (McCaw *et al*, 2005; Yan *et al*, 2001). This kinase is ubiquitously expressed, and gene knockout studies show global deletion of ERK5 is embryonic lethal due to what was initially thought to be cardiac defects (Regan *et al*, 2002). However, cardiomyocyte specific inactivation of ERK5 results in normal development, indicating that the lethality from the global knockout is due to defects in vascular formation (Hayashi *et al*, 2004; Hayashi and Lee, 2004). Diverse biological roles of ERK5 are also identified, including cell survival, differentiation, proliferation, and growth. ERK5 is reported to play a physiological role in neuronal survival, endothelial cell response to sheer stress, prostate and breast cancer, cardiac hypertrophy, and atherosclerosis (Hayashi and Lee, 2004; Nishimoto and Nishida, 2006; Wang and Tournier, 2006).

ERK5 is activated in response to both growth and stress stimuli. This includes a wide variety of growth factors [epidermal growth factor, nerve growth factor, vascular endothelial growth factor (VEGF), FGF-2], serum, phorbol ester, hyperosmosis, oxidative stress, laminar flow sheer stress, and UV radiation (Hayashi and Lee, 2004). Once activated, ERK5 exerts its kinase activity on a number of other protein kinases and transcription factors in both the cytosol and the nucleus. Furthermore, unlike other MAPKs, ERK5 has been shown to function directly as a transcriptional activator (Akaike *et al*, 2004; Kasler *et al*, 2000).

ERK5 signalling, in true MAPK fashion, is influenced by such things as scaffold proteins, docking sites, phosphatases, and other members of the MAPK family. However, because ERK5 is less well studied than the other MAPKs previously discussed, less is known about these forms of regulation. Adaptor and scaffold proteins such as Lck-associated adaptor (Lad) and Grb-2-associated binder 1 (Gab 1) as well as

muscle specific A-kinase anchoring protein (mAKAP) have all been shown to play an integral role in ERK5 signalling (Wang and Tournier, 2006). Furthermore, MEK5 (the MAP2K of ERK5) uses its Phox/Bem 1P (PB1) domain to bind and tether together the upstream MAP3K (MEKK2/3) and the downstream ERK5 to facilitate signalling (Nakamura *et al*, 2006; Nakamura and Johnson, 2003). While regulation of ERK5 activity has been shown to be regulated by specific protein phosphatases, such as MKP1 and -3 (Kamakura *et al*, 1999) and the phosphotyrosine specific phosphatases PTP-SL (Buschbeck *et al*, 2002), much less is known about this type of regulation than is with the other MAPKs.

MITOGEN-ACTIVATED PROTEIN KINASES IN HEART FUNCTION AND DISEASE

The following sections focus on the role of MAPKs in various pathological aspects of cardiac diseases, with particular emphasis on hypertrophy, cardiac remodelling, and myocardial cell death.

Cardiac hypertrophy is a common response to external stressors, including mechanical overload, neurohormonal stimulation, and oxidative stress. Hypertrophy can be a compensatory response to augment contractility and maintain cardiac output without adverse pathology. However, when stressors persist, this compensatory process can evolve into a decompensated state with profound changes in gene expression profile, contractile dysfunction, and extracellular remodelling (Diwan and Dorn, 2007; Selvetella *et al*, 2004). Although physiological versus pathological hypertrophy can be clearly differentiated by a number of qualitative and quantitative parameters, the underlying mechanisms and their interrelationship remain controversial. Most importantly, the signalling mechanisms mediating the critical transition from compensated hypertrophy to decompensated heart failure remain poorly understood (Dorn and Force, 2005; Frey and Olson, 2003; Selvetella *et al*, 2004). Furthermore, while some cardiomyopathies are genetic and others idiopathic, many are the result of some sort of insult or injury to the myocardium. Myocardial ischemia and/or infarction due to partial or complete occlusion of a coronary artery and the subsequent reperfusion of the tissue (ischemia-reperfusion or IR) are among the most significant causes of

injury to the heart. Most of the efforts in the past have focused on the underlying mechanisms of IR-induced myocardial injury or on cardiac protection offered by preconditioning or postconditioning (Balakumar *et al*, 2008). The signalling mechanisms involved in these events (injury versus cardiac protection) are distinctly different. However, recent work has shown that protective events are diminished in various pathological conditions commonly associated with cardiovascular disease (hyperglycemia, hypertension, cardiac hypertrophy, aging, obesity), pointing to the importance of understanding the signalling pathways involved (Balakumar *et al*, 2009). Finally, pathological manifestations in end-stage failing hearts share many common features regardless of the underlying etiologies, such as ventricular wall thinning, chamber dilation, cardiomyocyte dropout, and dramatically increased interstitial fibrosis (Dorne and Force, 2005), suggesting that intracellular signalling pathways elicited by different stressors may converge to some common targets. As highly conserved signalling pathways, MAPKs may be common mediators in these pathological remodelling processes. Normal cardiac function and pathological remodelling involve fibroblasts, the coronary vascular system, and inflammatory cells. Although much of the recent progresses are made through advanced wizardry of genetic manipulation in model organisms such as mice, it is important to appreciate some of the limitations of this powerful approach. Genetic manipulation through complete knockout and nonphysiological overexpression can produce a phenotype that may not truly reflect the functional role of the targeted molecule or pathway in a particular pathological condition. Compensatory, secondary, or off-target effects can arise from such non-physiological manipulation to obscure correct interpretations. In addition, some of the genetic manipulation itself can lead to unwanted side effects, including cytotoxicity of GFP, Cre, and tamoxifen induction (Buerger *et al*, 2006; Huang *et al*, 2000; Koitabashi *et al*, 2009). Therefore, results from genetic studies should be interpreted with plenty of caution by taking into account some of these caveats.

A. ERK1/2

1. Cardiac hypertrophy

Many studies have implied a role for the Ras/Raf/MEK1/ERK signalling pathway in promoting cardiac hypertrophy. Hunter *et al*. (1995) initially showed that transgenic

expression of a constitutively active Ras (H-Ras-V12) in mouse heart led to left ventricular hypertrophy associated with cardiomyocyte hypertrophy but not increased cardiac fibrosis. Subsequently, Zheng *et al.* (2004) observed characteristic features of familial hypertrophic cardiomyopathy (HCM) in another H-Ras-V12 transgenic model, including fetal-gene induction, myofilament disarray, and interstitial fibrosis which led to diastolic dysfunction (Zheng *et al.*, 2004). While both of these studies used the same constitutively activated H-Ras-V12 mutant, different promoters were used to drive its expression (MLC-2v versus α -MHC, respectively), possibly reflecting dose-dependent effects of Ras signalling driving hypertrophy versus cardiomyopathy. Gene expression profiling in temporally regulated α MHC-H-Ras-V12 transgenic mice suggests that overactivation of this pathway induces early response genes, loss of mitochondria function, and alteration in ion channel proteins, all of which lead to pathological changes in the extracellular matrix, reduced cardiac output, and electrophysiological abnormalities (Mitchell *et al.*, 2006). Ras mRNA expression in HCM patients identified a positive correlation with the severity of hypertrophy (Kai *et al.*, 1998). Likewise, patients suffering from so-called RAS/MAPK syndromes, a group of autosomal dominant disorders linked to mutations causing augmented Ras/Raf/MEK/ERK activity (e.g., Noonan and LEOPARD syndromes), exhibit hypertrophic cardiomyopathy (Aokiet *et al.*, 2008). Finally, in response to mechanical unloading afforded by use of a left ventricular assist device (LVAD), reverse remodelling and reduction in myocyte hypertrophy in the post-LVAD heart is associated with decreased ERK activity (Flesch *et al.*, 2001). Conversely, an endogenous inhibitor of the ERK pathway, Sprouty-1, has been reported to be induced in human hearts during hypertrophy regression following LVAD support (Huebert *et al.*, 2004). Overexpression of MEK 1, the upstream activator of ERK1/2, has shown similar overactivation of Ras. Constitutively active MEK1 leads to cardiomyocyte hypertrophy *in vitro*, while dominant negative MEK1 attenuates this response (Ueyama *et al.*, 2000). *In vivo*, cardiac-specific expression of constitutively activated MEK1 also promotes hypertrophy (Bueno *et al.*, 2000). However, unlike Ras overactivation, the MEK1 transgenic heart has no increase in fibrosis and displays preserved cardiac function, suggesting MEK-ERK may not be the critical downstream signalling pathway for Ras-induced pathological remodelling.

Complimentary to these gain-of-function approaches, Harris *et al.* (2004) have demonstrated that inhibition of the ERK pathway via dominant negative Raf attenuated

hypertrophy and fetal gene induction in response to pressure overload. Likewise, Yamaguchi et al. (2004) have shown that cardiac specific deletion of c-raf-1 leads to heart failure without hypertrophy in the absence of external stress. Both groups found that, while there was an apparent lack of hypertrophy, there was a significant increase in apoptosis associated with Raf inactivation. This is consistent with the observation that overactivation of the ERK pathway causes both hypertrophy and a partial resistance to apoptosis (Bueno *et al*, 2000). However, the antiapoptotic activity of Raf appears to be primarily due to Raf binding to and directly suppressing the proapoptotic kinases Ask1 and Mst2 independent of MEK/ERK activities (Chen and Sytkowski, 2005; Chen *et al*, 2001; Yamaguchi *et al*, 2004). Similar results were also obtained when the protein tyrosine phosphatase Shp2 was deleted from the myocardium. Shp2 is an essential component of RTK signalling through the Ras/Raf/MEK/ERK pathway, and a gain-of-function mutation in this protein causes craniofacial and cardiovascular defects in Noonan syndrome. Deletion of Shp2 in the myocardium leads to dilated cardiomyopathy without transition through hypertrophy at baseline or following pressure overload associated with diminished ERK activation (Kontaridis *et al*, 2008). These findings, specifically the onset of dilated cardiomyopathy without transitioning through hypertrophy, are similar to what was observed in the c-raf-1 knockout animals. Furthermore, GSK3 α has been shown to block cardiac hypertrophy both in vitro and in vivo via inhibition of ERK signalling (Zhai *et al*, 2007). While all of these findings strongly suggest that ERK contributes to hypertrophy in the myocardium, one study by Purcell et al. (2007) suggests that reduction in ERK activity is not sufficient to prevent hypertrophy in response to various forms of hypertrophic stimuli in vivo. Achieved by either overexpression of dual specific phosphatase 6 or deletion of ERK (*ERK1*^{-/-} or *ERK2*^{+/-}), these modifications led to an increase in apoptosis without a significant impact on hypertrophy. These results suggest that ERK activity is an important pathway for cardioprotection but that cardiac hypertrophy can proceed via ERK-independent mechanisms.

In addition to growth factor-mediated signalling through RTKs (Clerk et al, 2006), signalling via G protein-coupled receptors (GPCRs) has also been shown to promote cardiac hypertrophy (Salazar et al, 2007), and in a number of settings, this has been shown to be mediated via ERK signalling. β -adrenergic agonists promote cardiomyocyte hypertrophy via direct interaction between ERK and β -arrestin (Barki-

Harrington *et al*, 2004; Salazar *et al*, 2007). Interestingly, signalling from β -adrenergic receptors, which can lead to detrimental effects in the failing heart, utilize β -arrestin to transactivate RTK signalling via ERK (Noma *et al*, 2007). This β -arrestin-dependent, G protein-independent signalling by those receptors is thought to be cardioprotective. This is exemplified by the recent discovery that carvedilol, a nonsubtype-selective β -adrenergic receptor antagonist that has been shown to be particularly effective in treatment of heart failure, promotes signalling via β -arrestin-dependent ERK1/2 activation in the absence of G protein activation (Wisler *et al*, 2007). Likewise, other GPCRs, including α -adrenergic receptors (Kuster *et al*, 2005; Xiao *et al*, 2001; Xiao *et al*, 2002), angiotensin receptors (Aoki *et al*, 2000; Yang *et al*, 2007), and endothelin receptors (Chen *et al*, 2005; Cullingford *et al*, 2008; Kennedy *et al*, 2006; Lu *et al*, 2009; Yue *et al*, 2000), have been shown to signal through ERK to promote cardiomyocyte hypertrophy. In addition to arrestin-mediated ERK activation, Wright *et al*. (2008) provided other evidence that nuclear targeted α -adrenergic receptor might activate ERK located in caveolae, although the underlying molecular basis remains unclear. More recently, Lorenz *et al*. (2009) have identified heterotrimeric G protein-mediated autophosphorylation of ERK as yet another hypertrophic signaling mechanism leading to ERK activation. In these studies, activation of G_q -coupled receptors was sufficient to mediate a protein-protein interaction between $G\beta\gamma$ and ERK, leading to autophosphorylation and translocation to the nucleus and activation of prohypertrophic substrates. This novel autophosphorylation-mediated ERK activation was sufficient to induce hypertrophy both in vitro and in vivo and was also shown to be present in failing human hearts. Finally, a recent report by Cervante *et al*. (2010) suggest that cross-talk of GPCRs can be orchestrated by arrestin to achieve spatiotemporal activation of ERKs in nucleus versus cytoplasm, leading to different functional outcome. In addition to ligand-mediated mechanisms, Ras activation can be facilitated by direct oxidative modification of its thiol groups (Kuster *et al*, 2005; Yamamoto *et al*, 2003), thus providing another possible molecular link between oxidative stress and the onset of cardiac hypertrophy. In short, Ras-Raf-MEK1-ERK1/2 pathway is generally regarded as a prohypertrophic and prosurvival pathway that can be a significant but not a necessary signaling component in cardiomyocyte hypertrophy.

2. Cardioprotection versus myocardial cell death

The cardioprotective effects of two classes of drugs commonly used to treat cardiac related diseases, Ca²⁺ channel blockers and β -adrenergic receptor blockers, have been reported to be mediated in part through ERK1/2 activity (Kovacs *et al*, 2009). In vivo studies in which c-Raf-1 activity in the heart was lost showed an increase in apoptosis both at baseline and in response to pressure overload (Harris *et al*, 2004; Yamaguchi *et al*, 2004). Similarly, the Molkenin group has identified specific MEK-ERK2 signalling as a mediator of cardioprotection (Lips *et al*, 2004). In response to ischemia-reperfusion injury, MEK transgenic hearts were better protected from injury and apoptosis than wild-type controls, an effect that was lost when ERK2 was specifically deleted. Indeed, ERK1/2 signalling has been identified as one of the major components of the RISK (reperfusion injury salvage kinase) pathway. A plethora of studies have subsequently shown that activation of the ERK pathway by various stimuli leads to cardioprotection during reperfusion (reviewed in Ref. Hausenloy and Yellon, 2007). While the role of ERK signaling in preventing reperfusion-induced injury is well established, its role in preconditioning is less well understood, and conflicting results have been reported (Downey *et al*, 2007; Hausenloy *et al*, 2005). ERK's cardioprotective role has also been investigated in relation to the chemotherapeutic agent doxorubicin (DOX). DOX is known to induce myocardial damage, including cardiomyopathy and myocyte apoptosis (Takemura and Fujiwara, 2007). While the mechanism of DOX-induced cardiac damage is multifaceted, downregulation of ERK1/2 activity has been suggested to play a role. Indeed, DOX-induced cardiotoxicity was prevented by the administration of substrates that increased ERK1/2 activity (Suet *et al*, 2006; Xiang *et al*, 2009). Conversely, recent work done in cultured myocytes has suggested a functional link between ERK1/2 and p53 actually promotes apoptosis in response to DOX (Liu *et al*, 2008).

While much work has been done identifying upstream activators of cardioprotective ERK1/2 signaling, much less is known regarding the exact mechanism by which it imparts this protection. Multiple mechanisms may exist for prosurvival effects of ERK1/2. Work by Das *et al*. (2007) has shown that the protective effect of ANG II-mediated preconditioning is due in part to ERK1/2 dissociating from caveolin. Similarly, ERK1/2 has been shown to play a role in cGMP-dependent protein kinase (PKG)-mediated cardioprotection in response to IR (Das *et al*, 2009; Das *et al*, 2008). ERK1/2 activation in this case resulted in increase expression of inducible nitric oxide

synthase (iNOS), endothelial NOS (eNOS), and Bcl-2. ERK1/2 has also proposed to exert its cardioprotective effects by phosphorylating and activating the transcription factor GATA4, which can then increase the expression of antiapoptotic proteins in neonatal ventricular myocytes (Arier *et al*, 2004; Kobayashi *et al*, 2006; Liang *et al*, 2001; Morimoto *et al*, 2000). However, recent work has shown that this does not hold true in adult cells. While GATA4 still promotes survival, it was found not to be downstream of ERK1/2 signalling in response to α_1 -adrenergic receptors, a previously described survival pathway in cardiomyocytes (Huang *et al*, 2008, Huang *et al*, 2007). ERK1/2 may also promote survival of cardiomyocytes by interacting with other signalling pathways. IL-10 mediated ERK1/2 activation was shown to inhibit TNF- α -induced apoptotic signalling by blocking IKK phosphorylation and subsequent NF κ B activation (Dhingra *et al*, 2009). Likewise, ERK1/2 has also been shown to compensate for loss of Akt activity in postinfarct myocardium and promote cardioprotection in response to erythropoietin (Miki *et al*, 2007). Finally, ERK1/2 has been found to suppress gap junction permeability in response to mitoK_{ATP} channel opening during IR, thus reducing myocardial damage (Naitoh *et al*, 2006). As noted above, the ERK-independent cardioprotective activity of Raf is mediated through direct suppression of proapoptotic kinases, Ask1 and Mst2 (Chen and Sytkowski, 2005; Chen *et al*, 2001; Yamaguchi *et al*, 2004). In short, Ras-Raf-MEK-ERK1/2 may exert strong cardioprotective effects via multiple downstream targets, but much remains to be done to delineate their specific contribution under particular circumstances.

3. Cardiac remodeling

As discussed above, unregulated Ras-Raf-MEK-ERK signalling can lead to both hypertrophy and pathological remodelling in heart. Gene expression profiling in temporally regulated α -MHC-H-Ras-v12 transgenic mice suggests that overactivation of this pathway induces early response genes, loss of mitochondrial function, and alteration in ion channel proteins, all of which can contribute to extracellular matrix remodelling, reduced cardiac output, and electrophysiological abnormalities observed in HCM (Mitchell *et al*, 2006). In addition, Ras activation can have a direct impact on SR calcium cycling in ventricular myocytes both in vitro and in vivo. In vitro expression of Ha-Ras-V12 in cultured myocytes leads to downregulation of L-type Ca²⁺ channel

expression and activity in an ERK-dependent manner (Ho *et al*, 2001). Furthermore, activation of Ras leads to decreased expression of SERCA in cultured myocytes (Ho *et al*, 1998). In vivo studies, while finding no change in L-type Ca^{2+} channels or sarcomeric structure, showed decreased Ca^{2+} transients secondary to suppressed SR Ca^{2+} uptake as a result of decreased SERCA expression and hypophosphorylation of phospholamban (Zheng *et al*, 2004). More recently, Ruan *et al.* (2007) reported that $\text{G}_i\alpha 1$ induction and subsequent impairment of PKA signaling appears to be one of the key downstream mediators in Ras-induced SR calcium defects and arrhythmia. Yada *et al.* (2007) also reported a role for another Ras-like small GTPase, Rad, in modulating calcium homeostasis and electrophysiological properties in ventricular myocytes. Therefore, unregulated Ras signalling may have a direct impact on cardiac function and electrophysiology, but downstream signalling appears to be different from the canonical MEK-ERK cascade. The molecular basis is just beginning to emerge. LIF, a hypertrophic stimulus in cardiomyocytes, leads to increased L-type Ca^{2+} transients in an ERK-dependent manner (Hagiwara *et al*, 2007; Takahashi *et al*, 2004). These findings imply that the specific outcomes of ERK activation may be dependent on the activating stimulus, again demonstrating the complexity of these signalling networks. In addition to playing a role in Ca^{2+} channel regulation, ERK signalling also plays a role in regulation of other ion channels including potassium channels and the Na^+/H^+ exchanger in the myocardium (Fliegel, 2008; Fliegel, 2009; Teos *et al*, 2008; Walsch *et al*, 2001). In short, the Ras-Raf-MEK-ERK pathway can induce SR calcium defects and arrhythmias in the heart by modulating ion channels, exchangers, and pumps and serves as a potential contributor to the contractile defects and sudden cardiac arrest prevalent in hypertrophic cardiomyopathy.

In summary, both classic RTK-mediated and GPCR-mediated ERK activation have significant roles in cardiac hypertrophy and cardioprotection. However, the functional outcome of ERK activation can be modulated and altered by scaffolds in a specific spatiotemporal pattern. This complexity in ERK pathway leads to different phenotypes from “physiological” form of compensated hypertrophy and cardioprotection to pathological form of hypertrophic cardiomyopathy and remodelling. Therefore, the intricate ERK activation mechanisms must be carefully considered when we attempt to target ERK pathway as a potential therapy for heart failure.

B. JNK

1. Cardiac hypertrophy

The role that JNK plays in cardiac hypertrophy is less clear. JNK activity is substantially upregulated (as quickly as 10–15 min after application of pressure overload) and reaches a maximal level at ~30 min (Fischer *et al*, 2001; Nadruz *et al*, 2004). While JNK2 is activated in the cytosol, there is a significant increase in translocation of activated JNK1 to the nucleus (Nadruz *et al*, 2004). The transient activation of JNK is clearly seen in severe pressure overload (85% constriction of the aorta) but not volume-overloaded hearts. In pressure overload, activation peaks between 10 and 30 min (Sopontammaraket *et al*, 2005). In contrast, mild pressure overload (35% constriction of the aorta) exhibits a transient increase in JNK activity at 30 min, but higher levels are seen at 1 and 2 days post-constriction. In contrast, another recent study in rat has shown that in response to pressure overload, JNK activity is actually decreased in the first 24 h post-aortic banding (Roussel *et al*, 2008). In this particular study, ERK activity was also decreased despite an upregulation of angiotensin receptors. These findings fit with other findings which show that there was no significant increase in JNK1/2 activity after 24 h in either pressure- or volume-overload experiments (Miyamoto *et al*, 2004). Mechanical stretch of cultured myocytes also activates JNK in a rapid and phasic manner (Nadruz *et al*, 2005; Pan *et al*, 2005). Furthermore, exercise, an acute form of stress, has been shown to also cause a rapid transient increase in JNK activity that is not present in exercised trained rats which exhibited a physiological cardiac hypertrophy (Boluyt *et al*, 2003). Taken together, these findings indicate that JNK activation is most likely a dynamic signalling event that can be influenced by the nature of the stimuli and that different JNK isoforms may play separate, nonredundant roles in the process.

Initial studies in cultured neonatal cardiomyocytes indicated that overactivation of JNK by MKK7, an upstream MAP2K, and leads to a hypertrophic phenotype (Wang *et al*, 1998). Correspondingly, dominant negative MKK4, another upstream MAP2K, was able to attenuate the endothelin-1-induced hypertrophic response in cultured myocytes (Choukroun *et al*, 1998). Likewise, initial *in vivo* studies in rats showed that dominant negative MKK4 abrogated JNK activity and pressure overload-induced hypertrophy (Choukroun *et al*, 1999). These findings would suggest that JNK activity is responsible,

in part, for the promotion of cell hypertrophy. In contrast, recent work by Lui et al. (2009) has shown that cardiac-specific deletion of MKK4 sensitizes the myocardium to pathological hypertrophy following pressure overload or chronic β -adrenergic stimulation. Similarly, disruption of JNK activity (dominant negative JNK) in the heart contributes significantly to hypertrophy following pressure overload (Liang *et al*, 2003). This is shown to be due in part to the ability of JNK to inhibit the translocation of the prohypertrophic transcription factor NFAT into the nucleus (Liang *et al*, 2003; Liu *et al*, 2009; Molkenin *et al*, 2004). Deletion of JNK shows similar results. In one study, *JNK1*^{-/-}, *JNK2*^{-/-}, and *JNK3*^{-/-} mice all show hypertrophy after pressure overload; however, the degree of hypertrophy is not significantly greater than wild-type mice (Tachibana *et al*, 2006). The same studies indicated that JNK1 in particular was required to maintain cardiac contractility and prevent heart failure under sustained mechanical overload. As mentioned previously, JNK1 is found to have increased translocation to the nucleus in response to pressure overload, which may explain why this particular isoform shows a more severe phenotype when deleted. This somewhat mirrors the JNK1 translocation to the nucleus that is also seen during IR (Mizukami *et al*, 1997). Interestingly, another group showed that loss of MEKK1-JNK signalling in the heart attenuates Gq-induced hypertrophy (Minamino *et al*, 2002). However, subsequent studies using this model have shown that loss of MEKK1-JNK signalling does not prevent hypertrophy in response to pressure overload (Sadoshima *et al*, 2002). Other studies have demonstrated that JNK signaling is an important part of endothelin-1-mediated hypertrophic signalling in cultured myocytes (Irukayama-Tomobe *et al*, 2004; Shimojo *et al*, 2006). This further indicates that JNK may have differential roles dependent on the stimuli. Furthermore, in vivo JNK activation in various transgenic animal models failed to induce cardiac hypertrophy. Activation of JNK in the heart by overexpression of constitutively active MKK7 activated the fetal gene program and ventricular remodelling, but did not induce hypertrophy (Petrich *et al*, 2004; Petrich *et al*, 2002). Utilizing a cre-loxP-mediated gene-switch approach, Petrich et al. (2003) were able to temporally regulate JNK activation in the adult myocardium. As with other studies, JNK activation in this manner led to pathological remodelling in the absence of ventricular hypertrophy but with a marked induction of fetal gene expression.

Given the conflicting results that have been obtained from both in vitro and in vivo studies, it has been hard to delineate the exact mechanism behind the JNK signalling

during hypertrophy. As mentioned previously, JNK's regulation of NFAT may be one mechanism (Liang *et al*, 2003; Liu *et al*, 2009). JunD, a downstream target of JNK, has been shown both in vivo and in vitro to block the cardiomyocyte hypertrophic response to both pressure overload and phenylephrine (PE) (Hilfiker-Kleiner *et al*, 2006; Hilfiker-Kleiner *et al*, 2005; Ricci *et al*, 2005). It has been suggested that this may be one explanation for the lack of hypertrophy in response to JNK activation. However, at least in vitro, phosphorylation of JunD by JNK is not required for its ability to prevent PE-induced hypertrophy (Hilfiker-Kleiner *et al*, 2006). Finally, recent work has shown that binding of growth arrest and DNA-damage-inducible beta (GADD45B) to MKK7 decreases its activity and prevents JNK-mediated cardiac hypertrophy (Wang *et al*, 2008). While studies in vitro have suggested that JNKs are prohypertrophic, the majority of studies in vivo do not support that conclusion; rather, JNKs appear to be more antihypertrophic, acting in part via excluding NF-ATs from the nucleus and upregulating JunD.

2. Cardioprotection versus myocardial cell death

Similar to the hypertrophy scenario, JNK's role in IR is also unclear. Numerous studies both in vitro and in vivo have shown the JNK is activated as a result of reoxygenation upon reperfusion (Fryer *et al*, 2001; Knight and Buxton, 1996; Laderoute and Webster, 1997; Sekoet *et al*, 1997; Yin *et al*, 1997). While its activation during the ischemic phase is less well established, a few studies have suggested that it occurs (Ping *et al*, 1999; Shimizu *et al*, 1998; Yue *et al*, 2000). As a stress-induced signaling pathway, JNK has both protective and pathological roles in different cell types. This dichotomy is also observed in cardiomyocytes. JNK1, but not JNK2, has been shown to be proapoptotic during in vitro IR experiments (Hreniuk *et al*, 2001). Likewise, treatment with various JNK-selective inhibitors reduces infarct size and apoptosis in response to IR (Ferrandi *et al*, 2004; Milano *et al*, 2007). Furthermore, JNK activity contributes to the detrimental effects of a number of proteins known to increase myocardial injury following IR, including the receptor for advanced glycation end-products (RAGE) (Aleshin *et al*, 2008), PKC- β (Kong *et al*, 2008), β -adrenergic receptors (Remondino *et al*, 2003), uncleaved HB-EGF (Uetani *et al*, 2009), Rho-kinase (Zhang *et al*, 2009), and poly(ADP-ribose) polymerase (Song *et al*, 2008). Most recently, JNK has been shown to be activated and promote apoptosis during IR by atrogin-1, an E3 ubiquitin ligase (Xie *et al*, 2009). Atrogin-1 targets MAPK phosphatase-1 (MKP-1) for degradation,

resulting in a sustained activation of JNK and increased apoptosis through increasing cleaved caspase-9, caspase-3, and Bax and by decreasing Bcl-2. JNK has been reported to associate with the mitochondria, possibly interacting with proapoptotic proteins (Aoki *et al*, 2002; Baines *et al*, 2002), and has also been shown to mediate apoptosis-inducing factor (AIF) translocation from the mitochondria to the nucleus (Song *et al*, 2008; Zhang *et al*, 2009). However, convincing as these data are, the complexity of the system is probably best exemplified by Kaiser *et al*. (2005), who reported enhanced myocyte survival after IR with both JNK activation and inhibition. JNK has also been viewed as antiapoptotic in response to nitric oxide (NO) *in vitro* (Andreka *et al*, 2001). Similarly, blocking JNK activity increased apoptosis and the activity of both caspase-9 (Dougherty *et al*, 2002) and caspase-3 (Engelbrecht *et al*, 2004) in another *in vitro* IR model. This has been proposed to be mediated by the interaction of JNK with Apaf-1, which delays the activation of caspase-9 by the apoptosome (Tran *et al*, 2007). It has also been suggested that part of JNK's cardioprotective effect is due to activation of Akt, a key prosurvival protein in postischemic cardiomyocytes (Shao *et al*, 2006). In short, like in hypertrophy, the role of the JNK pathway in IR injury remains controversial, perhaps reflecting the complexity of multistage, multi-targeted signalling networks involved in this process.

3. Cardiac remodelling

Transgenic activation of the JNK pathway in the heart resulted in a lethal restrictive cardiomyopathy with selective extracellular matrix remodelling (Petrich *et al*, 2004). (Collagen deposition was not increased, but fibronectin levels were markedly increased.) Prolonged activation of JNK activity in heart was also associated with abnormal gap junction structure, loss of the main component (connexin-43), and slowed conduction velocity in the heart (Petrich *et al*, 2002). Recent evidence suggests that the loss of gap junctions in JNK-activated heart is associated with the loss of connexin-43 protein expression as well as improper intracellular targeting (Ursitti *et al*, 2007). On the other hand, deletion of JNK1 in the heart resulted in an increase in fibrosis following pressure overload (Tachibana *et al*, 2006). Similarly, chronic treatment with a JNK inhibitor led to increased apoptosis and cardiac fibrosis in the cardiomyopathic hamster model (Kyojima *et al*, 2006). Likewise, another study showed the loss of toll-like receptor 4 (TLR4) improved cardiac function and reduced cardiac remodelling following ischemic injury in the heart (Riad *et al*., 2008). In this study, the wild-type

animals displayed a significant decrease in JNK activity following ischemia that did not occur in the TLR4 animals. Interestingly, the higher JNK level in the TLR knockout animals following ischemia was also accompanied by a significant decrease in calcineurin, indicating that the cross-talk between these two pathways as discussed previously may also play an important role in cardiac remodelling. These results indicate that JNK activity functions to keep some aspects of cardiac remodelling in check while promoting the dysregulation of others.

JNK has also been implicated in promoting cardiac remodelling downstream of various pathways. For example, ASK-1/JNK has been shown to play a role in β -adrenergic-induced cardiac remodelling and apoptosis in vivo (Fan *et al*, 2006). Hsp20, a protein with known cardioprotective effects (Fan *et al*, 2005), inhibited the activation of JNK in this setting. In a rat model of pressure overload, treatment with RA inhibited cardiac remodelling by inhibiting MAPK signaling, including JNK activity, by upregulating MKP-1 and MKP-2 (Chouldhary *et al*, 2008). Likewise, in a model of ANG II-induced hypertrophy, mice deficient for ASK1-JNK signalling demonstrated an attenuation of cardiac fibrosis and remodelling (Izumiyae *et al*, 2003). JNK activation downstream of ET-1 has also been implicated in perivascular remodelling in rat (Jesmi *et al*, 2006). Finally, matrix metalloproteinases (MMP) are well known to contribute to cardiac remodelling. Recent in vitro studies have shown that in response to β -adrenergic signalling, extracellular matrix metalloproteinase inducer (EMMPRIN) expression and MMP-2 activity was increased in a JNK-dependent manner in cardiomyocytes (Siwik *et al*, 2008). These findings are supported by other in vitro work in which JNK activation in H9c2 cardiomyoblasts resulted in the upregulation of MMP-2 (but not MMP-9) activity (Chen *et al*, 2009). Likewise, in vivo studies on the loss of β 1-integrins showed increased JNK activity was associated with increased MMP-2 but not MMP-9 activity, which corresponded with less cardiac fibrosis in this setting (Krishnamurthy *et al*, 2007). ROS signalling is emerging as an important player in cardiac remodeling. Since JNK activation is a downstream consequence of ROS induction, there might be a larger role for JNK in cardiac remodelling than originally thought (Anilkumar *et al*, 2009; Hori and Nishida, 2009). Finally, ASK-1/JNK is a downstream pathway of ER stress signalling (Nagai *et al*, 2007), which is also gaining more appreciation as an important aspect of stress signalling in the diseased heart (Toth *et al*, 2007, Xu *et al*, 2005). For example, Kerkela and co-workers (Force and Kerkela, 2008; Kerkela *et al*, 2006) have

found that ER stress and ensuing JNK activation is responsible for mitochondrial defects and severe cardiomyopathy as a result of anticancer therapy targeted to the tyrosine kinase c-abl.

These results may indicate that JNK's role in cardiac pathological remodelling may depend on the activating stimuli. However, because hypertrophy and remodelling often go hand in hand, it is hard to determine whether the remodelling observed in some of these cases is a specific and direct result of JNK activation or secondary to the ensuing hypertrophy recruitment of other signalling pathways.

C. p38

1. Cardiac hypertrophy

Despite a great deal of interest in p38, much of its role in the heart is yet to be clarified. Initial in vitro studies of this pathway suggested that p38 promotes cardiac growth and hypertrophy. Inhibition of the pathway using small molecule inhibitors (SB203580 or SB202190) or dominant negative p38 adenovirus inhibits myocyte growth in response to hypertrophic stimuli (Liang and Molkenin, 2003; Nemoto *et al*, 1998; Zechner *et al*, 1997). In addition, multiple groups have shown that overactivation of the p38 pathway induces hypertrophic changes in vitro (Nemoto *et al*, 1998; Wang *et al*, 1998; Zechner *et al*, 1997). However, other studies suggest that p38 is not necessary for agonist-induced hypertrophy in cultured myocytes (Choukroun *et al*, 1998) and that p38 inhibition is actually associated with calcineurin induced hypertrophy via induced expression of MAPK phosphatase-1 (Lim *et al*, 2001).

Results from in vivo studies showed that targeted activation of p38 in the heart did not produce any significant degree of cardiac hypertrophy (Liao *et al*, 2001). Instead, transgenic overexpression of either MKK3 or MKK6 in the heart increased interstitial fibrosis, ventricular wall thinning, and premature death due to cardiac failure. These findings are supported by Klein *et al*. (2005) in which loss of PKC- ϵ resulted in increased activation of p38 in the myocardium following pressure overload. These animals displayed a similar phenotype to the MKK3/MKK6 animals, including no increase in hypertrophy but a significant increase in fibrosis and impaired diastolic function. These findings indicate that, in vivo, p38 activity alone is not sufficient to

promote cardiomyocyte hypertrophy. Conversely, initial studies involving cardiac-specific p38 dominant negative transgenic mice showed that loss of p38 activity either had no effect on hypertrophy (Zhang *et al*, 2003) or sensitized the heart to hypertrophy (Braz *et al*, 2003) in response to pressure overload. The enhanced hypertrophy in this setting is suggested to be the result of loss of p38's antagonizing effect on NFAT-mediated transcriptional activity (Braz *et al*, 2003; Molkentin, 2004; Yang *et al*, 2002). Cardiac-specific deletion of p38 did not alter pressure overload hypertrophy. It resulted in a similar degree of myocyte hypertrophy between p38 CKO and wild-type animals following pressure overload (Nishida *et al*, 2004). However, these mice did exhibit an increase in apoptosis, fibrosis, and chamber dilation as well as reduced LV function (Nishida *et al*, 2004). Taken together, these findings would indicate that p38 activity is not involved in promoting hypertrophy *in vivo*, but may play an important role in pathological remodelling.

Recent findings have implicated p38 in physiological hypertrophy. In response to swimming, loss of p38, either by deletion of ASK1 (an upstream activator) or by conditional knockout of p38 from the myocardium, resulted in increased hypertrophy without increasing fibrosis (Taniike *et al*, 2008). These authors proposed that the loss of p38 activity resulted in an increase in AKT activity, a known inducer of physiological hypertrophy. Conversely, p38 dominant negative transgenic mice did not experience an increase in hypertrophy in response to swimming (Watanabe *et al*, 2007). This may mirror the different results obtained from the dominant negative transgenic model and the conditional knockout model in response to pressure overload discussed above. Furthermore, an increase in p38 activation in response to loss of the regulatory protein 14-3-3 resulted in maladaptive hypertrophy with increased fibrosis and apoptosis in response to swimming (Watanabe *et al*, 2007).

While gain-of-function and loss-of-function studies through genetic manipulation have shown that p38 is not sufficient for hypertrophy, at least *in vivo*, studies involving upstream activators still imply a role for p38 in the hypertrophic process. Multiple studies have shown that the protective effects of estrogen on the myocardium are mediated in part through activation of the p38 pathway. In response to both pressure overload and activation of G_qα signalling, administration of estrogen *in vivo* blocks hypertrophy in a p38-mediated manner (Babiker *et al*, 2006; Satoh *et al*, 2007).

Likewise, p38 dominant negative transgenic female mice exhibited greater hypertrophy than either males or ovariectomized females in response to pressure overload (Liu *et al*, 2006). In vitro studies have produced similar results. In contrast, activation of thyroid receptor (TR α 1) has been shown to cause myocyte hypertrophy via TAK-1/p38 activity in vitro (Kinugawa *et al*, 2005). Likewise, leptin induces hypertrophy of cultured neonatal myocytes as a result of caveolae and RhoA-mediated phospho-p38 translocation to the nucleus (Zeidan *et al*, 2008). These results and others like them may indicate that the role of p38 in cardiac hypertrophy is a conflicting one. While acute activation of p38 appears to be prohypertrophic, chronic activation of p38 can lead to suppression of hypertrophic growth in heart. However, it is clear from both in vitro and in vivo studies that p38 activation has a detrimental effect on cardiac function and normal gene expression. Therefore, p38 induction is more closely related to pathological form of hypertrophy than to physiological compensation.

2. Cardioprotection versus myocardial cell death

The role of p38 during IR has been well reported in the literature. However, the conclusions are often contradictory, with some evidence pointing toward a protective role and other results indicating a detrimental role (Clark *et al*, 2007; Steenbergen, 2002). Similar conflicting results have also been noted regarding the role of p38 in ischemic preconditioning (Bell *et al*, 2008; Steenbergen, 2002). These contradictions are likely due, at least in part, to a number of variables including use of different protocols, species, method of p38 inhibition, and measured outcomes. That said, some studies that employed similar species and protocols still resulted in opposing conclusions (Bell *et al*, 2008).

Shortly after its identification, investigators demonstrated that p38 was robustly activated by ischemia in the isolated perfused rat heart (Bogoyevitsch *et al*, 1996). This activation is both rapid in its onset and transient in its duration after induction of ischemia. To date, however, the exact role that this temporal activation plays in ischemia still eludes investigators. A number of studies have indicated that activation of p38 during ischemia leads to increased injury (Barancik *et al*, 2000; Bellet *et al*, 2008; Ma *et al*, 1999; Mackay and Mochly - Rosen, 1999; Martin *et al*, 2001; Nagarkatti and

Sha'afi, 1998, Sanada *et al*, 2001; Saurin *et al*, 2000). Likewise, an equal number of studies have shown that p38 activity during ischemia serves a protective role (Martin *et al*, 1999; Mauliket *al*, 1998; Mocanu *et al*, 2000; Weinbrenner *et al*, 1997; Zechner *et al*, 1997). This last point is seen mostly in the context of ischemic preconditioning, the process by which small repeated periods of ischemia impart cardioprotection against more sustained ischemic periods. A number of investigators have shown that p38 activity increases during preconditioning (Steenbergen, 2002). Interestingly, this too appears to be phasic in nature. Ping *et al*. (1999) have shown that p38 activity is increased with brief periods of ischemia, but with repetitive cycles of ischemia and reperfusion, the level of p38 activity returns to baseline within 6 cycles. Furthermore, multiple cycles of ischemia and reperfusion lead to less p38 activation during sustained periods of ischemia following the preconditioning when compared with nonpreconditioned hearts (Gysemberghet *al*, 2001; Maraiset *al*, 2001; Schneider *et al*, 2001). Furthermore, inhibiting p38 activity during prolonged periods of ischemia reduces infarct size only in non-preconditioned hearts and that inhibition of p38 during preconditioning eliminates its cardioprotective effects (Béguinet *al*, 2007; Gysembergh *et al*, 2001; Sanada *et al*, 2001). Although appearing to be contradictory, these results may be reconciled based on the hypothesis that a negative-feedback mechanism recruited by the modestly induced p38 activity during preconditioning contributes to minimize the detrimental impact of IR. Identifying the molecular basis of this preconditioning-induced protective mechanism remains a major challenge in the biology of ischemia and has the potential to translate this phenomenon into a viable therapy for ischemic disease. In addition, Engel *et al*. (2006) have suggested that inhibiting p38 activity can help preserve cardiac function following ischemia by reducing scarring and promoting myocyte proliferation. This new aspect of p38-mediated cardioprotection opens up a new and exciting avenue by which p38 may be manipulated for therapeutic benefit in the heart.

Another confounding factor adding to the complexity of p38 study is the presence of multiple p38 isoforms in the heart. While p38 α is the predominant isoform in the heart, p38 β is also present and has been shown to have different physiological consequences. Initial studies in neonatal rat ventricular myocytes revealed that overexpression of p38 α impart pro-apoptotic effects, while overexpression of p38 β leads to myocyte hypertrophy (Wang *et al*, 1998). Studies investigating the role of different p38 isoforms

during ischemia have discovered possible differential roles for the α - and β -isoforms. Following adenoviral-mediated overexpression and simulated ischemia, Saurin et al. (2000) have shown that p38 α activity is increased while p38 β activity is decreased. Furthermore, these authors demonstrate that inhibition of only the α -isoform was protective. Subsequently, multiple studies have indicated that p38 β may be the isoform that imparts cardioprotection (Kim *et al.*, 2005; Kim *et al.*, 2006). Recently, in vivo studies utilizing overexpression of a cardiac-specific kinase dead p38 β mutant revealed that loss of p38 β , but not p38 α , activity in the myocardium resulted in increased ischemic injury (Cross *et al.*, 2009). This is similar to previous work in which mice either overexpressing a dominant negative form or lacking one allele of p38 α were significantly protected from IR injury (Kaiser *et al.*, 2004; Otsu *et al.*, 2003). These results may provide some clue as to the discrepancy of previous results regarding the protective versus detrimental role of p38 during ischemia. Many early studies utilized p38 inhibitors that block both the α - and β -isoform. If the two isoforms do indeed have different activation profiles and functional roles during ischemia, then experimental results may be confounded by inadvertently blocking both isoforms. Furthermore, it has been shown that the most common p38 inhibitor, SB203580, can actually inhibit other kinases depending on the concentration used (Borsch-Haubold *et al.*, 1998; Clerk and Sugden, 1998; Hall-Jackson *et al.*, 1999; Lali *et al.*, 2000). Finally, it has begun to be recognized that p38 activation can be mediated by more than the canonical kinase cascade as described earlier, but also via a noncanonical mechanism involving TAB-1 induced autophosphorylation (Ge *et al.*, 2002). Indeed, TAB-1-mediated p38 activation is observed in ischemic heart and implicated in cardiac injury (Li *et al.*, 2005; Tanno *et al.*, 2003). However, although one study showed TAB-1 induced p38 activation in cardiomyocyte caused apoptosis similar to canonically activated p38 activity, another showed TAB-1 interaction with p38 led to its intracellular localization and downstream signalling distinct from the canonical pathway (Fiedler *et al.*, 2006; Lu *et al.*, 2006). Although mainly observed in brain and thymocytes, p38 can also function as an alternative mechanism of GSK-3 β inactivation, thus further complicating the functional outcome of p38 activation/inactivation in the heart (Thornton *et al.*, 2008).

The upstream and downstream signalling that contributes to p38's role in insulin resistance has yet to be fully determined. Multiple studies, however, have begun to examine such events. For instance, in a setting of insulin-induced cardioprotection, rat

hearts treated with insulin followed by IR showed improved functional recovery and an increase in phospho-Hsp27 (Li *et al*, 2008). This protective effect was abolished by treatment with the p38 inhibitor SB203580. p38-mediated Hsp27 activation has also been shown to play a protective role during IR in response to pretreatment of the hearts with H₂O₂ (Blunt *et al*, 2007). In this case, the protective effect was determined to be due to Hsp27's ability to prevent Ca²⁺-induced proteolysis of myofilament proteins. Hsp27 has been shown in other studies to have cardioprotective properties (Hollander *et al*, 2004; Martinet *et al*, 1999; Martin *et al*, 1997). p38's ability to activate Hsp27 may explain some of the results showing that p38 is cardioprotective. However, transgenic expression of both wild-type and a nonphosphorylatable form of Hsp27 were both cardioprotective following IR, suggesting that phosphorylation by p38 is not an absolute requirement for its cardioprotective effects (Hollander *et al*, 2004). Interestingly, Gorog *et al*. (2009) have demonstrated that loss of MAPK APK2, the kinase that functions between p38 and Hsp27, resulted in the loss of ischemia-induced Hsp27 phosphorylation but did not exacerbate the ischemic injury.

While the previous examples discuss p38 activation and signaling in terms of cardioprotection, other studies have investigated how inhibition of p38 is cardioprotective. As mentioned previously, p38 activity in myocytes can be proapoptotic. Work by Dhingra *et al*. (2007) has shown that p38 activity is important in TNF- α -mediated myocyte apoptosis, in part, due to ROS production. Moreover, p38 inhibition has also been shown to prevent mitochondrial ROS production and Ca²⁺ overload during IR (Sucher *et al*, 2009). p38's role in mitochondrial-mediated cell death events was also examined by Schwertz *et al*. (2007). In their proteomic approach, they identified a number of proteins altered following IR in rabbit heart. Most interestingly, they noted that phosphorylation of VDAC-1, a mitochondrial porin with possible links to mitochondrial permeability transition pore (MPTP)-mediated cell death, was increased four fold following IR. This phosphorylation was significantly decreased, and cardioprotection was increased with treatment with the p38 inhibitor PD169316. p38 inhibition has also been shown to impart its cardioprotective effects by altering glucose utilization (Jaswal *et al*, 2007; Jaswal *et al*, 2007). Finally, endogenous p38 inhibition has also been shown to be cardioprotective during IR. Treatment of rats with the glucocorticoid dexamethasone was shown to be cardioprotective through induction of

the dual-specific phosphatase MKP-1 which resulted in a decrease in p38 phosphorylation (Fan *et al*, 2009).

As can be seen, the role of p38 in cardiac protection and injury is a complicated one. The specific contribution of p38 kinase in ischemic injury and protection is determined by the level, duration, mode, and timing of induction involving different isoforms and upstream/downstream pathways.

3. Cardiac remodeling

As with JNK, the other stress-activated MAPK, p38 appears to play an important role in cardiac remodelling after injury. Liao *et al*. (2001) discovered that targeted p38 activation in the myocardium led to a restrictive cardiomyopathy with significant amounts of interstitial fibrosis. In this setting, p38 was shown to induce cytokine release from myocytes, including TNF- α and IL-6 (Liet *al*, 2005). Interestingly, in these *in vitro* studies, blocking p38 activity did not appear to prevent cytokine production in the myocytes, only their release from the cell. Proinflammatory cytokines such as TNF- α and IL-6 are known to act in both autocrine and paracrine fashions. Acting in an autocrine fashion, they are known to have negative inotropic effects (Prabhu, 2004). Acting in a paracrine fashion, they play a large role in myocardial remodeling (Nian *et al*, 2004). These initial studies are supported by findings of Tenhunen *et al*. (2006) in which DNA microarray analysis of animals with cardiac-specific overexpression of p38 revealed that genes related to inflammation and fibrosis were among the most significantly upregulated.

p38 is also activated by proinflammatory cytokines, including transforming growth factor (TGF)- β . This type of p38 activation also contributes to cardiac remodelling. Indeed, p38 is activated via a TGF- β 1/TAK1-dependent mechanism in myocytes following myocardial infarction in rats (Matsumoto-Ida *et al*, 2006). As discussed previously, p38 activity can induce cytokine production, thus creating a type of feed-forward mechanism for cytokine action and production. This autocrine and paracrine signalling can lead to recruitment and proliferation of cardiac fibroblasts and inflammatory cells resulting in remodelling. Recent work in aged hypertensive rats (which naturally develop significant amounts of cardiac fibrosis) has shown that treatment with a TGF- β antagonist dramatically reduces both hypertrophy and

interstitial fibrosis. This was accompanied by a decrease in phospho-p38 levels. This fits with other studies that have shown inhibition of p38 reduces remodelling following myocardial infarction (Liu *et al*, 2005; See *et al*, 2004). Interestingly, recent work by Frantz *et al*. (2007) indicated that long-term (9 wk) inhibition of p38 starting 1 wk after induced cardiac ischemia reduced cytokine production but did not affect other aspects of cardiac remodelling, including collagen deposits (Frantz *et al*, 2007). This finding, however, is in contrast to work by others which showed significant reduction in cardiac fibrosis and hypertrophy following IR with long-term p38 inhibition (Kompa *et al*, 2008). While the protocols for these two studies were similar, the difference in outcome may be due to the different p38 inhibitors used (SB239063 and RWJ67657, respectively).

In addition to extracellular matrix remodelling, p38 can also regulate myocyte contractility. Activation of p38 has been shown to have negative inotropic effects in myocytes (Chen *et al*, 2003; Liao *et al*, 2002; Zechner *et al*, 1997). Moreover, recent work by Szokodi *et al*. (2008) has shown that increased contractility in response to ET-1 treatment was due to ERK signalling and was further augmented by inhibition of p38. In this setting, it appears that p38 may play a regulatory function by counterbalancing the effects of ERK. While the precise mechanism by which p38 influences myocyte contractility is not fully understood, it appears to be due, at least in part, to modifications of structural proteins. Initial work described p38's role in contractility as Ca^{2+} transient independent (Liao *et al*, 2002), but suggested that it may be due to modifications of sarcomeric proteins (Chen *et al*, 2003). Most recently, Vahebi *et al*. (2007) have suggested that a p38-mediated decreased phosphorylation of α -tropomyosin is one of the mechanisms involved. Furthermore, p38 has the potential to affect myocyte contractility by promoting transcription of the $\text{Na}^+/\text{Ca}^{2+}$ exchanger (NCX1), a key regulator of Ca^{2+} homeostasis in both the healthy and pathological myocardium (Menich *et al*, 2007). Interestingly, a recent study found that inhibiting NCX1 actually resulted in upregulation of the NCX1 gene in a p38-dependent manner and that this increase was accompanied by NCX-p38 complex formation (Xu *et al*, 2009). With the proposal of NCX1 inhibitors as a therapeutic treatment for heart failure, more work needs to be done to better understand the interplay between these two proteins. Finally, p38 has also been shown to downregulate SERCA expression and prolong the Ca^{2+} transient in cultured myocytes (Andrews *et al*, 2003). Although more work needs to be

done, given the importance of Ca^{2+} handling in cardiac pathologies, it is important to better understand the role the p38 signalling may play on this front. In short, chronic induction of p38 activity in postinjury hearts plays an important role in cellular and myocardial remodelling by affecting both the contractility of myocytes and the extracellular matrix.

Akt module

AKT is a serine/threonine protein kinase that regulates a variety of cellular functions in different tissues. AKT is the effector of PI3K and is essential during postnatal cardiac development that is achieved predominantly by hypertrophy rather than hyperplasia of individual cardiomyocytes (Shiojima and Walsch, 2006). There are three isoforms of AKT, AKT1, AKT2, and AKT3. It has been shown that AKT1 KO mice have slightly diminished growth and that these mice are susceptible for spontaneous and stress-induced apoptosis (Chen *et al*, 2001; Cho *et al*, 2001). AKT2 KO mice have normal body size but are mildly insulin resistant (Cho *et al*, 2001), while AKT3 KO mice have reduced brain size that is attributed to decrease in cell number and cell size (Easton *et al*, 2005). The combined deletion of AKT1 and AKT2 or AKT1 and AKT3 genes result in perinatal lethality with multiple developmental defects, indicating a large degree of functional overlap between the three isoforms of AKT (Bae *et al*, 2003; Peng *et al*, 2003). On the other hand, increased AKT signalling in β -cells promotes hypertrophy and hyperplasia (Jetton *et al*, 2005), whereas increased AKT function in T-lymphocytes and prostate cells promotes lymphoma (Rathmell *et al*, 2003) and prostate cancer (Majumder and Sellers, 2005), respectively.

In the heart, short-term AKT1 activation promotes physiological hypertrophy (Shiojima *et al*, 2002) whereas long-term AKT1 activation induces pathological hypertrophy (Kemi *et al*, 2008; Matsui *et al*, 2003). Physiological and pathological hypertrophy are morphologically, functionally, and molecularly distinct from each others. Physiological hypertrophy occurs during postnatal cardiac development and in trained athletes and is characterized by normal or enhanced contractile function, normal architecture, and organization of cardiac structure without increases in interstitial fibrosis. Clinically, pathological hypertrophy is observed in patients with uncontrolled hypertension,

myocardial infarction, and aortic stenosis. In its advanced stages, it is characterized by contractile dysfunction, interstitial fibrosis, and expression of foetal cardiac genes such as atrial natriuretic peptide and β -myosin heavy chain (β -MHC) (Mann *et al*, 2010; Shah and Solomon, 2010). Pathological hypertrophy is associated with increased morbidity and mortality and eventually the sustained pressure overload leads to myocardial contractile dysfunction, dilatation, and development of heart failure (HF) through poorly understood mechanisms (Mann *et al*, 2010; Shah and Solomon, 2010). In endothelial cells, brief AKT activation attenuates damage to ischaemia, whereas prolonged AKT activation leads to increased but unorganized blood vessel formation, reminiscent of tumour vasculature (Phung *et al*, 2006). Hence, AKT signalling plays an important role in maintaining vascular homeostasis and that tight control of the AKT signal in endothelial cells is required for normal vascular patterning and remodelling. Growth factors such as insulin and insulin growth factor as well as exercise activate AKT through its recruitment to the cell membrane and its phosphorylation at Thr 308 and Ser 473 by PDK1 and mTORC2, respectively. On the other hand, absence of growth factors and sedentary lifestyle lead to decreased phosphorylation and hence inactivation of AKT (Kemi *et al*, 2008; Longnus *et al*, 2005). However, in stressed cardiac myocytes, such as in oxidative stress or in ischaemia reperfusion, AKT signalling and its interaction with its downstream effectors are altered or are overridden by other signalling pathways as discussed below. This review will address the role of AKT in promoting coronary angiogenesis and in modulating cardiac function with specific emphasis on the role of AKT in altering programmed types of cell death, such as autophagic and apoptotic cell death in cardiomyocytes and in HF.

AKT and angiogenesis

In endothelial cells, AKT phosphorylates a wide variety of target proteins that regulate cell proliferation, survival, permeability, release of nitric oxide, and cell migration (Shiojima and Walsch, 2002; Somanath *et al*, 2006). AKT is essential in vascular endothelial growth factor (VEGF)-mediated angiogenesis and regulates the migration of endothelial cells necessary for vessel sprouting, branching, and the formation of networks during angiogenesis via the phosphorylation of Girdin, an actin binding protein, at Ser 1416 to regulate its subcellular localization and cell migration in fibroblasts (Enomoto *et al*, 2005). Kitamura *et al*. (2005) have shown that the delivery

of adenovirus harbouring Girdin short interfering RNA in Matrigel embedded in mice, markedly inhibited VEGF-mediated angiogenesis. Targeted disruption of the Girdin gene in mice impaired vessel remodelling in the retina and angiogenesis from aortic rings; however, Girdin was unessential for embryonic vasculogenesis. These findings demonstrate that the AKT/Girdin signalling pathway is essential in VEGF-mediated postneonatal angiogenesis. Short-term AKT activation in inducible transgenic AKT1 mice induces physiological hypertrophy with maintained vascular density. Coronary angiogenesis is enhanced to keep pace with the growth of the myocardium. The increase in vascular density is directly related to the increase in VEGF and angiopoietin-2 during short-term AKT1 activation (Shiojima and Walsch, 2002; Kitamura *et al*, 2008). On the other hand, prolonged AKT activation leads to pathological hypertrophy. Under these conditions, VEGF and angiopoietin-2 are downregulated and capillary density is reduced. The decrease in coronary angiogenesis could in part explain the decrease in cardiac function during long-term AKT activation. It has been shown that VEGF blockade in pressure overload reduces capillary density and results in an accelerated transition from compensated hypertrophy to HF (Izumiya *et al*, 2006). Thus, the balance between cardiac growth and coronary angiogenesis is critical and that the cross-talk between cardiac myocytes and coronary vasculature is essential for the maintenance of the contractile function, especially in pathological hypertrophy and in HF.

AKT and cell death

Cardiac myocyte loss in HF via the form of necrotic, apoptotic, and autophagic cell death may in part contribute to the worsening in cardiac contractile function and to left ventricular remodelling. Strong evidence in the literature suggests that short-term activation of AKT have beneficial effects via the inhibition of apoptotic cell death. Matsui *et al* (1999) showed that adenoviral gene transfer of activated AKT1 protects cardiomyocytes from apoptosis in response to hypoxia *in vitro*. Cardiomyocytes were infected with either a control adenovirus (Ad.EGFP) or adenoviruses carrying constitutively active forms of PI 3-kinase (Ad.BD110) or AKT (Ad.myr-AKT-HA). Ad.BD110 significantly inhibited apoptosis of hypoxic cardiomyocytes compared with Ad.EGFP. Ad.myr-AKT-HA even more dramatically inhibited apoptosis of hypoxic cardiomyocytes. Moreover, adenovirus-mediated AKT1 gene transfer in the heart diminishes cardiomyocyte apoptosis and limits infarct size following

ischaemia/reperfusion injury (Matsui *et al*, 2001) and ameliorates doxorubicin-induced contractile dysfunction (Taniyama and Walsch, 2002). Beside its anti-apoptotic effect, AKT1 controls autophagic cell death by phosphorylating and thus inhibiting the translocation of forkhead box O (FOXO) family, particularly FOXO3a, from the cytoplasm into the nucleus and thus inhibits FOXO3a effector, BNIP3, from initiating mitochondrial autophagy and mitochondrial defragmentation (Mammucari *et al*, 2008). This effect of AKT is mainly seen in the presence of growth stimuli and is lost with their absence such as during starvation (Mammucari *et al*, 2007; Sandri, 2008). However, in stressed cardiomyocytes, AKT regulates the autophagic activity, on the short term, via c-Jun N-Terminal Kinases (JNKs) signaling. Our data suggest that the expression of the mitochondrial autophagic marker (BNIP3) is significantly upregulated 2h after cardiomyocyte stress with phenylephrine (PE). Moreover, Shao *et al* (2006) showed that JNKs can mediate reactivation of AKT and cardiomyocyte survival after hypoxic injury *in vitro* and *in vivo*. The authors demonstrate that reactivation of AKT after resolution of hypoxia is regulated by JNKs and suggest that this is likely a central mechanism of the myocyte protective effect of JNKs.

AKT and calcium cycling proteins

AKT1 signalling may also improve contractile function by influencing myocardial calcium cycling, which plays a critical role in contractility and relaxation of cardiomyocytes. During excitation of the cardiomyocyte, small calcium influx via the L-type calcium channels (LTCC) leads to massive release of calcium from the endoplasmic reticulum via the ryanodine receptors, a phenomenon known as calcium-induced calcium release. The increase in intracellular calcium leads to contraction of the cardiomyocyte and to the activation of the sarcoendoplasmic reticulum calcium ATPase (SERCA2a), which pumps calcium from the cytoplasm into the sarcoplasmic reticulum. The activity of SERCA2a is inhibited by phospholamban (PLB). During diastole there is inhibition of PLB by its phosphorylation at two different sites; one is activated by protein kinase A (PKA) in response to β -adrenergic stimulation and the other is activated by calcium ions and calmodulin, thus promoting and enhancing the activity of SERCA2a. One of the other proteins that affects the function of SERCA2a is the protein phosphatase 1 (PP1) and its inhibitor-1 (I-1). Phosphatase 1 is a serine/threonine phosphatase that is localized to the sarcoplasmic reticulum and is inhibited by I-1,

which becomes active upon phosphorylation of threonine-35 of PLB protein by PKA. This results in inhibition of PP1 and therefore enhanced PKA-mediated phosphorylation of PLB, leading to amplification of the β -adrenergic response in the heart. AKT1 appears to positively regulate contraction by increasing calcium influx through the LTCC (Catalucci *et al*, 2009), by increase in SERCA2a protein levels (Kim *et al*, 2008), and by augmenting PLB phosphorylation (Catalucci *et al*, 2009), possibly through down-regulation of PP1. Whether AKT1 is directly involved in the phosphorylation of LTCC, PLB, or in the activation of I-1 awaits further investigation.

AKT and metabolism

AKT1 modulates glucose and fatty acid metabolism. AKT may promote glucose oxidation by enhancing glucose uptake through glucose transporters and attenuates fatty acid oxidation through down-regulation of peroxisome proliferator-activated receptor- α (PPAR α) and its coactivator, PPAR γ coactivator-1(PGC-1), which transcriptionally activate the genes in fatty acid oxidation pathway. Under normal conditions, adenosine triphosphate (ATP) is produced up to 10–40% from oxidation of glucose and lactate and up to 60–90% from β -oxidation of free fatty acids. Fatty acids generate more ATP per gram of substrate than lactate or glucose, and are energy efficient, whereas glucose and lactate generate more ATP than fatty acids for each mole of oxygen and are oxygen efficient. Therefore, if the supply of oxygen is limited, glucose oxidation will provide more energy per equal amount of oxygen and support more work than fatty acids. Moreover, during ischaemia the accumulation of free fatty acids is toxic and induces damage to the cell membrane and death of the cell. Stimulation of glucose oxidation may be beneficial under ischaemic conditions, and the cardioprotective effects of glucose–insulin–potassium (GIK) infusion in the reperfusion phase or fatty acid oxidation inhibitors as shown in animal models of ischaemia reperfusion (Zhang *et al*, 2006) support this notion (Diaz *et al*, 2007). Therefore, the cardioprotective and beneficial effect of short-term activation of AKT1 in the reperfusion phase may be attributed in part to the switch from fatty acid to glucose metabolism leading to the efficient myocardial consumption of oxygen.

Exercise and AKT signalling in heart failure

Heart failure is a growing problem in the industrialized world and has reached epidemic proportions in the USA. Although the central effects of HF are pulmonary and peripheral vascular congestion, many patients believe that exercise limitation is the most troubling feature. Traditional therapies, such as angiotensin-converting enzyme inhibitors, β -blockers, and spironolactone show impressive reductions in mortality with somewhat less significant improvement in functional capacity. Exercise training was once prohibited in HF patients out of concern for patient safety. However, it is now recognized as a therapeutic option for improving functional capacity, especially that mechanical function and functional capacity do not always have a direct correlation in HF subjects (Davies *et al*, 2010). Clinical trials of exercise training in HF show improvements in exercise time, functional capacity, and peak oxygen consumption and that exercise training seemed to be safe and well tolerated in HF patients (O'Connoret *et al*, 2009; Whellan *et al*, 2007; Gianuzzi *et al*, 1997; McKelvie *et al*, 1995). The cardiomyocyte signalling pathways driving this beneficial effect of exercise were not fully understood until recently. Miyachi *et al.*(2009) explored the signalling pathways involved in the beneficial effect of exercise on left ventricular geometry in a HF model of Dahl Salt-Sensitive hypertensive rats. The authors found that exercise training had a beneficial effect on cardiac remodelling and attenuated HF in hypertensive rats, with these effects likely being attributable to the attenuation of left ventricular concentricity and restoration of coronary angiogenesis through the activation of phosphatidylinositol 3-kinase(p110 α)-AKT-mammalian target of rapamycin signalling (Miyachi *et al*, 2009). Moreover, Konhilas *et al.* (2004) have shown that there are sex differences with regard to exercise-induced cardiac adaptation in mice. The authors found that sex/gender is a dominant factor in exercise performance and found that female animals have greater capacity to increase their cardiac mass in response to similar amounts of exercise. They attributed these differences to significant increase in calcium/calmodulin-dependent protein kinase (CaMK) activity in females compared with males in response to exercise. The phosphorylation of glycogen synthase kinase-3 (GSK-3) was evident after 7 days of cage-wheel exposure in both sexes and remained elevated in females only by 21 days of exercise. However, there were no sex differences with regard to exercise-induced AKT phosphorylation (Konhilas *et al*, 2004).

Exercise also has beneficial effects on the musculoskeletal system in HF subjects (Ventura-Clapier *et al*, 2007; You Fang and Marwick, 2003). Skeletal muscle abnormalities in patients with HF include atrophy of highly oxidative, fatigue-resistant type I muscle fibres, decreased mitochondrial oxidative enzyme concentration and activity, reduced mitochondrial volume and density, and reduced muscle bulk and strength (Ventura-Clapier *et al*, 2002). Exercise enhances cardiac and skeletal muscle metabolism by increasing mitochondrial biogenesis and by enhancing fatty acid β -oxidation via PGC-1 α signalling (Ventura-Clapier *et al*, 2007). Recently, Toth *et al.*(2011) have shown that chronic HF reduces AKT phosphorylation in human skeletal muscle compared with patients with normal cardiac function. The decrease in AKT phosphorylation in skeletal muscle of HF subjects could partly be related to the decrease in blood and nutrient supply to the highly oxidative, fatigue-resistant type I muscle fibres. Decrease in phosphorylated AKT in skeletal muscle will lead to decrease in protein synthesis and enhances protein breakdown via the activation of FOXO transcription factors and the transcription of E3 ubiquitin ligases important for muscle proteolysis such as Atrogin-1 and MurF-1. Hence, the cardiovascular and the musculoskeletal systems are interrelated in the sense that functional deterioration in one system is negatively reflected on the other one.

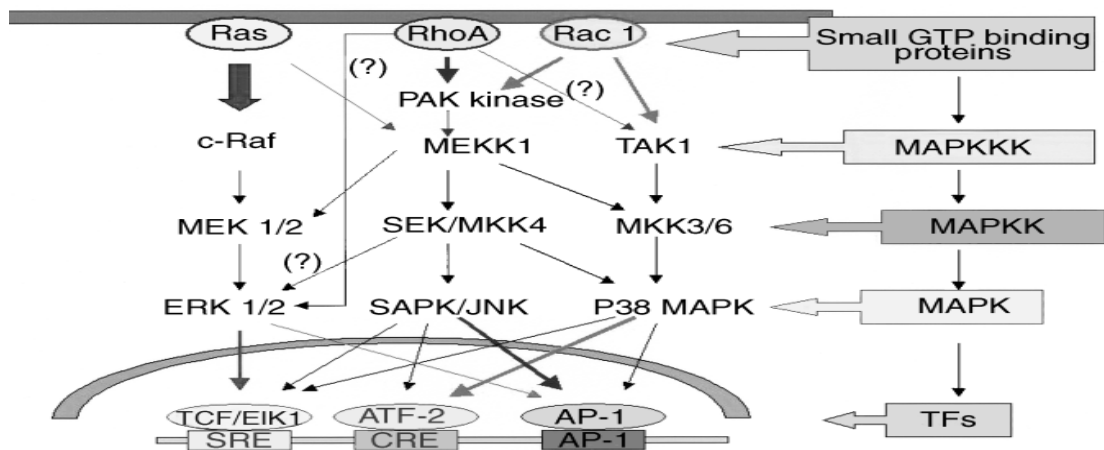


Figure 1.7: Three different MAPK signaling pathways named ERK pathway, SAPK/JNK pathway, and p38 pathway are well established and involved in the intracellular signaling of myocardial remodelling. From these MAPK pathways, various transcription factors such as Elk1, ATF-2 (CREB), AP-1, NF- κ B, and Sp1 are activated and start the transcription of target genes (Taken from Diwan and Dorn, 2007).

Protein kinase C

Protein kinase C (PKC) is a family of serine/threonine kinases. PKCs are major mediators of signal transduction pathways and have been shown to regulate sets of biological functions as diverse as cell growth, differentiation, apoptosis, transformation and tumorigenicity (Nishizuka, 1984; Nishizuka, 1992; Nishizuka, 1995). All PKCs have a common general structure with 2 principal modules: a NH₂-terminal regulatory domain that contains the membrane-targeting motifs and a COOH-terminal catalytic domain that binds ATP and substrates. Throughout the primary sequence of the enzymes, there is an alternation of conserved (C1–C4) and variable (V1–V5) regions. According to differences in the binding capability of their regulatory domain, the presently known 10 members of the PKC family have been grouped into 3 classes: the classical PKCs (α , β with 2 isoforms β 1 and β 2, γ) which are regulated by calcium, diacylglycerol (DAG) and phospholipids, the novel PKCs (δ , ϵ , θ) which are regulated by DAG and phospholipids but lack the calcium binding domain and the atypical subgroup (ζ , λ or i , the mouse ortholog of λ in humans) which are insensitive to both calcium and DAG. The relative content of each isozyme in the heart has been a controversial issue since it was found as different in different species. In one of the first reports characterizing the expression of PKC isozymes in the heart, PKC ϵ was described as the principal, if not the only PKC isozyme to be expressed in the rat heart (Bogoyevitsch *et al*, 1993). Later, many other PKC were found in the heart, principally PKC α , PKC δ , and PKC ζ (see Mackay and Mochly-Rosen, 2001 for review). Even PKC γ , that was considered to be present only in the brain was found by us (Rouet-Benzineb *et al*, 1996) and others (Ping *et al*, 1997) in the rabbit heart. However, PKC γ present in the heart originates from non-muscle cells and 2 PKC isozymes of the group of novel PKC isozymes, PKC ϵ and PKC δ , are among the principally expressed PKCs in cardiomyocytes along with PKC α in human and rodent hearts.

Although they are members of the same subgroup (the so-called novel group), PKC δ and PKC ϵ mediate contrasting and even opposing effects. Overexpression of PKC ϵ stimulates growth and is oncogenic in mouse, rat, and human fibroblasts (Mischak *et al*, 1993; Cacace *et al*, 1993; Perletti *et al*, 1996). In contrast, PKC- δ inhibits cell growth in fibroblasts (Mischak *et al*, 1993; Watanabe *et al*, 1992). When overexpressed in vascular smooth muscle cells, PKC δ but not PKC ϵ induces apoptosis in response to PMA

(phorbol 12-myristate 13-acetate) treatment (an activator of classical and novel PKCs) (Mischak *et al*, 1993). In salivary gland acinar cells, PKC- δ is essential for etoposide-induced apoptosis (Reyland, 1999).

In general, PKC ϵ appears thus as the “bad” due to its oncogenic properties. It has even been proposed as a tumor marker (Gorin and Pan, 2009). In contrast, PKC δ appears as the “good” with proapoptotic properties in cancers and it is an antioncogene. Surprisingly, for cardiologists, at least in the domain of ischemia, PKC ϵ is the “good” since it has been shown to be a major actor in the mechanisms inducing preconditioning (the process by which short periods of ischemia protect the heart against a long ischemic period of ensuing ischemia). In contrast, inhibition of PKC δ during reperfusion protects the heart from reperfusion-induced damage (Budas *et al*, 2007) although both were shown to have parallel hypertrophic effects (Chen *et al*, 2001).

PKC delta and epsilon

PKC δ and PKC ϵ have a 41% amino acid homology with 9% gaps. This score is relatively low. It can be compared to that between PKC α and PKC β that shows 81% homology with 0% gaps and it is similar to that between PKC δ and PKC ζ (39% homology with 5% gaps) which are members of 2 different subgroups (novel and atypical). The structural differences between PKC δ and PKC ϵ lie not only in the variable domains but also in the C1 and C2 regions of the regulatory domain.

In contrast with preconditioning to ischemia in which PKC δ and PKC ϵ have opposite roles, both act in the same direction during the development of hypertrophy (Chen *et al*, 2001). The activation of PKC ϵ may be a factor that induces ventricular hypertrophy with its positive effect on cell growth. In this line, the relation between PKC ϵ and the cytoskeleton is a mechanism that potentially initiates hypertrophy via phosphorylation of proteins in the costameres, which then transmit signalling to the Z-disk for parallel or series addition of thin filaments regulated via actin capping (Russel *et al*, 2010).

The activation of PKC ϵ was shown during stretch of cardiomyocytes (Vincent *et al*, 2006). In isolated guinea-pig hearts, stretch, one of the principal activators of ventricular

hypertrophy, has been shown to induce a PKC ϵ translocation to membranes that was partially inhibited by losartan (Paul *et al*, 1997). In vivo, an induction of concentric cardiac hypertrophy with an overexpression of constitutively active PKC ϵ (Takeishi *et al*, 2000) or with the expression of cardiac specific PKC ϵ activator (Mochly-Rosen *et al*, 2000) was shown. The effect of PKC ϵ is in general considered to lead to a concentric hypertrophy. However, in mice overexpressing PKC ϵ (Goldspink *et al*, 2004), the evolution of hypertrophy was quite deleterious since it led to a dilated cardiomyopathy. Thus, the effect of PKC ϵ may differ depending upon its level of expression.

PKC activity has been generally described as increased with different behaviours of different isozymes. In general, PKC ϵ and PKC δ increased content and translocation towards the membrane fraction were found but this is not a universal finding in all types of hypertrophy. In aortic banding in rats (Gu and Bishop, 1994), guinea pigs (Takeishi *et al*, 1999) and in severe human aortic stenosis (Simonis *et al*, 2007) an increased concentration of PKC ϵ was found in membranes. In contrast, PKC δ content was found as unchanged in nuclear–cytoskeletal fraction in the model of rat aortic banding (Gu and Bishop, 1994). Other workers found the same translocation in a completely different type of hypertrophy, right ventricular hypertrophy induced by pulmonary hypertension due to chronic hypoxia in rats (Morel *et al*, 2003). However, opposite results were described in hypertrophy or heart failure by others (Mohammadi *et al*, 1997; Fryer *et al*, 1998; Rouet-Benzineb *et al*, 1996; Braun *et al*, 2004; Koide *et al*, 2003; Bowling *et al*, 1999). In human failing hearts, left ventricular PKC ϵ content was decreased (Bowling *et al*, 1999). In rabbit left ventricular hypertrophy (Mohammadi *et al*, 1997) and heart failure (Rouet-Benzineb *et al*, 1996), researchers have found a decreased cardiac content of PKC ϵ and a similar down-regulation was demonstrated in a model of genetic hypertension while PKC δ was unaffected (Fryer *et al*, 1998). In contrast, PKC ϵ activity was found to be unchanged in rat aorto-caval fistulas while PKC δ was increased (Braun *et al*, 2004). During the development of heart failure in Dahl salt sensitive rats, PKC ϵ and PKC δ contents were increased in the hypertrophy phase but PKC ϵ content tended to be in heart failure while PKC δ remained elevated (Koide *et al*, 2003). Thus, although PKC ϵ is an actor in the development of hypertrophy, its expression in the myocardium and its translocation are not found as increased in all models.

Many interactions of PKC ϵ with other proteins have been published. Using proteomic analysis, PKC ϵ was shown to be associated with at least 36 proteins including the potential downstream targets of PKC ϵ , such as Src and Lck tyrosine kinases, mitogen-activated protein kinases (p38 MAPKs, JNKs, and ERKs), and upstream modulators of PKC ϵ , such as PI3 kinases and their substrate, PKB/Akt (Ping *et al*, 2001). As previously noted, these kinases had also been implicated in preconditioning, suggesting a potentially important mechanism for the transmission and integration of signals during preconditioning. The presence of two isozymes of nitric oxide synthase (NOS) (inducible [iNOS] and constitutive [eNOS]) in the PKC ϵ signalling complexes was also found (Ping *et al*, 2001).

PKC ϵ has been shown to bind scaffold proteins. The first interaction of this type has been that of PKC ϵ with AKAP79/150 that also binds the phosphatase PP2B, calcineurin (Klauck *et al*, 1996). PKC ϵ and calcineurin were shown to bind an anchoring protein called CG-NAP in the Golgi in a hypophosphorylated inactive form PKC ϵ and we also found a direct interaction between this kinase and this phosphatase during cellular stretch (Vincent *et al*, 2006). Actin filaments also function as scaffold proteins for signaling complexes. In the central nervous system, a protein–protein interaction of PKC ϵ with actin, unique to PKC ϵ (Prekeris *et al*, 1996), was shown to be sufficient to maintain PKC ϵ in a catalytically active conformation, thereby, eventually regulating cytoskeletal dynamics (Prekeris *et al*, 1998; Nakhost *et al*, 1998). In the heart, F-actin bound PKC ϵ selectively over PKC δ (Huang and Walker, 2004) and it was shown that the binding interface between PKC ϵ and cardiac myofilaments was mainly on the V1 region of PKC ϵ and the interface between PKC ϵ and F-actin was mainly on the C1 region of PKC ϵ (Huang and Walker, 2004).

PKC α

With respect to the conventional isoforms, PKC α is the predominant subtype expressed in the mouse, human, and rabbit hearts, while PKC β and PKC γ are detectable but expressed at substantially lower levels (Hambleton *et al*, 2006; Pass *et al*, 2001; Ping *et al*, 1997). Numerous reports have also associated PKC α activation or an increase in PKC α expression with hypertrophy, dilated cardiomyopathy, ischemic injury, or

mitogen stimulation (Dorn and Force, 2005). For example, haemodynamic pressure overload in rodents promotes translocation and presumed activation of PKC α during the hypertrophic phase or during the later stages of heart failure (Gu and Bishop, 1994; Jalili et al, 1999; De Windt et al, 2000; Bayer et al, 2003; Braun et al, 2002). Increased expression of PKC α was also observed following myocardial infarction (Wang et al, 2005; Simonis et al, 2007). Human heart failure has also been associated with increased activation of conventional PKC isoforms, including PKC α (Simonis et al, 2007; Bowling et al, 1999). Thus, PKC α fits an important criterion as a therapeutic target; its expression and activity are increased during heart disease.

A number of independent molecular mechanisms have been associated with the known protection from heart failure by PKC α inhibition, although all of these mechanisms have so far been associated with modulation of cardiac contractility. The first identified mechanism whereby PKC α inhibition enhances cardiac contractility is through SR Ca²⁺ loading (Braz et al, 2004). Specifically, PKC α phosphorylates inhibitor 1 (I-1) at Ser67, resulting in greater protein phosphatase 1 activity, leading to greater phospholamban (PLN) and less activity of the SR Ca²⁺ ATPase (SERCA2) pump (Braz et al, 2004). Less SERCA2 activity reduces SR Ca²⁺ load leading to reduced Ca²⁺ release during systole, hence reduced contractility. Thus, inhibition of PKC α with a drug or dominant negative mutant would reduce PP1 activity for PLN, making PLN less inhibitory towards SERCA2 and leading to mild enhancements in SR Ca²⁺ load to augment contractility. Greater SR Ca²⁺ loads and cycling have been shown to benefit the mouse from numerous insults that would otherwise cause heart failure (Dorn and Molkenin, 2004). Indeed, gene therapy trials using SERCA2 overexpression in the hearts of humans with failure have already shown early promise.

Another mechanism whereby PKC α can directly alter cardiac contractility is through phosphorylation of G-protein-coupled receptor kinase 2 (GRK2). Indeed, cardiac-specific activation of PKC α led to increased GRK2 phosphorylation and activity, blunted cyclase activity, and impaired β -agonist-stimulated ventricular function (Malhota et al, 2010). GRK2 is known to directly control β -adrenergic receptor function and cardiac contractility (Koch, 2004). Consistent with these observations, mice overexpressing the cPKC activating peptide in the heart showed uncoupling in β -adrenergic receptors (Hahn et al, 2003).

PKC α also appears to directly phosphorylate key myofilament proteins including cardiac troponin I (cTnI), cTnT, titin, and myosin binding protein C, which leads to decreased myofilament Ca²⁺ sensitivity and reduced contractility in myocytes (Belin et al, 2007; Sumandea et al, 2003; Kooij et al, 2010; Hidalgo et al, 2009). These myofilament proteins could also be phosphorylated by other cPKC isoforms (Huang et al, 2001; Wang et al, 2006). Moreover, PKC α has also been shown to phosphorylate the α 1c subunit of the L-type Ca²⁺ channel, an effect that could alter contractility as well (Yang et al, 2009). Similarly, PKC β I, β II, and γ can also phosphorylate serine residues in the α 1c subunit (Yang et al, 2009). These data further suggest the possible promiscuous nature of the cPKCs in the regulation of protein phosphorylation, Ca²⁺ cycling, and cell contractility. Despite these similarities in targets, PKC α functions are different from PKC β and γ in altering contractility because adult cardiac myocytes from PKC β overexpressing TG mice showed increased Ca²⁺ transients and increased contractility (Huang et al, 2001), while PKC α overexpressing TG mice showed depressed cardiac contractility (Braz et al, 2004). Moreover, myocytes from adult PKC α null hearts showed increased contractility and augmented Ca²⁺ transients (Braz et al, 2004).

In addition to these specific molecular targets that all appear to alter cardiac contractility, it remains possible that inhibition of PKC α protects the myocardium through other unknown mechanisms that are unrelated to contractility. For instance, PKC-mediated phosphorylation has been correlated with myofibril degeneration in cardiomyocytes, while preservation of myofilament integrity may represent another potential mechanism for the beneficial effects of PKC inhibition (Sussman et al, 1997). Other potential PKC α targets may include structural proteins, signalling proteins, and transcription factors (Palaniyandi et al, 2009). Outside of a myocyte intrinsic effect, PKC α inhibition can also protect the entire cardiovascular system by limiting thrombus formation through a platelet specific mechanism (Konopatskaya et al, 2009).

The results in genetically modified animal models and in isolated adult myocytes clearly show a cardioprotective effect with PKC α inhibition. Such results suggested that a nontoxic and tissue available pharmacological inhibitor with selectivity toward PKC α might be of significant therapeutic value. Thus, the effects of cPKC inhibitors of the bisindolylmaleimide class, such as ruboxistaurin (LY333531), Ro-32-0432, or Ro-31-

8220, were tested in different rodent heart failure models. For example, short-term infusion of Ro-32-0432 or Ro-31-8220 significantly enhanced contractility and left ventricular developed pressure in isolated mouse hearts (Hambleton et al, 2006). Importantly, Ro-31-0432 or Ro-31-8220 did not significantly augment cardiac contractility in *PKCα*^{-/-} mice, strongly supporting the conclusion that the biological effect of the bisindolylmaleimide compounds on contractility are due to PKCα. Moreover, general activation of both classic and novel PKC isozymes in the heart by short-term infusion of PMA produces a dramatic decrease in contractility in wild type mice but not in *PKCα*^{-/-} mice (Hambleton et al, 2006). This result also suggests that PKCα is the primary negative regulator of cardiac contractility after global activation of all PKC isozymes in the heart. With respect to heart failure, short-term or long-term treatment with Ro-31-8220 in the *Csrp3* null mouse model of heart failure augmented cardiac contractility and restored pump function. PKC inhibition with Ro-31-8220 or Ro-32-0432 also reduced mortality and cardiac contractile abnormalities in a mouse model of myotonic dystrophy type 1 (DM1) (Wang et al, 2009).

Another PKCα/β inhibitor, ruboxistaurin, has been through late-stage clinical trials for diabetic macular edema and shown to be well tolerated and hence was extensively analyzed in both mouse and rat models of heart failure (The PKC-DRS Study Group, 2007). Although ruboxistaurin was originally reported to be PKCβ selective (Jirousek et al, 1996), it is equally selective for PKCα (IC50 of 14 nmol/L for PKCα versus 19 nmol/L for PKCβII). Moreover, given that PKCα protein levels are much higher than PKCβ in the human and mouse hearts (Hambleton et al, 2006), it further suggests that ruboxistaurin functions predominantly through a PKCα-dependent mechanism. Ruboxistaurin increased baseline contractility by 28% in rats with acute infusion (Hambleton et al, 2006). Acute infusion of ruboxistaurin also augmented cardiac contractility in wild type and *PKCβγ*^{-/-} mice but not *PKCα*^{-/-} mice (Liu et al, 2009). These results indicate that ruboxistaurin enhances cardiac function specifically through effects on PKCα but not PKCβ or PKCγ. Ruboxistaurin also prevented death in wild type mice throughout 10 weeks of pressure overload stimulation, reduced ventricular dilation, enhanced ventricular performance, reduced fibrosis, and reduced pulmonary edema comparable to or better than metoprolol treatment (Liu et al, 2009). Ruboxistaurin when administered to *PKCβγ* null mice subjected to pressure overload, resulting in less death and heart failure, further suggesting PKCα as the primary target

of this drug in mitigating heart disease (Liu et al, 2009). In addition, Boyle et al. (2005) showed that ruboxistaurin reduced ventricular fibrosis and dysfunction following myocardial infarction in rats. Ruboxistaurin treatment also significantly decreased infarct size and enhanced recovery of left ventricular function and reduced markers of cellular necrosis in mice subjected to 30 min of ischemia followed by 48 h of reperfusion (Kong et al, 2008). Connelly et al. (2009) demonstrated that ruboxistaurin attenuated diastolic dysfunction, myocyte hypertrophy, collagen deposition, and preserved cardiac contractility in a rat diabetic heart failure model. These results in rodents overwhelmingly support the contention that PKC α inhibition with ruboxistaurin, or related compounds, protects the heart from failure after injury. Hence, cPKC inhibitors, such as ruboxistaurin, should be evaluated in heart failure patients, especially given its apparent safety in late phase clinical trials in humans (The PKC-DRS Study Group, 2007). A related cPKC inhibitory compound from Novartis, AEB071, was also shown to be safe in human clinical trials for psoriasis and could be a candidate for translation in the heart failure area (Skvara et al, 2008).

While there is a clear need for novel inotropes to support late-stage heart failure, there may also be a therapeutic niche in the earlier stages of heart failure if the inotrope is selective. One unique aspect associated with PKC α inhibition is that contractility is only moderately increased, which may have a safer profile compared with traditional inotropes. In addition, PKC inhibition is not subject to significant desensitization as is characteristic of β -agonists (Hambleton et al, 2006). More importantly, PKC α inhibition has a prominent effect on SR Ca²⁺ cycling and the myofilament proteins as a means for altering cardiac contractility. These mechanisms of action are significantly downstream of how traditional β -adrenergic receptor agonists function and hence might bypass the negative effects of traditional inotropes that promote arrhythmia and myocyte death. The inhibition of PKC α may also benefit a failing myocardium independent of contractility regulation because PKC α is involved in reactive signalling within the heart that participates in hypertrophy, pathological remodelling, and decompensation.

The diabetic heart

Diabetic Cardiomyopathy; phenotypic characteristics and potential pathophysiological mechanisms

The diabetic cardiomyopathy's progression seems to be divided into three stages. The early stage is characterized by metabolic disturbances (glucose, fatty acid metabolism, Ca homeostasis etc), without significant functional and structural cardiac changes. At the middle stage, necrosis and apoptosis of the myocytes lead to fibrosis and hypertrophy. The left ventricle's mass begins to increase and the diastolic function is altered. The systolic function may be normal. Hypertrophy and diastolic abnormalities are observed most commonly and earlier than systolic abnormalities. The late stage of the diabetic cardiomyopathy is characterized by changes in the small vessels and increased left ventricle's mass. Both the diastolic and systolic function is altered (Fang et al, 2004).

The body weight is significantly smaller in streptozotocin-induced diabetic rats than in control rats. On the contrary heart weight and the left ventricular weight normalized for the body weight were higher in diabetic rats. The higher left ventricular mass normalized for body weight reveals the eccentric hypertrophy in this ventricle. The end-diastolic and the end-systolic dimensions were similar in diabetic and control animals, but when corrected for body weight were higher in the diabetic groups (Bollano et al, 2006). The left ventricular end-diastolic pressure was higher, but the dP / dT was depressed in these animals. These results indicate the diastolic and systolic dysfunction in the diabetic heart. The heart rate was significantly lower in diabetic rats. There was also a collagen content significantly higher in diabetic left ventricular tissues (Bollano et al, 2006).

Changes in contractile proteins

Alterations in proteins involved in the regulation of the actomyosin system, (Malhotra and Sanghi, 1997) and a shift in the myosin heavy chain from type α to β (Takeda et al, 1998), have been observed in diabetic myocardium resulting in reduced systolic tension development. Calcium homeostasis is also affected in diabetic heart. Sarcoplasmic

reticulum calcium pump protein (SERCA2a) expression is reduced with reduced sarcoplasmic reticulum calcium sequestration and intracellular calcium overload, a situation which may account for the impaired relaxation (Depre et al, 2000). There is also a reduction in the sarcoplasmic reticulum Ca-ATPase (Abe et al, 2002) and in sarcolemmal Na/K ATPase and Calcium-binding activities.

Changes in metabolism

Metabolic changes in diabetic heart consist of a defect in the utilization of the glucose (Chen et al, 1984). This is caused by the depletion of glucose transporters (GLUT 1-GLUT 4), that carry glucose across the sarcolemmal membrane (Eckel and Reinauer, 1990; Garvey et al, 1993) and by the down-regulation of the glycolytic proteins. The glucose uptake from the diabetic heart is also reduced because of the insulin deficiency or resistance (Kaestnet et al, 1991; Kinulainen et al 1994). Insulin deficiency reduces the activation of glycogen synthase and phosphatase activity (Miller, 1983). Furthermore, the enhanced fatty acid oxidation exerts an inhibitory effect on glucose oxidation (Liedtke et al, 1988) and consequently on the entry of glucose into the cardiac cell. Thus, the cardiac metabolism is shifted from the glucose utilization towards the free fatty acids. The enhanced fatty acid metabolism leads to the accumulation of toxic intermediates (Rodrigues et al, 1998). The inhibition of glucose oxidation by the fatty acids could be a major factor for the development of diabetic cardiomyopathy.

Apoptosis/necrosis

Increased cell death is another characteristic of diabetic cardiomyopathy. Loss of myocytes leads to impaired cardiac function, in adult myocardium. Oxidative stress caused by reactive oxygen and nitrogen species due to hyperglycemia may activate the process of apoptosis and myocyte necrosis (Venero et al, 2005). On the other hand, necrosis causes extracellular widening and deposition of collagen in a diffuse or scattered manner (Falcao-Pires et al, 2009; Jin et al, 2009). Collagen deposition is referred to an increase in type III collagen in the diabetic heart (Falcao-Pires et al, 2009).

The Streptozotocin-induced type 1 diabetic rat model

A significant part of the current understanding of the pathophysiology and pathogenesis of cardiac disease in DM can be attributed to experimentation in the rodent model system. The rodent model shares many phenotypic similarities to human disease and meaningful correlates can be drawn in metabolism and physiology. With regard to the influence of DM on cardiac structure and function, rat models have been effectively used to study structural phenotypes, physiology of altered energy flux and storage, insulin secretion and action and numerous other metabolic parameters (McNeill, 1999; Kahn, 2005). Considering the limitations of invasive testing in human tissues and ethical and logistical constraints herewith, rat models provide invaluable opportunities to study detailed molecular mechanisms underlying the pathophysiology of diabetes in controlled conditions accounting for microbiological, chemical, genetic and environmental factors. Other advantages include relatively short generation intervals, adaptability to invasive testing and other economic considerations.

Rat models mimicking physiological and pathological states unique to each diabetes subtype have been developed to investigate inherent etiopathologic heterogeneities. Chemically induced type-1 diabetes is by far the most common model of animal DM and frequently involves administration of agents that produce the desired pathology by producing toxic effects on the beta cells of the pancreas. Alloxan and STZ are widely used diabetogenic agents owing to their specific action on β cells resulting in lesions that quite accurately resemble β cell destruction characteristic of T1DM and the sustenance of a relatively permanent diseased state to enable investigation of chronic effects of DM (Lenzen, 2008). Compared to alloxan (cyclic urea analog), STZ is reported to have a greater specificity to β cells, a longer half life and is associated with lower mortality rates (Lenzen, 2008), making it the agent of choice for chemical induction of experimental diabetes in this study.

The antimicrobial STZ [2-deoxy-2(3-methyl-3-nitrosourea)1-D-glucopyranose], is a product of *Streptomyces achromogens* and has been used as a chemotherapeutic alkylating agent. Declared diabetogenic in 1963, by Rakieta *et al.*, STZ results in a metabolic milieu characterised by insulinopenia termed ‘STZ-diabetes’ resulting from targeted β cell necrosis via processes of methylation, free radical generation and NO production. Post administration, the GLUT-2 transporter transports STZ into pancreatic

cells wherein it generates highly reactive carbonium ions (CH^3+) that alkylate and fragment DNA bases along a defined sequence of events. DNA damage results in the activation and overstimulation of the pro-survival, cell repair nuclear enzyme poly(ADP-ribose) polymerase and concomitant reduction in β cell NAD^+ and ATP stores (Sandler and Swenne, 1983; Elsner *et al.*, 2000). This alteration in redox states and histological changes in the affected cells ultimately result in β cell necrosis. Other supplementary hypotheses in the diabetogenic potential of STZ include its ability to act as an intracellular nitric oxide (NO) donor, generating 3',5'-cyclic guanosine monophosphate (cGMP) and NO that participate in DNA damage by inhibiting aconitase (Turk *et al.*, 1993). Finally, the participation of STZ in xanthine metabolism has been associated with increases in ROS that may further accelerate cell death and inhibition of insulin synthesis (Nukatsuka *et al.*, 1990). In aggregate, these mechanisms result in deficits in insulin biosynthesis, glucose-induced insulin secretion and glucose transport and metabolism culminating in diabetes that resembles human hyperglycemic nonketotic DM (Weir *et al.*, 1981).

Impact of diabetes on cardiac remodeling after myocardial infarction

Cardiac remodelling may be viewed as stress response to an index event such as myocardial ischaemia or imposition of mechanical load which leads to a series of structural and functional changes in the viable myocardium. Early in the course of this process, a variety of compensatory mechanisms are in operation, such as activation of neuro-hormonal and inflammatory systems. In the short term, this response seems to restore cardiovascular function to a normal homeostatic range but with time, sustained activation of these systems can lead to secondary end-organ damage (Swynghedauw, 1999).

Conflicting data are available concerning the effects of diabetes on post-AMI LV remodelling. Furthermore, considerable controversy exists regarding the underlying pathophysiological mechanisms. In streptozotocin (STZ)-induced hyperglycemia, AMI exacerbated LV chamber dilatation and contractile dysfunction (Shiomi *et al.*, 2003). In diabetic MI mice models, apoptosis in association with interstitial fibrosis were more enhanced in diabetic post-MI hearts (Matsusaka *et al.*, 2006). Similarly, STZ-induced diabetes in rats resulted in prolonged cardiomyocyte apoptosis after MI (Backlund *et al.*,

2004). Enhanced apoptosis was found to be in parallel with increased LV enlargement and fibrosis (Backlund et al, 2004).

In a model of type 2 diabetes in rats, heart failure progression was accelerated 8 wk after coronary artery ligation as assessed by enhanced LV remodelling and contractile dysfunction, (Chandler et al, 2007). This response was accompanied by greater increases in atrial natriuretic factor and skeletal alpha-actin, while a decrease in peroxisome proliferator-activated receptor-alpha-regulated genes in association with increased myocardial triglyceride levels were observed (Chandler et al, 2007). These results indicate that diabetes may accelerate post-MI remodelling through mechanisms which are not fully understood.

New insights in cardiac remodelling:the role of thyroid hormone

Heart failure remains one of the main causes of death in the modern world despite the advances in the treatment of this syndrome (Morrissey et al., 2010; Roger, 2010). Current therapies are rather limited to medical treatments aiming to optimize cardiac haemodynamics than to restore the damaged myocardium. The potential of rebuilding the injured heart has only recently been appreciated with cell base therapies to be a promising therapeutic approach. However, despite the progress made in this field, there still remain issues of the optimal cell type to transplant, cell delivery, homing of the cells, electrical coupling and so forth (Tongers et al., 2011).

A growing body of evidence obtained from studies on nature's models of regeneration reveals that a natural healing process may exist in the heart (Chablais et al., 2011; Schnabel et al., 2011). The concept of tissue regeneration has been described in Greek mythology with chained Prometheus to watch his own liver regenerate every time it was devoured by an eagle and Hydra to regenerate its many heads. The potential of cardiac muscle regeneration has been an issue discussed as early as 1852. Interestingly, Zielonko, in 1874, under the supervision of Virchow, did the first experimental work studying hearts from rabbits and frogs and came to the conclusion that hypertrophy is not only due to the enlargement of individual muscle fibers but also to cellular hyperplasia. Since then the issue remains largely controversial due to the lack of

understanding of the underlying mechanisms of this process (King, 1940; Robledo, 1956).

The importance of thyroid hormone (TH) in organ remodelling has been recently revealed in studies concerning models of tissue and organ regeneration such as the amphibian metamorphosis or the zebra fish regeneration (Bouzaffour et al., 2010; Furlow and Neff, 2006; Jopling et al., 2010; Sato et al., 2007; Slack et al., 2008). Intriguingly, the process of amphibian metamorphosis that allowed life to emerge from the aquatic environment to earth is entirely dependent on TH. This gene programming is evolutionary conserved in mammals with TH being critical for embryonic heart development and the control of various aspects of regeneration by reactivating developmental gene programming later in adult life (Pantos et al., 2011a).

Thyroid hormone and cardiac remodeling

Re-activation of the fetal phenotype: a window for regeneration

Cardiac remodeling is a stress response process to an index event such as ischemia, mechanical loading, metabolic alterations etc. Early in this process, a variety of compensatory mechanisms are in operation, such as activation of the inflammatory and neuro-hormonal systems. In the short term, this response seems to restore cardiovascular function to a normal homeostatic range but with time, sustained activation of these systems can lead to end-organ damage. One of the main characteristics of this response is the reactivation of the fetal gene programming that drives cells to de-differentiate. Thus, features of fetal heart metabolism re-emerge and include the preference of glucose metabolism over fatty acids as substrates for energy provision while early response genes, such as c-myc and c-fos are highly expressed with isoform switches of many other proteins, including metabolic enzymes and sarcomeric proteins (decrease in α -MHC and increase in β -MHC expression) (Rajabi et al., 2007; Swynghedauw, 1999; Taegtmeyer et al., 2010). The physiological relevance of the return of the heart to fetal gene programming remains still a debatable issue. Heart failure physiologists view this process as a maladaptive response which leads to the progressive decline in cardiac function. However, fetal re-programming may also result in a 'low energy state' which adapts and protects the damaged myocardium upon stress

(Rajabi et al., 2007). In fact, the remodeled myocardium appears to be resistant to hypoxia or ischemia–reperfusion injury (Pantos et al., 2005b; Pantos et al., 2007b). An expanded view regarding the biological significance of the reactivation of fetal phenotype after stress comes recently from observations showing that amphibians or mammals can retain the ability to regenerate at early stages of development (Slack et al., 2008; Herdrich et al., 2011; Porrello et al., 2011). Thus, the return to fetal phenotype which occurs after stress may be thought as a permissive state for regeneration (Witman et al., 2011). In fact, de-differentiated cells retain the ability to proliferate and / or grow and then to re-differentiate to specialized cells that comprise the regenerated structure or organ (Bouzaffour et al., 2010; Jopling et al., 2010; Odelberg, 2002). This mechanism appeared early in species evolution and allowed living organisms to adapt to the environmental stresses (Sanchez Alvarado, 2000). The molecular control of this process until now remains largely unknown.

Thyroid hormone (TH) : the same player in organ embryonic development and response to stress

The potential link of TH to organ development and regeneration has been revealed in studies on the amphibian metamorphosis (Sato et al., 2007). Amphibian metamorphosis is one of the nature's paradigms of tissue and organ remodeling and this process seems to be entirely controlled by TH. Almost 100 years ago, Gudernatsch made the remarkable discovery that equine thyroid extracts could accelerate the metamorphosis of tadpole into juvenile frogs (Gudernatsch, 1912). Since then, several studies, if not all, have shown that the morphological and functional changes of metamorphosis are the result of alterations in the transcription of specific sets of genes induced by TH (Berry et al., 1998; Shi et al., 2001; Furlow et al., 2004; Furlow and Neff, 2006).

Action of TH

Thyroxine (T4) is secreted by thyrocytes and enters the cell through various mechanisms. Passage of T4 may be passive, given the lipophilic nature or transporter- and energy-dependent (Hennemann, 2005). T4 is converted to triiodothyronine (T3) by deiodinases which are seleno-proteins (type-1 and type-2 deiodinases, D1 and D2),

while T3 is degraded by type-3 deiodinase, D3 (Bianco et al., 2002). D1 can also inactivate TH by converting T4 to reverse T3 (rT3) (Bianco and Kim, 2006). Cellular actions of TH may be initiated within the cell nucleus, at the plasma membrane, in the cytoplasm, and at the mitochondrion.

Thyroid hormone system seemsto be an ancestral hormone system and interestingly, thyroid hormone receptor (TR) genes present at the base of biletarians before TH production, indicating an importantphysiological role of this receptor. Living organisms acquired the ability of producing THwith increasing evolutionary complexity (Bianco et al., 2002).TH nuclear receptors (TRs) mediate the biological activities of T3 via transcriptional regulation. Two TR genes, α and β , encode four T3-binding receptor isoforms (α 1, β 1, β 2, and β 3). The transcriptional activity of TRs is regulated at multiple levels. Besides being regulated by T3, transcriptional activity depends on the type of TH response elements located on the promoters of T3 target genes, by the developmental- and tissue-dependent expression of TR isoforms, and by nuclear co-regulatory proteins. Nuclear co-regulatory proteins modulate the transcription activity of TRs in a T3-dependent manner. In the absence of T3, co-repressors act to repress the basal transcriptional activity, whereas in the presence of T3, co-activators function to activate transcription. In addition to ligand binding, phosphorylation events play important roles in nuclear receptor action at the molecular level including modulation of hormone binding, co-factor recruitment, ligand-dependent gene transcription and cytosolic-nuclear trafficking. Phosphorylation of TRs is mediated via kinase intracellular signaling (Nicoll et al., 2003).

The distinct function of TR isoforms has been identified by phenotypic analysis of mutant mice strains, in transfection studies and in studies using thyroid analogs (Kinugawa et al., 2001; Flamant and Samarut, 2003; Kinugawa et al., 2005; Pantos et al., 2005a; Pantos et al., 2007d; Pantos et al., 2008c). TR α 1 seems to be critical for most of TH actions in cardiac and non cardiac tissues. Thus, TR α 1 ensures the maintenance of homeostasis by controlling heart rate (Wikstrom et al., 1998; Tavi et al., 2005), adaptive thermogenesis (Wikstrom et al., 1998) stress response (Venero et al., 2005), and food intake (Pantos et al., 2005a; Pantos et al., 2007d). Furthermore, TR α 1 controls DNA damage-induced tissue repair (Kress et al., 2008). TR α 1 is predominantly expressed in the myocardium and regulates important genes related to the contractile function, pacemaker activity, conduction and metabolism. Thus, myosin isoform expression (Kinugawa et al 2001; Flamant and Samarut, 2003; Kinugawa et

al., 2005; Pantos et al., 2005a; Pantos et al., 2007d; Pantos et al., 2008c), SERCA inhibitory protein phospholamban (PLB) (Belakavadi et al., 2010), connexin-43 (Stock and Sies, 2000), potassium channels (Gloss et al., 2001; Mansen et al., 2011) and glucose utilization are all found to be regulated by TR α 1 (Esaki et al., 2004).

TH and the developing heart : the relevance of TR α 1 receptor

The role of TH as developmental signal has been demonstrated in several studies with *Xenopus laevis* to be an ideal system for ascertaining the developmental roles of TH and its receptor (Slack et al., 2008). Interestingly, this system reveals that regulation of TH/TR axis can allow the same simple molecule TH to induce completely opposite morphological responses in distinct tissues. In this context, TR α seems to play an important physiological role due to its dual function (liganded vs un-liganded state). Thus, at early developmental stages in which TH is low, TR α receptor is highly expressed and at its un-liganded state acts as a repressor of TH positive regulated genes and prevents precocious metamorphosis (Sato et al., 2007). At later stages, the rise in TH levels results in the conversion of the un-liganded to the liganded TR α state and triggers cell differentiation and completes metamorphosis (Furlow & Neff, 2006). Similarly, in mammals, during fetal life, TR α 1 is increased while TH levels remain low and decreases after birth with the rising of the circulating TH (White et al., 2001).

Based on this evidence, subsequent studies using mammal cell based models have shown that this developmental program has been conserved in mammals. Thus, in the embryonic heart derived cell line (H9c2) which is considered an established model to study skeletal and heart muscle differentiation, TH was shown to be critical in this process (van der Putten et al., 2002; van der Heide et al., 2007). In fact, intracellular T4 and T3 increase during the progression of cell differentiation with a concomitant increase in the expression of TR α 1 and this response could be prevented by pharmacological inhibition of thyroid hormone binding to TR α 1 (van der Putten et al., 2002; van der Heide et al., 2007; Meischl et al., 2008; Pantow et al., 2008c). The potential role of TR α 1 in cell differentiation/de-differentiation process has been further documented in transfection studies using neonatal cardiomyocytes. Thus, neonatal cardiac cells over-expressing TR α 1 and treated with TH were able to differentiate into adult cardiac cells (Kinugawa et al., 2005). On the contrary, untreated cardiomyocytes remained undifferentiated and this response was characterized by an increase in cell

growth with a fetal pattern of myosin heavy chain (MHC) isoform expression (Kinugawa et al., 2005). This novel action was shown to be a unique feature of TR α 1 receptor. In fact, the over-expression of TR β 1 could promote cell differentiation regardless the presence or absence of TH.

The effect of TH on cell differentiation appears to be mediated via the activation of distinct kinase signalling pathways. Thus, transient activation of ERK is involved in TH induced changes in cell shape while the effect on cell growth is p38 MAPK and/or mTOR dependent (Kinugawa et al., 2005; Pantos et al., 2007e; Ojamaa, 2010). These data have recently been confirmed in fetal ovine cardiomyocytes (Chattergoon et al 2011).

TH and the response of the myocardium to stress: the relevance of TR α 1 receptor

There is a growing body of evidence that a fetal pattern of thyroid hormone signalling is reactivated in the damaged myocardium which may be of physiological relevance (Witman et al., 2011). Thus, myocardial ischemia was shown to induce various changes in TH–TR homeostasis which closely resemble those occurring during embryonic development of the heart (Pantos et al., 2008b). The most characteristic feature of this response is the re-expression of TR α 1 along with the increased activation of growth kinase signaling (ERK and mTOR) during the development of reactive cardiac hypertrophy and its decline during the transition to heart failure (Pantos et al., 2010). This association indicates that a potential link of TR α 1 to growth signalling may exist. Thus, in a model of phenylephrine (PE, an α 1-adrenergic agonist) induced pathological cell growth, PE resulted in a redistribution of TR α 1 receptor from the cytosol to nucleus. This unique response was found to be an ERK dependent process which required an intact mTOR signaling. These changes were subsequently shown to be of physiological relevance regarding the cellular response to stress. With the removal of TH from culture medium, TR α 1, which remained un-liganded, displayed a repressive action resulting in cell de-differentiation with large cells of undefined shape and filopodia like structures containing disoriented, dense myofibrils and increased amount of β -MHC (Pantos et al., 2008). On the contrary the addition of TH in the culture medium resulted in cell differentiation by switching the TR α 1 to the liganded state (Pantos et al., 2008). These series of experiments revealed for the first time that

TH signaling is critical for the response of the cardiac cell to stress and TH can rescue cardiomyocytes from the stress induced cell de-differentiation.

TH promotes endogenous regeneration by activating developmental gene programming

In accordance with the observations made in cell based models, several proofs of concept studies in animals with myocardial infarction showed that that thyroid hormone, while having a detrimental effect on healthy tissue, could have a reparative effect on the injured myocardium (Ojamaa et al., 2000; Degens et al., 2003; Pantos et al., 2007c; Chen et al., 2008; Pantos et al., 2008a; Henderson et al., 2009; Pantos et al., 2009a; Pantos et al., 2009b; Forini et al., 2010). Thus, TH or thyroid analogues treatment early after coronary ligation in animals reduced apoptosis (Chen et al., 2008; Kalofoutis et al., 2010) and limited the extent of infarct size (Forini et al., 2010; Abohashem-Aly et al., 2011). More importantly, TH could favorably remodel the viable, non-ischemic myocardium. TH accelerated the development of cardiac hypertrophy characterized by an adult pattern of MHC isoformexpression. This response caused an early normalization of wall stress which is known to be a critical determinant of oxygen consumption and myocardial performance (Grossman et al., 1975; Dorn, 2007). TH treatment had also a striking effect on cardiac geometry which critically determines the mechanical efficiency of the myocardium (Coghlan and Hoffman, 2006; Sehgal and Drazner, 2007). TH either early or late after myocardial infarction could reshape the heart from spherical to the elipsoid shape (Pantos et al., 2008a; Pantos et al., 2009b). These favorable changes were the result of the TH effect on cardiomyocyte remodelling as indicated by the characteristic changes seen at the molecular level (Pantos et al., 2007e; Pantos et al., 2008c). Thus, factors involved in mitochondrial DNA transcription and biogenesis, calcium handling proteins and cardio-protective molecules such as HSP70 were all found to be over-expressed with TH treatment (Pantos et al., 2008a; Forini et al., 2010). Furthermore, TH modulated the regulatory role of PKC ϵ and PKC α on contractile function (Pantos et al., 2007c).

Akt : a critical player in TH-induced favorable effects on cardiac remodeling

One of the major players in the response of the cardiac cell to stress is the Akt signaling pathway. Moreover, Akt is a critical regulator of physiological growth. Thus, chronic Akt blockade aggravates pathological hypertrophy while inhibits exercise-induced physiological hypertrophy (Buss et al. 2011). Furthermore, the effect of stem cell transplantation after myocardial infarction in mice was shown to be Akt dependent (Tseng et al. 2010). However, the level of phosphorylation of this kinase is of important physiological relevance. In fact, in transgenic animals, chronic Akt activation caused a spectrum of phenotypes from moderate cardiac hypertrophy with preserved systolic function and cardio-protection to massive cardiac dilatation and sudden death. Along this line, TH administration in mice with myocardial infarction had a beneficial or detrimental effect depending on the extent of Akt phosphorylation induced by TH. Thus, mild activation of Akt caused by the replacement dose of TH resulted in favorable effects on the myocardial performance of the post-infarcted heart, while further induction of Akt by higher dose of TH was accompanied by detrimental effects (Pantos, 2010).

Thyroid hormone and cardio-preservation: The thyroid hormone ‘paradox’

Unlike the long held belief, TH can protect the heart against ischemia despite the fact that it increases oxygen consumption (by accelerating heart rhythm and increasing cardiac contractility) and depletes the heart from glycogen (Pantos et al., 2001; Pantos et al., 2002; Pantos et al., 2003a; Pantos et al., 2003b; Pantos et al., 2006). TH pre-treatment and ischemic pre-conditioning had a similar functional response to ischaemic insult which was characterized by a marked increase in post-ischaemic recovery of function despite the exacerbation of diastolic dysfunction during the ischemic period (ischemic contracture). This effect was shown to be mediated via the suppression of the pro-apoptotic p38 MAPK signalling pathway (Pantos et al., 2003b). The explanation of this paradox lies on the fact that the differentiation/physiological growth process can share common pathways with those involved in stress response. Thus, the activation of redox regulated signaling pathways which mediate cell differentiation, results also in the up-regulation of redox regulated cardio-protective molecules, such as heat shock

proteins which can increase tolerance of the cell against ischemia (Strandness and Bernstein, 1997; Pantos et al., 2003a; Pantos et al., 2006).

Studies in the isolated rat heart models further revealed that TH is able to acutely protect the myocardium via its non genomic action. Thus, T₃, although had no effect on uninjured myocardium, it significantly improved post-ischemic recovery of function and limited apoptosis in the injured myocardium. This effect was also mediated by the suppression of the pro-apoptotic p38 MAPK. Intriguingly, the non-genomic effect of T₃ was shown to be initiated at the cytosolic TR α 1 receptor, a mechanism which probably explains the failure of T₄ to limit reperfusion injury (Pantos et al., 2009a; Pantos et al., 2011b).

Clinical implications

Can ‘low T₃ syndrome’ be either a bystander or player? An expanded overview

Several studies have provided evidence that TH metabolism is altered under cardiac and non-cardiac illnesses and after cardiac surgery, a condition known as non thyroidal illness or ‘low T₃ syndrome’ . The cause of low T₃ state seems to be multi-factorial with cytokines to be major contributors to this response (Abo-Zenah et al., 2008). Thus, interferon- α and interleukin-6 (IL-6) can cause a response similar to “‘low-T₃ syndrome’” and in patients with acute myocardial infarction a negative correlation between IL-6 or CRP and T₃ levels has been observed (Kimura et al., 2000).

The physiological relevance of “‘low-T₃ syndrome’” until now remains elusive. However, low T₃ levels have been correlated with the severity of the clinical assessment of heart dysfunction (NYHA) in patients with congestive heart failure and were the only predictor of NYHA at the multivariate analysis that included several neuro-hormonal parameters which change in heart failure (Iervasi et al., 2003; Pingitore et al., 2006). Along this line, total T₃ in plasma was strongly correlated with the maximal oxygen consumption (peak VO₂) in patients with dilated cardiomyopathy (ischaemic and non ischaemic) as assessed by cardio-respiratory stress testing (Pantos et al., 2007a). In addition low T₃ plasma levels were found to be an independent risk factor for increased mortality in patients with heart failure (Iervasi et al., 2003). T₃ levels in serum decline within 48 h after acute myocardial infarction (Eber et al., 1995)

or within 6–24 h after cardiac surgery (Holland et al., 1991). Lower T3 levels appear to be an independent predictor of mortality after myocardial infarction (Friberg et al., 2002). Furthermore, T3 levels are strongly correlated to early and late recovery of cardiac function with T3 levels at six months to be an independent predictor of the recovery of the myocardium (Lymvaios et al., 2011). Interestingly, patients who spontaneously recover T3 levels in plasma after myocardial infarction are those with markedly improved cardiac functional recovery (Lymvaios et al., 2011). It is of interest that T3 has also been found to be an independent determinant of atherosclerosis progression (Barth et al., 1987; Baxter and Webb, 2009; Ichiki, 2010).

TH in cardiac surgery

TH has long been used in cardiac surgery as inotrope and vasodilator. The efficacy and safety of TH as postoperative treatment has been recently assessed in a systematic review of all the randomized controlled studies comparing T3 to placebo (Kaptein et al., 2010). Thus, both high- and low-dose iv T3 therapy were shown to improve cardiac index after coronary artery bypass surgery. Mortality was not significantly altered by high-dose iv T3 therapy and could not be assessed for low-dose iv or oral T3. Effects on systemic vascular resistance, heart rate, pulmonary capillary wedge pressure, new onset atrial fibrillation, inotrope use, serum TSH and T4 were inconclusive. This study calls for further large scale investigations with particular emphasis on T3 effects on reperfusion injury (Kaptein et al., 2010).

The potential effect of T3 on limiting reperfusion injury has recently been addressed in patients undergoing cardiac surgery and has been compared to an established cardioprotective regime the glucose-insulin potassium (GIK) treatment. A total of 440 patients were recruited and randomized to either placebo (5% dextrose) (n = 160), GIK (40% dextrose, K⁺ 100 mmol L⁻¹, insulin 70 µL⁻¹) (0.75 mL kg⁻¹ h⁻¹) (n = 157), T3 (0.8 µg kg⁻¹ followed by 0.113 µg kg⁻¹ h⁻¹) (n = 63) or GIK + T3 (n = 60). GIK/placebo therapy was administered from start of operation until 6 h after removal of aortic cross-clamp (AXC) and T3/placebo was administered for a 6-h period from removal of AXC. Serial hemodynamic measurements were taken up to 12 h after removal of AXC and troponin I (cTnI) levels were assayed to 72 h. Cardiac index (CI) was significantly increased in both the GIK and the GIK/T3 group in the first 6 h compared with placebo and T3 therapy (Ranasinghe et al., 2006). T3 therapy increased CI versus placebo between 6

and 12 h after AXC removal but combination therapy did not. Release of cTnI was lower in all treatment groups at 6 and 12 h after removal of AXC (Ranasinghe et al., 2006).

The potential of pre-operative TH treatment to precondition the myocardium has also been explored. Thus, eighty patients undergoing coronary artery bypass grafting with a preoperative EF% less than 30% were randomized to the T3 group (125 µg/day orally for 7 days preoperatively and from the first postoperative day till discharge) and to the placebo group. Patients in the T3 group had a higher cardiac index than patients in the placebo group in the entire post-CPB periods. Furthermore, mean inotropic requirements remained lower in the T3 group than in the placebo group (Sirlak et al., 2004).

TH in myocardial infarction

A phase II, randomized, double blind, placebo-controlled study has been recently initiated testing the use of substitutive doses of synthetic T3 in patients with STEMI (ST-Elevation Myocardial Infarction) and borderline/reduced circulating T3 (Pingitore et al., 2011). Treatment with either synthetic TH or placebo starts during the in hospital period in presence of stable haemodynamic conditions (i.e. 48-72 hrs after STEMI) and will be taken for further 6 months after hospital discharge (Gerdes and Iervasi, 2010; Pingitore et al., 2011).

Working hypothesis: Distinct change in thyroid hormone receptor can lead to cardiac remodelling during diabetes-induced heart failure in STZ-induced diabetic rats following acute myocardial infarction.

Main aims of the study: Based on this evidence, the present study attempted to explore the following:

1. Can DM accelerate post MI remodelling?
2. Are these responses associated with changes in thyroid hormone signalling?
3. Can alterations in thyroid hormone signalling result in changes in growth kinase signalling and fetal like changes in contractile proteins?
4. Can thyroid hormone either prevent or reverse cardiac remodelling in STZ-induced diabetic heart

Some specific aims

1. To develop the STZ-induced type1 DM model and to undertake the relevant surgery to induce myocardial infarction.
2. To undertake physiological and biochemical studies measuring a number of physiological and molecular biochemical parameters including TH levels in the blood plasma.
3. To investigate protein expressions in TH receptors and other signalling proteins in the heart.
4. To analyze the data and write up the PhD thesis

CHAPTER 2

MATERIALS AND METHODS

Materials

Animals- Young adult male Wistar rats

Drugs: Streptozotocin, thyroid hormone, ketamine hydrochloride, thyroid hormones, aspirin, iodoacetic acid, phenylbutazone,, sodium salicylate,

Reagents; SDS-PAGE gel electrophoresis, 2 –mercaptoethanol, Elisa assay kits, buffer solutions, acrylamide, agents for western Blotting, specific antibodies for the different proteins and kinases, EGTA,EDTA,PMSE.

Chemicas; Analar grade chemicals

Equipment; Langendorff's perfusion set up, ecocardiograph equipment, equipment for Westerbn Blotting, SDS-PAGE systemCCD camera, chemiluminescence equipment, glucose merer.

Methods

Animals

Male Wistar rats weighing between 280-360 g, were maintained on a 12 h light/dark cycle and fed with a standard chow *ad libitum*. The rats were handled in accordance with the Guide for the Care and Use of Laboratory Animals published by the US National Institutes of Health Guide (NIH Pub. No. 83-23, Revised 1996). Approval was also granted by the Ethics Review Board Committees of the University of Athens and the University of Central Lancashire.

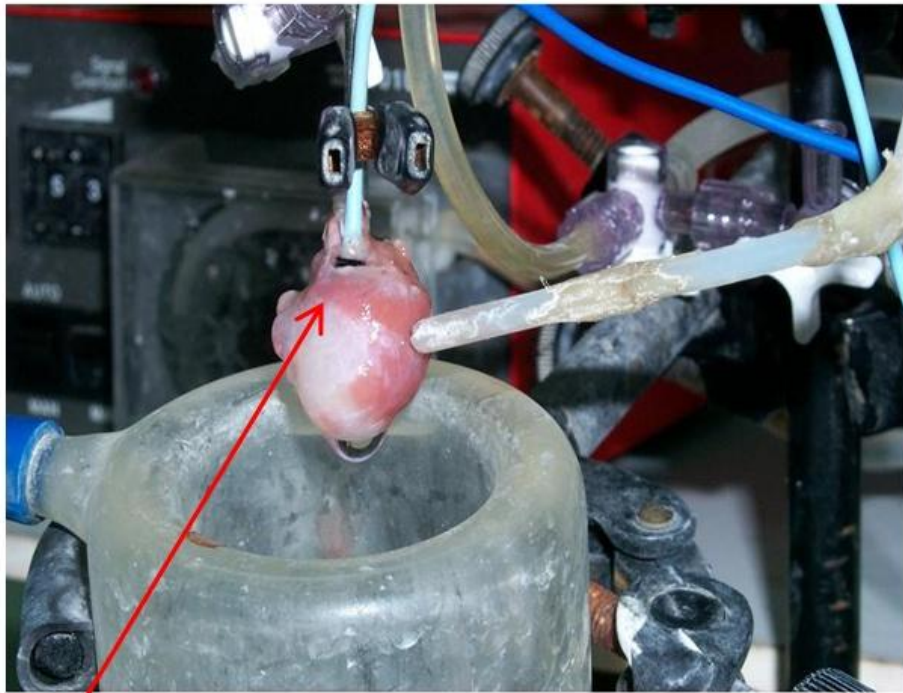
Induction of Diabetes

Diabetes mellitus (DM) was induced by a single injection of streptozotocin (STZ; either 35 mg/kg bw or 60 mg/kg bw; i.p) prepared in 0.1 M sodium citrate buffer, pH 4.5 (Sigma, Munich, Germany) as described previously (Shao et al, 2010; Kalofoutis et al, 2010; Lymvaios et al, 2011). STZ induced diabetes within 2-3 days following injection by destroying the pancreatic beta cells. Age-matched non-diabetic Wistar rats were injected with sodium citrate buffer alone and used as healthy controls. Diabetic animals and non-diabetic age –matched control group were kept in metabolic cages individually and separately under normal feeding and drinking conditions as well as metabolism control state for the first 4 days after STZ injection. Water consumption and urine volume were measured in (ml) on a daily basis. Four days after the injection of STZ, urine samples were tested for glucose and ketone levels using Keto-Diastix (Bayer). The dose of 35 mg/kg; i.p. STZ was selected after preliminary experiments that showed successful induction of glucosuria without significant keto-acidosis. In fact, urine volume increased in STZ-treated rats from 8.7 ± 0.6 ml on Day 0 to 31.9 ± 1.9 ml on day 4 while glucose concentration in urine had a mean value of 626 ± 54 mg/dL. Rats were subjected to surgical procedure 30 days after STZ injection.

Experimental model of myocardial infarction (MI)

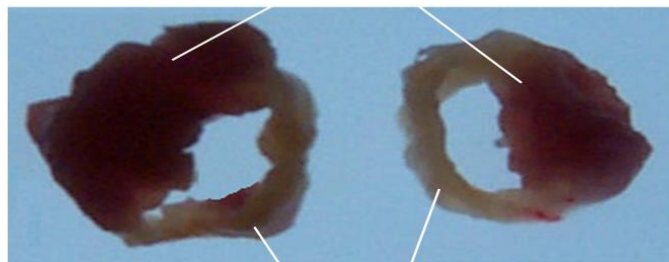
Myocardial infarction was induced by ligation of the left coronary artery as previously described (Pantos et al, 2007a, 2007b; Kalofoutis et al, 2010; Lymvaios et al, 2011). Rats were anaesthetized with an intraperitoneal (ip) injection of ketamine (70 mg/kg) and midazolame (0.1 mg/kg), intubated and ventilated via a tracheal cannula using a

constant-volume rodent ventilator (Harvard Apparatus, Inspira, 50 breaths/min, 1 ml/100 g tidal volume). Anaesthesia was maintained by inhalation of small doses of sevoflurane (1-2%). Left thoracotomy was performed at the fourth intercostal space followed by pericardiotomy. Left coronary artery was then ligated with a 6-0 silk round-bodied suture. The heart was quickly returned to the chest cavity, the chest was closed and the rats were allowed to recover using assist mode ventilation. Atelectasis was prevented by using positive end-expiratory pressure at the end of the surgical procedure. Continuous electrocardiogram (ECG) recordings were used to monitor heart rate and any changes due to ischaemia after coronary artery ligation. Body temperature was maintained at 37° C by using a heating blanket (Harvard Homeothermic Blanket, 50-7061). The mortality rate was up to 15-20% in the infarction control group, while it increased up to 30-40% in the diabetic infarction group in the first 24 h following the surgical procedure. Myocardial infarctions which produced a scar area of 60 mm² to 105 mm² were included in this study, corresponding to 25%-40% of the left ventricle (see Figure 2.1). The animals were left to recover for 2 weeks after myocardial infarction. The same procedure was followed for sham-operated control animals, but the coronary artery was not ligated.



(A) Ligation of coronary artery-acute MI in rats

Viable hypertrophic
myocardium



Scar tissue

(B)

Figure 2.1: Rat heart subjected to coronary artery ligation mounted on a Langendorff's apparatus (A). Scar area can be seen (upper image). Cross-sections of the left ventricle of post-infarcted rat heart. Scar tissue and viable hypertrophic myocardium can be seen ((B)). Typical of 7-8 such different experiments for control and diabetic hearts.

Functional and structural assessment

Echocardiography

Following 2 weeks of experimental surgery, rats were sedated with ketamine hydrochloric acid (100 mg/Kg) and heart function was evaluated by echocardiography as previously described (Pantos et al, 2007a, 2007b; Kalofoutis et al, 2010; Lymvaivos et al, 2011). Short and long-axis images were acquired using a digital ultrasound system (Vivid 7 version Pro, GE Healthcare) with the 14.0-MHz i13L probe. A large number of consecutive measurements were performed and analysed by two independent operators.

Left ventricular (LV) internal diameter at the diastolic phase (LVIDd), LV internal diameter at the systolic phase (LVIDs), posterior wall thickness at the diastolic phase (LVPW), systolic velocity of the posterior wall radial displacement (SVPW) and the ejection fraction (EF%) were measured. EF% was calculated using the Simpson equation. SVPW was measured from two-dimensional guided M-mode recordings obtained at the mid-ventricular level as previously described (Pantos et al, 2007a; 2007b; Shao et al, 2010; Kalofoutis et al, 2010; Lymvaivos et al, 2011). SVPW was used to assess the segmental contractile function of the non-infarcted myocardium, while EF% was used to determine the global contractile LV function. Wall tension index (WTI) was defined as the ratio $(LVIDd^2/Posterior\ Wall\ thickness)$ as previously described (Pantos et al, 2007a ; 2007b; Shao et al, 2010; Kalofoutis et al, 2010; Lymvaivos et al, 2011). WTI was measured in order to indirectly assess myocardial wall stress. In addition, sphericity index (SI), defined as the ratio of maximum long axis (in mm) to maximum short axis (in mm) of the left ventricle was determined in order to assess LV geometry. All measurements were averaged for at least 3 consecutive cardiac cycles (see Figure 2.2).

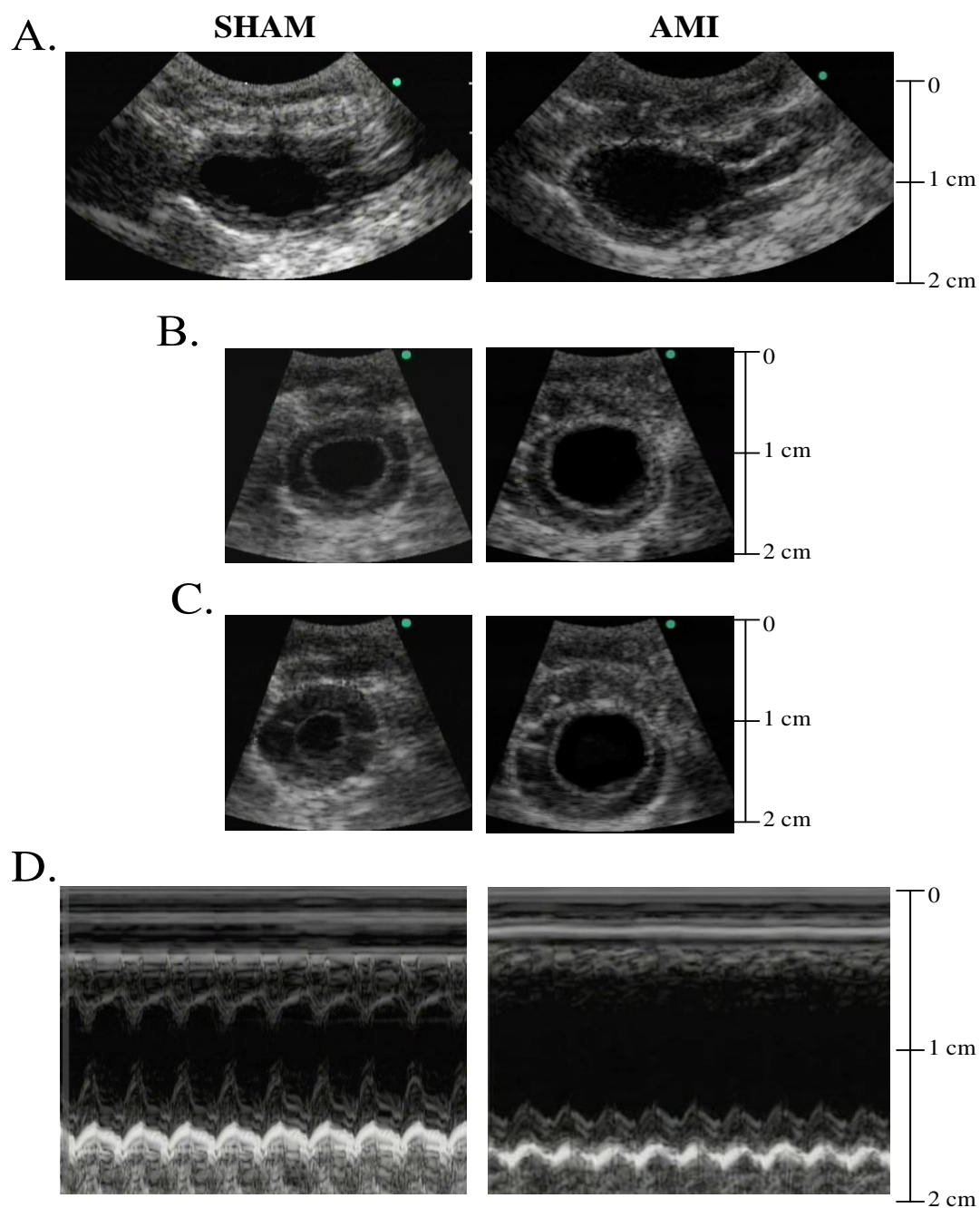


Figure 2.2: Long-axis view images (A), short-axis view images at diastole (B) and at systole (C) and (D) M-mode images obtained by transthoracic echocardiography. Typical of 7-8 such different experiments for either control or diabetic rats.

Echocardiographic analysis of myocardial deformation

The typical images in Figure 2.2 were processed in a workstation with software (EchoPAC Q analysis, General Electric). The method has been previously described (Pantos et al, 2007a ; 2007b; Shao et al, 2010; Kalofoutis et al, 2010; Lymvaivos et al, 2011) . The endocardial border was traced in an end-systolic frame. The software automatically selected 6 equidistant tissue-tracking regions of interest in the myocardium. The outer border was adjusted to approximate the epicardial border. The software automatically selected suitable stable acoustic objects for tracking, searched for them in the next frame using absolute differences algorithm. The computer provided a profile of radial strain (%) with time. On parasternal short-axis view, radial strain was deformation toward the LV center. Outcome measurements included end-systolic strain as the point during systole when the strain rate became zero from a previously positive value (radial strain rate) using the strain rate by time graph of the software analysis package. This time point of zero strain rate represented the transition from contraction to relaxation and had been previously used to define the end of systole and the initiation of diastole.

Isolated heart preparation

A non-ejecting isolated rat heart preparation was perfused at a constant flow according to the Langendorff's technique (Pantos et al, 2007a ; 2007b; Shao et al, 2010; Kalofoutis et al, 2010; Lymvaivos et al, 2011). Rats were anaesthetized with ketamine hydrochloric acid and heparin 1000 IU/kg was given intravenously before thoracotomy. The hearts were rapidly excised, placed in ice-cold Krebs-Henseleit buffer solution and mounted on the aortic cannula of the Langendorff's perfusion system(see Figure 2.3).. Hearts were paced at 320 beats/min with a Harvard pacemaker. An intra-ventricular balloon allowed measurement of contractility. Left ventricular balloon volume was adjusted to produce an average initial left ventricular end-diastolic pressure of 7-8 mmHg in all groups. The water filled balloon was connected to a pressure transducer and the LV pressure signal was transferred to a computer using data analysis software (IOX, Emka Technologies) which allowed continuous monitoring and recording of heart function.

Left ventricular developed pressure (LVDP), defined as the difference between left ventricular peak systolic pressure and left ventricular end-diastolic pressure, represented a contractility index obtained under isometric conditions. Left ventricular systolic function was assessed by recording the left ventricular developed pressure (LVDP, mmHg) and the positive and negative first derivative of LVDP; $+dp/dt$ (mm Hg/sec), $-dp/dt$ (mm Hg/sec).

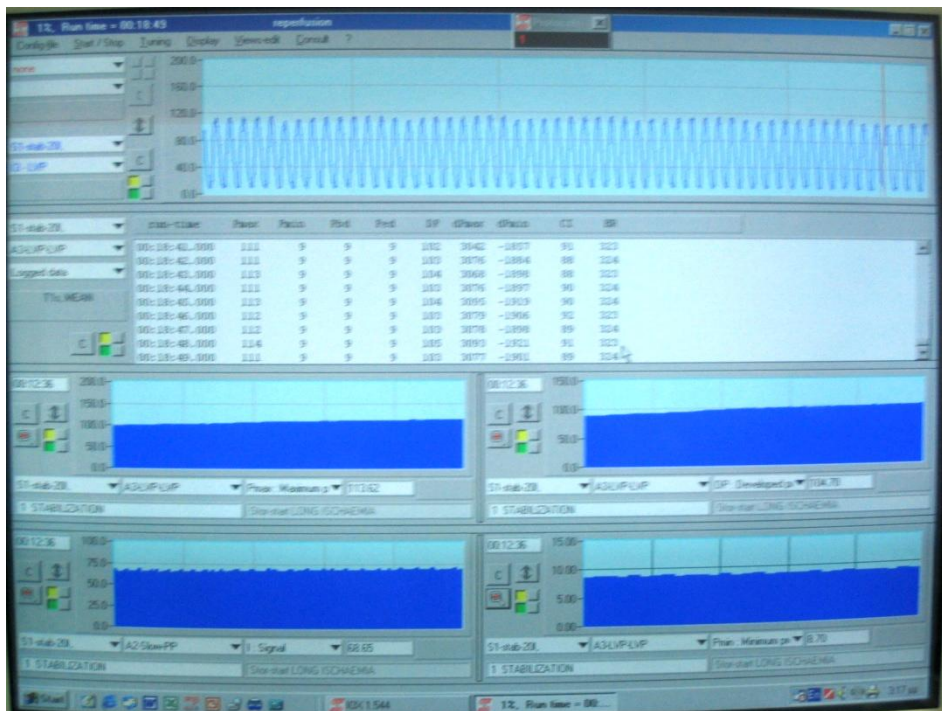
All preparations were perfused for 20 min and measurements were performed at the end of this period (Figure 2.3). The preparations included in this study were stable for at least the last 10 min of the perfusion period. Isolated hearts that did not produce stable measurements of LVDP, LV end-diastolic pressure and perfusion pressure for the last 10 min of the perfusion period were excluded from the analysis.



Figure 2.3: A photograph showing an isolated rat heart apparatus (Langendorff 's preparation).With organ bath,water jacket, transducer, stimulator chest recorder and computer to record the responses.



(A)



(B)

Figure 2.4: Photograph of a heart in the organ bath (A) and traces (B) showing procedure for protein isolation and measurement using sodium dodecyl sulfate-protein polyacrylamide (SDS-PAGE) gel electrophoresis and immuno detection system.

Measurement – Protein expressions

Left ventricular tissues were homogenized in an ice-cold buffer solution (A) containing 10 mM Hepes (pH: 7.8), 10 mM KCl, 0.1 mM EDTA, 0.1 mM EGTA, 0.5 mM PMSF, 1 mM DTT and 10 µg/ml leupeptin. A volume of 200 µl of 10% Igepal was added and samples were left in ice for 30 min. Homogenization was repeated and a small fraction of total lysis was kept for myosin heavy chain isoform analysis. The rest of the homogenate was centrifuged at 1000 g for 5 min, 4°C and the pellet containing the nuclear fraction, was washed again in buffer (A) with 1% Igepal, while the supernatant containing the cytosolic fraction was stored at -80°C. The final pellet was resuspended in 300 µl buffer (B) containing 20 mM Hepes (pH: 7.8), 420 mM NaCl, 1 mM EDTA, 1 mM EGTA, 0.5 mM PMSF, 1 mM DTT, 10 µg/ml leupeptin and 10% glycerol. The samples were incubated at 4°C for 60 min (under agitation) followed by centrifugation at 10000 g for 5 min, 4°C. The supernatant containing the nuclear fraction was separated and stored at -80°C, while the pellet containing cellular debris and cytoskeleton were discarded (Pantos et al 2007a; 2007b; Kalofoutis et al 2010). TRs protein expression was determined in nuclear fraction and signal transducing kinases were determined in cytosolic fraction. Protein concentrations were determined by the BSA method. Cytosolic samples were prepared for sodium dodecyl sulphate polyacrylamide gel electrophoresis (SDS-PAGE) by boiling for 5 min in Laemmli sample buffer containing 5% 2-mercaptoethanol. Either 20 µg (nuclear fraction) or 35 µg (cytosolic fraction) of total protein was loaded onto 7% or 10% (w/v) acrylamide gels and subjected to SDS-PAGE in a Bio-Rad Mini Protean gel apparatus. For Western blotting, following SDS-PAGE, proteins were transferred electrophoretically to a nitrocellulose membrane (Hybond ECL) at 100 V and 4 °C, for 1.5 h using Towbin buffer. After Western blotting, filters were probed with specific antibodies against After Western blotting, membranes were probed with specific antibodies against total and phospho-ERK, total and phospho-AKT (Ser 473), total and phospho-JNKs and total and phospho-p38 (Cell Signalling Technology, dilution 1:1000) overnight at 4°C, SERCA (Affinity Bioreagents, MA3-919, dilution 1:1000, o/n at 4°C), phospholamban (Affinity Bioreagents, MA3-922, dilution 1:1000, o/n at 4°C), PKCα (BD Biosciences, 610108, dilution 1:1000, 2h at R.T.) and PKCε (Affinity Bioreagents, BD Biosciences, 610086, dilution 1:1000, o/n at 4°C). Membranes were incubated with appropriate anti-mouse (Amersham) or anti-rabbit (Cell Signaling) HRP secondary antibodies.

Immunoreactivity was detected by enhanced chemiluminescence using Lumiglo reagents (New England Biolabs). Chemiluminescence was detected by the image analysis system FluorChem HD2 (AlphaInnotech Corporation, 14743, Catalina Street, San Leandro, CA) equipped with a CCD camera and analysis software. Five samples from each group were loaded on the same gel. Histone H3 protein expression was used in order to normalize slight variations in nuclear protein loading.

Measurement of myosin heavy chain isoform content

Homogenates of all samples were diluted 40 fold with Laemmli sample buffer containing 5% 2-mercaptoethanol. The composition and preparation of the gels was carried out as previously described (Pantos et al, 2007a ; 2007b; Shao et al, 2010; Kalofoutis et al, 2010; Lymvaivos et al, 2011). Briefly, the stacking and separating gels consisted of 4 and 8% acrylamide (wt/vol), respectively, with Acryl:bis-Acryl in the ratio of 50:1. The stacking and separating gels included 5% (vol/vol) glycerol. The upper running buffer consisted of 0.1 M Tris (base), 150 mM glycine, 0.1% sodium dodecyl sulphate (SDS) and 2-mercaptoethanol at a final concentration of 10 mM. The lower running buffer consisted of 0.05 M Tris (base), 75 mM glycine and 0.05% SDS. The gels were run in Biorad Protean II xi electrophoresis unit at a constant voltage of 240 V for 22 h at 4°C. The gels were fixed and silver-stained (Biorad silver stain kit). Gels were scanned and quantified using the AlphaScan Imaging Densitometer (Alpha Innotech Corporation, USA).

Measurement of thyroid hormones

Plasma L-thyroxine and 3,5,3' tri-iodothyronine quantitative measurements were performed with ELISA, using kits obtained from Alpha Diagnostic International, Texas, USA (No 1100 for total T₄ and No 1700 for total T₃), as previously described. (Pantos et al 2005) L-thyroxine and 3,5,3' triiodothyronine levels were expressed as nmol/L of plasma. Absorbance measurements were performed at 450 nm with TecanGenios ELISA reader (Tecan, Austria).

Measurement of T3

In this study, the total T3 ELISA kit was based on competitive binding of thyroxine from serum samples and enzyme-labelled T3 to T3-specific antibodies immobilized on microtiter well plates. In the assay, total T3 was released from its binding proteins by a

releasing agent present in the assay buffer. After a washing step, chromogenic substrate was added and colour developed. The enzymatic reaction (blue color) was inversely proportional to the amount of T3 present in the sample. The reaction was terminated by adding stopping solution (converts blue to yellow). Absorbance was then measured on a micro-titer well ELISA reader at 450 nm and the concentrations of T3 in samples and control were read off from the standard curve. All values were expressed as nM.

Detection Limit

Based on sixteen replicates determinations of the zero standard, the minimum concentration of total T3 detected using this assay was 20 ng/dL. The detection limit was defined as the value deviating by 2 SD from the zero standard.

Precision

Intra-assay precision:

Three serum samples (mean total T3 concentrations 11, 18, and 160 ng/dL) were eluted in three separate runs. The samples showed good intra-assay precision with % CV of 6-11.

Inter-assay precision:

Three serum samples (160, 290, and 665 ng/dL) were run in duplicate in sixteen independent assays. The samples showed good inter-assay precision (3.0-10% CV).

Linearity

A serum sample containing 1000 ng/dL was diluted with a series of T3-free serum (Figure 2.5). The dilutions were tested and the T3 recoveries were compared with the expected concentration. The samples showed excellent mean recoveries of about 105% (range 80-113%).

Specificity

The specificity of total T3 ELISA kit was determined by measuring interference from high concentrations of T4, 3,3', 5-triiodothyronine (rT3, up to 1000 ng/ml), 3,5-diiiodothyronine (up to 10 ug/dL), Aspirin (10 mg/dL) iodoacetic acid (10 ug/dL), phenylbutazone (10 mg/dL), 3',5-diiiodothyronine (T2), and sodium salicylate. No significant cross-reaction was observed with any of these compounds.

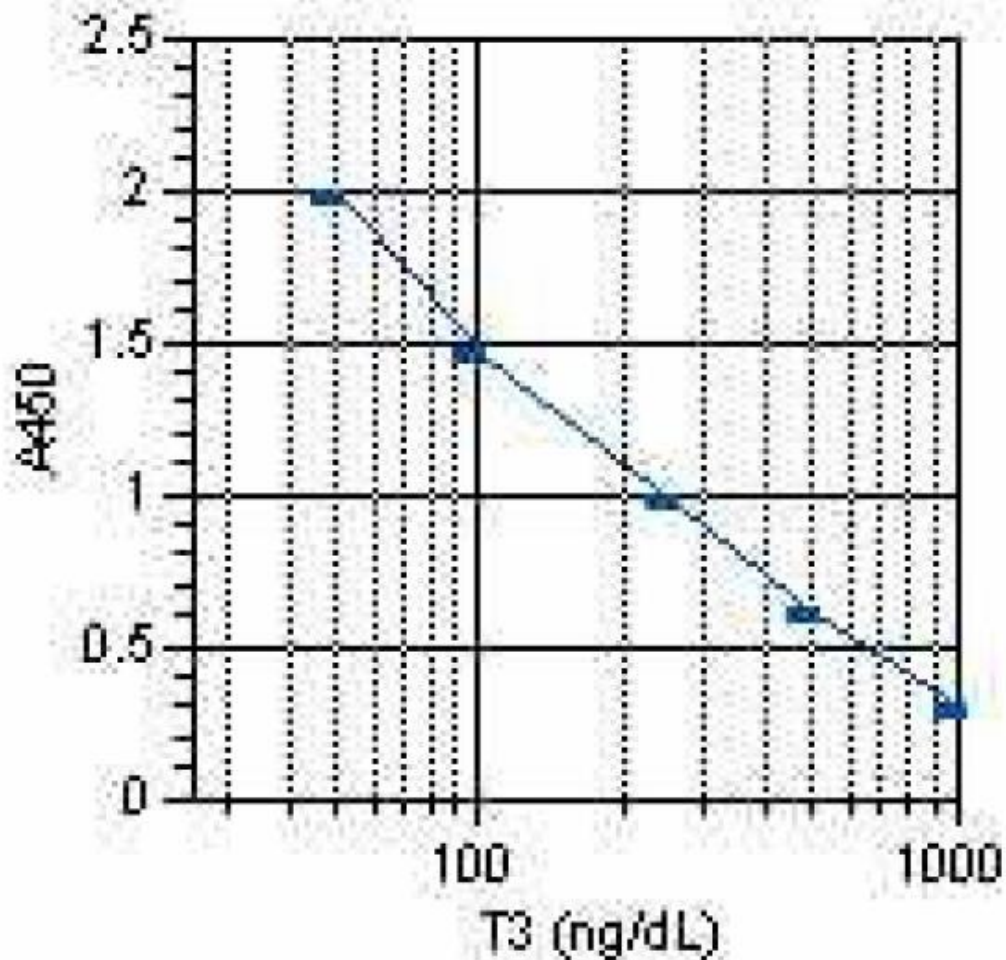


Figure 2.5: Standard assay curve for T3. Typical of 7-8 different such experiments

Measurement of T4

In this study, total T4 ELISA kit was based on competitive binding of human thyroxine from serum samples and enzyme-labeled T4 to T4-specific antibodies immobilized on micro-titer well plates. In the assay, total T4 was released from its binding proteins by a releasing agent present in the assay buffer. After a washing step, chromogenic substrate was added and colour developed. The enzymatic reaction (blue colour) was inversely proportional to the amount of T4 present in the sample. The reaction was terminated by adding stopping solution (converts blue to yellow). Absorbance was then measured on a micro-titer well ELISA reader at 450 nm and the concentration of T4 in samples and control was read off the standard curve (Figure 2.6). All values were expressed in nM.

Detection Limit

Based on sixteen replicates determinations of the zero standard, the minimum concentration of total T4 detected using this assay was 0.5 ug/dL. The detection limit was defined as the value deviating by 2 Standard deviation from the zero standard.

Precision

Intra-assay precision:

Three serum samples (mean total T4 concentrations 3.5, 6.8, 13.9 ug/dL) were run in five separate runs. The samples showed good intra-assay precision with % CV of 9-11.

Inter-assay precision:

Three serum samples (4-15 ug/dL) were run in duplicate in sixteen independent assays. The samples showed good inter-assay precision (2.7-4 % CV).

Specificity

The specificity of total T4 ELISA kit was determined by measuring interference from high concentrations of 3,5-diiodothyronine (up to 10 ug/dL), 3,3',5-triiodothyronine (rT3,,up to 1000 ng/ml), 3,3',5-triiodothyronine (T3,,up to 59nmol/l), 3,3',5-triiodothyroacetic acid (up to 42 nmol/l), 3,3',5-triiodothyropropionic acid (up to 63 nmol/l), Aspirin (10 mg/dL) iodoacetic acid(10 ug/dL), phenylbutazone (10 mg/dL). No significant cross-reaction was observed with any of these compounds.

Linearity

A serum sample containing 24 ug/dL was diluted with a series of T4-free serum. The dilutions were tested and the T4 recoveries were compared with the expected concentration. The samples showed excellent mean recoveries of about 102% (range 90-109%).

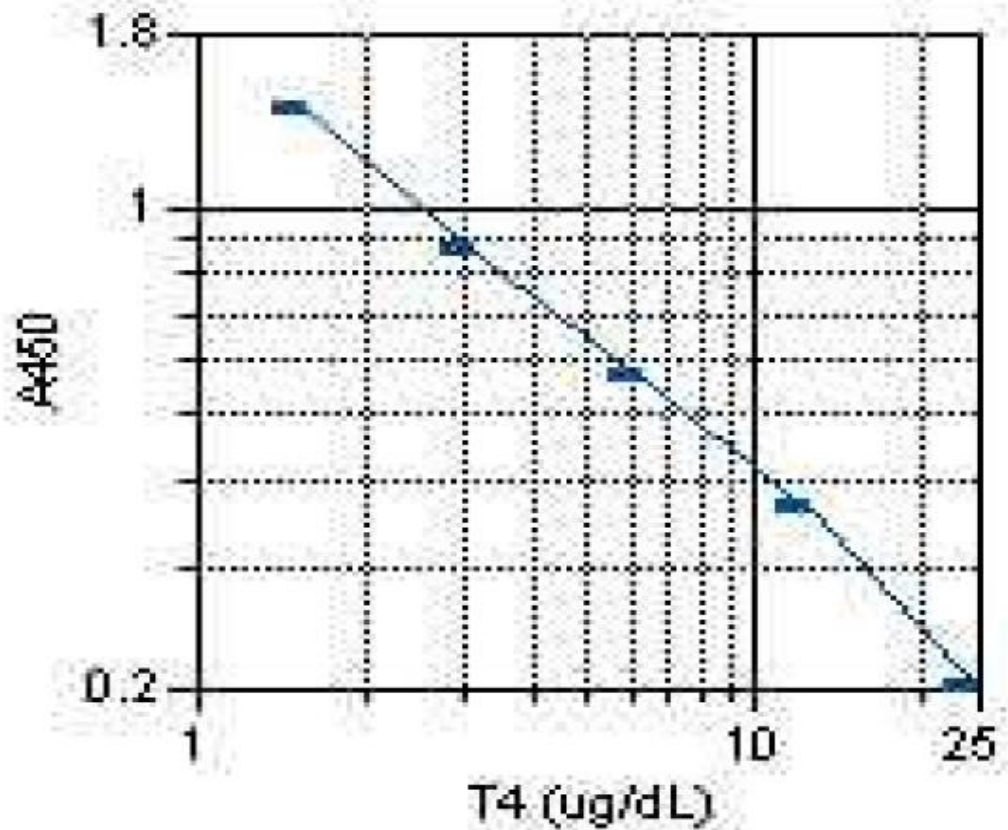


Figure 2.6: Standard assay curve for T4. Typical of 5-7 such different experiments.

General experimental protocol in this study

Rats were initially rendered diabetic with STZ. Four weeks after STZ-induced diabetes, some control and diabetic animals were induced with AMI. Two days after AMI induction, one group of rats (DM combined with AMI) were treated with TH (0.42 mg/mg T3 and 1.7 ug/mg T4 mixed with chow) for 2 weeks. Two weeks after the AMI surgical procedure, rats were anaesthetized with ketamine hydrochloride, subjected to echocardiography analysis and the hearts were removed and washed in ice-cold Krebs buffer. Left ventricle (LV) and right ventricle (RV) of the heart were separated and scar LV tissue was dissected out and the non- infarcted area was frozen in liquid nitrogen for further analysis. Blood was collected from the right atrium in order to measure total T₃ and T₄ in serum. The area of the scar tissue was measured in mm² and the weight in mg.

For the experimental protocol rats were separated in the following **five** experimental groups; **(1)** Control sham-operated rats (SHAM, n=20); **(2)** Diabetic sham-operated rats

(DM + SHAM, n=11); **(3)** Control rats subjected to myocardial infarction (AMI, n=19); **(4)** Diabetic rats subjected to myocardial infarction (DM + AMI, n=13) and **(5)** Diabetic rats subjected to myocardial infarction and thyroid hormone treatment (DM + AMI + TH, n=11).

Analysis of data and statistics

All the results are presented as means (\pm standard errors of the means). Unpaired Student's t-test and Mann-Whitney test were used to evaluate differences between groups in molecular protein analysis. One-way analysis of variance with Bonferroni or Dunnett correction was used for multiple comparisons. Significance was set at 0.05.

CHAPTER 3

RESULTS

A. Preliminary studies – Establishment of experimental model of type-1 diabetes

Streptozotocin (STZ) is a well known antibiotic and diabetogenic agent which can induce diabetes in rats by destroying the pancreatic beta cells (Bracken et al, 2004). The present study initially tested two different doses (35 mg/bw and 60 mg/bw) of STZ reported in literature to induce diabetes via intra-peritoneal (ip) injection (Qureshi et al, 2001; Howarth et al, 2002). Rats were kept in metabolic cages and urine was collected on a daily basis to determine volume and glucose and ketone concentrations in the urine. Tables 3.1 and 3.2 show analytical data including urine volume, urine glucose concentrations and urine ketone concentrations at baseline and 4 days after STZ injection employing 35 mg/bw and 60 mg/bw, respectively. The results show that 4 days after the injection of STZ, both doses (Table 3.1; 35 mg/bw and Table 3.2; 60 mg/bw) can increase significantly ($p < 0.05$) urine volume and glucose concentrations in the urine compared to base line measurements prior to the induction of diabetes. However, 35 mg/kg concentration had no significant effect on blood ketone concentration compared to 60mg/bw. Thus, a low dose of STZ injection (35 mg/bw) was selected as a more appropriate concentration for the rest of the since only small amounts traces of ketones were detected in urine samples. As such, the aim of the study was to avoid the development of keto-acidosis in blood secondary to high concentrations of glucose since acidic pH per se could be a cause of myocardial dysfunction. As a result, 35 mg/bw STZ was employed throughout this study.

Table 3.1: Table showing urine volume, urine glucose concentration and urine ketone concentration at base line and 4 days after STZ injection (ip) using 35 mg/bw.

GROUP	Base line prior to STZ injection			4 days after STZ injection		
	Urine volume (ml)	Urine Glucose (mg/dl)	Urine ketone (mg/dl)	Urine volume (ml)	Urine Glucose (mg/dl)	Urine ketone (mg/dl)
35mg/Kg	13,00	0	0	28,00	600	5,00
35mg/Kg	9,00	0	0	50,00	500	5,00
35mg/Kg	13,00	0	0	26,00	500	0,00
35mg/Kg	7,00	0	5	40,00	1000	0,00
35mg/Kg	10,00	0	0	34,00	750	0,00
35mg/Kg	10,00	0	0	40,00	1000	0,00
35mg/Kg	7,00	0	0	32,00	1000	5,00
35mg/Kg	8,00	0	5	23,00	500	5,00
35mg/Kg	12,00	0	0	10,00	250	5,00
35mg/Kg	5,00	0	0	32,00	1000	5,00
35mg/Kg	8,00	0	0	22,00	250	5,00
35mg/Kg	11,50	0	0	40,00	500	0,00
35mg/Kg	10,00	0	0	40,00	600	5,00
35mg/Kg	5,50	0	0	40,00	250	0,00
35mg/Kg	5,00	0	0	34,00	550	5,00
35mg/Kg	10,00	0	0	22,00	600	15,00
35mg/Kg	10,00	0	0	35,00	550	5,00
35mg/Kg	7,00	0	5	31,00	500	5,00
35mg/Kg	8,00	0	0	28,00	650	0,00
35mg/Kg	12,00	0	0	32,00	1000	0,00

Table 3.2: Table showing urine volume, urine glucose concentration and urine ketone concentration at base line and 4 days after STZ injection (ip) employing 60 mg/bw.

GROUP	Base line prior to STZ injection			4 days after STZ injection		
	Urine volume (ml)	Urine Glucose (mg/dl)	Urine ketone (mg/dl)	Urine volume (ml)	Urine Glucose (mg/dl)	Urine ketone (mg/dl)
60mg/K g	8,00	0	0	44,00	500	40,00
60mg/K g	9,00	0	0	55,00	1000	80,00
60mg/K g	10,00	0	0	60,00	2000	160,00
60mg/K g	7,00	0	0	50,00	1000	80,00
60mg/K g	12,00	0	0	48,00	1000	40,00
60mg/K g	8,00	0	0	52,00	1000	80,00
60mg/K g	10,00	0	0	58,00	2000	160,00
60mg/K g	11,00	0	5	48,00	1000	80,00
60mg/K g	14,00	0	0	40,00	500	40,00
60mg/K g	6,00	0	0	38,00	500	15,00

Contractile functions

Preliminary experiments in isolated rat heart preparation of normal and diabetic rats (treated with 35 mg/bw streptozocin) showed that indices of contractile function such as LVDP (Figure 3.1) and the positive and negative first derivative of LVDP (+dp/dt and -dp/dt) (Figure 3.2) were not significantly different between the 2 groups.

LVDP (mmHg)

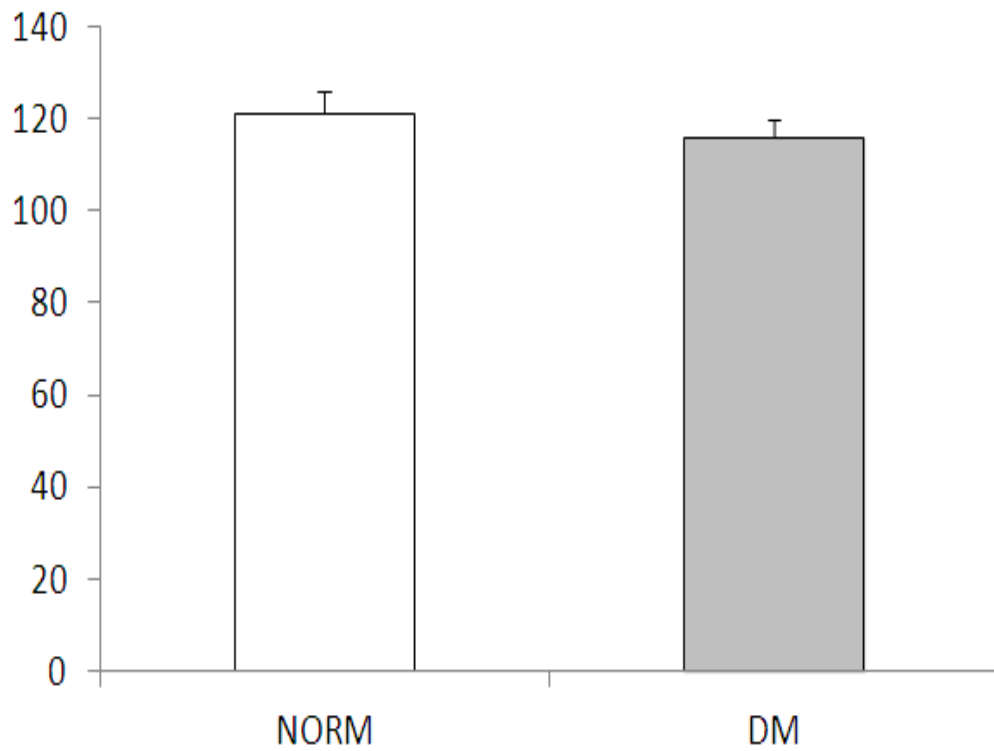
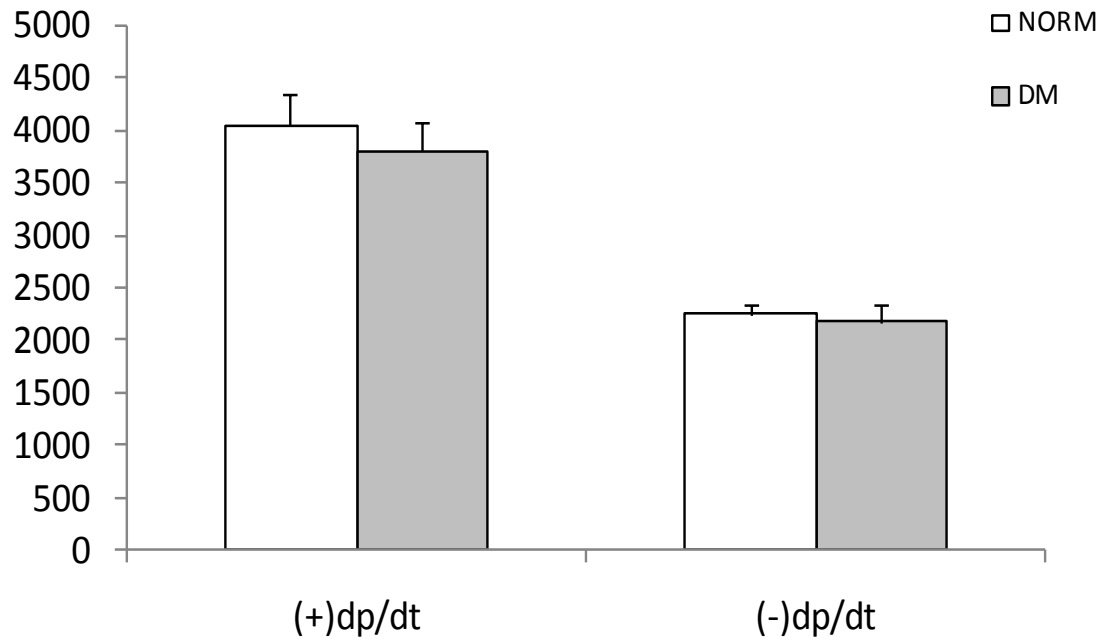


Figure 3.1: Bar chart showing that left ventricular developed pressure (LVDP in mm Hg) was not significantly different between normal (NORM) and diabetic (DM) rat hearts.). Data are mean and represent SEM., n=6-8 for each group.



(+) dp/dt and (-) dp/dt

Figure 3.2: Bar chart showing that the rate of increase (+dp/dt) and decrease (-dp/dt) of left ventricular developed pressure (LVDP) in mm Hg/sec were not significantly different between normal (NORM) and diabetic (DM) rat hearts. Data are mean \pm SEM., n=6-8 for each group.

B. General characteristics of all five groups of rats

Table 3.3: General characteristics of the experimental animals. (Student's t-test). Data are mean \pm SEM (numbers are represented in brackets). * $P < 0.05$ vs SHAM, ** $P < 0.05$ vs DM + SHAM and DM + AMI, $^{\&}P < 0.05$ vs DM + SHAM, $^{\#}P < 0.05$ vs DM + AMI

	SHAM (n=20)	AMI (n=11)	DM-SHAM (n=19)	DM-AMI (n=13)	DM-AMI+TH (n=11)
Initial Body weight (g)	356 (9)	343 (12)	367 (16)	372 (16)	352 (15)
Final Body weight (g)	363 (7)	340 (10)*	348 (13)*	336 (12)*	337 (14)*
Heart weight (mg)	845 (27)	859 (34)	767 (28)	908 (22) $^{\&}$	975 (34) $^{\&}$
HW/BW ratio	2.3 (0.06)	2.5 (0.07)	2.3 (0.08)	2.7 (0.14)*	2.93 (0.14)**
Heart Rate (bpm)	363 (12)	332 (13)	329 (16)	309 (11)*	370 (17)**
Lung Weight (LW in g)	1.25 (0.04)	1.33 (0.05)	1.15 (0.07)	1.75 (0.24)	1.43 (0.11)
LW/BW ratio	3.3 (0.1)	3.9 (0.19)	3.2 (0.13)	5.0 (0.8) $^{\&}$	3.8 (0.14) $^{\#}$

Table 3.3 shows the general characteristics of the rats from the five different experimental groups. The results show no significant difference in the initial and final body weights for all groups. However, it must be noted that the three groups of diabetic animals and the AMI control show a trend to decrease body weights between the beginning and the end of the experiment as compared to non-diabetic animals. This finding is expected due to increased catabolism observed in diabetes. The heart weights were also significantly ($P < 0.05$) increased the DM + AMI and DM + AMI+TH groups compared to either DM+SHAM or control SHAM groups. In addition, heart weight to body weight ratio was found to be significantly increased only in the DM + AMI

animals either with or without thyroid hormone treatment indicating the induction of cardiac hypertrophy. It should be also noted that lung weight to body weight ratio was significantly ($P<0.05$) increased in DM+AMI rats dictating the development of pulmonary congestion, while in animals treated with thyroid hormone the ratio was significantly decreased to almost normal values.

Physiological studies

Response of the diabetic heart after myocardial infarction

Cardiac hypertrophy, wall tension and geometry

The results presented in Table 3.4 and figures 3.3-3.13 show cardiac hypertrophy, wall tension and geometry. The ratio of left ventricular weight (LVW) to body weight (BW) was shown to be similar in SHAM, DM+SHAM, AMI and DM+AMI hearts, $p>0.05$ (figure 3.7). LVPW was found to be significantly ($p<0.05$) increased in AMI hearts as compared to SHAM indicating the development of mild cardiac hypertrophy (see table 3.4). On the contrary, LVPW was similar between DM+AMI and DM+SHAM hearts, indicating attenuation of this response in diabetic hearts (table 3.4). LV diastolic diameter (LVIDd) was found to be increased significantly ($p<0.05$) in AMI and DM+AMI hearts as compared to SHAM and DM+SHAM hearts respectively, with a trend towards an increased LVIDd in DM+AMI as compared to AMI hearts (figure 3.8). These changes were translated to marked alterations in the WTI. Thus, while a mild, but a significant ($p<0.05$) increase in WTI was observed in AMI as compared to SHAM hearts, a marked, but also a significant ($p<0.05$) increase in WTI was observed in DM+AMI as compared to AMI hearts (figure 3.6A). The results also show that sphericity index (SI) was found to be similarly decreased

significantly ($p < 0.05$) in AMI and DM+AMI hearts as compared to SHAM and DM+SHAM hearts, respectively (figure 3.6B).

Left ventricular function and heart rate

A small reduction in contractile function was found in DM+SHAM as compared to SHAM. In fact, only SVPW was found to be significantly ($p < 0.05$) reduced in DM+SHAM vs SHAM (figure 3.4), while EF% and LVIDs were similar between the 2 groups (figures 3.3 and 3.8, respectively). Significant ($p < 0.05$) reductions in all indices (EF%, LVIDs, SVPW, LVDP, $+dp/dt$ and $-dp/dt$) were seen in AMI as compared to SHAM hearts (figures 3.3-3.5;3.7-3.8). In addition, in DM+AMI hearts, further reductions in all contractile indices were observed as compared to AMI group (see table 3.4). Heart rate was found to be significantly ($p < 0.05$) reduced only in AMI hearts as compared to SHAM.

Systolic radial myocardial deformation

Regional systolic radial myocardial strain is also shown in table 3.6. Radial strain in antero-septal, anterior and antero-lateral segments corresponding to scar areas were greatly reduced almost equally in AMI and DM+AMI hearts as compared to SHAM and DM+SHAM (figure 3.9-3.13). Furthermore, in postero-lateral, posterior and postero-septal segments corresponding to viable remodeled myocardium, radial strain was significantly ($p < 0.05$) reduced in AMI as compared to SHAM, but further reduced in DM+AMI, as compared to AMI. In fact, global systolic radial myocardial strain of the left ventricle was significantly ($p > 0.05$) reduced in AMI vs SHAM and further reduced in DM+AMI as compared to AMI (figures 3.11-3.13).

Table 3.4: Left ventricular weight (LVW in mg), LVW to body weight ratio (LVW/BW, mg/g) and echocardiographic measurements of posterior wall thickness at diastolic phase (LVPW), wall tension index (WTI, LVIDd/2* LVPW) and sphericity index, left ventricular internal diameter at diastolic phase (LVIDd) and at systolic phase (LVIDs) and ejection fraction (EF%), in sham-operated rats (SHAM), sham-operated diabetic rats (DM-SHAM), post-infarcted rats (AMI) and post-infarcted diabetic rats (DM-AMI) after 2 weeks. (Student's t-test), Data are mean \pm SEM (number are shown in brackets); P<0.05 and ** P<0.01

Parameters measured	SHAM (n=20)	AMI (n=19)	DM-SHAM (n=11)	DM-AMI (n=13)
LVW/BW	1.87 (0.03)	2.0 (0.04)	2.04 (0.09)	1.94 (0.05)
LVPW(mm)	1.85 (0.02)	1.96 (0.03)*	1.92 (0.06)	1.91 (0.03)
WTI	1.74 (0.02)	2.03 (0.05)*	1.73 (0.05)	2.26 (0.07)**
Sphericity Index	1.94 (0.02)	1.63 (0.04)*	1.85 (0.04)	1.58 (0.03) ^{&}
LVIDd (mm)	6.5 (0.06)	8.0 (0.15)*	6.6 (0.1)	8.6 (0.15) ^{&}
LVIDs (mm)	3.7 (0.1)	6.1 (0.2)*	3.9 (0.1)	7.1 (0.2)**
EF%	75.7 (1.6)	49 (1.4)*	74.7 (1.9)	38.5 (1.7)**
SVPW (mm/s)	38.4 (1.4)	28.6 (1.0)*	31.3 (1.9)*	24.3 (0.9) [†]
LVDP	126 (1.8)	105.3 (2.6)*	113.5(5.9)	85.3 (4.9)**
+dp/dt	4517 (181)	3405 (127)*	3671 (269)*	2558 (144)**
-dp/dt	2361 (50)	2077 (47)*	2106(131)	1667 (110) [†]

* P<0.05 vs SHAM, ** p<0.05 vs DM-SHAM and AMI, [†] p<0.05 vs AMI, [&] p<0.05 vs DM-SHAM,

Thyroid hormones levels in plasma

Scar areas and weights as well as plasma levels of T₃, and T₄ and heart rate are shown in table 3.5. The results show no differences in either scar areas, scar weights and thyroid hormone levels in serum that were observed between groups. Heart rate was similar between SHAM, DM+SHAM and AMI hearts, while it was significantly ($p < 0.05$) reduced in DM+AMI as compared to SHAM.

Table 3.5: Thyroxine (T₄) and triiodothyronine (T₃) levels in plasma, heart rate (in beats per min) and the calculated area (mm²) of the scar tissue and the weight (mg) of the scar in non-diabetic sham-operated rats (SHAM), sham-operated diabetic rats (DM+SHAM), post-infarcted diabetic rats (DM+AMI) and post-infarcted diabetic rats treated with thyroid hormone (DM+AMI+TH) after 2 weeks are presented in this table. (Student's t-test) . Data are mean \pm SEM (numbers represented in brackets) * $P < 0.05$ vs SHAM.

Parameters Measured	SHAM (n=20)	AMI (n=19)	DM-SHAM (n=11)	DM-AMI (n=13)
T₄ (nM)	50.7 (2.9)	50.3 (2.3)	44.5 (2.8)	52.3 (3.1)
T₃ (nM)	1.01 (0.05)	1.02 (0.06)	1.08 (0.08)	1.09 (0.08)
Heart rate	363 (12)	332 (13)	329(16)	309 (11)*
Scar area (mm²)	-----	83.6 (3.4)	83.4 (3.4)
Scar weight (mg)	-----	188 (10.1)	167 (9.5)

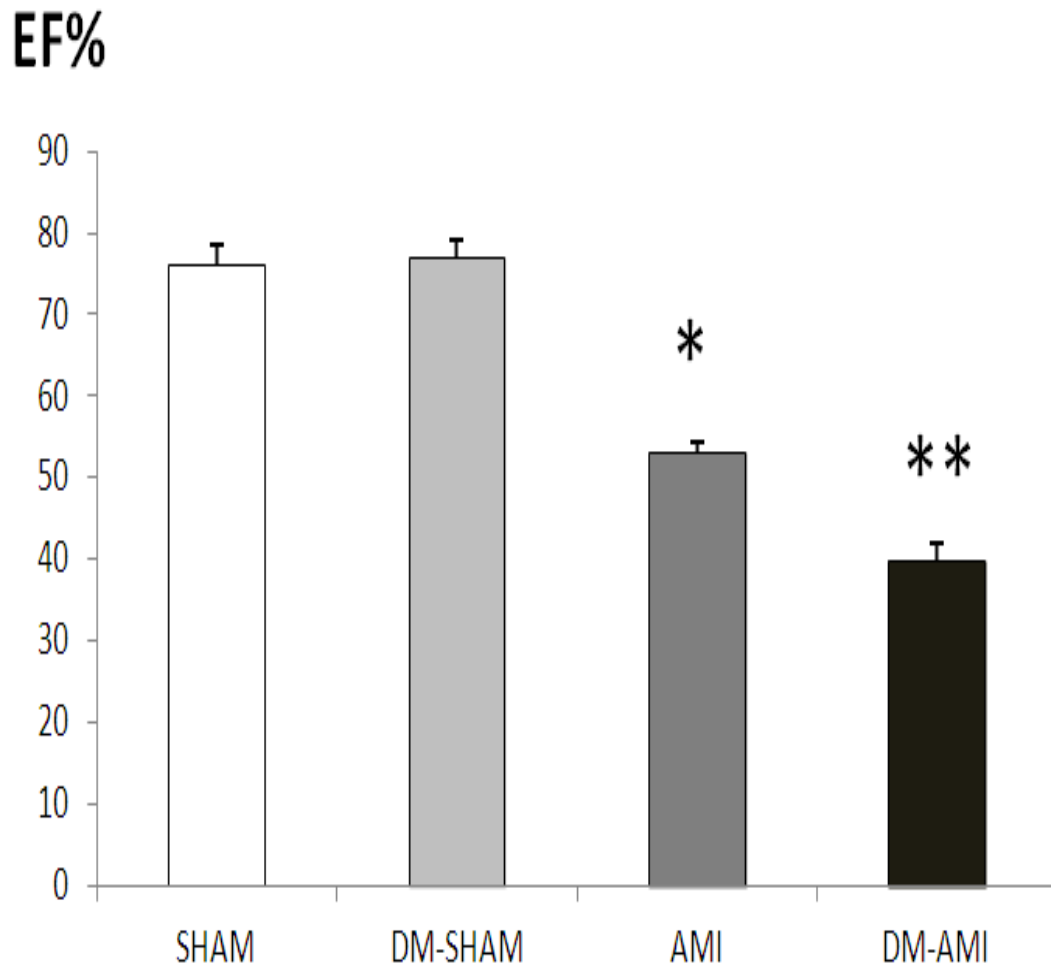


Figure 3.3: Bar chart showing ejection fraction (EF%) measured by echocardiography in sham-operated rats (SHAM), sham-operated diabetic rats (DM +SHAM), post-infarcted rats (AMI) and post-infarcted diabetic rats (DM + AMI) after 2 weeks. (ANOVA); Data are mean. Bars represent SEM. n=11-20; *P<0.05 for AMI as compared to SHAM. **P<0.05 for DM+AMI as compared to SHAM, DM + SHAM and AMI.

SVPW (mm/sec)

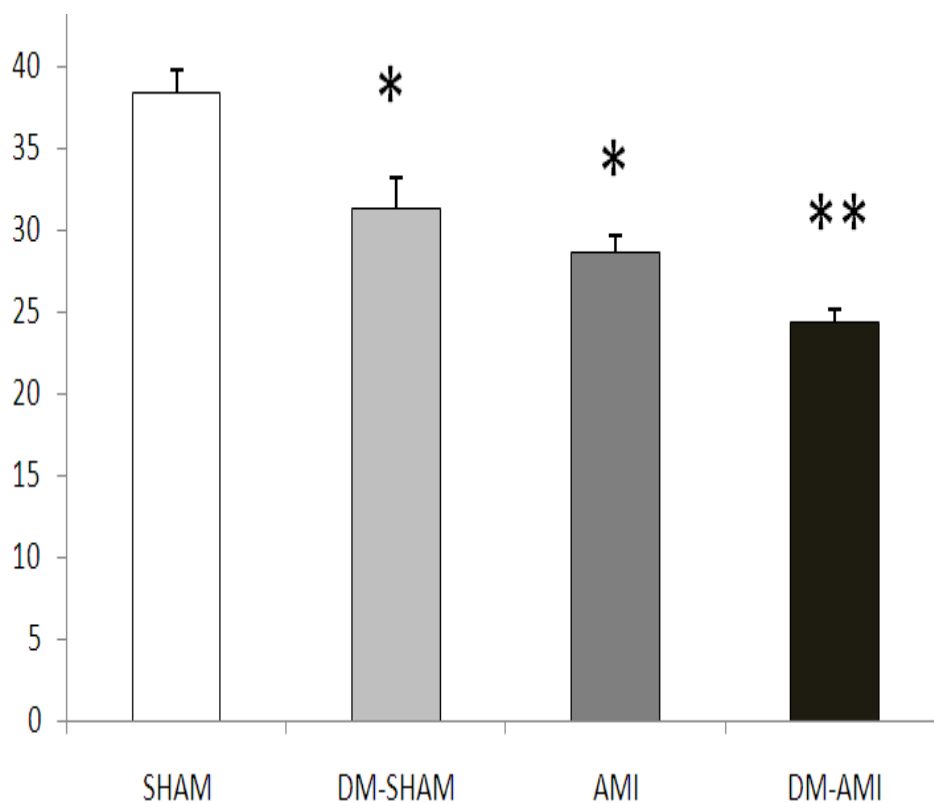
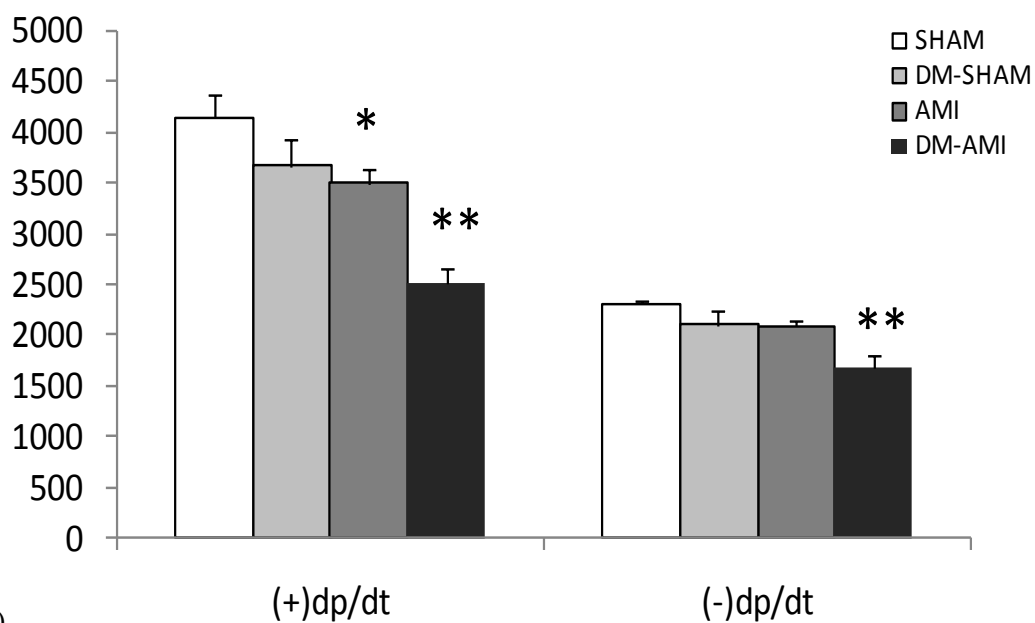
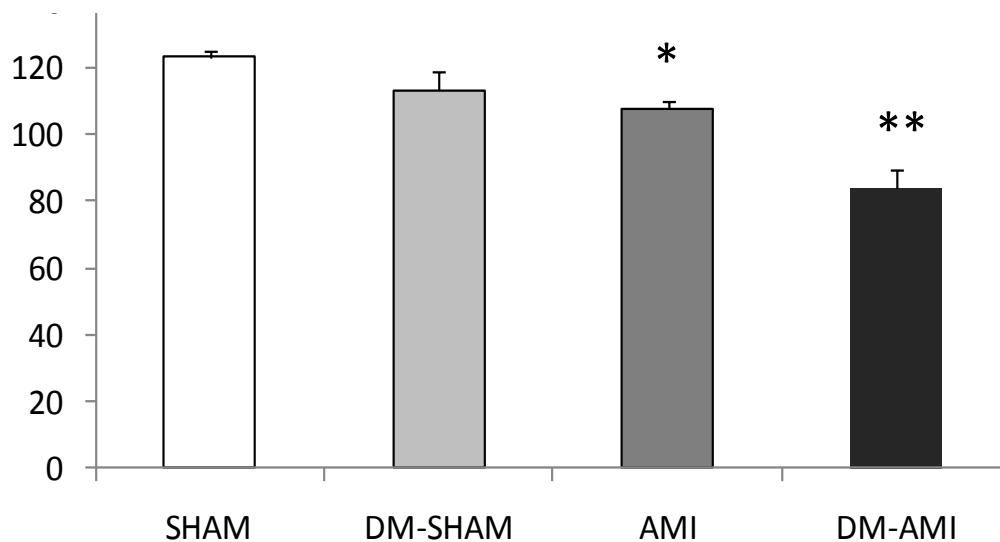


Figure 3.4: Bar chart showing regional systolic velocity of the posterior wall of the left ventricle (SVPW) measured by echocardiography is shown in sham-operated rats (SHAM), sham-operated diabetic rats (DM+SHAM), post-infarcted rats (AMI) and post-infarcted diabetic rats (DM+AMI) after 2 weeks. Data are mean. (ANOVA); Bars represent SEM. n=11-20; *P<0.05 as compared to SHAM. **P<0.05 as compared to SHAM, DM+SHAM and AMI.

(A)

LVDP (mmHg)

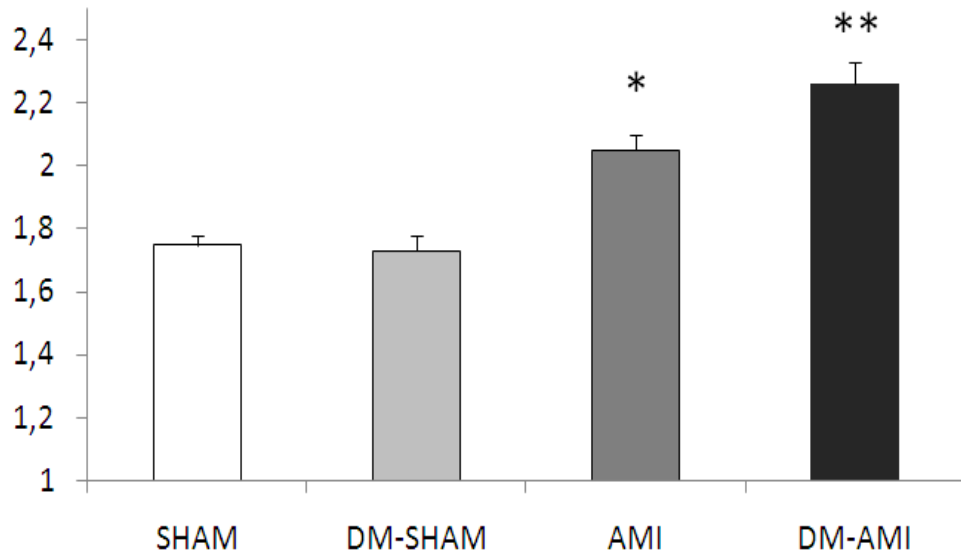


(B)

Figure 3.5: Left ventricular developed pressure (LVDP) (A) and the rate of increase and decrease of LVDP (+dp/dt and -dp/dt) (B) are shown in sham-operated rats (SHAM), sham-operated diabetic rats (DM+SHAM), post-infarcted rats (AMI) and post-infarcted diabetic rats (DM-AMI) after 2 weeks. (ANOVA); Data are mean \pm SEM. n=11-20, *P<0.05 vs SHAM. **P<0.05 vs SHAM, DM+SHAM and AMI.

(A)

Wall Tension Index



(B)

Sphericity Index

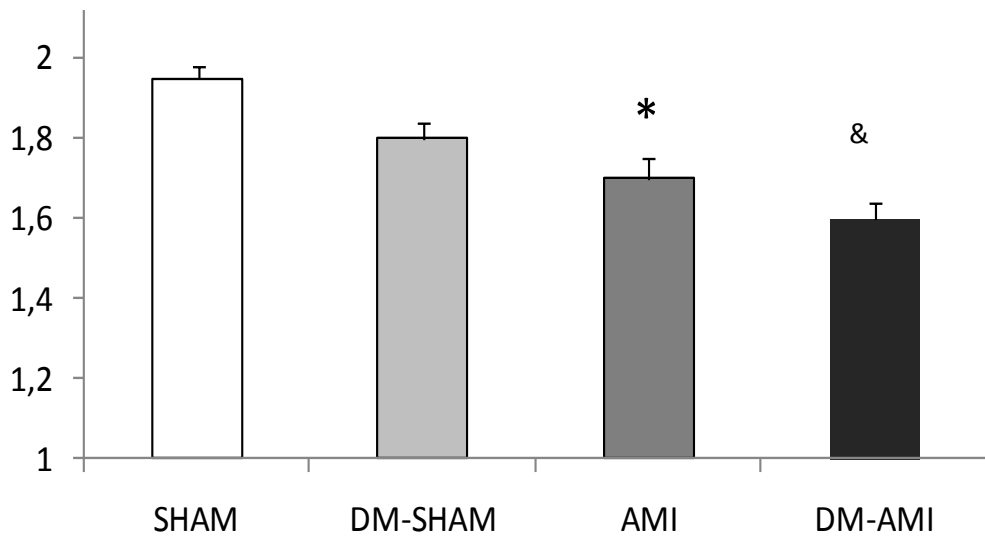
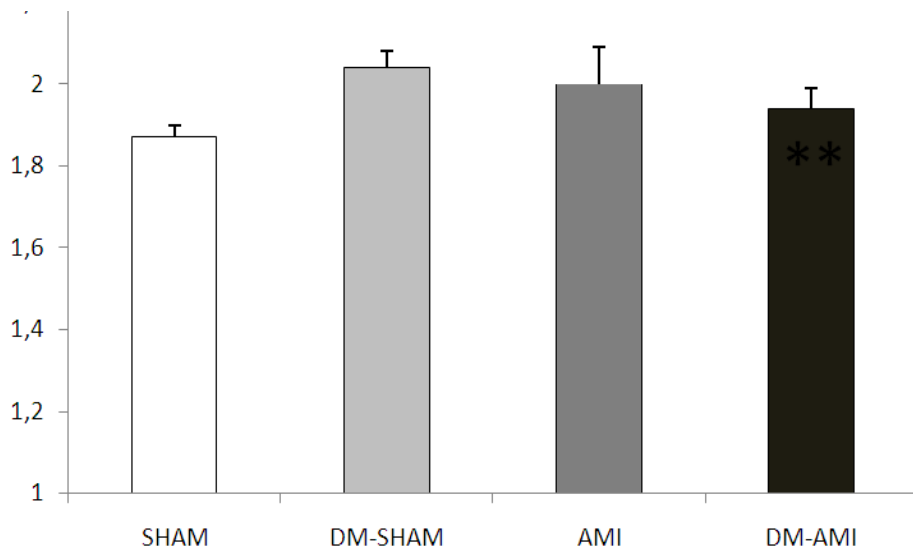


Figure 3.6: (A) Wall tension index (defined as the ratio of LVIDd to 2 x LVPW) and (B) Sphericity Index (defined as the ratio of diastolic LV length to diastolic LV diameter) in sham-operated rats (SHAM), sham-operated diabetic rats (DM+SHAM), post-infarcted rats (AMI) and post-infarcted diabetic rats (DM+AMI) after 2 weeks . (ANOVA); Data are mean \pm SEM. n=11-20. *P<0.05 vs SHAM. **P<0.05 vs SHAM, DM+SHAM and AMI. & P<0.05 vs SHAM and DM-SHAM

(A)

LVW/BW



(B)

LVPW (mm)

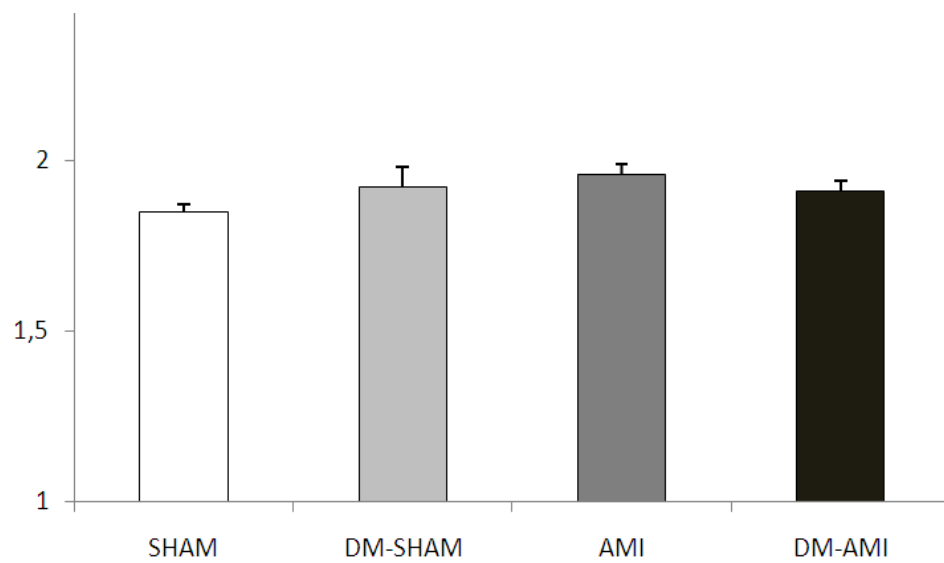
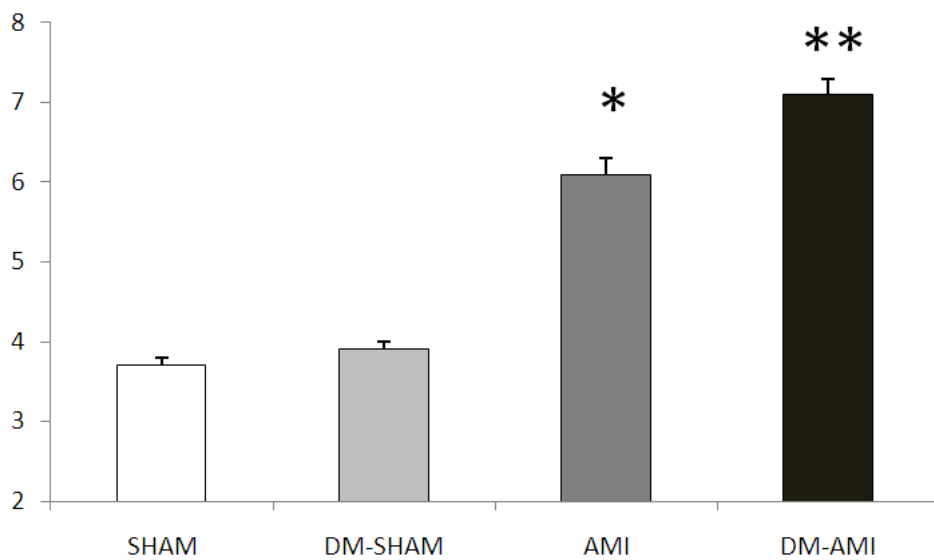
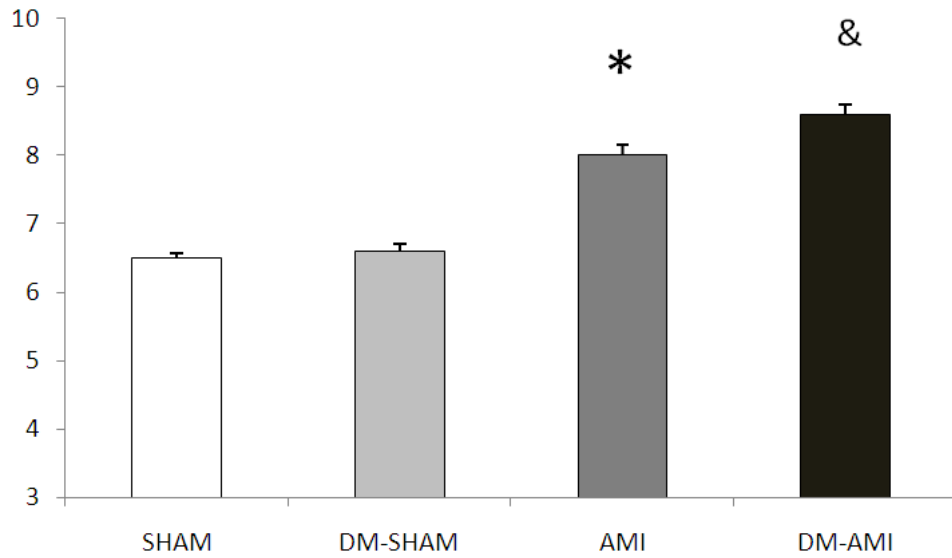


Figure 3.7: (A) Left ventricular weight to body weight (LVW/BW) and (B) Left ventricular wall thickness (LVPW) are shown in sham-operated rats (SHAM), sham-operated diabetic rats (DM-SHAM), post-infarcted rats (AMI) and post-infarcted diabetic rats (DM+AMI) after 2 weeks. Data are mean \pm SEM. n=11-21.

(A)

LVIDd (mm)



(B)

LVIDs (mm)

Figure 3.8: Left Ventricular Internal Diameter at (A) the end-diastole (LVIDd) and (B) at the end-systole (LVIDs) are presented in sham-operated rats (SHAM), sham-operated diabetic rats (DM+SHAM), post-infarcted rats (AMI) and post-infarcted diabetic rats (DM+AMI) after 2 weeks. (ANOVA); Data are mean \pm SEM. n=11-20. *P<0.05 vs SHAM. **P<0.05 vs SHAM, DM-SHAM and AMI. & P<0.05 vs SHAM and DM-SHAM

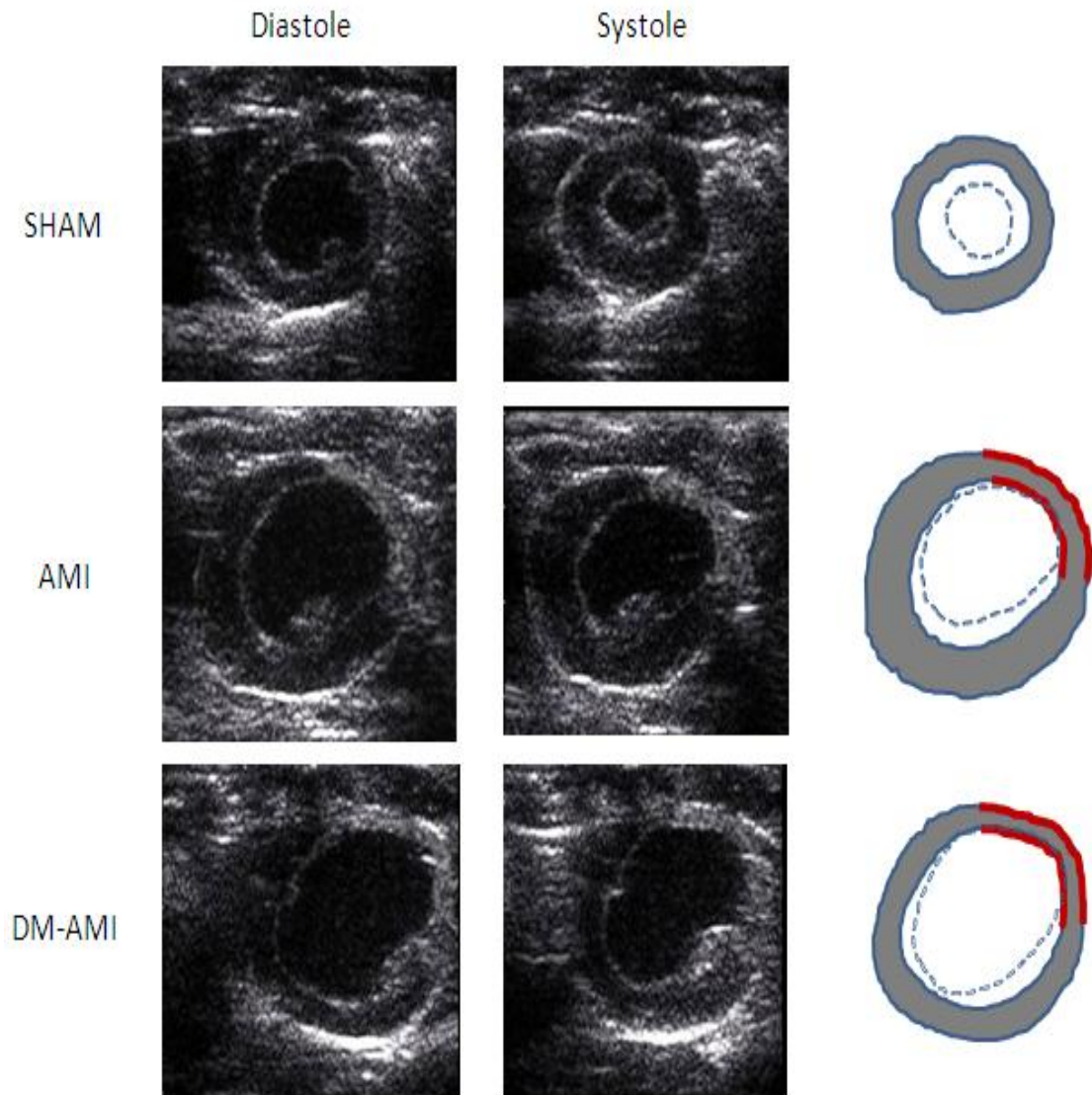


Figure 3.9: Representative short axis imaging echocardiographic views at diastole and at systole from sham-operated rats (SHAM), post-infarcted rats (AMI) and post-infarcted diabetic rats (DM+AMI) after 2 weeks. On the right, a schematic drawing of each image are shown for comparison. Grey colour represents viable myocardial tissue, red colour represents the scar area and dotted line represents the movement of the endocardial border during systole. Typical of 11-20 such different experiments for each group.

Table 3.6: Regional Systolic radial strain (%) at different segments of left ventricle (Student's t-test); * P<0.05 vs SHAM, ** p<0.05 vs DM-SHAM and AMI, † p<0.05 vs AMI, & p<0.05 vs DM-SHAM, (n=11-20)

		Antero-septal	Anterior	Antero-lateral	Postero-lateral	Posterior	Postero-septal
Strain	SHAM	46.3±3.8	48±4.9	45.2±4.1	39.6±4.2	39.1±4.2	41.8±4.0
	DM-SHAM	33±4.7*	41±12	41.7±10	40.6±10.9	38±9.8	34.3±6.4
	AMI	15.3±5.5*	6.4±4.8*	8.9±3.0*	17.3±4.5*	25.1±4.8	26.1±4.6*
	DM-AMI	9.5±2.6&	2.0±0.6&	4.9±3.2&	9.6±3.8*	13.4±4.2**	12.9±4.3*

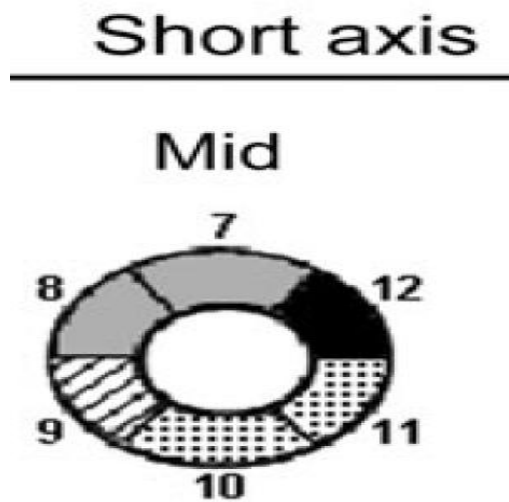


Figure 3.10: Short-axis imaging view of the left ventricle at the level of the papillary muscles was used to evaluate systolic radial strain. The evaluated segments of LV are shown according to international standards. 8=Antero-septal, 7=Anterior, 12=Antero-lateral, 11= Postero-lateral, 10= Posterior, 9= Postero-septal.

Global Systolic Radial Strain of LV (%)

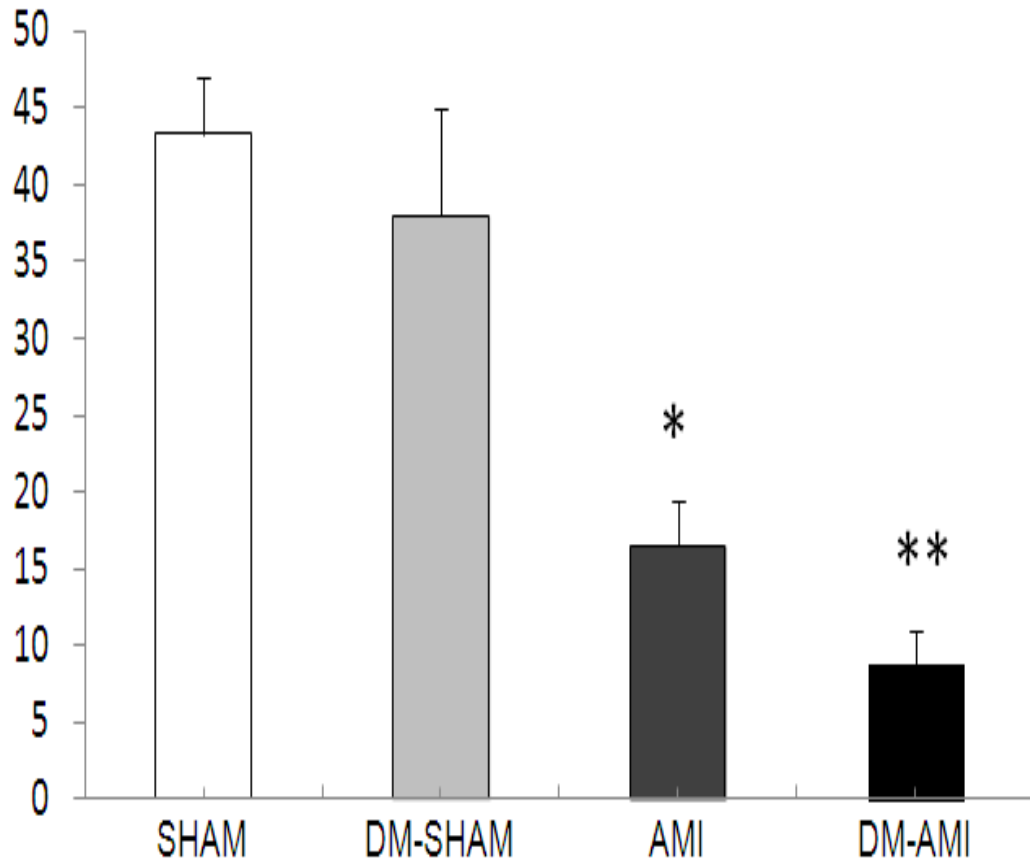


Figure 3.11: Global systolic radial strain of the left ventricle (defined as the mean of the regional systolic radial strains of the different segments of the LV) is shown in sham-operated rats (SHAM), sham-operated diabetic rats (DM+SHAM), post-infarcted rats (AMI) and post-infarcted diabetic rats (DM+AMI) after 2 weeks. (ANOVA); Data are mean. \pm SEM. $n=11-20$; * $P<0.05$ vs SHAM. ** $P<0.05$ vs SHAM, DM+SHAM and AMI.

SHAM

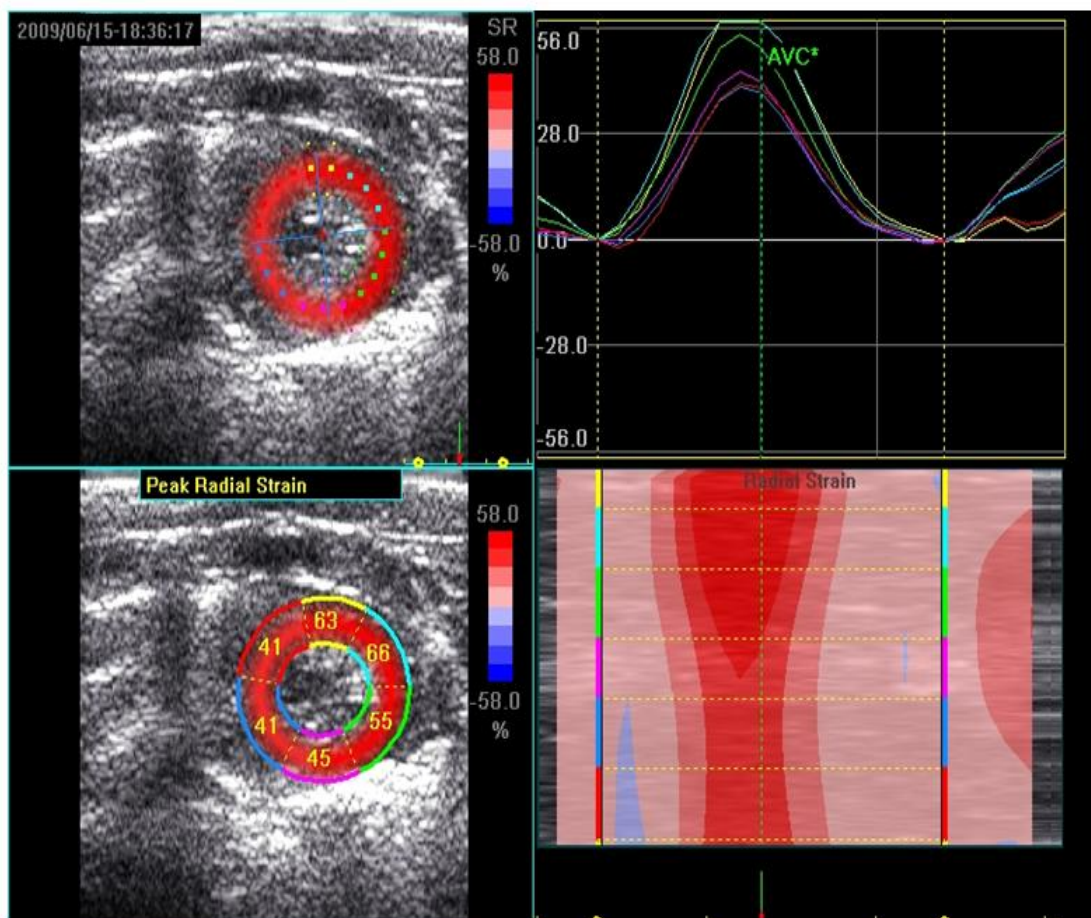
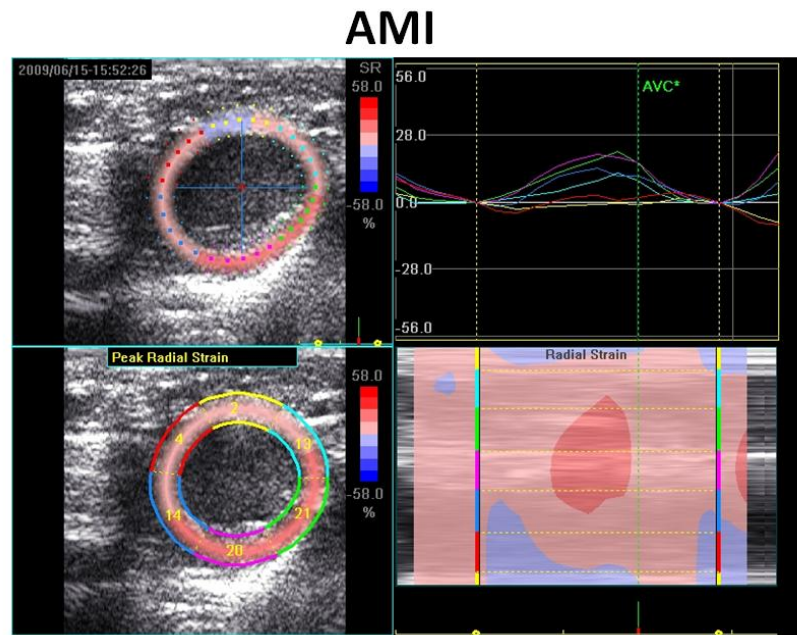


Figure 3.12: Image showing representative analysis of systolic radial strain of the left ventricle in sham-operated rat heart (SHAM). Typical of 11-20 such different experiments for each group.

(A)



(B)

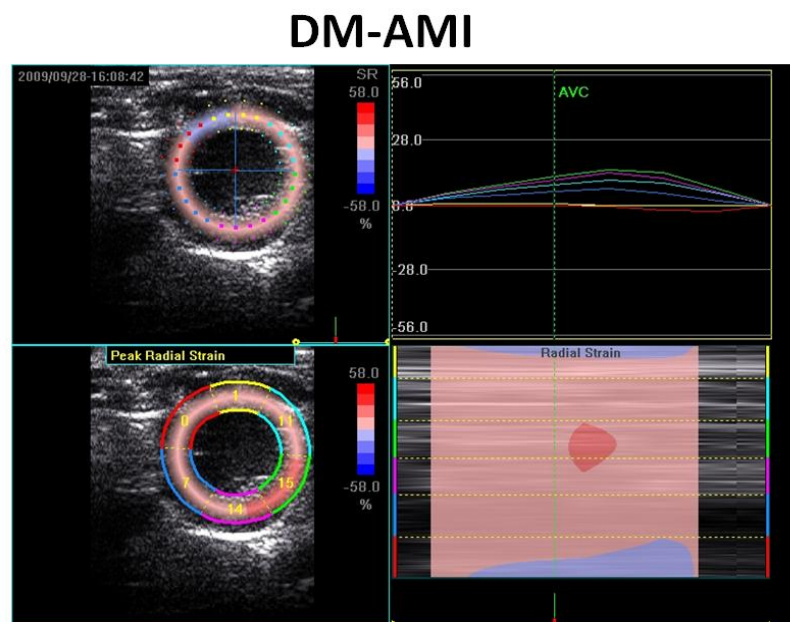


Figure 3.13: Images showing representative analysis of systolic radial strain of the left ventricle in (A) post-infarcted rat heart (AMI) and (B) diabetic post-infarcted rat heart (DM-AMI). Typical of 11-20 such different experiments for each group.

2. Effects of TH administration on the response of the diabetic heart after myocardial infarction

Heart rate and functional indices after myocardial infarction in diabetic rats

Scar areas and weights were similar in all the post-infarcted groups as shown in Table 3.7. Heart rate was found to be significantly ($p < 0.05$) reduced in DM+AMI hearts as compared to DM+SHAM. After thyroid hormone treatment, heart rate increased significantly ($p < 0.05$) by 20% in DM+AMI+TH hearts as compared to DM+AMI.

Left ventricular function

The results for left ventricular functions are shown in table 3.8 and figures 3.14-3.21. The data show significant ($p < 0.05$) reductions in contractile indices (EF%, LVIDs) for DM+AMI hearts as compared to DM+SHAM group. EF% and LVIDs were significantly ($p < 0.05$) improved in DM+AMI+TH as compared to DM+AMI hearts (see table 3.8; figures 3.14-3.15). Significant ($p > 0.05$) reductions were also seen in contractile indices measured under isometric conditions in Langendorff's preparations in DM+AMI hearts as compared to DM+SHAM. In fact, LVDP, +dp/dt and -dp/dt were all significantly ($p < 0.05$) reduced in DM+AMI vs DM+SHAM. Furthermore, in DM+AMI+TH hearts, LVDP, +dp/dt and -dp/dt were significantly ($p < 0.05$) improved as compared to DM+AMI hearts (figures 3.14-3.17; figure 3.21).

Systolic radial myocardial deformation

Regional systolic radial myocardial deformation ($\text{Strain}_{\text{Rad}}$) for all groups is shown in table 3.9 and figure 3.18-3.20). The results show that the mean global $\text{Strain}_{\text{Rad}}$ (%) was significantly ($p < 0.05$) decreased in DM+AMI hearts as compared to DM+SHAM hearts [$39 \pm 4.4\%$ vs $8.7 \pm 2.3\%$], respectively. Similarly, in DM+AMI+TH hearts,

Strain_{Rad} was improved in all segments and mean global Strain_{Rad} was significantly ($p<0.05$) increased [$22.5\pm 2.7\%$ vs $8.7\pm 2.3\%$] in DM±AMI.

Cardiac hypertrophy, wall tension and geometry

The ratio of LVW to body weight was shown to be similar in DM±SHAM and DM+AMI hearts, ($p>0.05$). LVPW was similar in DM+AMI and DM+SHAM hearts, indicating an attenuation of the hypertrophic response in the diabetic hearts (figure 3.17). LV diastolic diameter (LVIDd) was found to be significantly ($p<0.05$) increased in DM+AMI hearts as compared to DM+SHAM hearts (figure 3.14). These changes were translated to marked alterations in the WTI. Thus, a significant ($p<0.05$) increase in WTI was observed in DM+AMI as compared to DM+SHAM hearts (Table 3.8). Sphericity index (SI) was found to be significantly ($p<0.05$) decreased in DM-AMI hearts as compared to DM-SHAM hearts (Table 3.8; figure 3.19).

After TH treatment, both the ratio of LVW to body weight and LVPW were significantly ($p<0.05$) increased as compared to DM+AMI hearts, indicating the development of hypertrophy in those hearts (figure 3.17). In addition, LVIDd was significantly ($p<0.05$) reduced in DM+AMI+TH versus DM+AMI hearts (figure 3.14),. As a consequence, WTI was nearly normalized in DM+AMI+TH hearts and this was found to be significantly ($p<0.05$) reduced as compared to DM+AMI hearts (Table 3.8).

Table 3.7: Thyroxine (T4) and triiodothyronine (T3) levels in serum, heart rate (in beats per min) and the calculated areas (mm²) of the scar tissues and the weights (mg) of the scar tissues in sham-operated diabetic rats (DM-SHAM), post-infarcted diabetic rats (DM-AMI) and post-infarcted diabetic rats treated with thyroid hormone (DM-AMI+TH) after 2 weeks are presented in this table.(Student's t-test); The values are means ± (S.E.M) (numbers in brackets).* P<0.05 vs DM-SHAM, **P<0.05 vs DM-AMI, & P<0.05 vs DM-SHAM and DM-AMI ; n=11-20.

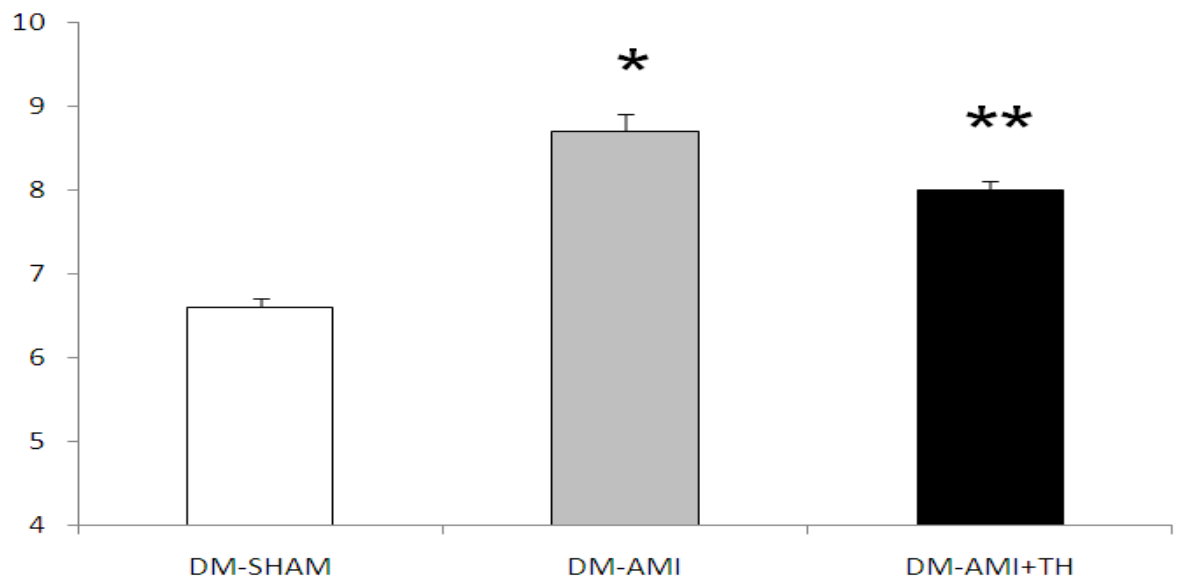
Parameters measured	DM-SHAM	DM-AMI	DM-AMI+TH
T4 (nM)	45.2 (3.1)	53.0 (3.1)	48.3 (2.5)
T3 (nM)	1.0 (0.08)	1.1 (0.07)	1.44 (0.07) ^{&}
Heart rate (bpm)	331(17)	299 (12)*	370 (17)**
Scar area (mm²)	82.5 (3.6)	83.9 (3.7)
Scar weight (mg)	165 (10)	188 (14)

Table 3.8: Left ventricular weight (LVW in mg), LVW to body weight ratio (LVW/BW, mg/g) and echocardiographic measurements of posterior wall thickness at diastolic phase (LVPW), wall tension index (WTI, LVIDd/2* LVPW) and sphericity index, left ventricular internal diameter at diastolic phase (LVIDd) and at systolic phase (LVIDs) and ejection fraction (EF%), in sham-operated diabetic rats (DM-SHAM), post-infarcted diabetic rats (DM-AMI) and post-infarcted diabetic rats treated with thyroid hormone (DM-AMI+TH) after 2 weeks. (Student's t-test); The values are means (S.E.M) (numbers in brackets). P<0.05 vs DM-SHAM, **P<0.05 vs DM-AMI & *P<0.05 vs DM-SHAM and DM-AMI

Parameters measured	DM-SHAM	DM-AMI	DM-AMI+TH
LVW (mg)	698 (18)	702 (12)	769 (30)
LVW/BW	2.08 (0.09)	1.97 (0.05)	2.37 (0.13)**
LVPW(mm)	1.95 (0.06)	1.92 (0.04)	2.10 (0.04)**
WTI	1.70 (0.05)	2.27 (0.08)*	1.91 (0.06) ^{&}
Sphericity Index	1.85(0.04)	1.56 (0.02)*	1.65 (0.03)*
LVIDd (mm)	6.6(0.1)	8.7 (0.2)*	8.0 (0.1) ^{&}
LVIDs (mm)	3.9(0.15)	7.2 (0.24)*	6.0 (0.22) ^{&}
EF%	74.5 (2.1)	37.9 (2.0)*	51.1 (1.0) ^{&}
SVPW (mm/s)	30.3 (1.9)	24.3 (0.9)*	37.3 (2.2)**
LVDP	113.5 (5.9)	85.3 (4.9)*	105 (5.8)**
+dp/dt	3671 (269)	2558 (144)*	3291 (253)**
-dp/dt	2106(131)	1667 (110)*	2206 (178)**

(A)

LVIDd (mm)



LVIDs (mm)

(B)

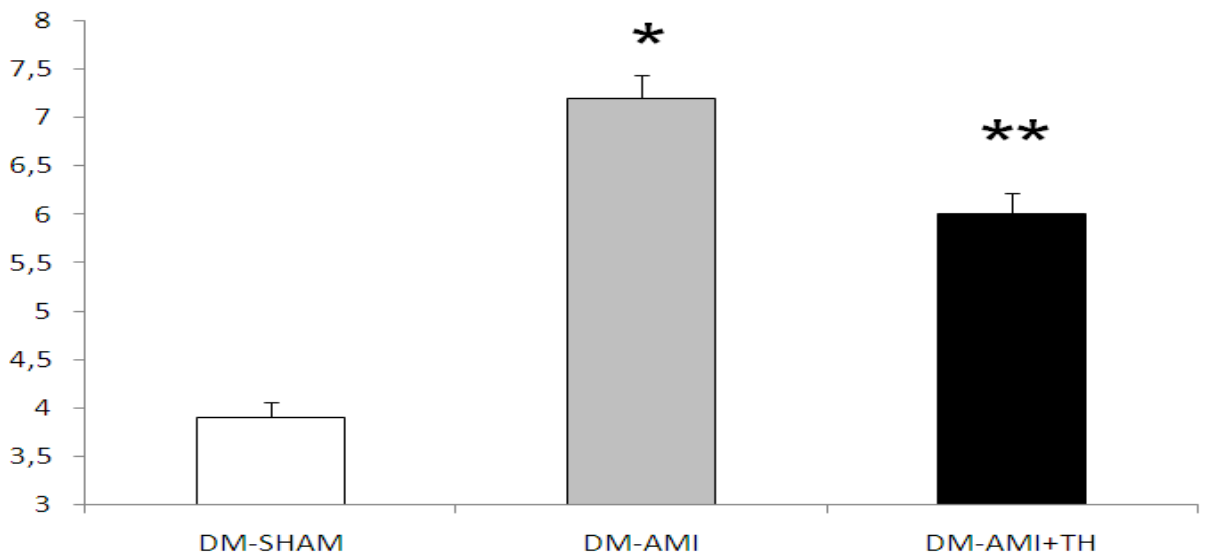
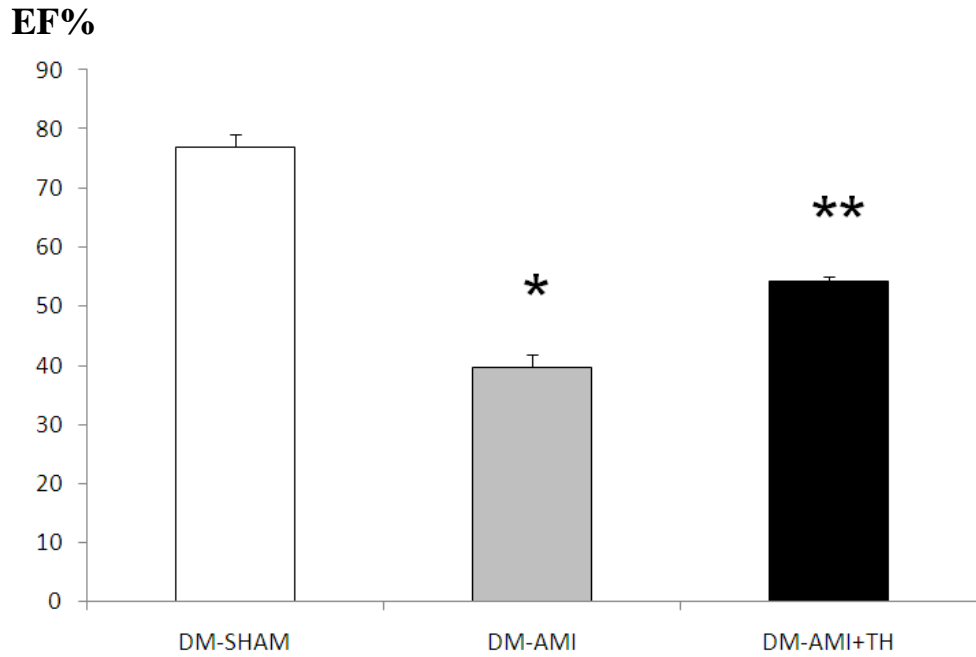


Figure 3.14: Left Ventricular Internal Diameter at (A) end-diastole (LVIDd) and at (B) end-systole (LVIDs) are presented in sham-operated diabetic rats (DM+SHAM), post-infarcted diabetic rats (DM+AMI) and post-infarcted diabetic rats with thyroid hormone treatment after 2 weeks. (ANOVA); Data are mean \pm SEM; * $P < 0.05$ vs DM+SHAM; ** $P < 0.05$ vs DM-SHAM and DM+AMI, $n = 11-20$.

(A)



(B)

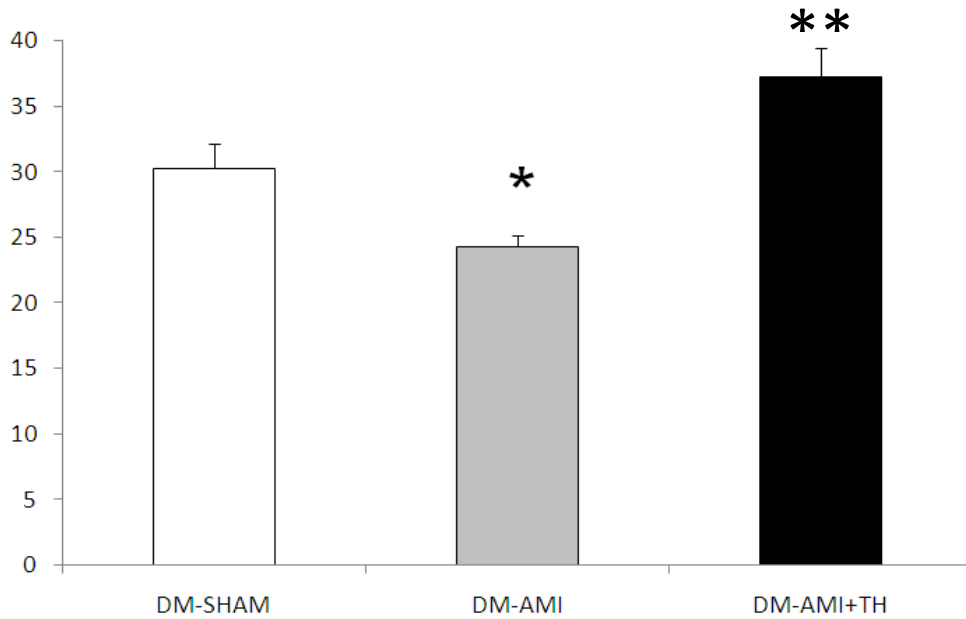
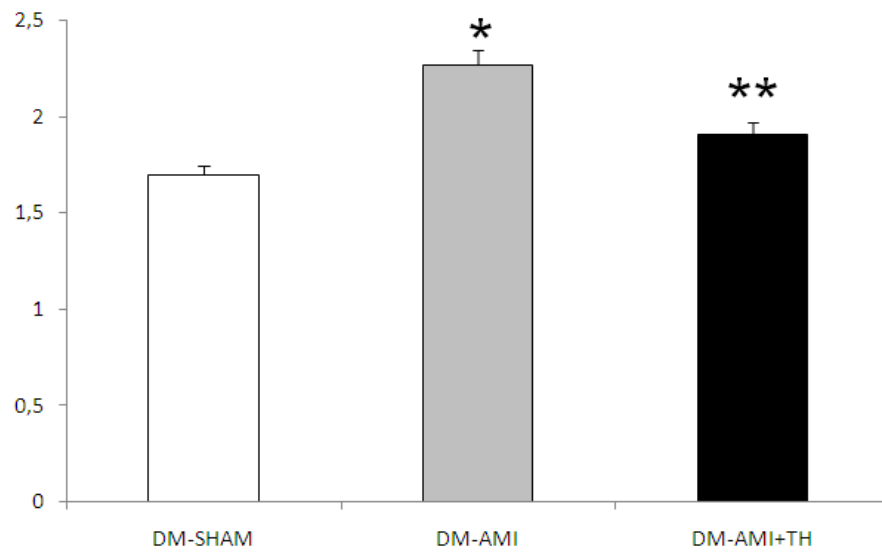


Figure 3.15 Ejection fraction (A) and (B) regional systolic velocity of the posterior wall of the left ventricle (SVPW) measured by echocardiography are shown in sham-operated diabetic rats (DM-SHAM), post-infarcted diabetic rats (DM+AMI) and post-infarcted diabetic rats with thyroid hormone treatment after 2 weeks. (ANOVA); Data are mean \pm SEM; n=11-21; *P<0.05 vs DM-SHAM; **P<0.05 vs DM+SHAM and DM+AMI

(A)

Wall Tension Index



(B)

Sphericity Index

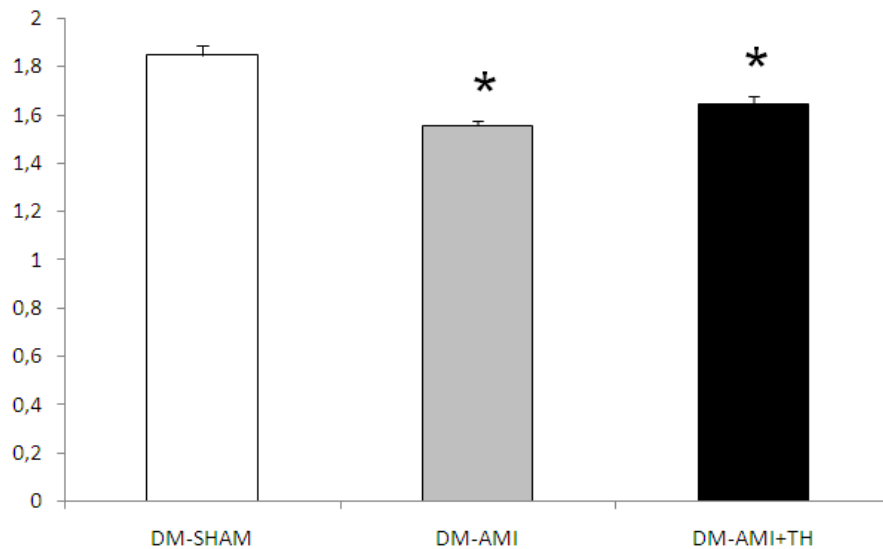
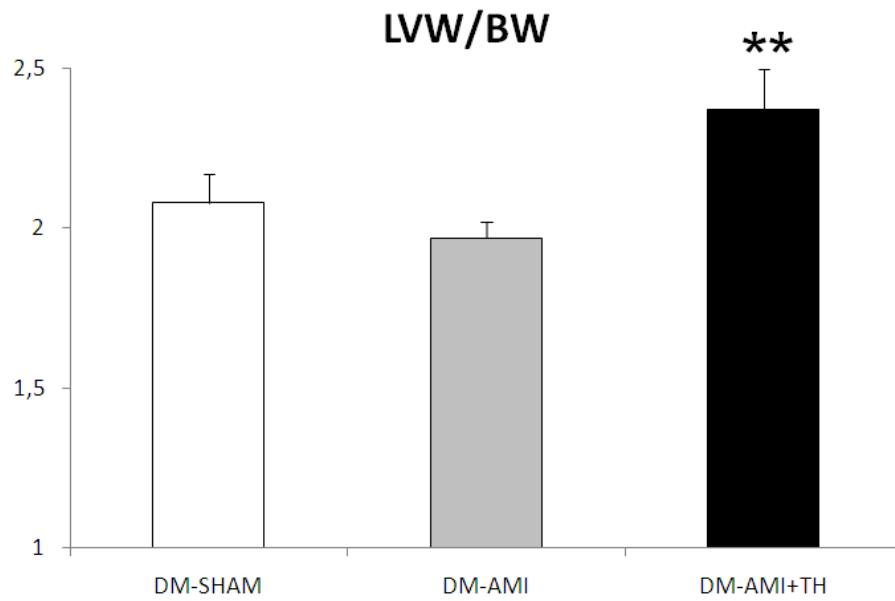


Figure 3.16: Wall tension index (defined as the ratio of LVIDd to 2 x LVPW) and Sphericity Index (defined as the ratio of diastolic LV length to diastolic LV diameter) are shown in sham-operated diabetic rats (DM+SHAM), post-infarcted diabetic rats (DM+AMI) and post-infarcted diabetic rats with thyroid hormone treatment after 2 weeks. (ANOVA); Data are mean ± SEM; n=11-20; *P<0.05 vs DM+SHAM; **P<0.05 vs DM+SHAM and DM+AMI.

(A)



(B)

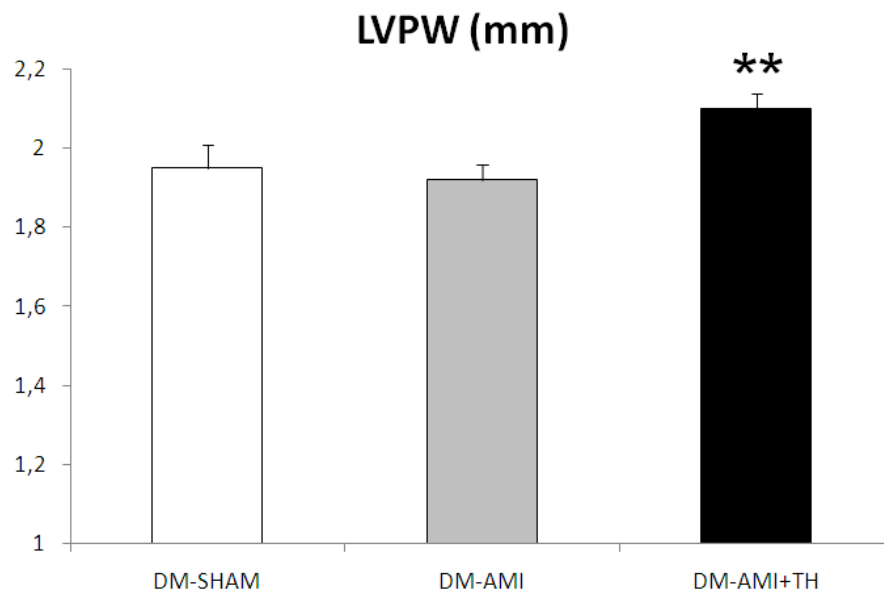


Figure 3.17: (A) Left Ventricular Weight to Body weight (LVW/BW) and (B) Left Ventricular Wall Thickness (LVPW) are shown in sham-operated diabetic rats (DM-SHAM), post-infarcted diabetic rats (DM-AMI) and post-infarcted diabetic rats with thyroid hormone treatment after 2 weeks. (ANOVA); Data are mean \pm SEM; n=7-20; **P<0.05 vs DM-SHAM and DM-AMI.

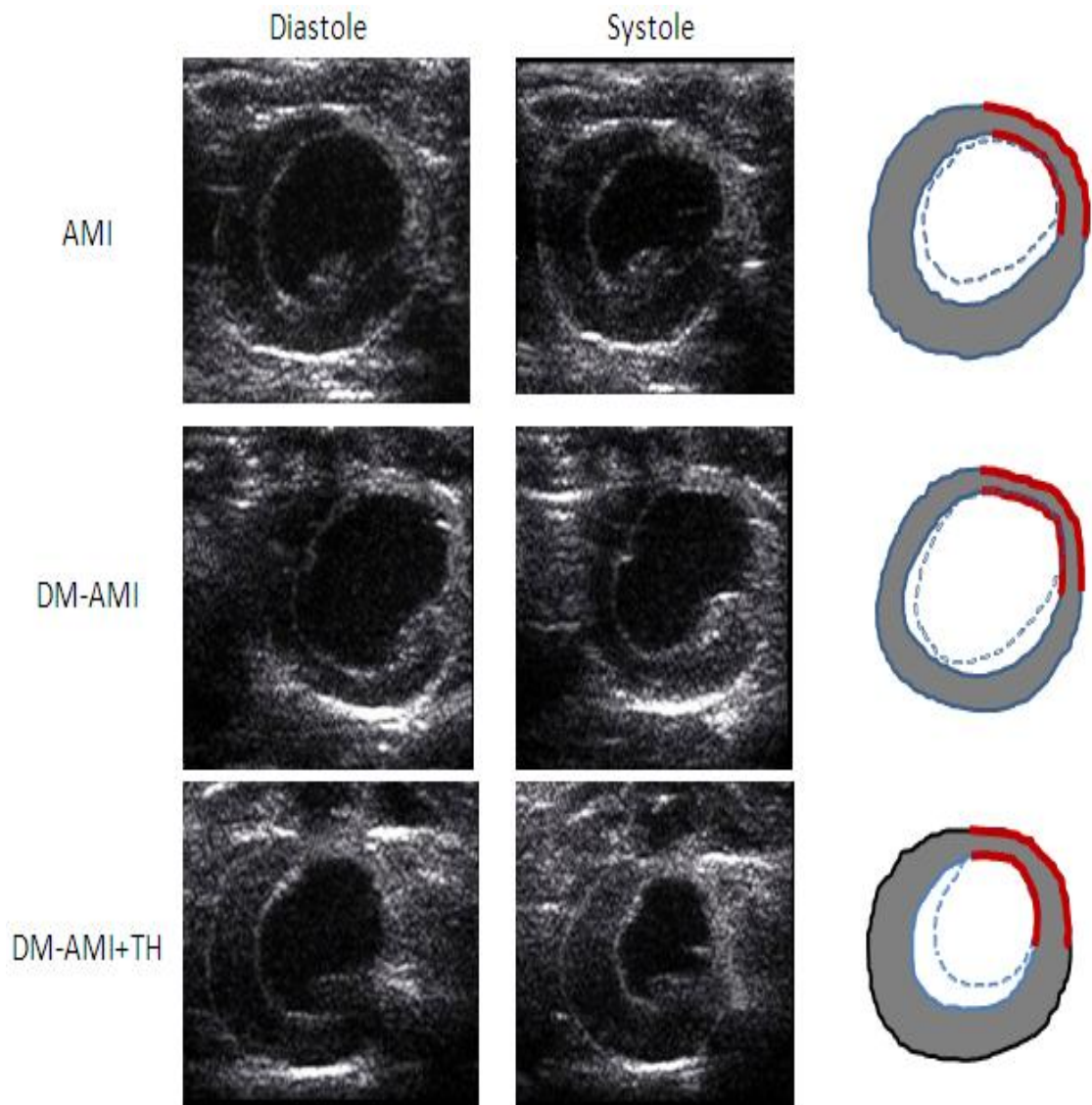


Figure 3.18: Representative short axis imaging echocardiographic views at diastole and at systole from sham-operated rats (SHAM), post-infarcted rats (AMI) and post-infarcted diabetic rats (DM+AMI) after 2 weeks. A schematic image of each is shown on the right for comparison. Grey colour represents viable myocardial tissue, red colour represents the scar area and dotted line represents the movement of the endocardial border during systole. Typical of 11-20 such different experiments for each group.

Table 3.9: Regional Systolic radial strain (%) at different segments of left ventricle. (ANOVA); Data are mean +_SEM, n=11-20; *P<0.05

		Antero-septal	Anterior	Antero-lateral	Postero-lateral	Posterior	Postero-septal
Strain _{Rad}	DM-SHAM	40.6±6.2	42±6.3	40.8±4.8	35.6±5.6	36.5±5.7	38.6±4.6
	DM-AMI	9.5±2.6*	2.0±0.6*	4.9±3.0*	9.6±3.8*	13.4±4.2*	12.9±4.3*
	DM-AMI+TH	28.9±6.2**	21.6±5.6&	17.2±3.5&	19.5±2.8*	21.6±2.8*	26.5±3.4**

Global Systolic Radial Strain (%)

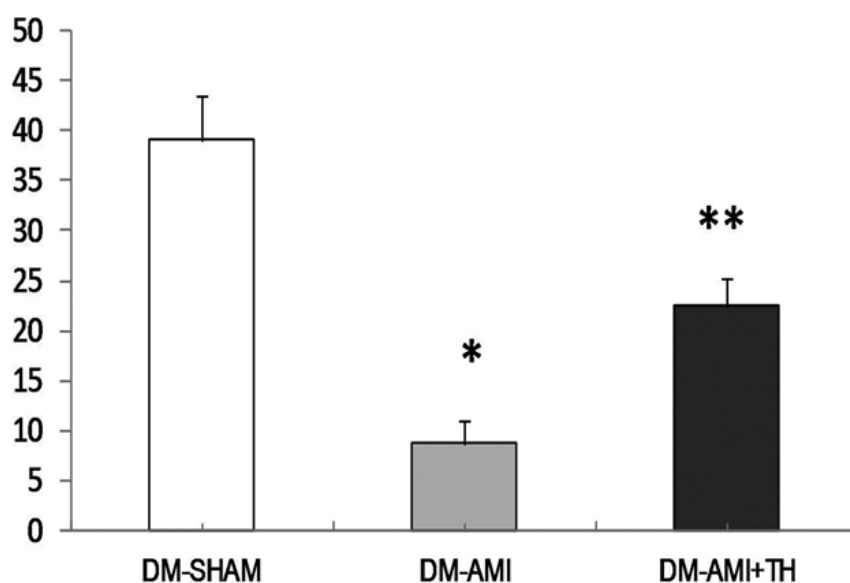
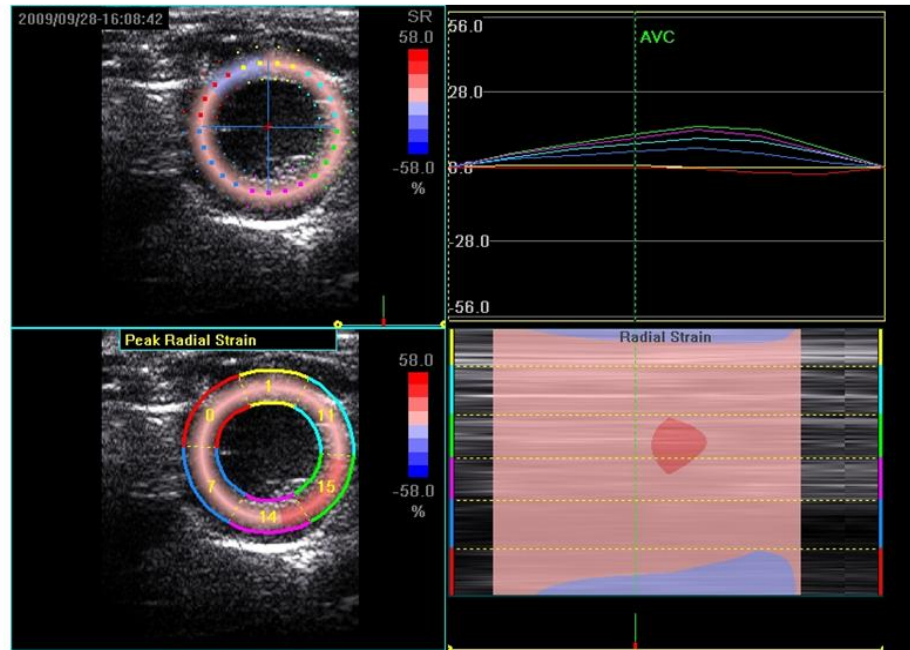


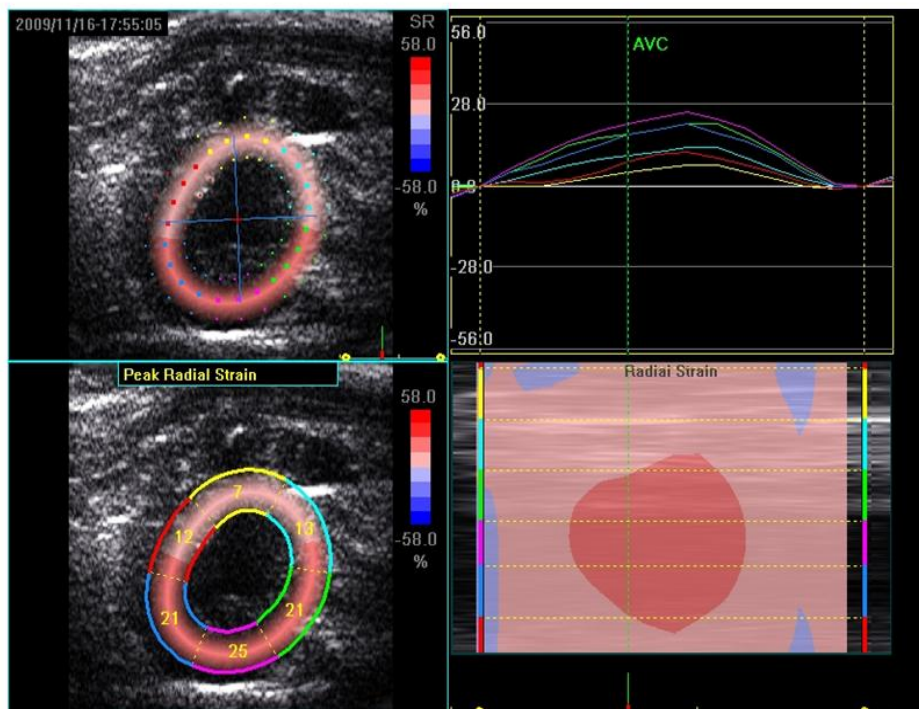
Figure 3.19: Global systolic radial strain of the left ventricle (defined as the mean of the regional systolic radial strains of the different segments of the LV) is shown in sham-operated diabetic rats (DM+SHAM), post-infarcted diabetic rats (DM+AMI) and post-infarcted diabetic rats with thyroid hormone treatment after 2 weeks.(ANOVA); ;Data are mean ± SEM; n=117-20; *P<0.05 vs DM+SHAM; **P<0.05 vs DM+SHAM and DM-AMI.

DM-AMI



(A)

DM-AMI+TH

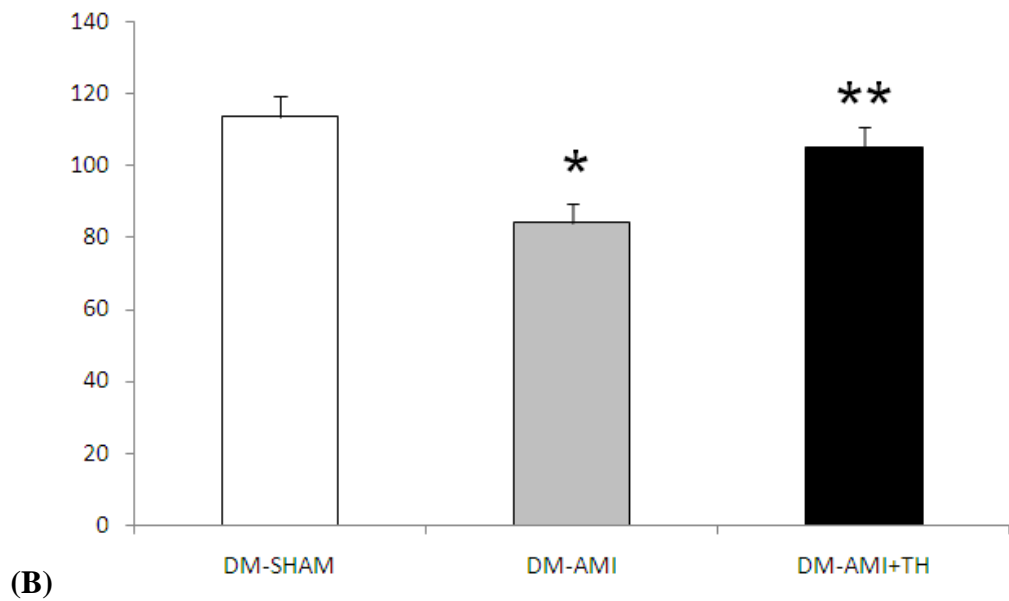


(B)

Figure 3.20: Images showing representative analysis of systolic radial strain of the left ventricle in diabetic post-infarcted rat heart (DM+AMI) and diabetic post-infarcted rat heart with thyroid hormone treatment (DM+AMI+TH). Typical of 11-20 such different experiments for each group.

(A)

LVDP (mmHg)



(B)

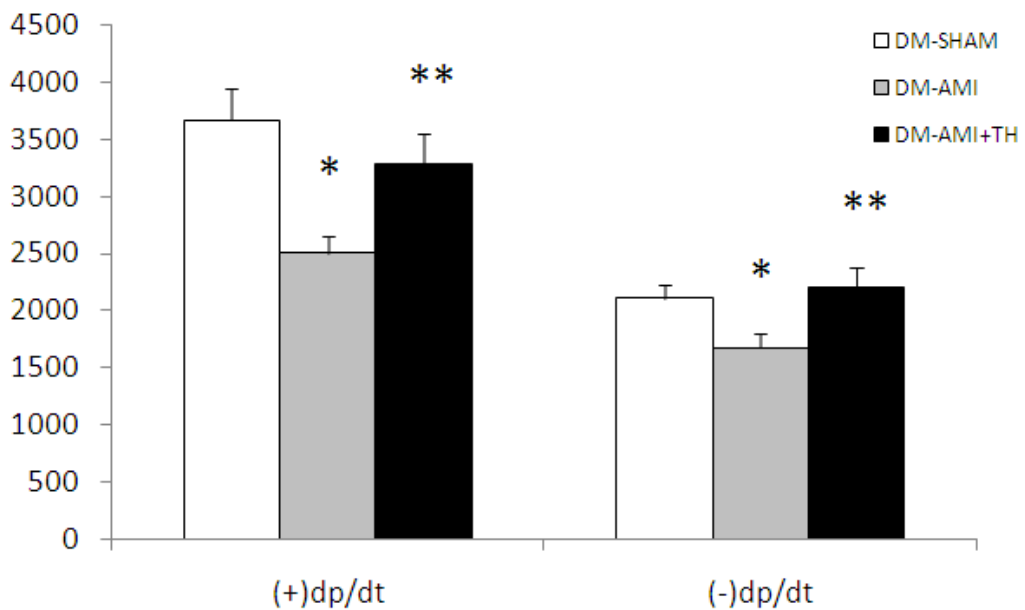


Figure 3.21: (A) Left ventricular developed pressure (LVDP) and (B) the rate of increase and decrease of LVDP (+dp/dt and -dp/dt) are shown in sham-operated diabetic rats (DM+SHAM), post-infarcted diabetic rats (DM+AMI) and post-infarcted diabetic rats with thyroid hormone treatment after 2 weeks. (ANOVA); Data are mean \pm SEM; n=11-20; *P<0.05 vs DM+SHAM; **P<0.05 vs DM+SHAM and DM+AMI.

C. Molecular Studies

Thyroid hormone nuclear receptor expression in the myocardium

Figures 3.22-3.23 show the protein expressions results for *thyroid hormone nuclear receptor*. The data show that nuclear TR α 1 and TR β 1 protein expressions were not significantly ($p>0.05$) different either between SHAM and DM+SHAM hearts, or between SHAM and NDM+AMI hearts. However, nuclear TR α 1 protein expression was found to be reduced significantly ($P<0.05$) by 2.1 fold in DM+AMI hearts compared to DM+SHAM (Figure 3.22). Similarly, nuclear TR β 1 protein expression was significantly reduced ($P<0.05$) by 2.0 fold in DM+AMI hearts compared to DM+SHAM (Figure 3.23).

Myosin isoform expression and calcium cycling proteins

Figures 3.24-3.25 show *myosin isoform expressions* and the *calcium cycling proteins in the heart under the different experimental conditions*. The results in figure 3.24 show significant ($P<0.05$) alterations in the pattern of myosin isoform expression in the viable myocardium. For example, the ratio of α -MHC to β -MHC expression was 6:1 in SHAM hearts as compared to 2:1 in both DM+SHAM and NDM+AMI hearts, $P<0.05$. Furthermore, in DM-AMI hearts α to β MHC ratio was 1:1, $p<0.05$ vs both DM+SHAM and NDM+AMI hearts. Figure 3.25 shows the expressions of SERCA and Phospholamban (PLB) under the different conditions. The results show that there was no significant difference in protein expressions for either SERCA or Phospholamban under the different experimental conditions.

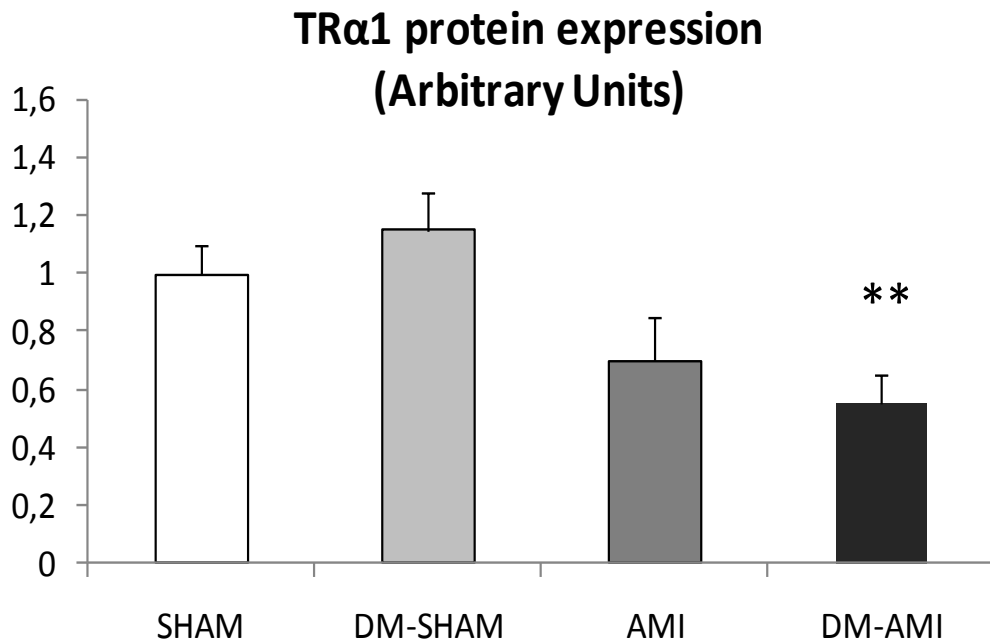
Expression of isoforms alpha, epsilon and delta of protein kinase C

Figure 3.26 shows the protein expressions of isoforms alpha, epsilon and delta of protein kinase C. The results show that the PKC δ was found to be significantly ($P < 0.05$) increased by 2.35 fold in AMI as compared to SHAM hearts. In DM+AMI hearts, PKC δ was also increased significantly ($p < 0.05$) by 2.5 fold as compared to DM+SHAM. No significant ($P > 0.05$) difference was seen between AMI and DM+AMI hearts. Similarly, no significant ($P > 0.05$) difference was found in PKC ϵ levels between all groups, PKC α protein expression was similar in SHAM and DM-SHAM hearts. However, there was a significant ($P < 0.05$) increase in PKC α levels by 2.5 fold in DM+AMI as compared to DM+SHAM hearts. A slight trend to increase was seen in PKC α in AMI hearts compared to SHAM.

Activation of intracellular kinase signalling

Figures 3.27-3.30 show the activation of a number of intracellular kinases under the different experimental conditions. The results show no significant ($P > 0.05$) difference in JNK kinase and phospho-Akt levels between all groups (Figures 3.28-3.29). In DM-SHAM hearts, phospho-p38 MAPK levels were also not significantly different from SHAM, but significantly ($P < 0.05$) increased in AMI hearts compared to DM combined with AMI hearts and significantly ($P < 0.05$) decreased in DM+AMI hearts (figure 3.27) compared to AMI hearts. In contrast, the protein expressions for phospho-p44 and p42 ERK kinases increased significantly ($P < 0.05$) by 1.8 and 2.0 folds, respectively as compared to SHAM hearts (figure 3.30). In AMI hearts, phospho-p38 MAPK levels were found to be increased 1.9 fold compared SHAM,, while phospho-p44 and p42 ERK kinases were significantly ($P < 0.05$) increased by 2.0 and 2.2 folds, respectively as compared to SHAM hearts. In DM+AMI hearts, phospho-p38 MAPK levels were found to be significantly ($P < 0.05$) reduced by 2.0 fold as compared to AMI, while remained unchanged as compared to DM+SHAM hearts, $P > 0.05$. In addition, phospho-p44 and p42 ERK kinases were unchanged in DM+AMI as compared to both AMI and DM-SHAM hearts, $P > 0.05$ (Figures 3.27 -3.30).

(A)



(B)

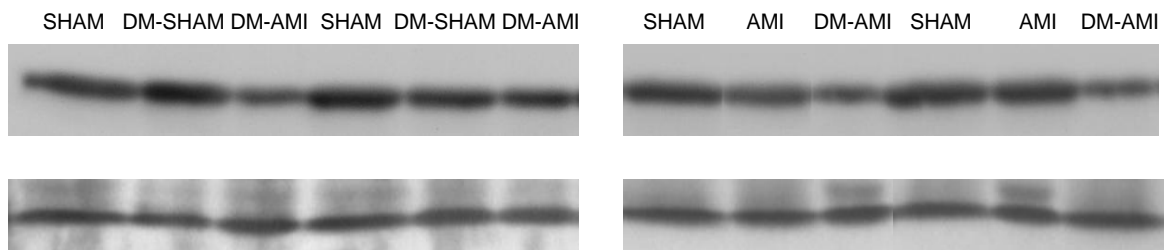
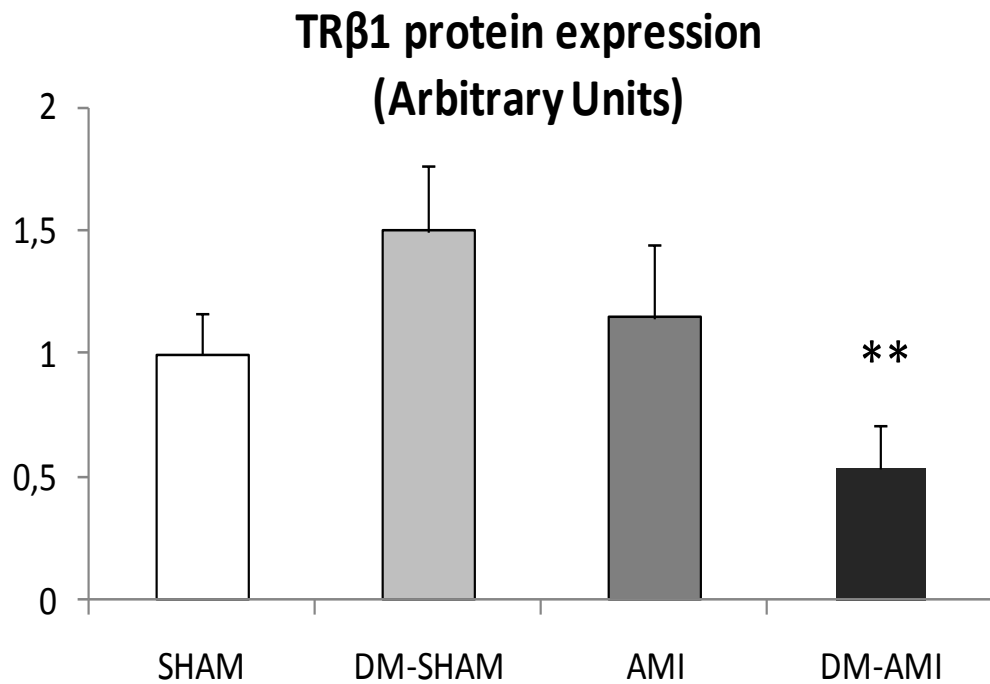


Figure 3.22: (A) Densitometric assessment in arbitrary units and (B) representative Western Blots of thyroid hormone receptor α 1 (TR α 1) protein expression in sham-operated rats (SHAM), sham-operated diabetic rats (DM+SHAM), post-infarcted rats (AMI) and post-infarcted diabetic rats (DM+AMI) after 2 weeks. Molecular weights of proteins (in kDa) were assessed by molecular weight markers. TR α 1 was detected as single band with molecular weights around 50 kDa, respectively. Histone H3 was used to normalize for slight variations in nuclear protein loading. (Columns are means of optical ratio or arbitrary units. (Mann-Whitney); Data are mean \pm SEM; n=11-20; **P<0.05 vs SHAM and DM-SHAM.

(A)



(B)

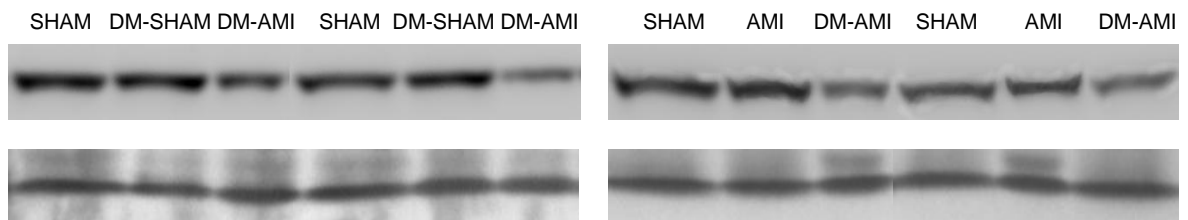
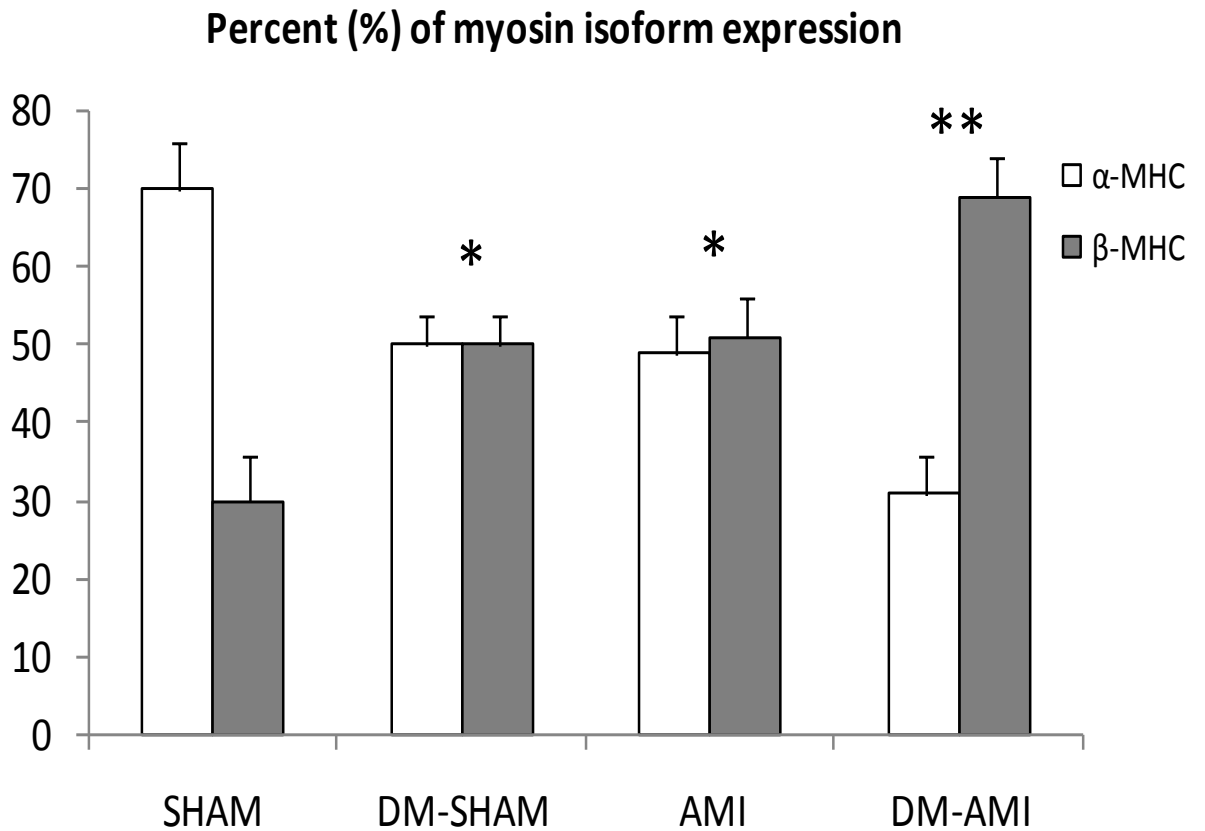


Figure 3.23: (A) Densitometric assessment in arbitrary units and (B) representative Western Blots of thyroid hormone receptor β 1 (TR β 1) protein expression in sham-operated rats (SHAM), sham-operated diabetic rats (DM+SHAM), post-infarcted rats (AMI) and post-infarcted diabetic rats (DM+AMI) after 2 weeks. Molecular weights of proteins (in kDa) were assessed by molecular weight markers. TR β 1 was detected as single band with molecular weight around 60 kDa, respectively. Histone H3 was used to normalize for slight variations in nuclear protein loading. (Columns are means of optical ratios or arbitrary units, \pm SEM; Mann-Whitney); ** $P < 0.05$ vs DM-SHAM and AMI.

(A)



(B)

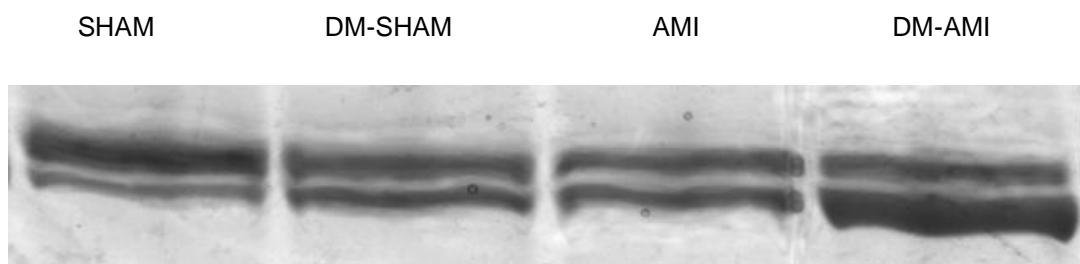
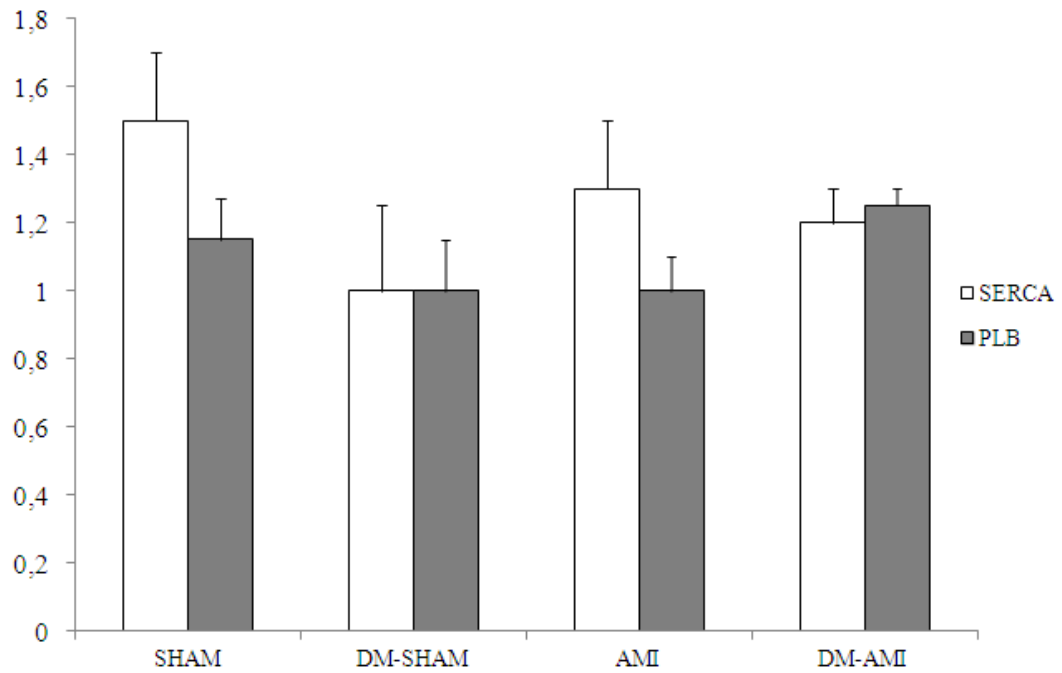


Figure 3.24: (A) Densitometric assessment in arbitrary units (%) and (B) representative images of myosin heavy chain isoform expression in sham-operated rats (SHAM), sham-operated diabetic rats (DM+SHAM), post-infarcted operated rats (AMI) and post-infarcted diabetic rats (DM+AMI) after 2 weeks. (Columns are means of optical ratios or arbitrary units, \pm SEM; ANOVA). * $P < 0.05$ vs SHAM; ** $P < 0.05$ vs DM+SHAM and AMI.

(A)

SERCA and PLB protein expression (Arbitrary Units)



(B)

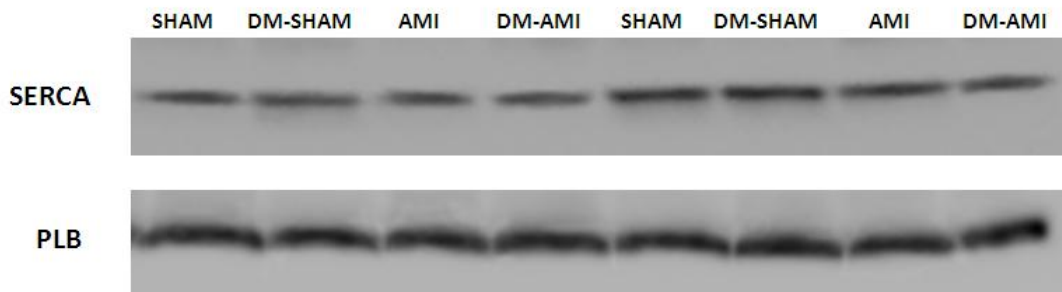
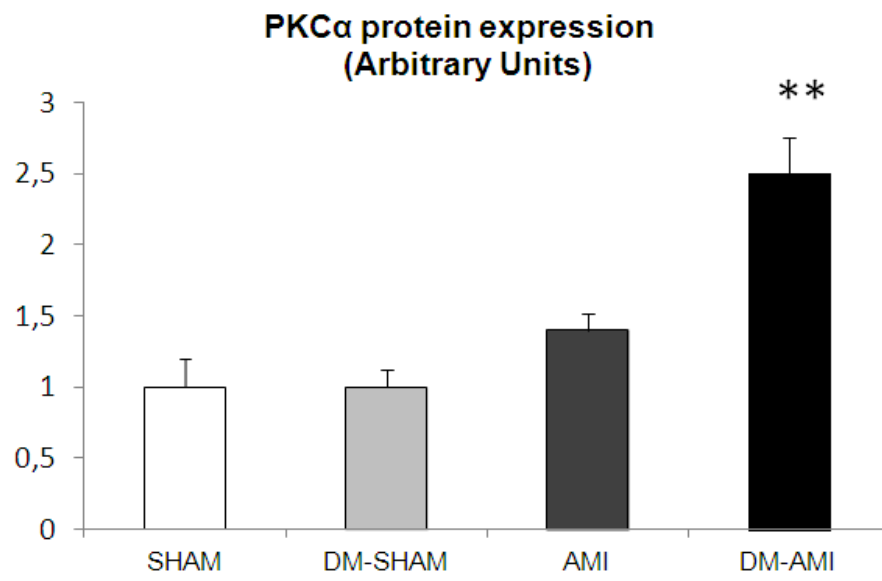
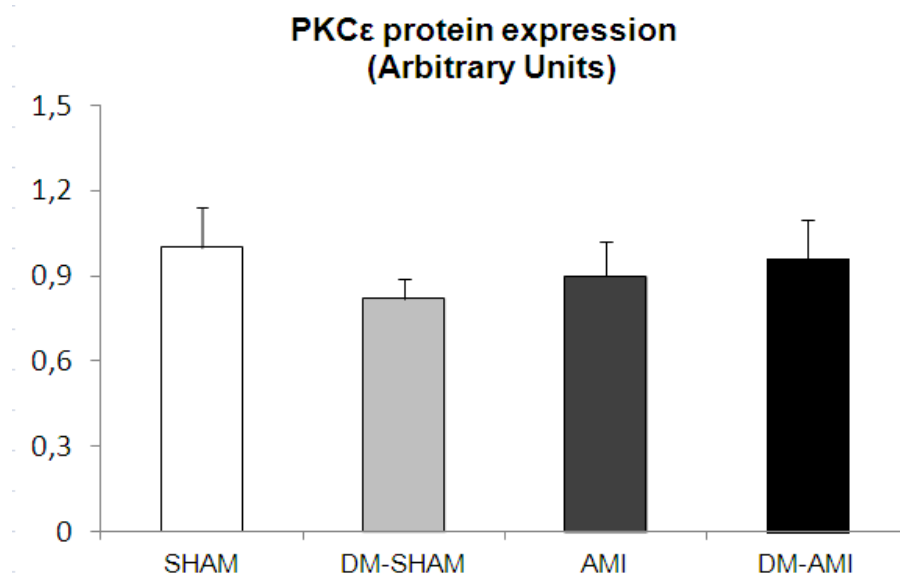


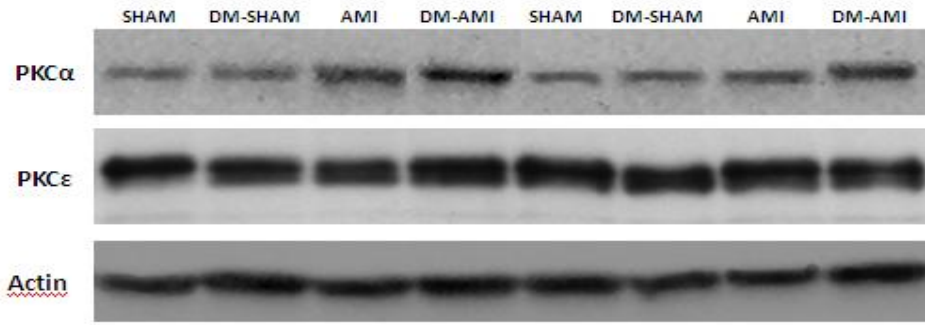
Figure 3.25: (A) Densitometric assessment in arbitrary units and (B) representative Western Blots of SERCA and phospholamban (PLB) protein expression in sham-operated rats (SHAM), sham-operated diabetic rats (DM+SHAM), post-infarcted rats (AMI) and post-infarcted diabetic rats (DM+AMI) after 2 weeks. (Columns are means of optical ratios or arbitrary units, \pm SEM; Mann-Whitney). Note that there was no significant difference in protein expressions for either SCERCA and PLB between the different parameters.

(A)



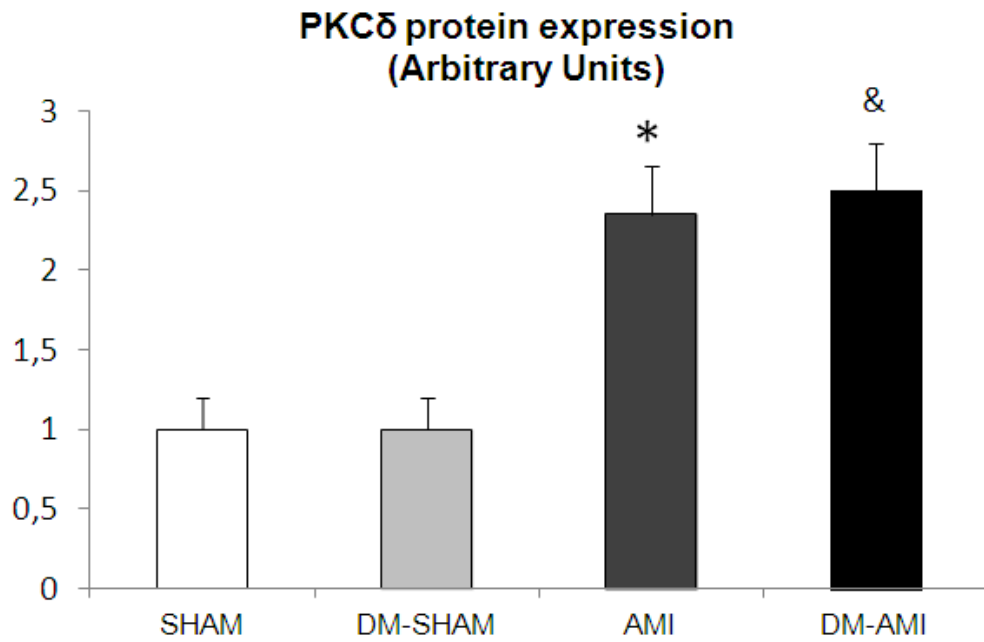
(B)





(C)

(D)

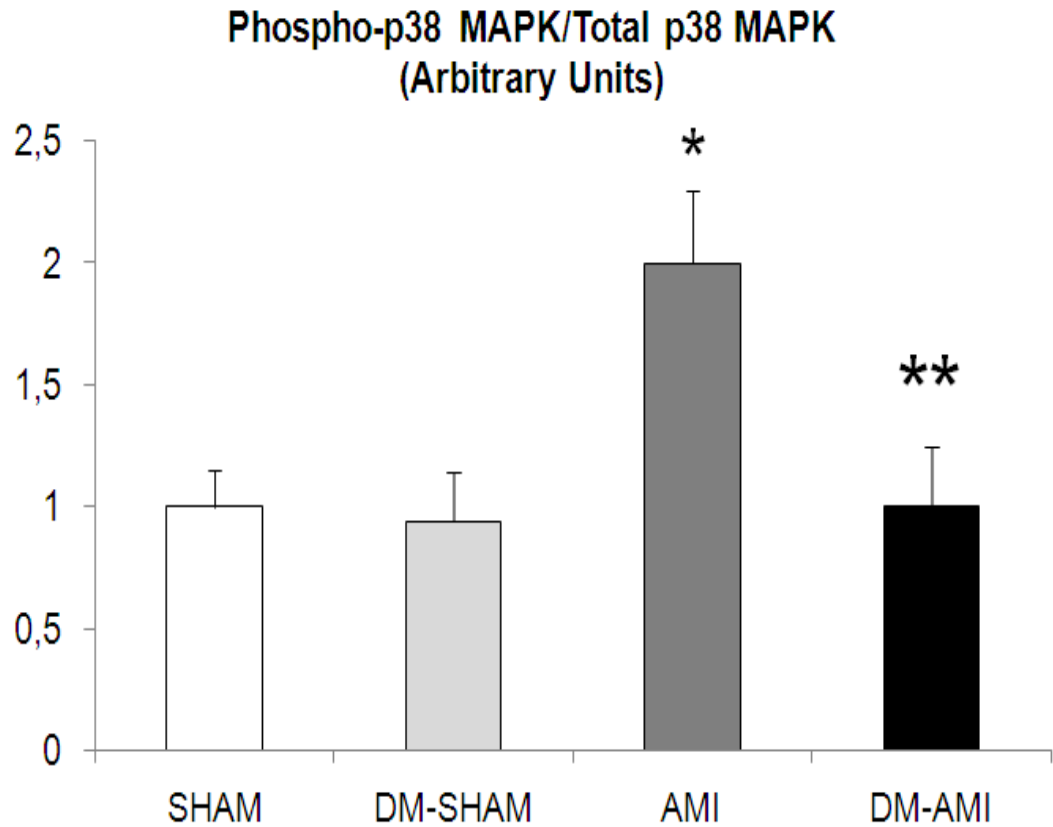


(E)



Figure 3.26: (A,B and D) Densitometric assessment in arbitrary units and (C and E) representative Western Blots of isoforms α , ϵ and δ of PKC in sham-operated rats (SHAM), sham-operated diabetic rats (DM-SHAM), post-infarcted rats (AMI) and post-infarcted diabetic rats (DM-AMI) after 2 weeks. (Columns are means of optical ratios or arbitrary units, \pm SEM; Mann-Whitney); $n=12=20$; * $P<0.05$ vs SHAM; ** $P<0.05$ vs DM-SHAM and AMI; & $P<0.05$ vs DM-SHAM

(A).



(B)

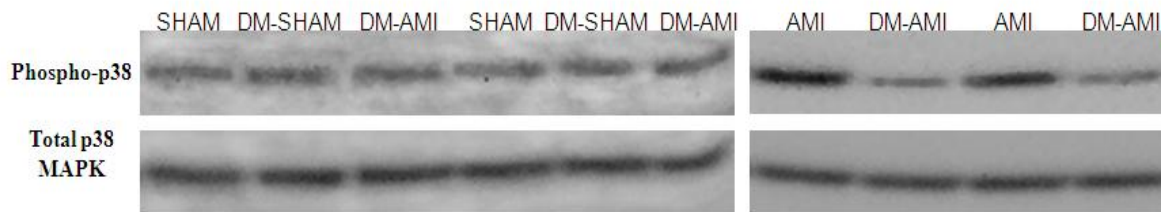
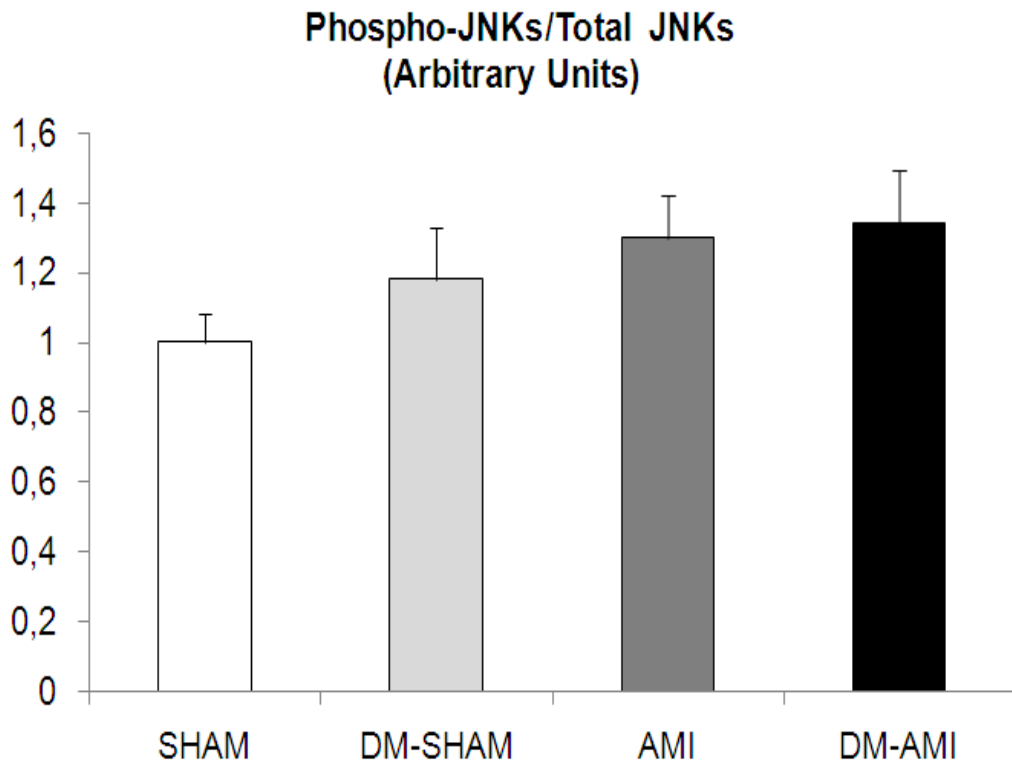


Figure 3.27: (A) Densitometric assessment in arbitrary units and (B) representative Western Blots of phosphorylated levels of p38 MAP kinase in sham-operated rats (SHAM), sham-operated diabetic rats (DM+SHAM), post-infarcted rats (AMI) and post-infarcted diabetic rats (DM+AMI) after 2 weeks. (Columns are means of optical ratios or arbitrary units, \pm SEM; Mann-Whitney); $n=11-20$; * $P<0.05$ vs SHAM, # $P<0.05$ vs DM+SHAM and DM+AMI

(A)

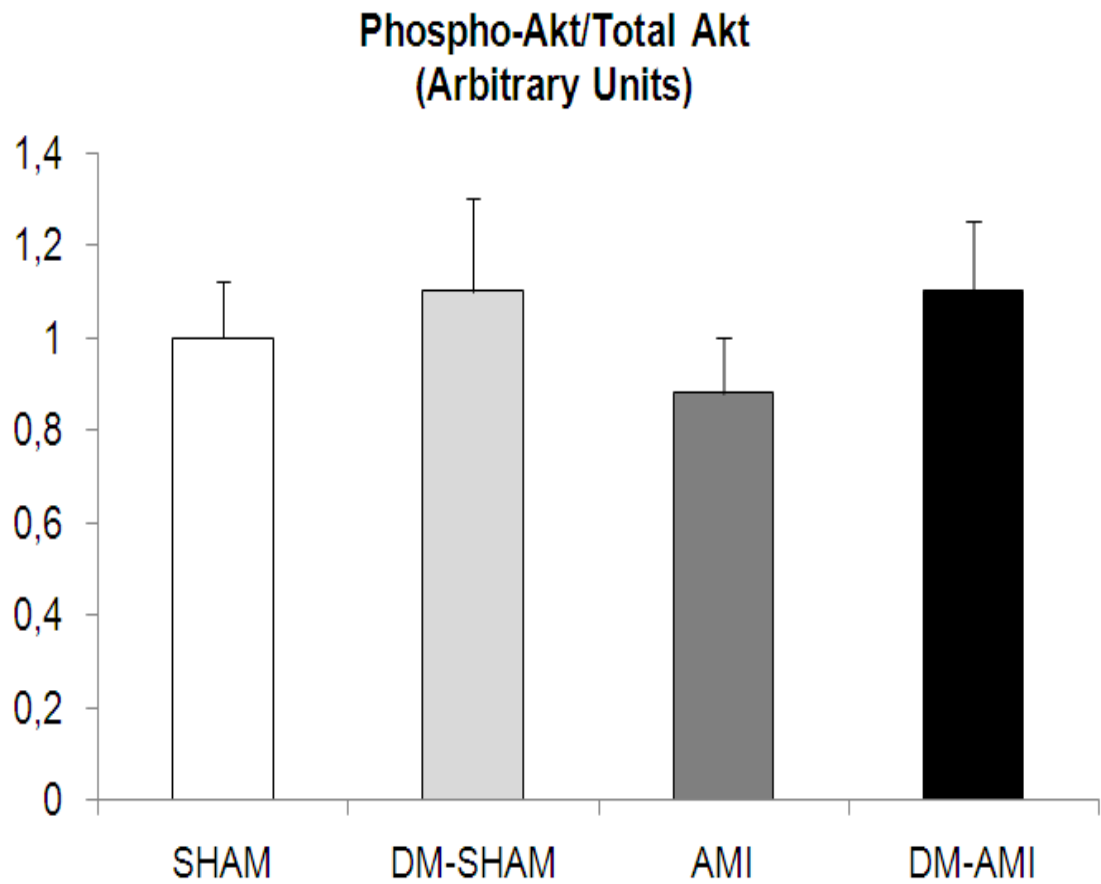


(B)



Figure 3.28: (A) Densitometric assessment in arbitrary units and (B) representative Western Blots of phosphorylated levels of p54 JNK in sham-operated rats (SHAM), sham-operated diabetic rats (DM+SHAM), post-infarcted rats (AMI) and post-infarcted diabetic rats (DM+AMI) after 2 weeks. (Columns are means of optical ratios or arbitrary units, \pm SEM; Mann-Whitney); n=11-20. There is no significant difference between the different parameters.

(A)



(B)

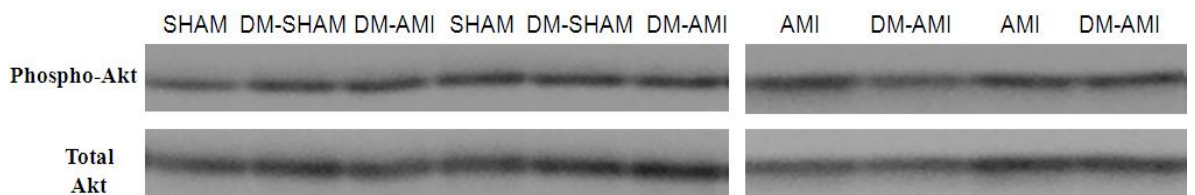
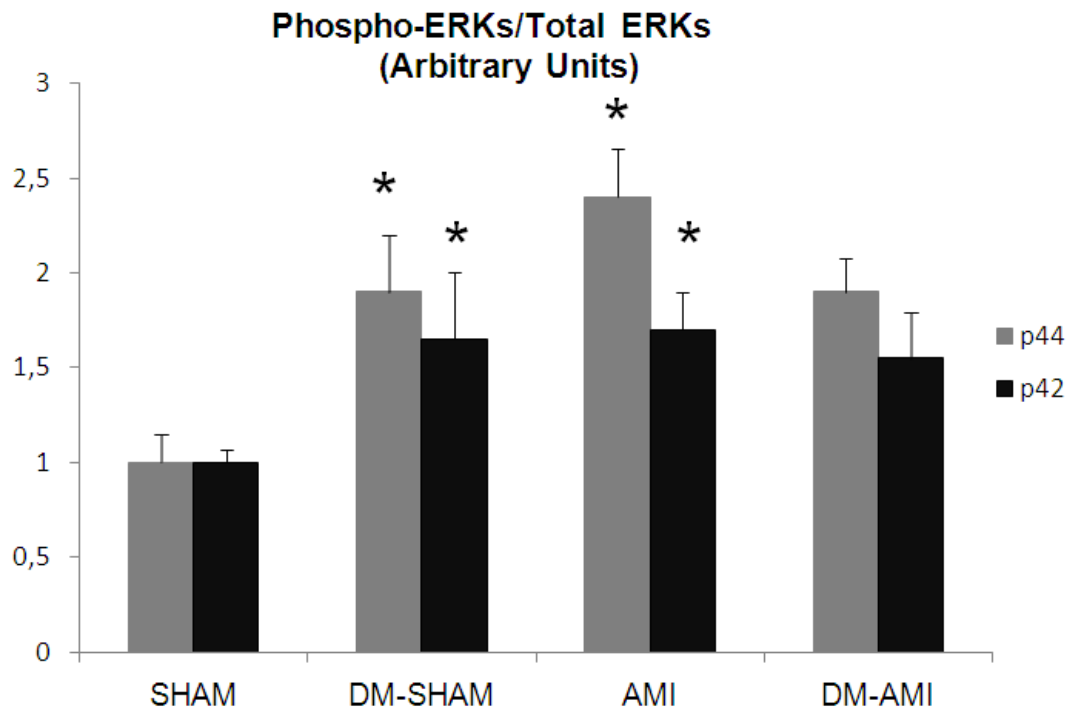


Figure 3.29: (A) Densitometric assessment in arbitrary units and (B) representative Western Blots of phosphorylated levels of Akt kinase in sham-operated rats (SHAM), sham-operated diabetic rats (DM+SHAM), post-infarcted rats (AMI) and post-infarcted diabetic rats (DM+AMI) after 2 weeks. (Columns are means of optical ratios or arbitrary units, \pm SEM; Mann-Whitney). Note that there was no significant difference between the different parameters .n=11-20.

(A)



(B)



Figure 3.30: (A) Densitometric assessment in arbitrary units and (B) representative Western Blots of phosphorylated levels of p44 and p42 ERKs in sham-operated rats (SHAM), sham-operated diabetic rats (DM+SHAM), post-infarcted rats (AMI) and post-infarcted diabetic rats (DM+AMI) after 2 weeks. (Columns are means of optical ratios or arbitrary units, \pm SEM; Mann-Whitney); $n=11-20$; $.* P<0.05$ vs SHAM, $^{\#}P<0.05$ vs DM+SHAM and DM+AMI

2. Effects of TH administration on the response of the diabetic heart after myocardial infarction

Thyroid hormone nuclear receptor expression in the myocardium

Figure 3.31 shows the thyroid hormone nuclear receptor expression in the myocardium. The results show that the nuclear TR α 1 protein expression was found to be reduced significantly ($P < 0.05$) by 2.1 fold in DM+AMI hearts compared to DM+SHAM. Moreover, nuclear TR β 1 protein expression was 2.0 fold less in DM+AMI hearts, $P < 0.05$ compared to DM+SHAM. . In DM+AMI+TH hearts, TR α 1 expression was increased as compared to DM+AMI hearts but not at a statistically significant level (Figure 3.31). Furthermore, in DM+AMI+TH hearts, TR β 1 expression was significantly ($P < 0.05$) increased by 2.0 fold as compared to DM+AMI hearts,. No significant changes T₄ plasma levels were observed, but there was a significant ($P < 0.05$) increase in plasma T₃ level for DM+AMI+TH compared to either DM+AMI or AMI+SHAM animals.

Calcium cycling proteins and myosin isoform expression

Figures 3.32-3.33 show that functional changes were accompanied by alterations in the pattern of myosin isoform expression (figure 3.32) and calcium cycling proteins (figure 3.33) in the viable myocardium. Thus, in DM+AMI hearts, SERCA was unchanged while phospholamban was found to be slightly increased 1.25 fold as compared to DM+SHAM but not at a statistically significant level, $p > 0.05$. Furthermore, the ratio of α -MHC to β -MHC expression was 2:1 in DM+SHAM as compared to 1:1 in DM+AMI hearts, $P < 0.05$ (Figure 3.33). TH treatment resulted in 1.8 fold increase in SERCA expression ($P < 0.05$) with no accompanying changes in PLB expression in DM+AMI+TH hearts as compared to DM+AMI hearts. DM+AMI+TH hearts were

found to express only α -MHC, as compared to 1:1 ratio of α -MHC to β -MHC expression in DM-AMI hearts, respectively; $P < 0.05$ (Figure 3.33).

Expression of isoforms alpha and epsilon of protein kinase C

Figure 3.34 shows the protein expressions of isoforms alpha and epsilon of protein kinase C. The results show that in DM+AMI hearts, PKC δ expression was found to be significantly ($P < 0.05$) increased by 2.5 fold as compared to DM+SHAM. TH treatment resulted in 2.0 fold increase ($P < 0.05$) in PKC δ in DM-AMI+TH hearts as compared to DM-SHAM hearts, while no significant ($P > 0.05$) difference was found between DM+AMI+TH and DM+AMI hearts (Figure 3.34). In DM+AMI hearts, PKC α expression was found to be increased 2.5 fold as compared to DM+SHAM ($P < 0.05$) while PKC ϵ remained unchanged as compared to DM+SHAM hearts, $P > 0.05$. (Figure 3.34). TH treatment resulted in 1.9 fold reduction in PKC α and 1.8 fold reduction in PKC ϵ in DM+AMI+TH hearts as compared to DM+AMI hearts, $P < 0.05$ (Figure 3.34).

Intracellular kinase signalling activation

Figures 3.36-3.38 show the intracellular kinase signalling activation proteins. The results show a significant ($P < 0.05$) difference in the protein expressions for phospho-p38 MAPK/total p38 MAPK (measured as arbitrary units) for DM+AMI+TH compared to DM+SHAM or DM+AMI. In contrast, the data show no significant difference in the gene expressions for phospho-Akt, phospho-ERK and phospho-JNK kinase levels between DM+SHAM, DM+AMI and DM+AMI+TH hearts; $P > 0.05$ (Figures 3.36-3.38)

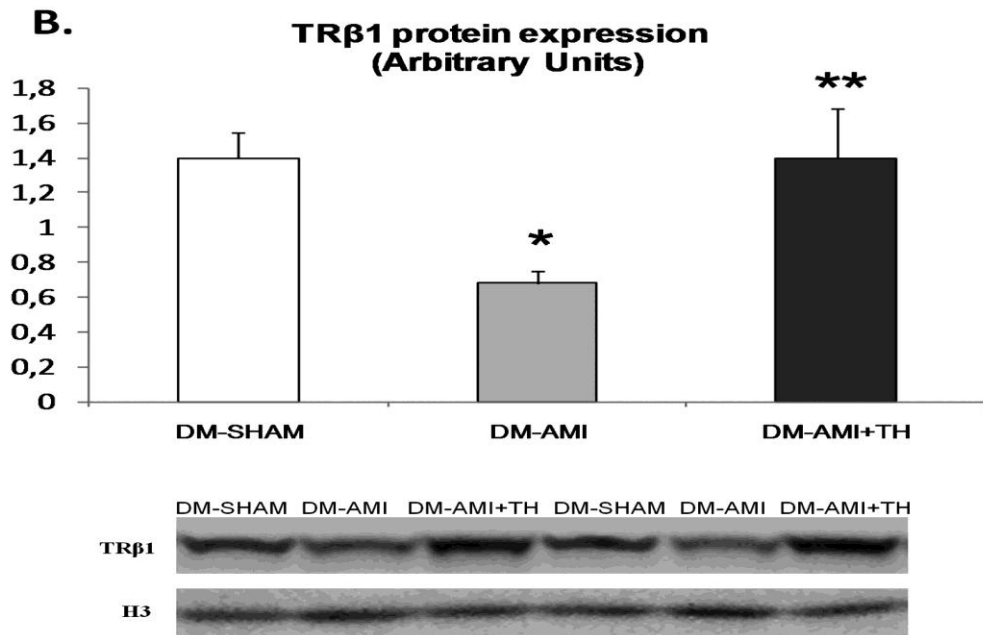
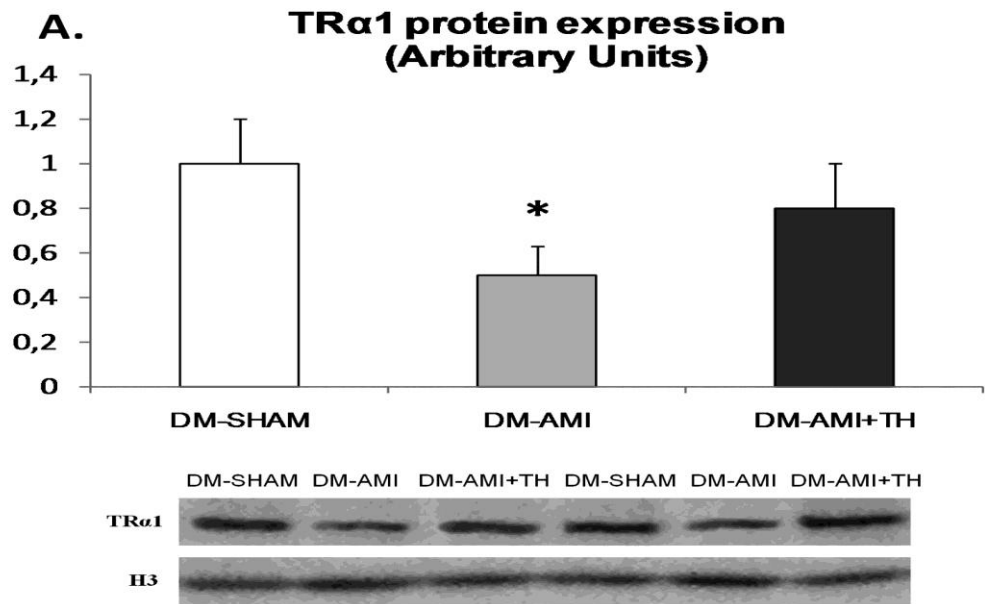
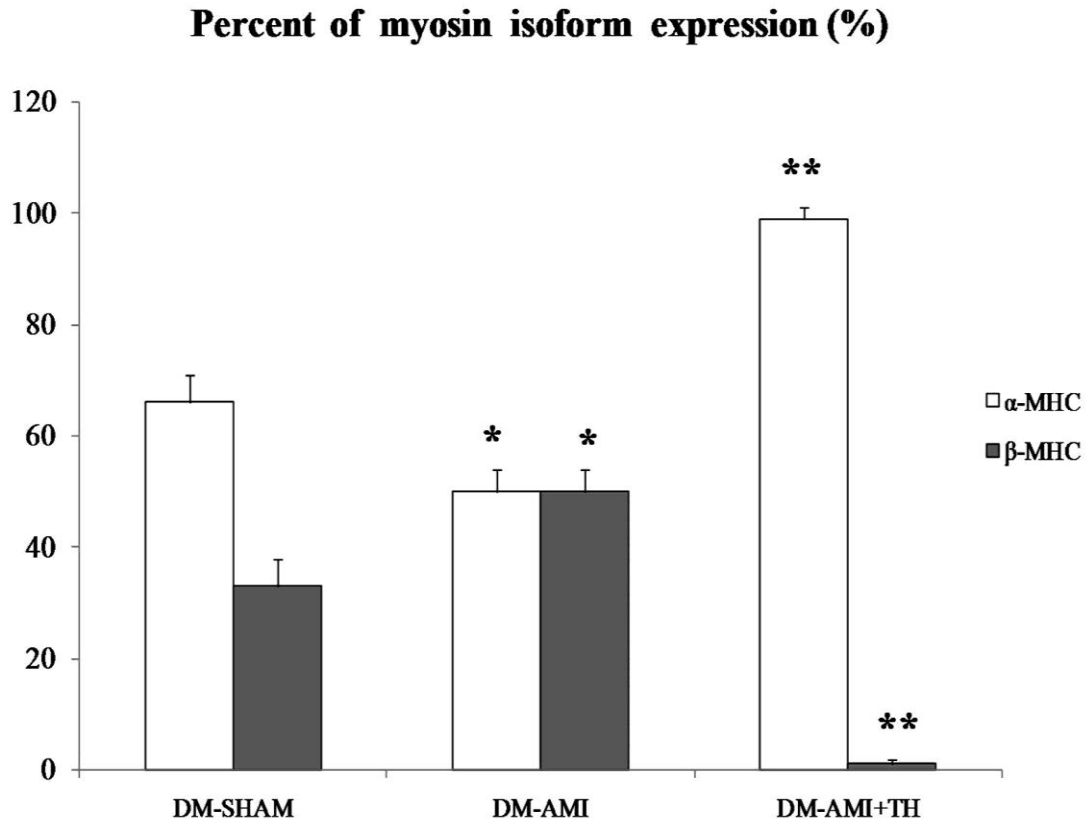


Figure 3.31: (A and B) Densitometric assessment in arbitrary units and (C) representative Western Blots of thyroid hormone receptor α 1 (TR α 1) and β 1 (TR β 1) protein expressions are shown in SHAM-operated diabetic rats (DM+SHAM), post-infarcted diabetic rats (DM+AMI) and post-infarcted diabetic rats with thyroid hormone treatment after 2 weeks. Histone H3 was used to normalize for slight variations in nuclear protein loading. Columns are means of optical ratios, bar=SEM; Mann-Whitney); n=11-20; * P<0.05 vs DM-SHAM, ** p<0.05 vs DM-AMIC

(A)



(B)

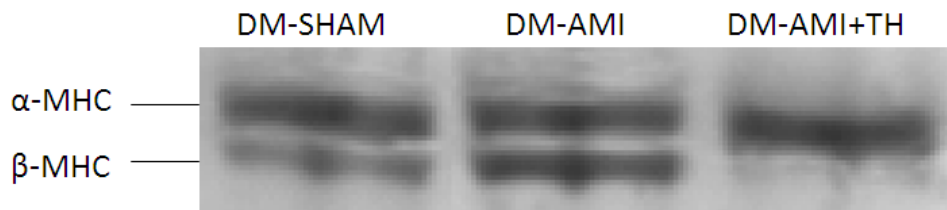
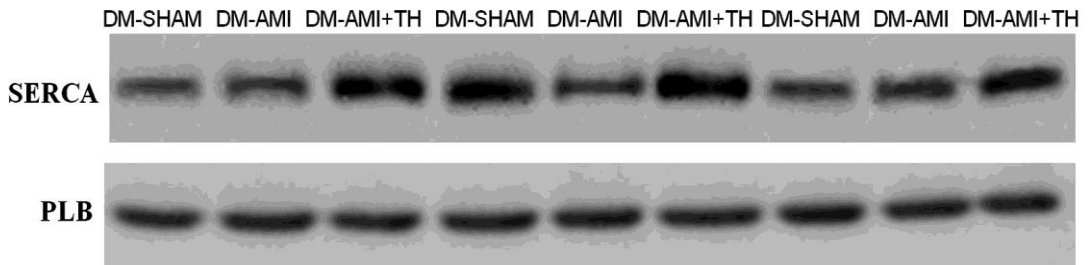
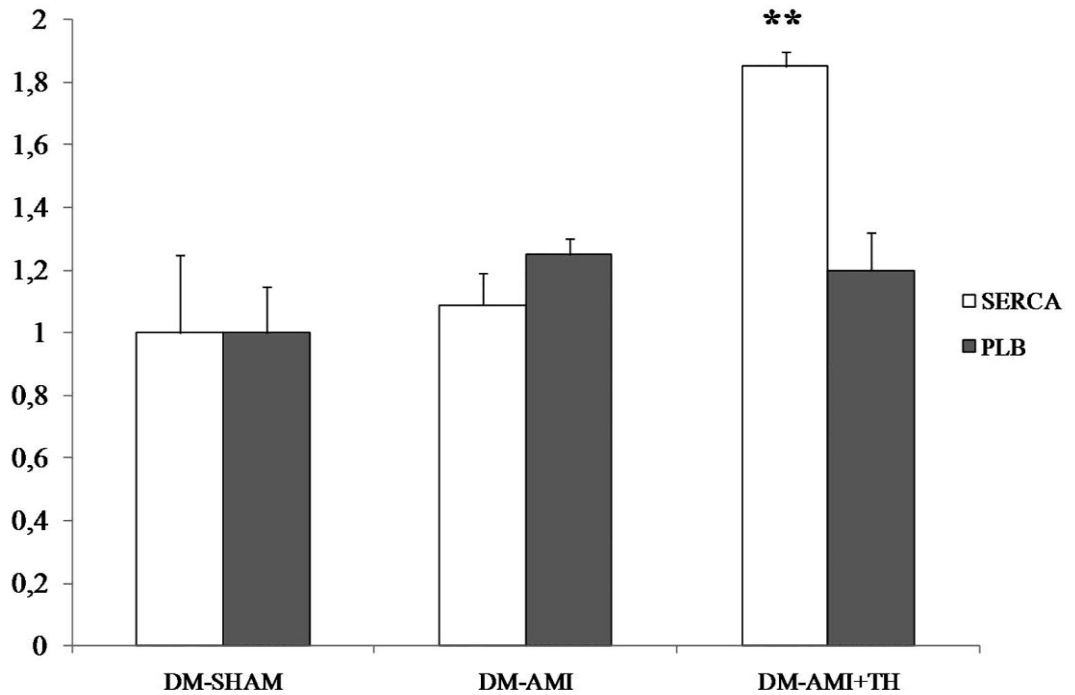


Figure 3.32: Densitometric assessment in arbitrary units and representative images of myosin heavy chain isoform expression shown in sham-operated diabetic rats (DM+SHAM), post-infarcted diabetic rats (DM+AMI) and post-infarcted diabetic rats with thyroid hormone treatment after 2 weeks. (Columns are means of optical ratios or arbitrary units, \pm SEM; ANOVA); $n=11-20$; * $P<0.05$ vs DM+SHAM, ** $P<0.05$ vs DM+SHAM and DM+AMI

(A)

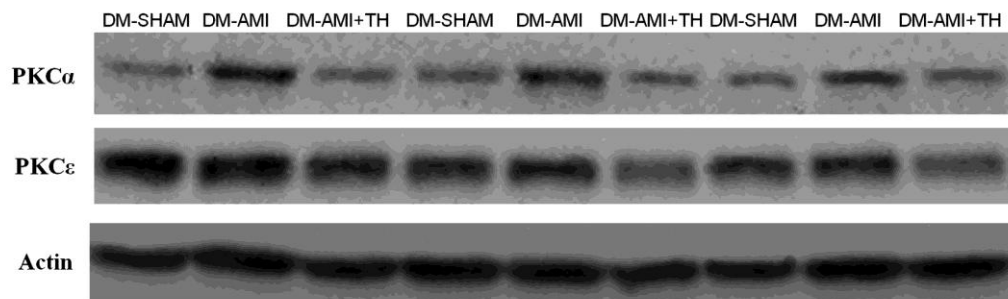
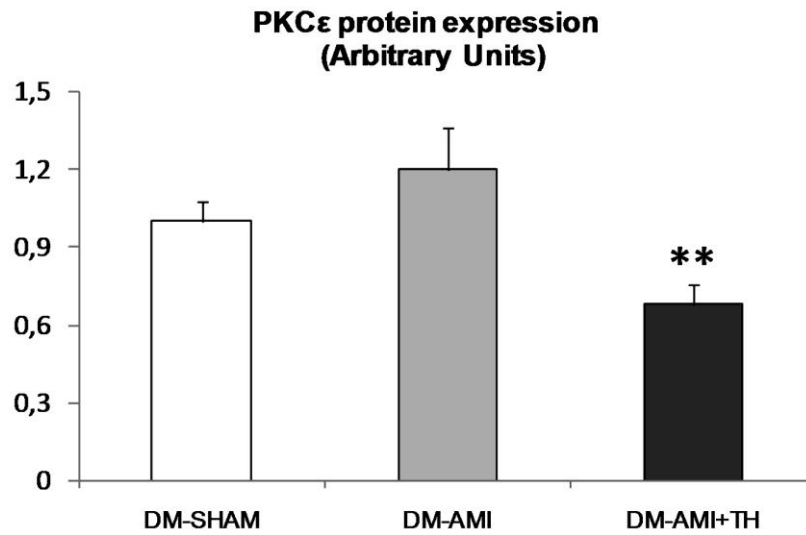
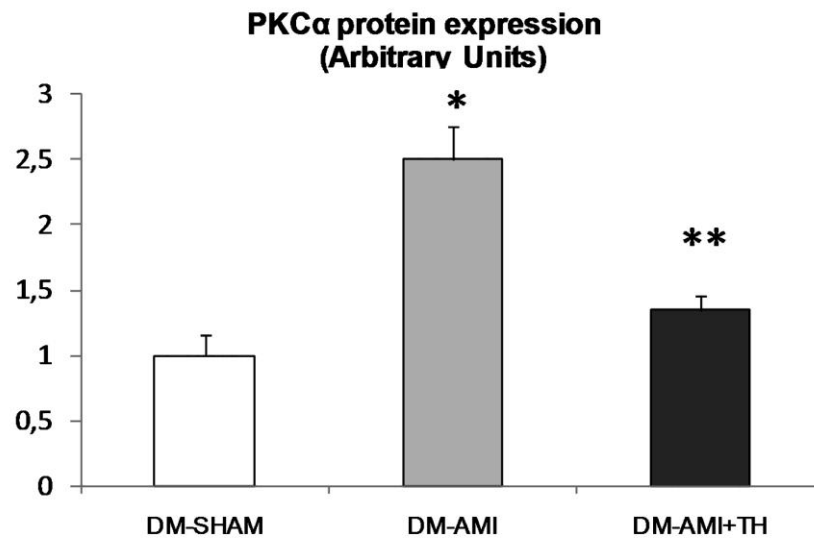
SERCA and PLB protein expression (Arbitrary Units)



(B)

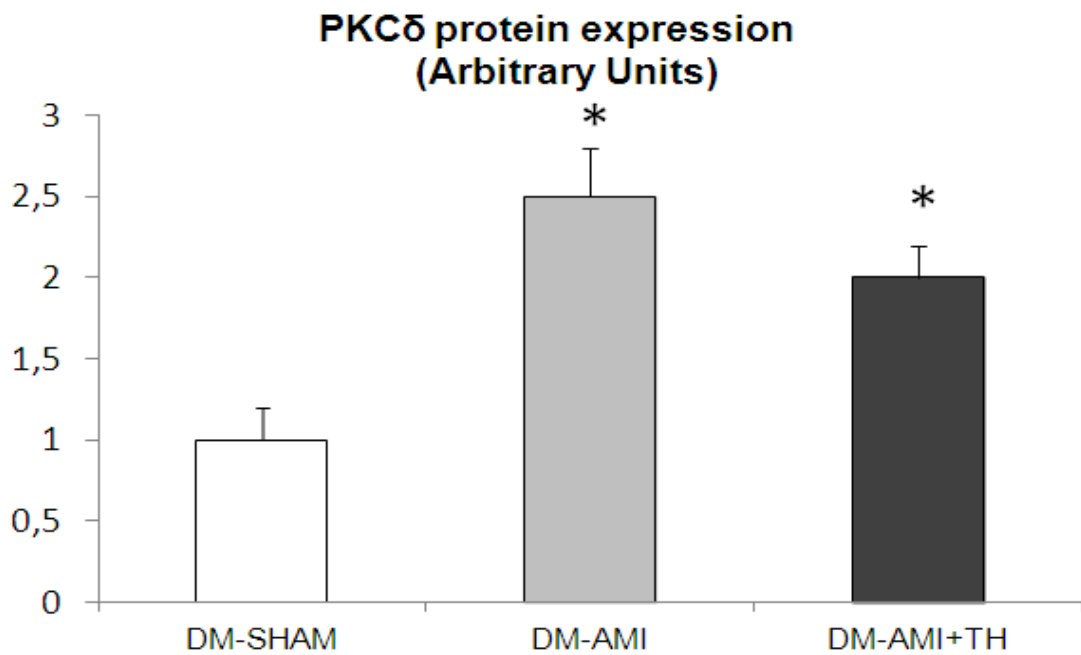
Figure 3.33: (A) Densitometric assessment in arbitrary units and (B) representative Western Blots of SERCA and phospholamban protein expressions are shown in sham-operated diabetic rats (DM+SHAM), post-infarcted diabetic rats (DM+AMI) and post-infarcted diabetic rats with thyroid hormone treatment after 2 weeks. (Columns are means of optical ratios or arbitrary units, \pm SEM; Mann-Whitney); n=11-20; ** P<0.05 vs DM-SHAM and DM-AMI.

(A)



(B)

(A)



(B)

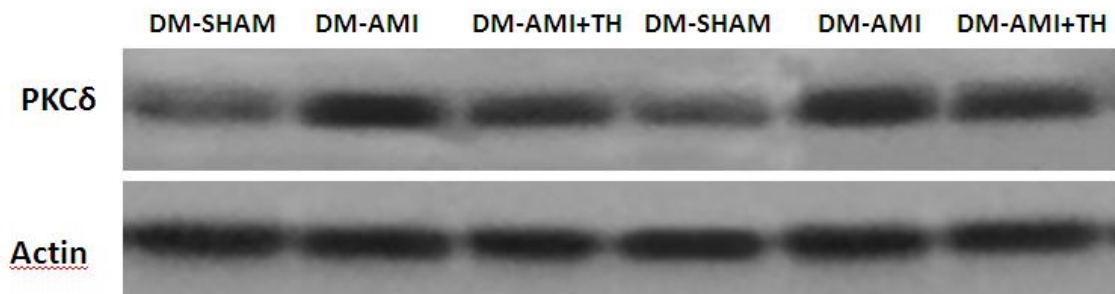
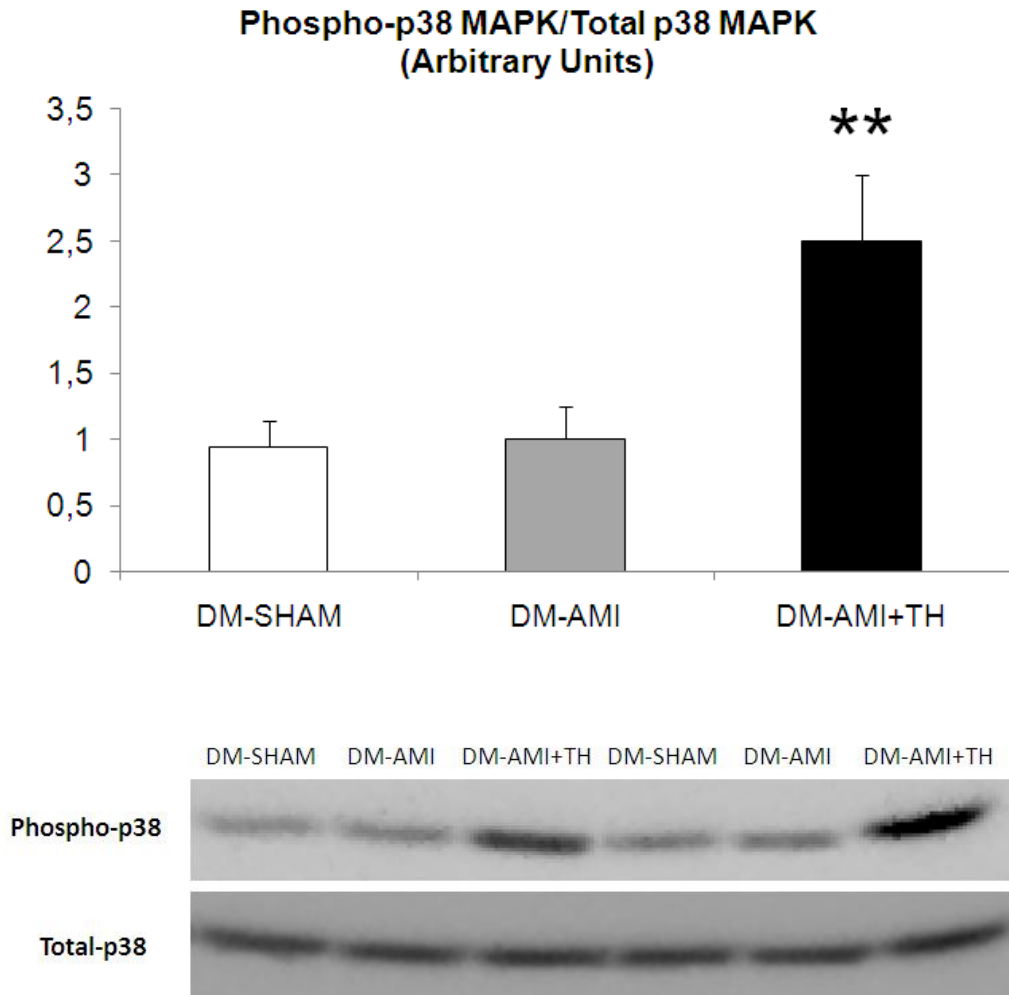


Figure 3.34: (A) Densitometric assessment in arbitrary units and (B) representative Western Blots of isoforms α , ϵ and δ of PKC are shown in sham-operated diabetic rats (DM+SHAM), post-infarcted diabetic rats (DM+AMI) and post-infarcted diabetic rats with thyroid hormone treatment after 2 weeks. (Columns are means of optical ratios or arbitrary units, \pm SEM; Mann-Whitney); $n=11-20$; * $P<0.05$ for DM +AMI vs DM+SHAM; * $P<0.05$ for DM+AMI + TH vs DM+SHAM and AMI.

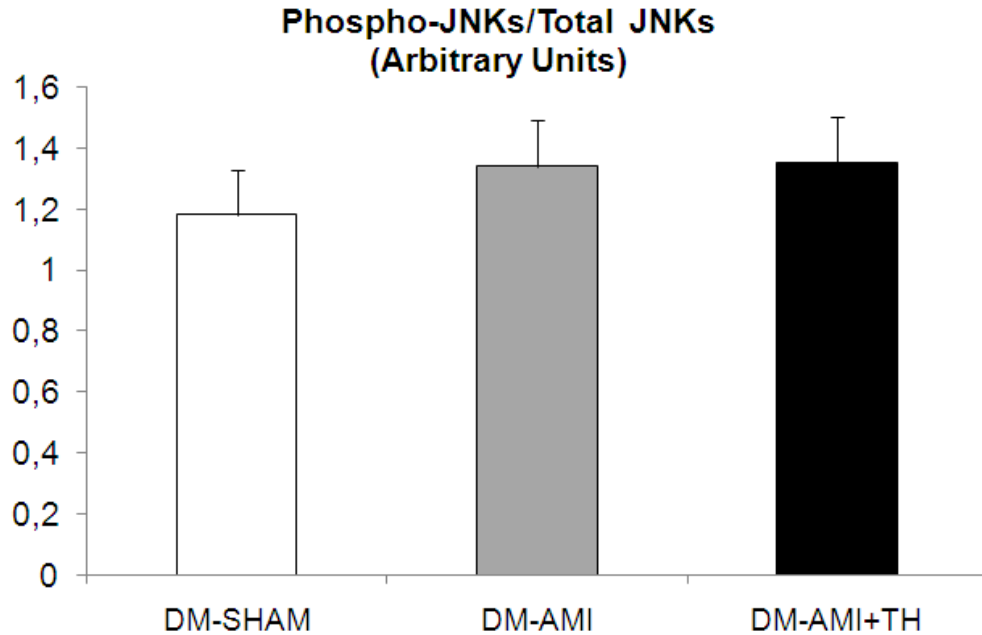
(A)



(B)

Figure 3.35: (A) Densitometric assessment in arbitrary units and (B) representative Western Blots of phosphorylated levels of p38 MAP kinase are shown in sham-operated diabetic rats (DM-SHAM), post-infarcted diabetic rats (DM-AMI) and post-infarcted diabetic rats with thyroid hormone treatment after 2 weeks. (Columns are means of optical ratios or arbitrary units, \pm SEM; Mann-Whitney); $n=11-20$; ** $P<0.05$ vs DM+SHAM and DM+AMI

(A)



(B)

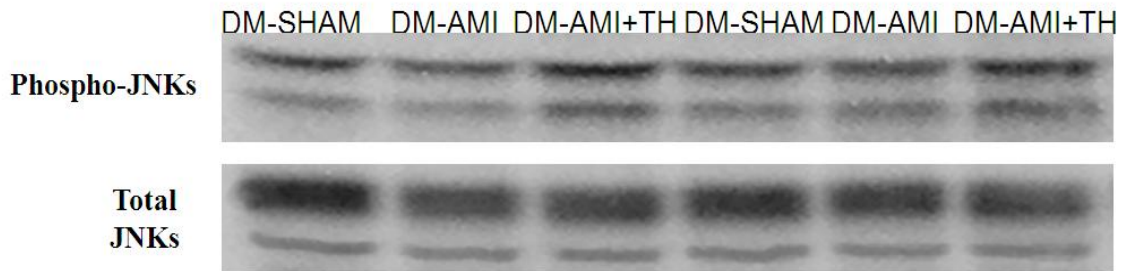
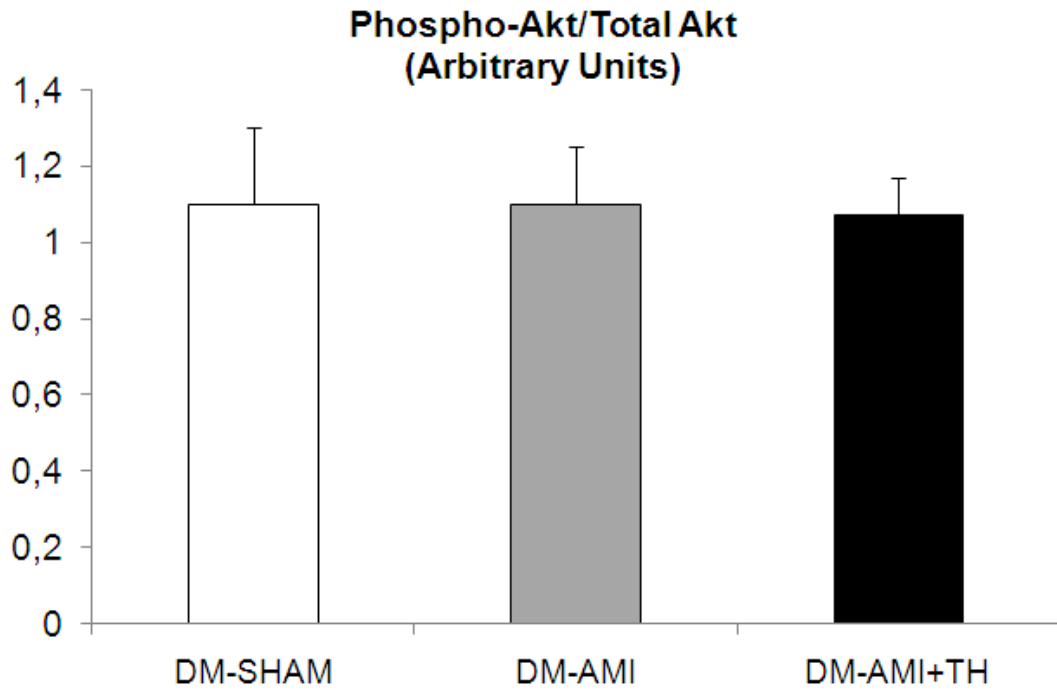


Figure 3.36: (A) Densitometric assessment in arbitrary units and (B) representative Western Blots of phosphorylated levels of p54 JNK in sham-operated diabetic rats (DM-SHAM), post-infarcted diabetic rats (DM+AMI) and post-infarcted diabetic rats with thyroid hormone treatment after 2 weeks. (Columns are means of optical ratios or arbitrary units, \pm SEM; Mann-Whitney); n=11-20; Note that there is no significant difference in the different parameters.

(A)



(B)

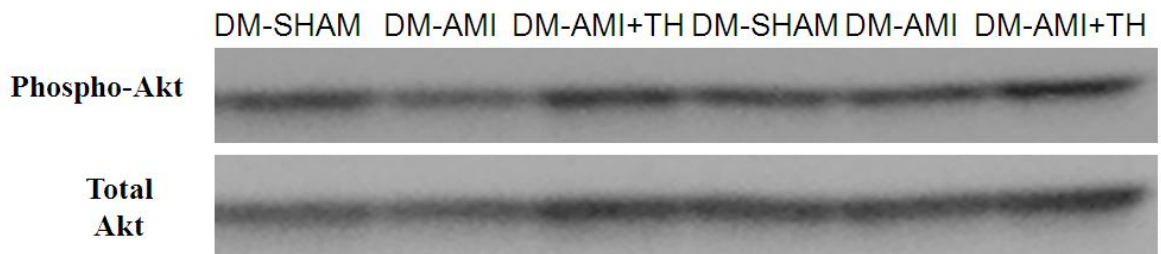
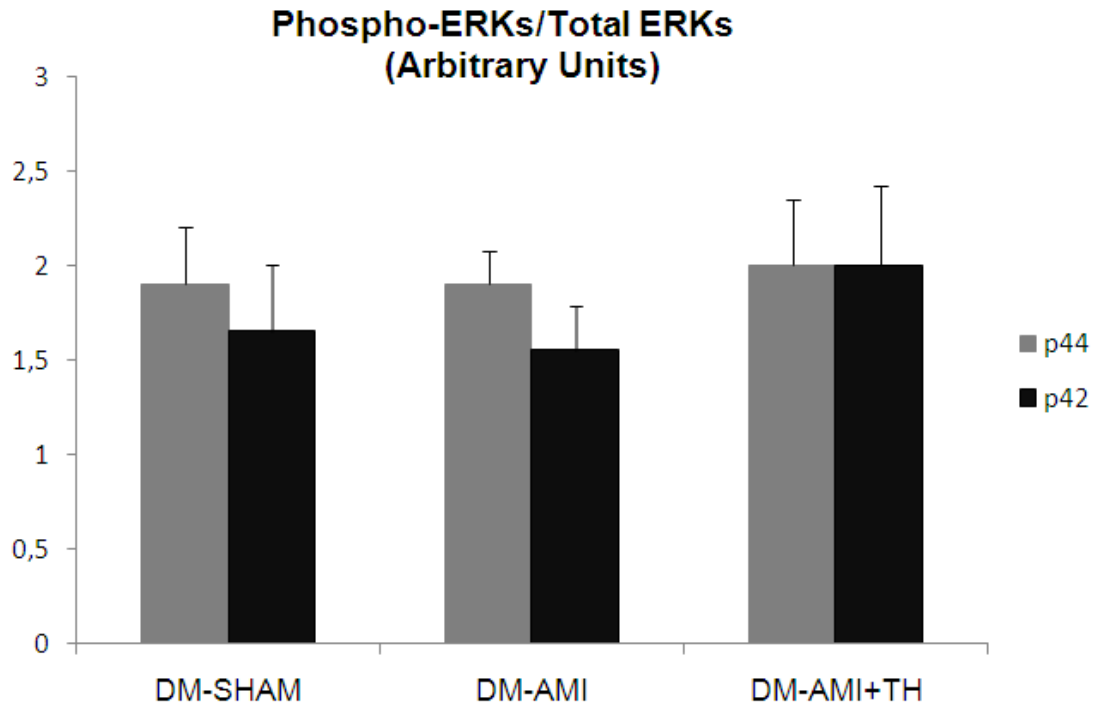


Figure 3.37 (A) Densitometric assessment in arbitrary units and (B) representative Western Blots of phosphorylated levels of Akt kinase are shown in sham-operated diabetic rats (DM-SHAM), post-infarcted diabetic rats (DM-AMI) and post-infarcted diabetic rats with thyroid hormone treatment after 2 weeks. (Columns are means of optical ratios or arbitrary units, \pm SEM; Mann-Whitney).; n=11-20. Note that there is no significant difference in the different parameters.

(A)



(B)

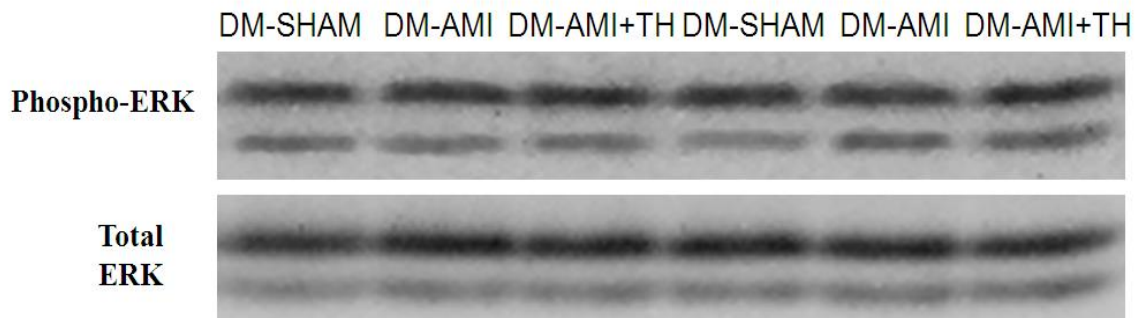


Figure 3.38: (A) Densitometric assessment in arbitrary units and (B) representative Western Blots of phosphorylated levels of p44 and p42 ERKs in sham-operated diabetic rats (DM-SHAM), post-infarcted diabetic rats (DM-AMI) and post-infarcted diabetic rats with thyroid hormone treatment after 2 weeks. (Columns are means of optical ratios or arbitrary units, \pm SEM; Mann-Whitney). n=11-20. Note that there is no significant difference in the different parameters

CHAPTER 4

GENERAL DISCUSSION

Preview to discussion

Diabetes mellitus (DM) is a major global metabolic disorder currently affecting more than 300 people worldwide. It is also estimated that another 100 million persons are undiagnosed and another 200 persons are pre-diabetics (Zimmet and Alberti, 2006; Kumar and Clark, 2007). If left untreated, DM can lead to a number of long term complications including neuropathy, nephropathy, retinopathy, cardiovascular diseases and others. In general, most diabetics will eventually suffer and subsequently die from heart diseases (Kumar and Clark, 2007). To date, we still do not understand fully how DM can induce heart failure and moreover, the cellular and molecular mechanisms involved in the process. As such, it is vitally important to unravel the scientific problem. Hence, this study employed the streptozotocin (STZ) -induced Type 1 diabetic (T1DM) rats to investigate plasma thyroid hormone levels, haemodynamic parameters and the cellular and molecular mechanisms of cardiac remodelling during diabetes mellitus (DM)-induced cardiomyopathy, acute myocardial infarction (AMI) and a combination of DM with AMI compared to age matched healthy sham controls. In another series of experiments, the investigation further explored the beneficial role(s) of thyroid hormone (TH) treatment in either preventing or reducing the effect of DM in combination with AMI on the heart compared to heart from DM sham animal. This discussion will be focussed on (a) the experimental model and the role of STZ in inducing DM, (b) the general characteristics of the animals, (c) the functional changes in the heart *in vivo and in vitro* employing echocardiography under the different experimental conditions and (d) the cellular and molecular mechanisms whereby either DM or AMI alone or when combined can induce remodelling of the heart comparing the absence and presence of thyroid hormone treatment and in age matched control animals..

STZ-induced diabetes mellitus

The STZ induced diabetic model has been in use for several years (Shaffer, 1991) to study the effect of type 1 DM on different physiological and biochemical parameters employing different organ systems including the heart (Bracken et al, 2003; 2004; Howarth and Singh, 1999). STZ, a naturally occurring broad spectrum compound (antibiotics), is produced by the bacterium *Streptomyces achromogenes* and it is a cytotoxic glucose analogue that can accumulate in the pancreatic β cells, thus inhibiting

insulin secretion via destruction of the beta cells causing a state of insulin-dependent DM. These two effects are attributed to the alkylating properties of STZ (Varva, 1959/1960). Many cellular actions have been attributed to the effect of STZ including damage to pancreatic cell mitochondria (Ganda et al, 1976). STZ is a nitroso-urea analogue which is lipophilic and it is rapidly taken up by the plasma membrane of tissues. STZ is taken up by the low-affinity GLUT2 transporters in the plasma membrane of the pancreatic β cells (Tjalve, 1976). The drug thus accumulates in the cell and the DNA alkylating activity of the methyl-nitroso-urea moiety, at the O6 position of the guanine is the main mechanism of toxicity by the drug. The methyl group is transferred from the drug to the DNA molecule causing damage to the pancreatic islets, thus resulting in the fragmentation of DNA, through a series of events (Yamamoto, 1981). The poly (ADP-ribose) polymerase, in an attempt to repair the DNA is overstimulated and thus diminishing cellular NAD⁺ and the ATP stores, resulting in cell necrosis. In addition,, protein methylation caused by STZ may contribute to the functional defects of the β cells after exposure to STZ (Bennett and Pegg, 1981).

An alternative hypothesis suggests that a part of the diabetogenic effect of STZ may be due to its potential to act as a donor of nitric oxide (NO). STZ contains a nitroso group enabling it to release NO, thus increasing the activity of guanylate cyclase and also, the formation of cGMP, both being characteristic effects of NO (Delaney, 1985). The generation of reactive oxygen species (ROS), such as superoxide and hydroxyl radicals deriving from hydrogen peroxide dismutation during hypoxanthine metabolism could accompany the effect of STZ, thus accelerating β cells destruction (Nukatsuka, 1990). Clinically symptoms and signs of DM are clearly seen in rats within 24 hours following single intraperitoneal injection of STZ including increased glucose concentration in the blood and urine, increase urine volume, and weight loss (Kumar and Clark, 2007; Adeghate et al ,2010). Some of these clinical changes depend upon the concentrations of the STZ employed in the study (Adephate et al, 2010). Following STZ-induced DM, the animals develop long term complications such as retinopathy, neuropathy, nephropathy, cardiomyopathy, exocrine gland insufficiencies, foot ulcers and many others (Howarth and Singh, 1999; Bracken et al, 2003; 2004; Kumar and Clark, 2007; Adeghate et al 2010).

General characteristics of the animals

The results of this study have also shown that the STZ-induced diabetic rats were hyperglycaemic and moreover, they had reduced body and heart weights compared to age-matched controls (see table 3.3). The reduction in body weight may be due to either the DM itself or the animals consumed less chow and more water due to the excess urination (polyurea). In addition, from physical examination, the gastrointestinal tract of the diabetic animals show signs of swelling and marked inflammation which may be associated with the indigestion or exocrine gland insufficiencies (Kumar and Clark, 2007). In addition, the results show that the heart weight to body weight and the lung weight to body weight in the diabetic rats increased significantly compared to age-matched control indicating signs of hypertrophy of the heart and congestion of the lungs. These characteristics are similar to those reported in the literature (Qureshi et al., 2001; Howarth and Singh, 1999; Bracken et al, 2004). One major long term complication of DM is cardiomyopathy, in which the heart is unable to pump blood efficiently. This could be due to several factors including reduced contraction, development of fibrosis, a derangement in calcium homeostasis and carbonylation of specific transporting proteins (Hatori et al, 2000; Choi et al, 2002; Bracken et al, 2003; D'Ssouza 2010; D'Souza et al, 2011; Shao et al, 2010; 2012).

Contractile dysfunction is frequently reported in human patients and in experimental animals with diabetes mellitus (DM) (Bracken et al. 2003; Kumar and Clark, 2007). This metabolic disorder is now accepted as a major risk factor for cardiovascular diseases rivalling cigarette smoking, stress, obesity, sedentary lifestyles, cholesterol disorders and hypertension (Standl and Schnell, 2000). In the UK alone, over 40,000 people die annually from DM-induced cardiomyopathy and it costs the National Health Service around £5-6 billion per year to diagnose, to treat and to care for diabetic patients (Currie, 1997). With over 300 million people affected globally by DM (Amos et al, 1997), most of whom may die from cardiovascular- related diseases, it is imperative that we understand the cellular and molecular mechanisms of DM-induced cardiomyopathy in order not only to prolong life, but also to provide a better quality of life for the diabetic patients globally.

Preliminary studies to establish baseline

The present study used young male Wistar rats which were maintained on a 12 h light/dark cycle and fed with a standard chow ad libitum. DM was induced by a single injection of STZ (Kalofoutis et al, 2010; Shao et al, 2010). Induction of experimental diabetes in the rat using STZ is very convenient and simple method to use resulting in a type 1 diabetic model. In this study, preliminary experiments using low (35 mg/bw) and high (60 mg/bw) dose of STZ were performed to select the appropriate dose resulting in diabetes with glucosuria but without keto-acidosis. The initial results showed that a low dose (35 mg/bw) of STZ was more convenient in inducing DM with very small traces of ketone in the blood compared to 60 mg/bw (Adeghate et al, 2010). Comparing the data presented in the tables 3.1 and 3.2 of this study, the results show that those rats which were injected with 60 mg/bw STZ had average urine glucose and ketone levels of 1050 mg/dl and 86.5 mg/dl, respectively. In contrast, rats injected with 35 mg/bw of STZ had mean urine glucose and ketone levels of 625 mg/dl and 3.5 mg/dl, respectively. With the very high dose of STZ, urine glucose level doubled and urine ketone concentration increased by almost 25 times. The rationale for these preliminary studies was to eliminate the ketosis in the animals (Kumar and Clark, 2017; Adeghate et al, 2010). It is well known that in chronic diabetes, because of the lack in glucose entering the cells where it can be used as a form of energy source, the body begins to use stores of fats as an alternative source of energy and in turn, the body produces either ketones or acidic by-products. There is much evidence that patients who suffer from heart failure are ketosis-prone since their ketonaemia is associated with increased circulating levels of free fatty acids, growth hormones and cortisol (Lommi et al, 1997; Kumar and Clark, 2007). Ketosis is due to the use of fatty acids as an energy source and this occurs during diabetes (Kumar and Clark, 2007). Ketosis is also an additional index to measure the severity of heart failure (Lommi et al, 1997).

Physiological and Biomolecular methods involved with the project

In tackling the scientific problems a number of novel scientific methods were involved in this study. They included STZ-induced diabetic model, induction of myocardial infarction, assessment of cardiac function *in vivo* and *in vitro* using the balloon method and echocardiography and molecular biological changes or expressions of different proteins in the heart (Kalofoutis et al, 2010; Shao et al, 2010). In brief, it is of

paramount importance to understand these methods by discussing their relevance in this study.

Induction of myocardial infarction (AMI)

Acute myocardial infarction is an effective method to induce heart failure and it was induced by ligation of the left coronary artery as previously described (Pantos et al, 2007; Kalofoutis et al, 2010). Rats were anaesthetized with an intraperitoneal (ip) injection of ketamine (70 mg/bw) and midazolame (0.1 mg/bw), intubated and ventilated via a tracheal cannula using a constant-volume rodent ventilator. Anaesthesia was maintained by inhalation of small doses of sevoflurane (1-2%). Left thoracotomy was performed at the fourth intercostal space followed by pericardiotomy. Left coronary artery was then ligated with a 6-0 silk round-bodied suture. Continuous electrocardiogram (ECG) recordings were used to monitor heart rate and any changes due to ischaemia after coronary artery ligation. Body temperature was maintained at 37° C by using a heating blanket (Harvard Homeothermic Blanket, 50-7061). This procedure resulted in 15-20% mortality within the first 24 h in the infarction control group, while it increased by up to 30-40% in the diabetic infarction group. The high mortality rate was probably due to a combination of DM with AMI since both DM and AMI individually can lead to cardiomyopathy (Kalofoutis et al, 2010). AMIs which produced a scar areas of 60 mm² to 105 mm² were included in this study, corresponding to 25%-40% of the left ventricle. The animals were left to recover for 2 weeks after myocardial infarction. The same procedure was followed for sham-operated control animals, but the coronary artery was not ligated (Pantos et al, 2010; 2011; 2012). In all these experiments involving the technique of AMI, special care was taken in order to reduce mortality. The method is rather tedious and it requires special training (Pantos et al 2010).

Isolated heart preparation

A non-ejecting isolated rat heart preparation was perfused at a constant flow according to the Langendorff's technique. Hearts were paced at a rate of 320 beats/min with a Harvard pacemaker. An intra-ventricular balloon allowed measurement of contractility (Pantos et al, 2010). Left ventricular balloon volume was adjusted to produce an average initial left ventricular end-diastolic pressure of 7-8 mm Hg in all groups. The water filled balloon was connected to a pressure transducer and the LV pressure signal

was transferred to a computer using data analysis software which allowed continuous monitoring and recording of heart function. Left ventricular developed pressure (LVDP), defined as the difference between left ventricular peak systolic pressure and left ventricular end-diastolic pressure, represented a contractility index obtained under isometric conditions. Left ventricular systolic function was assessed by recording the left ventricular developed pressure (LVDP, mm Hg) and the positive and negative first derivative of LVDP; $+dp/dt$ (mmHg/sec), $-dp/dt$ (mm Hg/sec). These are conventional methods used world wide by cardiac Physiologists in measuring cardiac function (Pantos et al, 2010; 2011; 2012; Shao et al, 2010; 2012). Like the induction of AMI, these experiments are tedious and they required an element of scientific skills.

Echocardiography

Echocardiography is an effective physiological tool to measure cardiac function in vivo (Kalofoutis et al, 2010; Shao et al, 2010; 2012). Short and long-axis images were acquired using a digital ultrasound system (Vivid 7 version Pro, GE Healthcare) with the 14.0-MHz i13L probe. A large number of consecutive measurements were performed and analysed by two independent operators. Left ventricular (LV) internal diameter (LVID) at the diastolic phase (LVIDd), LV internal diameter at the systolic phase (LVIDs), posterior wall thickness at the diastolic phase (LVPW), systolic velocity of the posterior wall radial displacement (SVPW) and the ejection fraction (EF%) were measured to determine cardiac function. EF% was calculated using the Simpson's equation. SVPW was measured from two-dimensional guided M-mode recordings obtained at the mid-ventricular level as previously described (Pantos, 2007; Shao, 2010; Kalofoutis, 2010; Shao et al, 2010; 2012). SVPW was used to assess the segmental contractile function of the non-infarcted myocardium, while EF% was used to determine the global contractile LV function. Wall tension index (WTI) was defined as the ratio $(LVIDd/2 * \text{Posterior Wall thickness})$ as previously described (Pantos et al, 2007; Shao et al, 2010; 2012). WTI was measured in order to indirectly assess myocardial wall stress. In addition, sphericity index (SI), defined as the ratio of maximum long axis (in mm) to maximum short axis (in mm) of the left ventricle was determined in order to assess LV geometry. All measurements were averaged for at least 3 consecutive cardiac cycles. These different measured parameters provide the scientist with relevant physiological data of left ventricular function since the left ventricle is the most important chamber in the heart to supply blood, nutrients and

oxygen to to the different organs and tissues of the body (Kumar and Clark, 2007; Vander et al 2007).

Assessment of Molecular changes

Cytosolic samples were prepared for sodium dodecyl sulphate polyacrylamide gel electrophoresis (SDS-PAGE) and for Western blotting, following SDS-PAGE and proteins were transferred electrophoretically to a nitrocellulose membrane using established methods (Pantos et al, 2007; Kalofoutis et al, 2010; Shao et al, 2010; 2012). Filters were probed with specific antibodies against total and phospho-ERK, total and phospho-AKT (Ser 473), total and phospho-JNKs and total and phospho-p38, SERCA, phospholamban, PKC α and PKC ϵ . Immunoreactivity was detected by enhanced chemiluminescence using Lumiglo reagents. Chemiluminescence was then detected by image analysis system. TRs protein expression was determined in nuclear fraction. Protein concentrations were determined by the BCA method. It is now well established that cardiac dysfunction is expressed not only at physiological level, but also at subcellular and molecular levels involving a number of regulatory proteins in the heart (Shao et al 2010; 2012)

Baseline characteristics of the unstressed diabetic myocardium

A mild cardiac dysfunction was observed in these animals with changes in dp/dt and a shift of myosin isoform expression towards β -MHC expression. Interestingly, this model appears to be similar to the CIRCO mice model in which insulin receptor has been deleted (Sena, 2009).

Diabetes-induced cardiomyopathy

As discussed above, more than 300 million people worldwide have DM mellitus and about 70 % of them will develop a unique type of heart failure referred to as diabetic cardiomyopathy (World Health Organisation, 2011; American Diabetes Association, 2011). A significant percentage of these individuals will also succumb prematurely from a fatal stress-induced ventricular arrhythmia (American Diabetes Association, 2011; Bertoni et al, 2004; MacDonald et al, 2008). To date, the mechanisms responsible for the reduced basal and stress-induced aberrant ventricular contractions in individuals

with diabetes mellitus remain incompletely defined and therapeutic strategies to slow their development and or progression is virtually non-existent. Some previous studies have shown that thyroid hormone may be of paramount importance in the remodelling of the heart during diabetes, thus either delaying or reducing mortality (Pantos et al, 2005; 2007; 2012).

This study investigated cardiac function and dysfunction during STZ-induced cardiomyopathy over a period of 4 weeks followed by induction of acute myocardial infarction for 2 weeks compared to controls. Two days after AMI, the DM+ AMI animals were treated with thyroid hormone for two weeks and there after the animals and isolated hearts were subjected to a number of in vivo and in vitro measurements. For comparison, the study employed 5 groups of experimental animals including control sham operated rats (sham), diabetic sham operated rats (DM+SHAM), diabetic rats subjected to acute myocardial infarction (DM+AMI) and diabetic rats subjected to acute myocardial infarction but treated with thyroid hormone (DM+AMI+TH) for comparison. It was of paramount importance to employ the appropriate controls throughout the study for comparison.

Physiological studies

The results of the study have clearly demonstrated that induction of acute myocardial infarction (AMI) can result in significant ($P < 0.05$) changes in all the different measured parameters including LVPW, WTI, sphericity index, LVID α , LVIDs, EF %, SVPW, LVDP, +dp/dt and -dp/dt, except for LVW/BW compared to control sham (see table 3.4.). These data have indicated that myocardial infarction can lead to a large, but a weak heart (left ventricle) which pumps significantly less blood than the sham control heart. The results also show that the diabetic sham heart was also significantly ($P < 0.05$) weak compared to control sham heart with marked decreases in SVPW, LVDP, +dp/dt and -dp/dt. Moreover, when the diabetic heart was induced with myocardial infarction there were further decreases in the various measured haemodynamic parameters compared to rats induced with myocardial infarction alone. These results have clearly demonstrated that acute myocardial infarction can lead to the development of a large (hypertrophy), but a weak heart and this can be exacerbated or even becomes weaker in the STZ -induced diabetic heart subjected to AMI (Pantos et al, 2012). Similarly, the results of the study have also shown that the sphericity index was significantly ($P < 0.05$)

decreased in acute myocardial infarction and in DM combined with AMI compared to the control sham. Similarly, the data presented in table 3.6 of this study have also shown that regional systolic radial strain was significantly ($P<0.05$) reduced in the different segments of the left ventricle of AMI and DM+AMI hearts compared to control sham animals (see table 3.6). In the diabetic left ventricle, only the antero-septal strain of the left ventricle was significantly ($P<0.05$) reduced compared to sham control non-diabetic left ventricle. The other measured areas of the left ventricle in the DM heart were reduced, but not significantly different from control left ventricle sham heart. These segments of the left ventricle became even weaker in the infarct diabetic heart compared to the normal infarct heart or the normal sham diabetic heart. These data also show that diabetes on its own can lead to a weak left ventricle compared to the control heart (see table 3.4). These parameters were only reduced, but not significantly different from control sham. Taken together, these physiological data have clearly demonstrated that diabetes mellitus can lead to the development of a weak left ventricle of the rat heart. Moreover, induction of myocardial infarction can enhance the weakness of the left ventricle and myocardial infarction in combination with diabetes can potentiate the weakness of the left ventricle, possibly leading to left ventricular failure (Pantos et al. 2012). The results of this study have also shown that the plasma levels of either T3 or T4 remained virtually unchanged under control sham, DM, AMI or DM in combination with AMI conditions. However, heart rate decreased significantly ($P<0.05$) in the DM+AMI group compared to the other groups (see table 3.5). However there was no significant change in either scar area or scar weight comparing AMI with DM+AMI hearts.

The question which this thesis attempted to answer is: whether thyroid hormone (TH) treatment can reverse these adverse pathophysiological effects of acute myocardial infarction in combination with DM compared to diabetic sham rats and STZ-induced diabetic rats subjected to AMI in the absence of TH treatment. Numerous studies have demonstrated that thyroid hormone treatment can both repair and regenerate the heart. It acts like a natural therapeutic agent leading to cardiac remodelling (Kalofoutis et al, 2010; Pantos and Mourouzis 2010a; 2010b; Pantos et al, 2010; Lymvaious et al, 2011; Pantos et al, 2012).

Thyroid hormone (TH) and its effect on the heart.

The results of the study have also shown that the serum level of the thyroxine (T4) increased slightly in DM-AMI-treated animals compared to the DM sham rats but the value was not significant. In contrast, serum levels of triiodothyroxine (T3) increased significantly in the thyroid-treated DM+AMI rats compared to the non-treated DM-sham and DM-AMI rats. Thyroid hormone increased heart rate significantly in DM+AMI rats compared to DM-sham and DM-AMI untreated rats. In addition, thyroid hormone evoked a marked increase in tissue scar weight, but it had no effect on the tissue scar area compared to non-treated DM+AMI animals (see table 2.7). These results have clearly shown that thyroid hormone treatment had marked beneficial effects on post-infarcted diabetic rats in relation to the blood levels of the hormones, heart rate and scar weight. These results are in total agreement with previous findings (Pantos et al, 2008; 2012).

Thus, the next logical step of this study was to determine the effect of thyroid hormone treatment in the DM+AMI hearts compared to non-treated DM-sham and DM+AMI hearts. The results show that thyroid hormone treatment over a period of two weeks had a marked and significant effect on the post infarcted heart compared to the non-treated hearts. LVW, LVW/BW, LVPW, wall tension, sphericity index, LVIDd, LVIDs, %EF SVPW, LVDP, +dp/dt and -dp/dt, all significantly ($P<0.05$) increased in the hearts of thyroid hormone- treated rats compared to hearts from the non-treated DM-sham and DM+AMI rats. In contrast, most of the measured haemodynamic parameters of the left ventricle of the heart decreased significantly ($P<.05$) in the non-treated DM+AMI rats compared to DM-SHAM rats and DM+AMI thyroid hormone treated rats (see table 3.8). Together, the present results show that acute myocardial infarction can have detrimental effects on the left ventricle of the STZ-induced diabetic rat heart. However, two weeks of treatment of the STZ-induced diabetic rats with thyroid hormone, not only reversed the detrimental effects of acute myocardial infarction, but it also enhanced the physiological status of the left ventricle compared to hearts from non-treated DM-sham rats (Pantos etl al, 2008; 2012).

Furthermore, the results presented in this study (see table 3.9) have also demonstrated that thyroid hormone can elicit significant beneficial effects on different parts or segments of the left ventricle. The data presented in table 3.9 show that the two weeks

of treatment of acute infarcted diabetic heart with thyroid hormone can lead to a significant ($P < 0.05$) increases in the athero-septal, the whole anterior, the antero-lateral and the posterior-lateral segments of the left ventricle compared to the non-treated DM-AMI left ventricle. The results have further demonstrated that acute myocardial infarction can evoke significant ($P < 0.05$) decreases in the sizes of various segments of the left ventricles compared to the diabetic+sham non-treated left ventricle. The thyroid hormone treatment over two weeks did not completely reverse the detrimental effects of acute myocardial infarction compared to DM-sham left ventricle, but the hormone had marked and significant beneficial effects compared to the left ventricle from DM-AMI non-treated rats (Pantos et al 2008; 2010; 2012).

These results have clearly highlighted the importance of thyroid hormone in cardiac repair and regeneration (Pantos et al, 2012). The hormone is acting like a natural healer for the heart during such adverse conditions as DM, AMI and AMI+DM. Numerous studies have previously shown the beneficial effects of thyroid hormone in organ and tissue remodelling and in repairing and in the regeneration process in the body (Forlow and Neff, 2006; Sato et al, 2007; Slack et al, 2008; Bouzaffour et al, 2010; Pantos et al, 2010; 2012). It is well known that thyroid hormone plays a major role in the development of the embryonic heart and in the control of various aspects of repair and/or regeneration. This is probably induced via thyroid hormone reactivating the development of gene programming in adult life (Pantos et al, 2011a/b; 2012). It has also been demonstrated that thyroid hormone plays a major role in both protecting and repairing the myocardium during adverse stress situations as in ischaemia and acute myocardial infarction (Pantos et al, 2011a/b; 2012).

The question which now arises is: what is responsible for the development of a weak left ventricle during diabetes, acute myocardial infarction or during diabetes in combination with AMI and how does thyroid hormone act to either protect the weak heart or to reverse the adverse effects of diabetes, AMI and DM in combination with AMI. In order to answer the question, it is of paramount importance to understand firstly the processes of contraction and relaxation of the heart.

Excitation – Contraction Coupling (ECC)

Excitation contraction-coupling (ECC) is a highly organised process of signal transduction pathways that overrides contractile force and function in the heart (Bers,

1991; Vander et al 2007). The process is initiated by the depolarisation of the cardiac cell membrane, during the cardiac action potential leading to Ca^{2+} entry via the voltage-gated L-type channels as inward Ca^{2+} current (I_{ca}) (Bers 1991a/b; Barry and Bridge 1993). The sodium/calcium (Na^+/Ca^+) exchanger operating in reverse mode has also been proposed as a candidate mechanism of Ca^{2+} entry into the myocyte (Lipp and Niggli, 1994; Leblanc and Hume, 1990). This small influx of Ca^{2+} triggers a much larger release of Ca^{2+} from ryanodine receptors (CaRyR) on the surface of the sarcoplasmic reticulum (SR). Following the activation of the SR and Ca^{2+} release, there is a transient rise in the cytosolic free Ca^{2+} concentrations $[\text{Ca}^{2+}]_i$, typically from a diastolic level of 100 nM to a peak systolic level of around 1 μM within a period of 20 and 40 msec after depolarisation (Beuckelmann and Weir, 1988; Kannel et al, 1987; Eisner and Trafford, 2000; Shaoa et al, 2012). This process is referred to as “ Ca^{2+} - induced Ca^{2+} release” (CICR) and is widely accepted as the main mechanism of Ca^{2+} release from the SR (Fabiato, 1983; Letwin and Bridge, 1998; Muller, 1965). Other mechanisms leading to the release of Ca^{2+} from the SR have been proposed, and include voltage-activated Ca^{2+} release (Levi and Ferrier, 1997) and inositol (King et al, 1998; Shaffer, 1991) trisphosphate (InsP3)- triggered Ca^{2+} release through (InsP3) receptors (Lipp et al.,, 2008). The process of contraction is initiated when the Ca^{2+} binds to the microfilament troponin-C, which in turn switches the contractile machinery (Bess, 1991a/b). Relaxation occurs when the Ca^{2+} transient decays and the Ca^{2+} dissociates from the troponin-C leading to the re-uptake of Ca^{2+} into the SR by a SR Ca^{2+} -ATPase-dependent pump (SERCA) (Bers, 1991a/b; Balk et al, 1994) and the extrusion of Ca^{2+} from the cell by $\text{Na}^+/\text{Ca}^{2+}$ exchanger and the Ca- ATPase pump (Barcenas-Russ et al, 1987; Jorgensen et al, 1982).

Calcium dysfunction in the diabetic heart

In the diabetic heart several workers have reported decreased responsiveness to the beta adrenergic stimulation (Seller et al, 2001) and marked changes in cellular calcium homeostatis (Howath and Singh, 1999; Bracken, 2003; 2004) including dysfunction of the L-type Ca^{2+} channels, the sodium-calcium exchanger, the ryanodine receptors and the SERCA pump (Bracken et al, 2002; 2003; 2004; Shao et al, 2010; 2012). All these proteins play a major role in regulating cellular Ca^{2+} transport during contraction and

relaxation of the heart. In cardiac myocytes, the resting cell $[Ca^{2+}]_i$ levels are determined mainly by Ca^{2+} leaking out of the cell. This is counter balanced by the sarcolemmal Ca-ATPase pump and the sarcolemmal Na^+ / Ca^{2+} exchanger (Shaffer and Mozattari, 1996). The Na^+ / Ca^{2+} exchanger provides the predominant mechanism for Ca^{2+} efflux during the cardiac diastole (Golden et al, 2001).

In a number of previous studies, it was demonstrated that STZ-induced diabetes mellitus over four to eight weeks can lead to elevated diastolic Ca^{2+} (Lagadic-Grossman et al., 1996; Hayashi and Noda 1997; Noda et al, 1992; Bracken et al, 2003; 2004; Shao et al, 2010; 2012). This elevated cellular calcium is due to asynchronous release of calcium from the SR via the ryanodine receptor operated channels (Shao et al, 2010; 2012) and dysfunction of the SERCA pump and the sodium calcium exchanger (Noda et al, 1992; Bracken et al, 2004). There is also much evidence that the activities of the L-type calcium channels are reduced during diabetes mellitus (Bracken et al, 2004). These changes in cellular Ca^{2+} homeostasis are responsible for the weak contraction of the heart during diabetes.

The next question which needs to be addressed is: how does acute myocardial infarction (AMI) result in the decrease in cardiac compliance and contraction either in the absence or the presence of diabetes mellitus. In order to answer this question, it is important to understand the relationship between diabetes and myocardial infarction and how the two when combined can worsen the problem.

Diabetes and myocardial infarction

Diabetic patients have been shown to suffer from more frequent (2.5-5 times) and severe myocardial infarction (MI) versus non-diabetics (Pell and Allonso, 1993). Studies conducted in the past have demonstrated that male diabetics have an increased likelihood of cardiovascular problems by 2 times the normal risk. Dhalla et al, (1985) have suggested three major risk factors that may account for the increased incidence of cardiovascular dysfunction in diabetic patients. They included atherosclerosis, microvascular alterations and primary myopathic disorder in cardiac muscle. Studies in the past have also demonstrated that two months after an AMI, the mortality in diabetic patients was approximately 41% in comparison to 15% in non-diabetic patients

(Partamian and Bradley, 1965). Even more alarming is the evidence that regardless of infarct size, diabetic patients still suffer a higher mortality rate than non-diabetics (Stone et al, 1989). The increased incidence of AMI in diabetics has been linked to glycaemic status (D'Souza et al, 2009). It has been shown that when the hyperglycaemic state of diabetics was stringently controlled, the incidence of AMI fell significantly (Clark et al, 1985). Hyperglycaemia has also been linked to accelerated atherosclerosis, endothelial dysfunction, coronary heart disease and hypertension (D'Souza et al, 2009). Moreover, hyperglycaemia is a hallmark of DM and it induces a variety of maladaptations at the subcellular and cellular levels of vascular tissues which may in part be accounted for the vascular complications. In fact, chronic hyperglycaemia has been suggested as the key factor in the pathogenesis of diabetic complications (D'Souza et al, 2009; 2011). The pathophysiological alterations due to hyperglycaemia during DM include glucose flux through the polyol-sorbitol pathway, hexosamine pathway, formation of advanced glycation-end products (AGEs) and the activation of protein kinase C (D'Souza et al, 2009). Another danger has been suggested that increases the mortality in diabetics is the occurrence of a silent AMI which has been suggested to be due to the damage of cardiac nerves and the inability of afferent nerves to transmit information as a result of visceral neuropathy (Faerman et al, 1977). Silent AMI was shown to be more common in the diabetic population (Niaken et al, 1986; Theoron et al; 1987) and it is of great concern because the patients are unaware that they have suffered an AMI and thus may not summon the proper medical attention (Soler et al, 1975). The survival of diabetic patients with AMI after 1, 2, and 5 years is 82%, 78% and 58%, whereas that for non-diabetic patients with AMI is 94%, 92% and 82%, respectively (Pantos et al. 2012).

In terms of the cellular mechanism of cardiac dysfunction, it is clear that cellular calcium homeostasis is further reduced in diabetes combined with myocardial infarction (Bracken et al, 2003; 2004). Acute myocardial infarction is normally associated with arrhythmias and beta adrenergic stimulation via the production of cyclic AMP and cellular calcium homeostasis overload and in turn, they are responsible for the AMI-induced arrhythmias (Welhelm et al, 1992). However, it would be expected that treatment of patients with calcium channel blockers could stabilize the AMI-induced arrhythmias. A previous study had earlier reported that calcium channel blockers did not reduce significantly the risk of initial recurrent infarction or death when given routinely to patients with acute myocardial infarction or unstable angina (Held et al, 1989).

The diabetic heart fibrosis and remodelling

In relation to the myocardium, the discussion so far addresses the processes of ECC and a derangement of cellular Ca^{2+} homeostasis during diabetes mellitus and diabetes in combination with AMI. The other issue of cardiac deformation during diabetes and AMI is the development of cardiac fibrosis (Martinet *et al*, 1990; D'Souza *et al*, 2010; 2011) leading to left ventricular remodelling. This is a process by which the size, shape and function of the ventricle are regulated by the mechanical, neuro-hormonal and genetic factors (Martin *et al*, 2000). Remodelling is both an adaptive and a physiological process during normal growth, a pathophysiological condition due to diabetes, AMI, cardiomyopathy, hypertension and other related heart diseases such as dysfunction of the valves (Feffer and Braunwold, 1990).

Heart failure (HF) may be viewed as a progressive disorder that is initiated in response to an index event (that may be acute i.e. AMI, chronic i.e. DM or hereditary) that results in either a loss or damage in the functioning of myocytes or alternatively produces a decline in the ability of the heart to function as a pump. Irrespective of the inciting event, several neurohormonal and inflammatory pathways are activated, including the renin-angiotensin-aldosterone system (RAAS), adrenergic system, inflammatory cytokine systems and a host of other autocrine and paracrine mechanisms as compensatory mechanisms to maintain stroke volume at a reduced ejection fraction (Packer, 1992; Fedak *et al*, 2005). Thus far, a multitude of mediators and proteins including norepinephrine, angiotensin II, endothelin, aldosterone, $\text{TGF}\beta 1$, tumour necrosis factor (TNF) have been implicated into the disease progression of the failing heart (Maytin and Colucci, 2002; Fedak *et al*, 2005; Swynghedauw *et al*, 2010). These processes are initially compensatory and beneficial and in most instances patients remain asymptomatic or minimally symptomatic following the initial decline in pumping capacity of the heart, or will develop symptoms only after the dysfunction has been present for some time (Maytin and Colucci, 2002). As such, the index event produces remodelling of the LV frequently along one of the two patterns, either hypertrophy or dilation. Myocardial hypertrophy associated remodelling results in increased LV mass without any effects on the LV volume in a process termed 'concentric remodelling' that is associated with preserved function, as the ventricle is

capable of generating greater force and higher pressure. The onset of LV dilation is characterised by ‘eccentric remodelling’ and substantial increases in intraventricular volume with comparable increases in the LV mass that represents a compensatory response to augment cardiac output in the face of diminished contractile function. Eventually, a functional demand of the myocardium is met; LV dilation progresses without appreciable increases in LV mass and in accordance with the Law of Laplace. The induction of excessive ventricular wall stresses is known to occur prior to the overt heart failure (Swynghedauw, 1999).

Molecular mechanism of cardiac remodelling

It is now well documented that cardiac remodelling occurs in response to cues generated by mechano-sensors (Connexins, integrins) that couple cellular signalling pathways to altered or mechanical stress/injury (D’Souza *et al*, 2009; 2011). In such cases, the nature and extent of signals that are transiently activated are far from fully understood. Moreover, it is now accepted that the myocardial response to either injury or altered mechanical load involves profound alterations in gene expressions including the activation of those that are normally involved in embryogenesis, also known as the foetal gene programme (Swynghedauw, 1999; Pantos *et al*, 2012). In the context of AMI-induced cardiac remodelling alone, genome-wide analyses have revealed significant coordinated changes in over 1400 genes early and 125 genes late in the infarct zone, and nearly 600 genes early and 100 genes late in the non-infarct heart (LaFramboise *et al*, 2005; Pantos *et al* 2012)

It is also now well known that foetal gene reprogramming, characteristic of pathological remodelling frequently involves an upregulation of foetal isoforms of genes whose products regulate cardiac contractility and Ca^{2+} handling. In turn these are paralleled by a down-regulation of their adult isoforms (i.e., up-regulation of β -MHC vs down-regulation of α -MHC) and often includes decreased SERCA2a and increased sodium calcium exchanger (NCX) expression (Hilfker-Kleiner *et al*, 2006). Another important feature is that the foetal gene phenotype is markedly expressed in the remodelled myocardium that involves the natriuretic peptides ANP and BNP. These are often detectable in the circulation where they are used as an indirect marker for myocardial injury/overload (D’Souza *et al*, 2011). These transcriptional changes culminate in several molecular and cellular alterations that characterise myocardial remodelling.

Moreover, they are broadly categorised into those that occur in the myocyte and changes that occur in the volume and composition of the extracellular matrix (ECM). Within the myocyte, in addition to the functional changes, the remodelling process is invariably associated with sarcomeric reorganisation. Dilation of the heart is associated with myocyte re-lengthening, mediated by the generation of new sarcomeres in series and enhancement of the length-to width ratio whereas a hypertrophic phenotype is the result of parallel addition of new sarcomeres. At the molecular level, hypertrophy appears to be characterised by increased expression of the adult isoforms of sarcomeric genes (Hilfker-Kleiner et al, 2006). Furthermore, biomechanical stretch signalling, altered redox states and pathological stimuli including hyperglycaemia and TGF β 1 may include the activation of the phosphatidylinositol 3-kinase (PI3-K)/ protein kinase B (Akt) – p70S6K, and/or activation of extracellular signal-regulated kinases (ERK) which co-ordinate the hypertrophic response (Selvetella et al, 2004; Wu and Derynck, 2009).

Outside changes in the myocyte and structural remodelling in the myocardium are associated with alterations in the structure and function of the ECM (D'Souza et al, 2011). Indeed, ECM deposition is a widely recognised alteration in the failing heart and the notion that progressive fibrosis underlies LV dilatation and HF progression has been supported by several experimental and clinical studies (Milner and Muller, 2005; Bowes et al, 2010). In pathological conditions, the ECM can be temporarily remodelled, reversibly remodelled or fully adapted to the changes in biomechanical load. However, prolonged overload results in detrimental collagen deposition that can render the heart electrically and structurally heterogeneous, resulting in excessive diastolic stiffness (Van Heerebeek et al, 2008) and/or induce LV dilatation altogether resulting in overt HF. Particular emphasis is now given to the collagenolytic MMPs and their inhibitors, the TIMPs in underlying LV dilatation. The balance of proteolytic and antiproteolytic activity appears to be an important determinant of the rate of ventricular enlargement. The general view is that disruption of this balance can result in progressive MMP activation leading to degradation of the ECM, myocyte, slippage, thinning of the ventricular wall, and ventricular dilation that occurs in the end stage of HF (Swynghedauw, 1999; D'Souza et al. 2011).

TGFβ1 in cardiac remodelling and failure

A central role for transforming growth factor beta 1 (TGFβ1) in the remodelling myocardium has come to light, given consistent myocardial upregulation in experimental models of AMI, cardiac hypertrophy and HF, and frequently in patients with dilated or hypertrophic cardiomyopathy (Dobaczewski et al, 2010). TGFβ1 is the most prevalent forms of TGFβs, a family of pleiotropic cytokines which are implicated in a wide variety of cell functions, including regulation of inflammation, ECM deposition, cell proliferation, differentiation and growth. The activating stimuli for TGFβ1 are varied and they include reactive oxygen species (ROS), integrins-mediated interactions and also MMP's 2 and 9, a phenomenon that couples matrix degradation with activation of a molecule that primarily mediates matrix integrity and stability (Annes et al, 2003; Shao et al, 2010). Beyond homeostatic roles, TGFβ1 mediates phenotype and function of several cell types crucial in tissue injury and repair processes including fibroblasts. In addition to enhancing ECM synthesis from fibroblasts, it exerts potent matrix preserving actions by suppressing the activity of the MMPs and by inducing synthesis of TIMPs (Schiller et al, 2004). TGFβ1 is a key upstream effector of CTGF, a fibrogenic mediator that acts in concert with TGFβ to promote persistent fibrosis (Leask et al, 2004). The hypertrophic effects of TGF-β1 stimulation on cardiomyocytes are by TGFβ1-mediated synthesis of foetal contractile proteins (Parker et al, 1990). Although there is substantial evidence indicating that TGFβ1 mRNA and protein induction is upregulated in the remodelling myocardium, direct evidence of increased activity is still lacking (Dobaczewski et al, 2010) and *in vivo* effects of TGFβ1 in promoting the myocardial fibrotic and hypertrophic response are supported by over expression experiments in transgenic mice (Rosenkranz 2002; Dobaczewski et al, 2010). Targeting regulatory mechanisms of ECM homeostasis that precedes transition to HF remains a vital goal in HF management. As TGF levels often reflect the development of cardiac remodelling (Villar et al, 2009), the TGFβ1 system is a promising therapeutic target for myocardial infarction and for cardiomyopathic conditions such as diabetic cardiomyopathy that are associated with fibrosis and hypertrophy. Also late, but not early, TGFβ blockade has been demonstrated to

attenuate remodelling in experimental MI and TGF β inhibition through administration of inhibitory peptides (Hermida et al, 2009), or neutralising antibodies has prevented the development of cardiac fibrosis in experimental pressure overload (Kuwahara et al, 2002).

The story so far is that STZ-induced diabetes, acute myocardial infarction and diabetes in combination with acute myocardial infarction can result in the development of weak left ventricular function and subsequent reduced cardiac output. This in turn is probably due to a derangement in cellular calcium homeostasis via its various transporting proteins and formation and development of fibrosis, all of which lead to the remodelling of the heart (Martin et al, 2002). The discussion attempted to show the various events including cellular Ca²⁺ homeostasis and development of fibrosis are both associated in left ventricular failure.

Molecular changes in the heart during a failure

The next logical question which this investigation needs to address is: what are the molecular events involved in the development of a weak left ventricle either during STZ-induced DM, AMI or AMI combined with DM compared to age-matched controls? This study measured the expressions of several cardiac proteins including calcium cycling proteins, several kinases and myosin isoforms expressions in control sham, DM-sham, AMI and DM+AMI. The data show variable changes in the different proteins under the different experimental measured conditions. The percentage of myosin isoforms expression for β MHC increased significantly ($P < .05$) during either DM, AMI or DM combined with AMI compared to sham control. In contrast, myosin isoforms expression for α MHC decreased significantly ($P < .05$) under the three experimental conditions compared to sham control. Similarly, there were no changes in either the protein expression for SERCA or phospholamban (PLB) in either diabetes, AMI or DM combined with AMI compared to sham control. These results indicate that the SERCA pump is not affected by either diabetes or AMI or during a combination of both DM and AMI.

The SERCA pump is activated by the phospholamban and it plays a major role in regulating cytosolic calcium during contraction. SERCA pumps calcium back to the SR

following contraction leading to relaxation of the heart and subsequent filling (Vander et al, 2007; Shao et al 2010; 2012). It is apparent from this study that neither DM, AMI nor DM combined with AMI had any significant effect on SERCA in the left ventricle of the heart compared to sham control hearts. The results also show significant ($P < 0.05$) increases in the β MHC and significant decreases in the α MHC in DM, AMI and DM combined with AMI compared to control. It is now well known that two isoforms of myosin heavy chain (MyHC), alpha and either beta exist in the mammalian ventricular myocardium and their relative expression is associated or correlated with the force of contraction of the heart (Nako et al, 1997). Several pathophysiological conditions including DM, AMI, DM combined with AMI and heart failure can shift the composition of both isoforms of MyHC in the ventricle from either alpha to beta isoforms. α MHC has a higher ATPase activity than the β MHC. In the heart, the velocity of contraction depends on MHC. Hearts expressing α MHC have more rapid contractile velocity as in a healthy heart. This allows for greater economy of free generation and pumping action of the myocardium. In contrast β MHC increases significantly in a faulty heart (Miyata et al, 2000; Reiser et al, 2001; Kalofoutis et al 2010).

The traditional view is that HF induced by either DM, AMI or hypertension as a functional disorder, is precipitated by impaired LV pump performance in response to increased haemodynamic burden of the heart and associated defects in myocyte contractility (Houser and Marguiles, 2003). HF is associated with a multitude of cellular and molecular defects that culminate in electrophysiological dysfunction, depressed myocyte contractility, fatal arrhythmias and pump failure. Numerous studies have suggested that the failing human cardiac myocytes undergo several changes that might be expected leading to a progressive loss of contractile function. These include decreased α -myosin heavy chain (MHC) gene expression with a concomitant increase in β (MHC) myosin heavy chain expression, progressive loss of myofilaments in cardiac myocytes and alterations in cytoskeletal proteins (Schaper et al, 1991; Gupta et al, 2000; Kalofoutis et al, 2010; Pantos et al 2012).

Together, the results obtained in this study following the induction of DM, AMI or DM plus AMI are in total agreement with several previous studies reported in the literature (see above). It is equally important to ascertain the cellular and molecular mechanisms involved in the decrease in expression of α MHC and increase in expressing β MHC during HF. It is possible that these changes occur as a result of carbonylation of the

regulatory proteins. In addition to oxidative stress, there is now much evidence in the literature that regulatory proteins (eg ryanodine receptors) in the heart, undergo carbonylation (Shao et al, 2010; 2012).

The present study has also shown that the expressions of protein kinase alpha (PKC α) increased significantly in DM-AMI and in AMI compared to sham control and DM+sham heart. In contrast, there was no significant change in the expression of PKC epsilon. The PKC isoenzymes have been implicated in such diverse cellular regulations including cell proliferation, cardiac contractility, hypertrophy, accelerated diabetic induced atherosclerosis and apoptosis (Pal et al, 2004; D'Souza et al, 2009). In a previous study, it was demonstrated that PKC α increased significantly in the weak diabetic heart (Kang et al, 1999). Several other studies have associated PKC α activation or an increase in PKC α expression with cardiac hypertrophy, dilated cardiomyopathy, ischaemia, and injury to mitogen stimulation (Dorn and Force, 2005). Elevated PKC α is also associated with later stages of heart failure (Bayer et al, 2003; Braun et al, 2002) and myocardial infarction (Wang et al, 2005; Simons et al, 2005). PKC α is an ideal protein to target during the treatment of either diabetes-induced cardiomyopathy or myocardial infarction. Further discussion of the role of PKC α is thoroughly reviewed in the introduction of the thesis.

The present results have also demonstrated no significant changes in phospho38 MAPK/Total p38 MAPK in DM-sham compared to sham and DM+AMI. However, there was a significant increase in the phospho38 MAPK/Total P38 MAPK in AMI hearts. This was significantly ($P < 0.05$) reduced during DM+AMI. In contrast, there were no significant changes in phosphoJNK/Total JNK and in phospho-Akt/Total Akt in either sham control, DM-sham, AMI or DM+AMI hearts. Interestingly, the results of the study show significant increases in phospho-ERKs/Total ERKs (p44 and p42) in DM-sham, AMI and DM+AMI sham compared to control sham.

The literature relating to P38-MAPK varied and some studies have reported that P38 plays a major role in cardiac growth and hypertrophy (Liang and Mollet, 2003; Nemoto et al., 1998). Another study has shown that activation of P38 had no significant effect on the degree of cardiac hypertrophy (Liao et al, 2001). However, there were marked increases in fibrosis and impaired diastolic function (D'Souza et al 2011). Together, these current results and others indicate that the role of p38 in cardiac

hypertrophy is a conflicting one. While acute activation of p38 appears to be prohypertrophic, chronic activation of p38 can lead to suppression of hypertrophic growth in the heart. However, it is clear from both *in vitro* and *in vivo* studies that p38 activation has a detrimental effect on cardiac function and normal gene expression. Therefore, p38 induction is more closely related to pathological form of hypertrophy than to physiological compensation (Pantos et al, 2012).

In the present study, P38-MAPK increases at least during acute myocardial infarction agreeing with some of the previous studies in the literature (Pantos et al 2012). The present results show no significant change in either phospho JNKs/Total JNKs and Phospho Akt/Total Akt in all the experimental conditions with either sham control, sham diabetes, AMI or DM+AMI. In contrast phospho-ERKs/Total ERKs increased significantly in DM+sham, AMI and DM+AMI conditions. Several other studies have demonstrated a relationship for Ras/Raf/MEK1/ERK signalling pathways with cardiac hypertrophy (Hunter et al, 1995; Zeng et al, 2004), similar to the results observed in the present study. Inhibition of the ERK pathway has been shown to alternate the diabetes or AMI induced hypertrophy of the heart (Ueyama et al, 2000; Kontaridis et al, 2008). Another study shows that reduction in the ERK activity is not sufficient to prevent hypertrophy of the myocardium during various types of hypertrophic stimuli *in vivo* (Purcell et al, 2007). Together, these results in the current and other studies suggest that ERK activity is an important biochemical pathway for cardioprotection, but also cardiac hypertrophy can proceed via ERK-independent mechanisms. In passing, it is particularly noteworthy that excessive beta adrenergic stimulation can also promote cardiomyocytic hypertrophy via an interaction between ERK and beta arrestin (Bark-Harrington, 2004; Salazar et al, 2007).

The role for JNK in the development of a large weak heart is unclear. The level of JNK increased in physiological cardiac hypertrophy due to acute forms exercise (Boluyt et al, 2003). There is some evidence that a disruption of JNK activity can result in cardiac hypertrophy following pressure overload (Liang et al, 2003). This effect is due to the ability of JNK to inhibit NFAT entry into the nucleus (Liang et al, 2003). From present study and those reported in the literature, it is clear that JNK has little or no effect on cardiac hypertrophy at least *in vitro* studies (Pantos et al, 2012).

The results of this study have shown no significant ($P < 0.05$) change in the activity of phosphor Akt/Total Akt in DM+sham, AMI and DM+AMI hearts. Akt is a serine/threonine protein kinase that regulates a number of cellular functions in different tissues including the heart (Shiojima and Walsch, 2006). Akt plays a major role in post natal cardiac development short term Akt activation can promote physiological hypertrophy (Shiojima et al, 2002) where as long term Akt activation can lead to a pathological hypertrophy (Kemi et al, 2008; Matsui et al, 2003). The latter is associated with morbidity and mortality leading to pressure over load, myocardial dysfunction, dilatation and subsequently heart failure (Mann et al, 2010; Shah and Soloman, 2010). Since no change in Akt was observed in this study, it is tempting to suggest that Akt plays no role in either diabetes or AMI-induced cardiomyopathy.

Role of thyroid hormone in DM, AMI and DM+AMI

The initial part of the discussion concentrated in the function – dysfunction of the heart and molecular events associated with DM+sham, AMI and AMI in combination with DM. This part of the discussion will now address the therapeutic or beneficial role of thyroid hormone in protecting the pathophysiological heart in the rat when DM was combined with AMI.

To date, heart failure remains one of the main causes of death in the world despite advances in drug and significant treatments (Roger, 2012; Mormsey et al, 2011). Most treatments aim at improving the pumping action of the heart or improving cardiac haemodynamic. The weak heart is deprived of myocytes and as such it becomes fibrotic in nature leading to a protective mechanism called remodelling (Martin et al, 2002; D'Souza et al. 2011; Pantos et al 2012). During failure, the heart has to regenerate and repair itself otherwise the failure process will be exacerbated. The potential for repair and regeneration has been evolutionary and it seems to be restricted in only developmental staged of life. In recent years, several studies have investigated the role of thyroid hormone in the repair and regeneration of several tissues in the body including the heart. Thyroid hormone is often described as nature's own wonder in repairing and regeneration of the body (Miyata et al, 2000; Pantos et al, 2001; Kalofoutis et al, 2010; Pantos et al, 2011, Lymvaios et al, 2011; Pantos et al 2012).

Thyroxine (T4) is secreted by the thyrocyte and enters the cell via different transport mechanism (Hennemann, 2005). In the body, T4 is converted to triiodothyronine (T3)

by the de-iodinase while T3 is degraded. Either type of the hormone T3 or T4 can be reconverted to one another by de-iodinase (Hennemann, 2005). Thyroid hormone initiates its effect in the body by activating its receptors which are located in the nucleus, the plasma membrane, in the cytoplasm and in mitochondria of the cell (Pantos et al, 2010). There are two types of the TH receptors (TRs), namely alpha and beta. The two TR genes, α and β encode four T3 binding receptor isoforms ($\alpha 1$, $\beta 1$, $\beta 2$ and $\beta 3$). TRs are usually phosphorylated in order to become active and this is mediated via a number of stimuli (Nicol et al, 2003). In the heart, the function of TR β is only apparent in the hypothyroid state and this is associated with angiogenesis (Pantos et al, 2010). In contrast, TR α ensures the maintenance of homeostasis by controlling heart rate, DNA damage, repairing of tissues stress responses and several others (Pantos et al, 2010).

In several previous studies, thyroid hormone has been shown to play a major role in the development and differentiation of cardiac cells (Van-Putten et al, 2002; Van-der Heide et al, 2007) via the expression of TR $\alpha 1$ (Meischl et al, 2008; Pantos et al, 2008c). The effect of TH on cell differentiation and development is believed to be mediated through the activation of a number of distinct endogenous pathways including ERK, P38-MAPK, mTOR and JNK (Kingawa et al, 2006; Pantos et al, 2007c; Ojamaa, 2010). The numerous beneficial role of TH via activation of its TR $\alpha 1$ and TR $\beta 1$ receptors have been reviewed in some details in the introduction of the thesis.

Since TH has been linked to repairing, regeneration and development as previously described in the literature (see introduction for details), it was relevant to investigate the effect of this “nature’s wonder” on the diabetic, AMI and AMI in consideration with DM during heart failure compared to sham healthy control hearts. The results of the present study have shown that TH (T4) did not increase significantly either in DM-sham, DM+AMI compared to the DM+AMI animals treated with TH. In fact, the DM+AMI treated rats seem to have a small decrease in plasma level of T4 compared to DM+AMI untreated animals (see table 3.7). However, in thyroid hormone treated DM+AMI rats, the circulating plasma level of T3 increased significantly compared to DM+sham or DM+AMI untreated animals. Moreover, thyroid hormone seemed to have a significant effect on heart rate in the treated rats compared to the untreated animals (Pantos et al, 2012). In addition, thyroid hormone treatment had no significant effect on cardiac scar area (see table 3.7), but there was an increase in scar weight compared to untreated DM+AMI hearts, but this was not significant (see table 3.7).

Thyroid hormone induced changes in the diabetic heart after myocardial infarction

Since DM+sham and DM+sham in combination with AMI can have adverse effects on the structure and function of the diabetic heart compared to either non diabetic or non AMI control sham, it was logical to investigate the effect of thyroid hormone (TH) treatment for comparison. The results show that pretreatment of the diabetic AMI rats for two weeks with thyroid hormone resulted in marked reversal and beneficial effects on the diabetic rat heart. Thyroid hormone was able to increase significantly ($P < 0.05$) the LVW, LVW/BW, LVPW, WTI, sphericity index, LVID α , LVIDs, %,EF SVPW, LVDP and +dp/dt and -dp/dt compared to the effect of DM+AMI hearts (see table 3.8). These results have clearly shown that TH can reverse the adverse effects of AMI in the diabetic heart to almost normal diabetic 'physiological' level. The results are in agreement with those observed in previous studies (Pantos et al, 2002; Lymvaivos et al, 2011).

The question which now arises is: how does TH act to reverse the deleterious effects of AMI on the heart. It is possible that during AMI, TH level is decreased or other events like activation of thyroid hormone receptors is decreased leading to a depletion in the protective effect of TH (Pantos et al, 2002; Lymvaivos et al, 2011). It is now well known that only after AMI, cardiac function is compromised because of ischaemic injury. As a result of these early changes, a number of neurohormonal and inflammatory events take place in the body leading to marked physiological changes. Decrease in TH level is a frequent observation in AMI (Pantos et al, 2010) and TH changes early after AMI can affect cardiac function adversely with marked haemodynamic consequences (Lymvaivos et al, 2011). It is also now well known that TH can regulate contractile function of the heart via several mechanisms including modulation of contractile protein function, enhanced calcium handling and cation channel activities (Iervasi et al, 2003; Pantos et al, 2008)

This study did not investigate the changes in cellular calcium homeostasis either during DM, DM + AMI or DM + AMI + TH treatment. However, the study measured a number of contractile proteins and signalling kinase molecules as well as changes in TR α 1 and TR β 1 protein expressions during the different conditions. The present results

have shown that thyroid hormone can significantly ($P < 0.05$) increase TR α 1 and TR β 1 protein expressions compared to the levels in DM+AMI hearts in the absence of thyroid hormone. Similarly, TH treatment significantly ($P < 0.05$) increased α MHC and decreased β MHC in the DM+AMI hearts compared to DM+AMI hearts in the absence of thyroid hormone. TH significantly increased SERCA protein expression, but not phospholamban protein expression in the DM+AMI hearts compared to DM+AMI hearts in the absence of the hormone.

The present results have also shown that two weeks of pretreatment of DM+AMI rats with thyroid hormone had marked and significant effects on a number of signalling molecules in the heart compared to the untreated DM+AMI rats. The hormone treatment resulted in significant ($P < 0.05$) decreases in the protein expression of PKC δ and significant ($P < 0.05$) increases in phospho-P38 MAPK/ Total P38 MAPK compared to untreated animals. However, there were no significant changes in the levels of either phospho-JNKs/ Total JNKs protein expressions or phospho-Akt/ Total Akt protein expressions in the DM+AMI heart compared to the thyroid hormone DM+AMI- treated hearts. Similarly, the present results show that thyroid hormone treatment had no significant effect on the protein expressions of phospho-ERK/Total ERK comparing non-treated DM+AMI group with treated DM+AMI groups. These results clearly show that TH seems to play a major role in reversing the deleterious effects of DM-AMI, by protecting the myocardium and thus, preventing the heart from further damage. Moreover, these findings suggest that TH seems to help in protecting the heart and in the repairing process (Pantos et al, 2008; Pantos et al, 2010; 2012)

Cardiac remodelling following acute myocardial infarction results in cardiac dysfunction due to myocardial loss and a series of changes in the non ischaemic myocardium including alterations in chamber size and shape and interstitial structure (Pantos et al, 2012). One main feature of cardiac remodelling is the recapitulation of foetal gene reprogramming leading to cell de-differentiation (Swynghedauw, 1999; Taegtmeier, 2010). The underlying mechanisms of this response are not fully understood. However, it is now recognized that hormone signalling related to cell differentiation, such as thyroid hormone (TH) may be of physiological relevance in the context of cardiac remodelling. Thus, distinct changes in TH–thyroid hormone receptor (TR) axis have been identified in the course of cardiac remodelling and have been linked to cardiac dysfunction (Pantos et al, 2005, 2007). Consequently, TH treatment

early after myocardial infarction can be favorable in remodelling the rat myocardium via its pleiotropic effects which include induction of physiological growth, expression of contractile proteins and enhanced protection of the myocardium from ischaemia (Pantos, 2005). Co-morbidities may abolish the beneficial effects of cardio-protective interventions. Diabetes is common in patients with coronary artery disease and significantly increases the risk of death from myocardial infarction (Kumar and Clark, 2007). Furthermore, recent experimental studies show that diabetes accelerates cardiac remodelling after myocardial infarction through mechanisms which are not fully understood (Lymvaivos et al, 2011).

Potential mechanisms

The mechanisms of impaired cardiac remodelling of the diabetic heart after myocardial infarction remain largely unknown. Thus, the present study made an attempt to give some fundamental new insights into the potential mechanisms which may implicate in this response. A complex kinase signalling has been implicated in cardiac remodelling with ERK and p38 MAPK to be mostly studied in the context of myocardial infarction (Gosselin 2006; Kumphune 2009). Activation of these cascades is increased due to myocardial stretch and mediates the development of the reactive hypertrophy. As previously reviewed in the introduction section, both classic RTK-mediated and GPCR-mediated ERK activation have significant roles in cardiac hypertrophy and cardioprotection. Furthermore, the Ras-Raf-MEK-ERK pathway can induce SR calcium defects and arrhythmias in the heart by modulating ion channels, exchangers, and pumps and serves as a potential contributor to the contractile defects and sudden cardiac arrest. Similarly, multiple groups have shown that over-activation of the p38 pathway induces hypertrophic changes in vitro with acute activation of p38 to be pro-hypertrophic and chronic activation of p38 to lead to the suppression of hypertrophic growth in heart. Based on this evidence, the present study explored whether a distinct pattern of ERK and p38 MAPK activation occurs in diabetic hearts subjected to myocardial infarction which may explain the impaired hypertrophic response seen in those hearts. Interestingly, the induction of myocardial infarction resulted in activation of both ERK1/2 and p38 MAPK (as assessed by the phosphorylated levels) in the non diabetic hearts. On the contrary, this response was different in diabetic hearts since p-ERK levels were found to be increased at baseline and no further increase was observed

after myocardial infarction. Moreover, p-p38 MAPK levels were also not shown to be increased in diabetic hearts after myocardial infarction. Here, it is of note that imposition of mechanical loading in diabetic heart also failed to result in ERK1/2 activation and increase wall thickening (Landau, 2008)

Collectively, these data point out that the response of the diabetic myocardium is impaired after myocardial infarction which may be, at least in part, be due to its inability to develop reactive hypertrophy to normalize wall stress. This is shown to be due to the defects in stretch induced kinase activation. The cause of this defect is not known. However, it has recently been shown that ischaemia can induce tissue hypothyroidism which can lead to myocardial atrophy (Pantos, 2005). Based on this evidence, this study explored whether changes in thyroid hormone receptors occurred in diabetic myocardium after myocardial infarction. Surprisingly, the molecular analysis in this study showed that, at this early stage, both TR α 1 and TR β 1 receptors were down regulated in the diabetic hearts while such a response was not observed in the non diabetic hearts. Circulating T4 and T3 levels remained unchanged. Thus, acute myocardial infarction appears to result early in tissue hypothyroidism in the diabetic hearts which may be implicated in the acceleration of post-ischaemic remodelling. Several lines of evidence support this notion. First, thyroid hormone is critical for cardiac growth and function, mitochondrial biogenesis, metabolism, angiogenesis and response to ischaemic stress (reviewed in introduction) and low thyroid function results in cardiac atrophy with chamber dilatation and marked increase of β -MHC expression (Tang, 2005) Second, hypothyroidism is shown to exacerbate post-ischaemic remodeling by altering myosin expression and cardiac geometry by preventing wall thickening and increasing chamber dilatation (Pantos, 2009).

The potential link of tissue hypothyroidism and impaired response of the diabetic heart to ischaemia has further been established in this study in experiments in which thyroid hormone was administered after myocardial infarction. Interestingly, TH treatment early after infarction, prevented changes in TRs receptor expression and resulted in significantly reduced β -MHC expression, increased wall thickening with reactivation of p38 MAPK levels and improved cardiac function in diabetic animals with myocardial infarction (Pantos et al, 2012)

From the data obtained in this study, it can be clearly seen that TH can reverse and or prevent cardiac damage at least in DM in combination with AMI. It is apparent that TH is promoting cell growth, differentiation and repairing of the heart following DM in combination with AMI through the distinct intracellular signaling events mentioned earlier in this discussion. The evidence from this study is that TH can indeed protect the heart against stress, insults and injuries induced by both DM and AMI via a regulation of cardiac cardioprotective signalling. The results present in this study were obtained from rat models of DM and AMI. It is of clinical importance to follow up this study using potential therapeutic application of TH in DM+AMI patients with heart failure (Pantos et al 2011a; 2011b)

CHAPTER 5

CONCLUSION

This study employed the STZ-induced diabetic rats which were subjected to AMI in the absence and presence of TH treatment in order to study the beneficial roles of TH on cardiac function compared to the appropriate controls. Preliminary experiments were done initially to establish a base line of STZ application. The results showed the STZ at 35 mg/kg bw was more effective in inducing DM with little or no ketosis compared to a high dose of 60 mg/kg bw. Having a good DM model, some animals were induced with AMI to investigate the relation between DM, AMI and DM+AMI on cardiac dysfunction in the absence and presence of TH measure physiological and biomolecular signals in the heart.

The main conclusions of the study are summarized in the flow diagram of figure 5.1A/B. It is proposed that myocardial ischaemia in the diabetic heart induces tissue hypothyroidism which results in hypertrophy, decreased haemodynamics, suppression of growth kinase signalling molecules and in turn, these result in the inability of the diabetic heart to develop reactive hypertrophy and to compensate for the early insult of acute myocardial infarction. Administration of TH to the diabetic/AMI animals prevents the hypothyroidism and in turn, helps to remodel the heart and thereby increasing the haemodynamic parameters. These processes evoked by TH seem to be mediated via the activation of growth kinase signalling in the myocardium.

In conclusion, the results have clearly show that TH treatment shortly after myocardial infarction has beneficial effects on the remodelling of the diabetic heart by preventing tissue hypothyroidism, increasing growth kinases and thus, elevating contractile function of the heart and in turn haemodynamics.

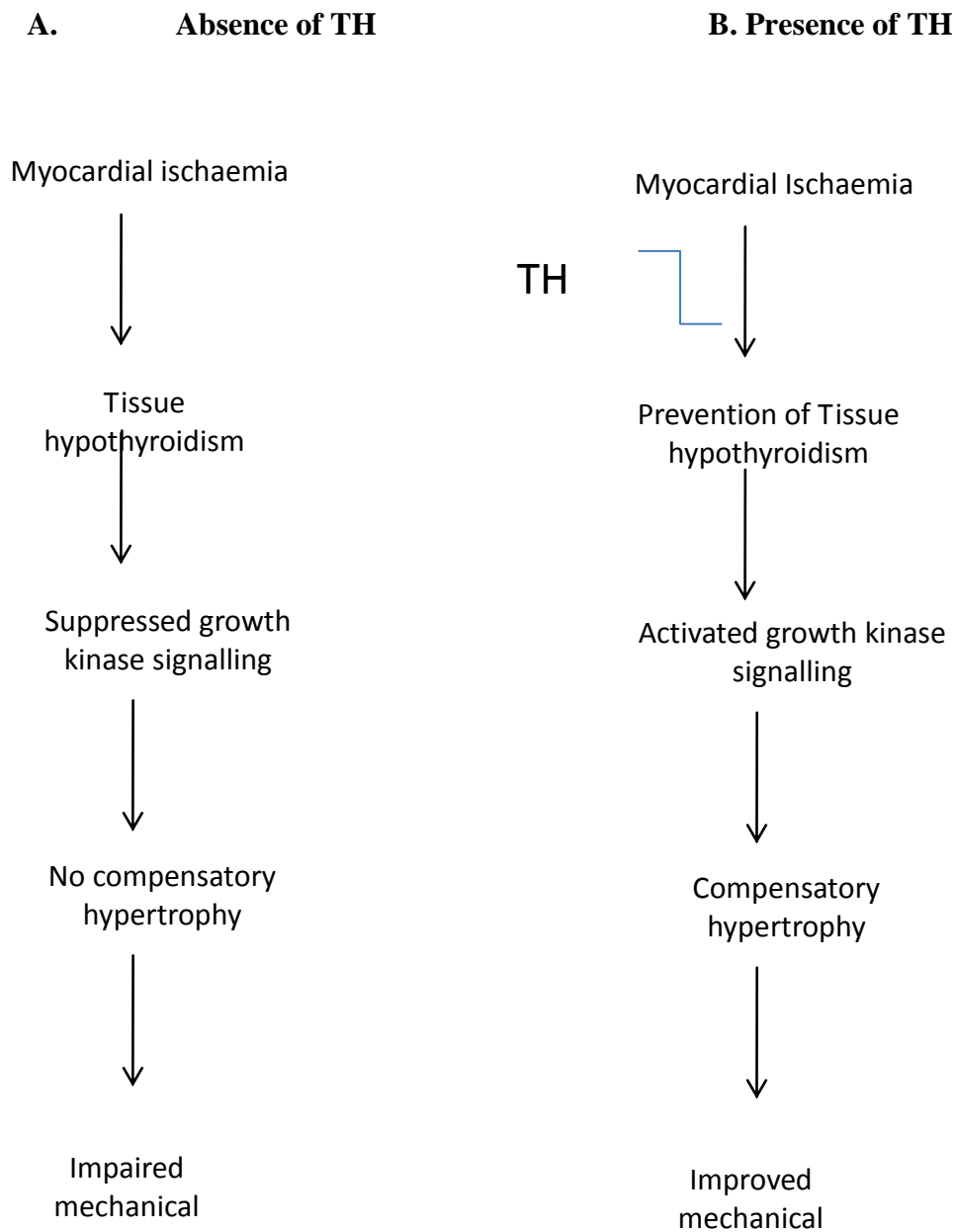


Figure 5.1: A schematic flow diagram showing the effect of myocardial infarction in the heart in the absence of TH (left) and in the presence of TH (right). The diagram shows clearly that thyroid hormone reverses all the deleterious effects of myocardial infarction, thus protecting the heart, preventing hypothyroidism, activating growth kinase signalling and improving cardiac contractile function and haemodynamic parameters.

CHAPTER 6

SCOPE FOR FUTURE RESEARCH

For future studies, a number of experiments have been proposed including:-

1. Investigating the gene expressions of other calcium handling proteins such as $\text{Na}^+/\text{Ca}^{2+}$ exchanger, the ryanodine receptor or L-type Ca^{2+} channel in the heart under different experimental conditions using Western Blotting techniques. These experiments will provide circumstantial evidence for a derangements in the different calcium transporting proteins in the heart and whether TH can repair and reverse any adverse effects.
2. Investigating the morphology and functions of cardiomyocytes obtained from whole hearts under different experimental conditions. Contractile function will be done by measuring myocyte kinetics (amplitude of contraction, rate of rise in tension, rate of relaxation etc) using the Video Edge System. These results will provide substantial evidence for myocyte dysfunction and the beneficial role of TH in reversing myocyte dysfunction. In addition, it is possible to measure the sizes (length and diameter) of the myocytes for hypertrophy.
3. Investigating the development of fibrosis and measuring gene expressions for the different collagens and related molecules under the different experimental conditions using morphological and molecular biological techniques in the absence and presence of thyroid hormone. The work will involve staining for the different fibrotic molecules and measuring the expressions for the different collagens and extracellular matrix factors (MMPS) and respective inhibitors.
4. Investigating the role of TH in type II diabetes mellitus experimental models employing the different experimental conditions. These studies will involve repeating all the experiments described in this thesis. It will also involve the measurements of contraction and cellular calcium homeostasis using established techniques.
5. Investigating the effect of thyroid hormone on intracellular free calcium concentrations and L-type calcium current activities under different experimental conditions. Calcium is the main stay in contraction and a derangement in its homeostasis is associated with cardiac dysfunction. Isolated myocytes will be loaded with fura -2 for the measurement of intracellular free calcium concentrations. Cells will be stimulated electrically and with caffeine. Experiments will involve the roles of SERCA, ryanodine receptors, calcium-

ATPase pump and the sodium calcium exchanger during calcium transport. From the data it will be possible to investigate the myofilament calcium sensitivity. The Patch Clamp Technique will be used to determine L-type calcium current activities under the different experimental conditions.

6. Investigating the effect of reactive oxygen species and carbonylation in the hearts from sham control, DM, AMI and AMI combined with DM in the absence and presence of TH treatment using established methods described in the literature.

REFERENCES

- Abe, T., Ohga, Y. and Tabayashi, N. et al. (2002). Left ventricular diastolic dysfunction in type 2 diabetes mellitus model rats. *Am J Physiol Heart Circ Physiol*, **282**:H138-148
- Abohashem-Aly, A. A., Meng, X., Li, J., Sadaria, M. R., Ao, L. and Wennergren, J., et al. (2011). DITPA, A Thyroid Hormone Analog, Reduces Infarct Size and Attenuates the Inflammatory Response Following Myocardial Ischemia. *J Surg Res*.**119**: 138-140
- Abo-Zenah, H. A., Shoeb, S. A., Sabry, A. A. and Ismail, H. A. (2008). Relating circulating thyroid hormone concentrations to serum interleukins-6 and 10 in association with non-thyroidal illnesses including chronic renal insufficiency. *BMC Endocr Disord*, **8** (1): 1-7.
- Adeghate E, Hameed RS, Ponery AS, Tariq S, Sheen RS, Shaffiullah M. and Donath T (2010). Streptozotocin causes pancreatic beta cell failure via early and sustained biochemical and cellular alterations. *Exp Clin Endocrinol Diabetes***118**, 699-707.
- Akaike, M., Che, W., Marmarosh, N., Ohta, S., Osawa, M., Ding, B., Berk, B., Yan, C. and Abe, J. (2004). The hinge-helix 1 region of peroxisome proliferator-activated receptor gamma 1 (PPARgamma1) mediates interaction with extracellular signal-regulated kinase 5 and PPARgamma1 transcriptional activation: involvement in flow-induced PPARgamma activation in endothelial cells. *Mol Cell Biol*, **24**: 8691– 8704.
- Aleshin, A., Ananthakrishnan, R., Li, Q, Rosario R, LuY, Qu W, Song F, Bakr, S., Szabolcs, M., D'Agati, V., Liu, R., Homma, S., Schmidt, A.M., Yan, S.F., and Ramasamy, R. (2008). RAGE modulates myocardial injury consequent to LAD infarction via impact on JNK and STAT signaling in a murine model. *Am J Physiol Heart Circ Physiol*, **294**:H1823–H1832.
- American Diabetes Association. Living with diabetes: Complications <http://www.diabetes.org/living-with-diabetes/complications> (Accessed on April 6th 2012)
- Andreka, P., Zang, J., Dougherty, C., Slepak, T.I., Webster, K.A., and Bishopric, N.H. (2001). Cytoprotection by Jun kinase during nitric oxide-induced cardiac myocyte apoptosis. *Circ Res*, **88**: 305–312.
- Andrews, C., Ho, P.D., Dillmann, W.H., Glembotski, C.C., and Mc-Donough, P.M. (2003). The MKK6-p38 MAPK pathway prolongs the cardiac contractile calcium transient, downregulates SERCA2, and activates NF-AT. *Cardiovasc Res*, **59**: 46–56.
- Anilkumar, N., Sirker, A. and Shah, A. (2009). Redox sensitive signaling pathways in cardiac remodeling, hypertrophy and failure. *Front Biosci*, **14**: 3168–1387.

- Aoki, H., Kang, P.M., Hampe, J, Yoshimura, K., Noma, T., Matsuzaki, M., and Izumo, S. (2002). Direct activation of mitochondrial apoptosis machinery by c-Jun N-terminal kinase in adult cardiac myocytes. *J Biol Chem*, **277**: 10244–10250
- Aoki, H., Richmond, M., Izumo, S., and Sadoshima, J. (2000). Specific role of the extracellular signal-regulated kinase pathway in angiotensin II-induced cardiac hypertrophy in vitro. *Biochem J*, **347**: 275–284.
- Aoki, Y., Niihori, T., Narumi, Y., Kure, S., and Matsubara, Y. (2008). The RAS/MAPK syndromes: novel roles of the RAS pathway in human genetic disorders. *Hum Mutat*, **29**: 992–1006.
- Aries, A., Paradis, P., Lefebvre, C. and Schwartz, R.J. (2004). Essential role of GATA-4 in cell survival and drug-induced cardiotoxicity. *Proc Natl Acad Sci USA*, **101**: 6975–6980.
- Avruch, J. (2007). MAP kinase pathways: the first twenty years. *Biochim Biophys Acta*, **1773**: 1150–1160.
- Babiker, F.A., Lips, D., Meyer, R., Delvaux, E., Zandberg, P., Janssen, B., van Eys, G., Grohe, C., and Doevendans, P.A. (2006). Estrogen receptor α protects the murine heart against left ventricular hypertrophy. *Arterioscler Thromb Vasc Biol*, **26**: 1524–1530.
- Backlund, T., Palojoki, E., Saraste, A. et al. (2004). Sustained cardiomyocyte apoptosis and left ventricular remodelling after myocardial infarction in experimental diabetes. *Diabetologia*, **47**: 325–330
- Bae SS, Cho H, Mu J, and Birnbaum MJ. (2003). Isoform-specific regulation of insulin-independent glucose uptake by Akt/protein kinase B. *J Biol Chem*, **278**: 49530–49536.
- Baines, C.P., Zhang, J., Wang, G.W., Zheng, Y.T., Xiu, J.X., Cardwell, E.M., Bolli, R., and Ping, P. (2002). Mitochondrial PKC α and MAPK form signaling modules in the murine heart: enhanced mitochondrial PKC α -MAPK interactions and differential MAPK activation in PKC α -induced cardioprotection. *Circ Res*, **90**: 390–397.
- Balakumar, P., Rohilla, A. and Singh, M. (2008). Pre-conditioning and postconditioning to limit ischemia-reperfusion-induced myocardial injury: what could be the next footstep? *Pharmacol Res*, **57**: 403–412.
- Balakumar, P., Singh, H., Singh, M., and Anand-Srivastava, M.B. (2009). The impairment of preconditioning-mediated cardioprotection in pathological conditions. *Pharmacol Res*, **60**: 18–23.
- Balke CW, Egan TM, and Wier WG (1994). Processes that remove calcium from the cytoplasm during excitation-contraction coupling in intact rat heart cells. *J Physiol* **474**, 447-462.
- Bao, J.E., Dixon, G.Z. and Zhao, Q. (1995). Components of a new human protein kinase signal transduction pathway. *J Biol Chem*, **270**: 12665–12669.
- Barancik, M., Htun, P., Strohm, C., Kilian, S., and Schaper, W. (2000). Inhibition of the cardiac p38-MAPK pathway by SB230580 delays ischemic cell death. *J Cardiovasc Pharmacol*, **35**: 474–483.

- Barcenas-Ruiz L, Beuckelmann DJ, and Wier WG (1987). Sodium-calcium exchange in heart: membrane currents and changes in $[Ca^{2+}]_i$. *Science* **238**, 1720-1722.
- Barki-Harrington, L., Perrino, C., and Rockman, H.A. (2004). Network integration of the adrenergic system in cardiac hypertrophy. *Cardiovasc Res*, **63**: 391–402.
- Barr, R.K. and Bogoyevitch, M.A. (2001). The c-Jun N-terminal protein kinase family of mitogen-activated protein kinases (JNK MAPKs). *Int J Biochem Cell Biol*, **33**: 1047–1063.
- Barry WH and Bridge JH (1993). Intracellular calcium homeostasis in cardiac myocytes. *Circulation* **87**, 1806-1815.
- Barth, J. D., Jansen, H., Kromhout, D., Reiber, J. H., Birkenhager, J. C., and Arntzenius, A. C. (1987). Progression and regression of human coronary atherosclerosis. The role of lipoproteins, lipases and thyroid hormones in coronary lesion growth. *Atherosclerosis*, **68**(1-2): 51-58.
- Baxter, J. D., and Webb, P. (2009). Thyroid hormone mimetics: potential applications in atherosclerosis, obesity and type 2 diabetes. *Nat Rev Drug Discov*, **8**(4): 308-320.
- Bayer, A.L., Heidkamp, M.C., Patel, N., Porter, M., Engman S., and Samarel, A.M. (2003). Alterations in protein kinase C isoenzyme expression and autophosphorylation during progression of pressure overload-induced left ventricular hypertrophy. *Mol Cell Biochem*, **242**: 145–152.
- Béguin, P.C., Belaidi, E., Godin-Ribuot, D., Lévy, P., and Ribuot, C. (2007). Intermittent hypoxia-induced delayed cardioprotection is mediated by PKC and triggered by p38 MAP kinase and Erk1/2. *J Mol CellCardiol*, **42**: 343–351.
- Belakavadi, M., Saunders, J., Weisleder, N., Raghava, P. S., and Fondell, J. D. (2010). Repression of cardiac phospholamban gene expression is mediated by thyroid hormone receptor- α 1 and involves targeted covalent histone modifications. *Endocrinology*, **151**(6): 2946-2956.
- Belin, R.J. , Sumandea, M.P. , Allen, E.J. , Schoenfelt, K. , Wang H., and Solaro, R.J. et al. (2007). Augmented protein kinase C- α -induced myofilament protein phosphorylation contributes to myofilament dysfunction in experimental congestive heart failure. *Circ Res*, **101**: 195–204.
- Bell, J.R., Eaton, P., and Shattock, M.J. (2008). Role of p38-mitogen-activated protein kinase in ischaemic preconditioning in rat heart. *Clin Exp Pharmacol Physiol*, **35**: 126–134.
- Bennett RA and Pegg AE (1981). Alkylation of DNA in rat tissues following administration of streptozotocin. *Cancer Res* **41**, 2786-2790.
- Berry, D. L., Rose, C. S., Remo, B. F., and Brown, D. D. (1998). The expression pattern of thyroid hormone response genes in remodeling tadpole tissues defines distinct growth and resorption gene expression programs. *Dev Biol*, **203**(1): 24-35.
- Bers DM (1991). Excitation-contraction coupling and cardiac contractile force. Dordrecht, The Netherlands: Kluwer Academic publishers
- Bers, D.M. (1991). Ca regulation in cardiac muscle, *Med Sci Sports Exer*,

23(10):1157-1162.

- Bertoni AG, Hundley WG, Massing MW, Bonds DE, Burke GL, and Goff DC, Jr. (2004). Heart failure prevalence, incidence, and mortality in the elderly with diabetes. *Diabetes Care* **27**, 699-703.
- Beuckelmann DJ and Wier WG (1988). Mechanism of release of calcium from sarcoplasmic reticulum of guinea-pig cardiac cells. *J Physiol* **405**, 233-255.
- Bianco, A. C., and Kim, B. W. (2006). Deiodinases: implications of the local control of thyroid hormone action. *J Clin Invest*, **116**(10): 2571-2579.
- Bianco, A. C., Salvatore, D., Gereben, B., Berry, M. J., and Larsen, P. R. (2002). Biochemistry, cellular and molecular biology, and physiological roles of the iodothyronine selenodeiodinases. *Endocr Rev*, **23**(1): 38-89.
- Blunt, B.C., Creek, A.T., Henderson, D.C., and Hofmann, P.A. (2007). H₂O₂ activation of HSP25/27 protects desmin from calpain proteolysis in rat ventricular myocytes. *Am J Physiol Heart Circ Physiol*, **293**:H1518–H1525.
- Bogoyevitch, M.A. (2006). The isoform-specific functions of the c-jun N-terminal kinases (JNKs): differences revealed by gene targeting. *Bioessays*, **28**: 923–934.
- Bogoyevitch, M.A., Gullepie-Brown, J., Ketterman, A., Fuller, S., Ben-Levy, R., Ashworth, A., Marshall, C.J., and Sugden, P. (1996). Stimulation of the stress-activated mitogen-activated protein kinase subfamilies in perfused heart: p38/RK mitogen-activated protein kinases and c-Jun N-terminal kinases are activated by ischemia/reperfusion. *Circ Res*, **79**: 162–173.
- Bogoyevitch, M.A., and Kobe, B. (2006). Uses for JNK: the many and varied substrates of the c-Jun N-terminal kinases. *Microbiol Mol Biol, Rev* **70**: 1061–1095.
- Bogoyevitch, M.A., Parker, P.J., and Sugden, P.H. (1993). Characterization of protein kinase C isotype expression in adult rat heart. Protein kinase C-epsilon is a major isotype present, and it is activated by phorbol esters, epinephrine, and endothelin. *Circ Res*, **72**:757–67.
- Bollano, E., Omerovic, E., Svensson, H. et al. (2006). Cardiac remodeling rather than disturbed myocardial energy metabolism is associated with cardiac dysfunction in diabetic rats. *Int J Cardiol*,
- Boluyt, M.O., Loyd, A.M., Roth, M.H., Randall, M.J., and Song, E.Y.M. (2003). Activation of JNK in rat heart by exercise: effect of training. *Am J Physiol Heart Circ Physiol*, **285**: H2639–H2647.
- Borsch-Haubold, A.G., Pasquet, S. and Watson, S.P. (1998). Direct inhibition of

- cyclooxygenase-1 and -2 by the kinase inhibitors SB 203580 and PD98059. SB 203580 also inhibits thromboxane synthase. *J Biol Chem*, **273**: 28766–28772.
- Bouzaffour, M., Rampon, C., Ramage, M., Courtin, F., and Vriza, S. (2010). Implication of type 3 deiodinase induction in zebrafish fin regeneration. *Gen Comp Endocrinol*, **168**(1): 88-94.
- Bowers, S. L., Borg, T.K. and Baudino, T.A. (2010). The dynamics of fibroblast-myocyte-capillary interaction in the heart. *Ann NY Acad Sci*, **1188**:143-152.
- Bowling, N., Walsh, R.A., Song, G., Estridge, T., Sandusky G.E. and Fouts, R.L, et al. (1999). Increased protein kinase C activity and expression of Ca²⁺ - sensitive isoforms in the failing human heart. *Circulation*, **99**: 384–391.
- Boyle, A.J., Kelly, D.J., Zhang, Y., Cox, A.J., Gow, R.M. and Way, K., et al. (2005). Inhibition of protein kinase C reduces left ventricular fibrosis and dysfunction following myocardial infarction. *J Mol Cell Cardiol*, **39**: 213–221.
- Bracken, N., Howarth, F.C. and Singh, J. (2006). Effects of streptozotocin-induced diabetes on contraction and calcium transport in rat ventricular cardiomyocytes. *Annals N.Y. Acad. Sci* :**1084**, 208-222.
- Bracken, N.K., Singh, J., Winlow, W., and Howard F.C. (2003). Mechanism underlying contractile dysfunction in streptozotocin-induced type 1 and type 2 diabetic cardiomyopathy. In *Atherosclerosis, Hypertension and Diabetes*. G.N. Pierce, M. Nagano, P.Zahradka & N.S. Dhalla, Eds.: 387–408. Qureshi, M.A., Bracken, N.K. Winlow, W. et al. 2001. Time dependent effects of streptozotocin-induced diabetes on contraction in rat ventricular myocytes. *Emirates J*. **19**: 35–41.
- Bracken, N.K., Woodall, A.J. Howarth, F.C. and Singh, J., (2004). Voltage dependence of contraction in streptozotocin-induced diabeticmyocytes. *Mol Cell Biochem*,**261**: 235–243.
- Braken, N.K., Singh, J, Wintow, W. and Howarth, F.C. (2003). Mechanisms underlying contractil dysfunction in Streptozotocin-induced Type I and Type II diabetic cardiomyopathy. *Progr Exp Card*, **9**(111): 387-408.
- Braun, M.U., LaRosee, P., Schon, S., Borst M.M. and Strasser, R.H.(2002). Differential regulation of cardiac protein kinase C isozyme expression after aortic banding in rat. *Cardiovasc Res*, **56**: 52–63.
- Braun, M.U., LaRosee, P., Simonis, G., Borst, M.M., and Strasser, R.H. (2004). Regulation of protein kinase C isozymes in volume overload cardiac hypertrophy. *Mol Cell Biochem*, **262**:135–143.
- Braz, J.C., Gregory, K., Pathak, A., Zhao, W., Sahin, B., and Klevitsky, R. et al. (2004). PKC- α regulates cardiac contractility and propensity toward heart

failure. *Nat Med*, **10**: 248–254.

- Braz, J.C., Bueno, O.F., Liang, Q., Wilkins, B.J., Dai, Y.S., Parsons, S., Braunwart, J., Glascock, B.J., Klevitsky, R., Kimball, T.F., Hewett, T.E., and Molkenin, J.D. (2003). Targeted inhibition of p38 MAPK promotes hypertrophic cardiomyopathy through upregulation of calcineurin-NFAT signaling. *J Clin Invest*, **111**: 1475–1486.
- Budas, G.R., Churchill, E.N. and Mochly-Rosen, D. (2007). Cardioprotective mechanisms of PKC isozyme-selective activators and inhibitors in the treatment of ischemia-reperfusion injury. *Pharmacol Res*, **55**: 523–536.
- Budina, S. and Abel, E.D. (2007). Diabetic cardiomyopathy revisited. *Circulation*, **115**(25): 3213–3223.
- Bueno, O., De Windt, L.J., Tymitz, K.M., Witt, S.A., Kimball, T., Klevitsky, R., Hewett, T., Jones, S., Lefer, D., Peng, C., Kitsis, R., and Molkenin, J. (2000). The MEK1-ERK1/2 signaling pathway promotes compensated cardiac hypertrophy in transgenic mice. *EMBO J* **19**: 6341–6350.
- Buerger, A., Rozhitskaya, O., Sherwood, M.C., Dorfman, A.L., Bisping, E., Abel, E.D., Pu, W.T., Izumo, S., and Jay, P.Y. (2006). Dilated cardiomyopathy resulting from high-level myocardial expression of Cre-recombinase. *J Card Fail*, **12**: 392–398.
- Buschbeck, M., Eickhoff, J., Sommer, M.N., and Ullrich, A. (2002). Phosphotyrosine-specific phosphatase PTP-SL regulates the ERK5 signaling pathway. *J Biol Chem*, **277**: 29503–29509.
- Cacace, A.M., Guadagno, S.N., Krauss, R.S., Fabbro, D., and Weinstein, I.B. (1993). The epsilon isoform of protein kinase C is an oncogene when overexpressed in rat fibroblasts. *Oncogene*, **8**: 2095–2104.
- Cannell MB, Berlin JR and Lederer WJ (1987). Effect of membrane potential changes on the calcium transient in single rat cardiac muscle cells. *Science* **238**, 1419-1423.
- Catalucci, D., Latronico, M.V., Ceci, M., Rusconi, F., Young, H.S., Gallo, P., Santonastasi, M., Bellacosa, A., Brown, J.H., Condorelli, G. 2009. Akt increases sarcoplasmic reticulum Ca²⁺-cycling by direct phosphorylation of phospholamban at Thr17. *J Biol Chem*, **284**: 28180–28187.
- Catalucci, D., Zhang, D.H., DeSantiago, J., Aimond, F., Barbara, G., Chemin, J., Bonci, D., Picht, E., Rusconi, F., Dalton, N.D., Peterson, K.L., Richard, S., Bers, D.M., Brown, J.H., and Condorelli, G. (2009). Akt regulates L-type Ca²⁺ channel activity by modulating Cav α 1 protein stability. *J Cell Biol*, **184**: 923–933.

- Cervantes, D., Crosby, C. and Xiang, Y. (2010) Arrestin orchestrates crosstalk between G protein-coupled receptors to modulate the spatiotemporal activation of ERK MAPK. *Circ Res*, **106**: 79–88.
- Chablais, F., Veit, J., Rainer, G., and Jazwinska, A. (2011). The zebrafish heart regenerates after cryoinjury-induced myocardial infarction. *BMC Dev Biol*, **11**: 21-25
- Chandler, M.P., Morgan, E.E., McElfresh, T.A. et al. (2007). Heart failure progression is accelerated following myocardial infarction in type 2 diabetic rats. *Am J Physiol Heart Circ Physiol*, **293**:H1609-1616
- Chandrashekar, I.R., Dike, A. and Cowslik, S.M. (2004). Membrane-induced structure of the mammalian tachikinin neuropeptide gamma. *J Struct Biol*, **148**(3):315-325.
- Chen, C. and Sytkowski, A.J. (2005). Apoptosis-linked gene-2 connects the Raf-1 and ASK1 signalings. *Biochem Biophys Res Commun*, **333**:51–57.
- Chen, J., Fujii, K., Zhang, L., Roberts, T., and Fu, H. (2001). Raf-1 promotes cell survival by antagonizing apoptosis signal-regulating kinase 1 through a MEK-ERK independent mechanism. *Proc Natl Acad Sci USA*, **98**: 7783–7788.
- Chen, L., Hahn, H., Wu, G., Chen, C.H., Liron, T., Schechtman, D., et al. (2001). Opposing cardioprotective actions and parallel hypertrophic effects of delta PKC and epsilon PKC. *Proc Natl Acad Sci USA*, **98**:11114–11149.
- Chen, V., Ianuzzo, C.D., Fong, B.C. et al. (1984). The effects of acute and chronic diabetes on myocardial metabolism in rats. *Diabetes*, **33**:1078-1084
- Chen, W.S., Xu, P.Z., Gottlob, K., Chen, M.L., Sokol, K., Shiyanova, T., Roninson, I., Weng, W., Suzuki, R., Tobe, K., Kadowaki, T., and Hay, N. (2001). Growth retardation and increased apoptosis in mice with homozygous disruption of the Akt1 gene. *Genes Dev*, **15**:2203–2208.
- Chen, Y. F., Kobayashi, S., Chen, J., Redetzke, R. A., Said, S., and Liang, Q., et al. (2008). Short term triiodo-L-thyronine treatment inhibits cardiac myocyte apoptosis in border area after myocardial infarction in rats. *J Mol Cell Cardiol*, **44**(1): 180-187.
- Chen, Y., Rajashree, R., Liu, Q., and Hofmann, P. (2003). Acute p38 MAPK activation decreases force development in ventricular myocytes. *Am J Physiol Heart Circ Physiol*, **285**: H2578–H2586.
- Cheng, T.H., Shih, N.L., Chen, S.Y., Lin, J.W., Chen, Y.L., Chen, C.H., Lin, H., Cheng, C.F., Chiu, W.T., Wang, D.L., and Chen, J.J. (2005). Nitric oxide inhibits endothelin-1-induced cardiomyocyte hypertrophy through Cgmp mediated suppression of extracellular-signal regulated kinase phosphorylation. *Mol Pharmacol*, **68**: 1183–1192.
- Cheng, Y.C., Kuo, W.W., Wu, H.C., Lai, T.Y., Wu, C.H., Hwang, J.M., Wang, W.H., Tsai, F.J., Yang, J.J., Huang, C.Y., and Chu, C.H. (2009). ZAK induces MMP-

- 2activity via JNK/p38 signals and reduces MMP-9 activity by increasing TIMP-1/2 expression in H9c2 cardiomyoblast cells. *Mol Cell Biochem*, **325**: 69–77.
- Cho, H., Mu, J., Kim, J.K., Thorvaldsen, J.L., Chu, Q., Crenshaw, E.B. 3rd, Kaestner, K.H., Bartolomei, M.S., Shulman, G.I., and Birnbaum, M.J. (2001). Insulin resistance and a diabetesmellitus-like syndrome in mice lacking the protein kinase Akt2 (PKB beta). *Science*, **292**:1728–1731.
- Cho, H., Thorvaldsen, J.L., Chu, Q., Feng, F, and Birnbaum MJ. (2001). Akt1/PKBalpha is required for normal growth but dispensable for maintenance of glucose homeostasis in mice. *J Biol Chem*, **276**:38349–38352.
- Choi, K.M., Zhong, Y., Hoit B.D. et al. (2002). Defective intracellular Ca²⁺ signaling contributes to cardiomyopathy in type 1 in diabetic rats. *Am J Physiol* **283**: H1398–H1408.
- Choudhary, R., Palm-Leis, A., Scott, R.C. III, Guleria, R.S., Rachut, E., Baker, K.M., and Pan, J. (2008). All-trans retinoic acid prevents development of cardiac remodeling in aortic banded rats by inhibiting the reninangiotensin system. *Am J Physiol Heart Circ Physiol*, **294**: H633–H644.
- Choukroun, G., Hajjar, R., Fry, S., del Monte, F., Haq, S., Guerrero, J., Picard, M., Rosenzweig, A., and Force, T. (1999). Regulation of cardiac hypertrophy in vivo by the stress activated protein kinases/c-JunNH2-terminal kinases. *J Clin Invest*, **104**: 391–398.
- Choukroun, G., Hajjar, R., Kyriakis, J.M., Bonventre, J.V., Rosenzweig, A., and Force, T. (1998). Role of the stress-activated protein kinases in endothelin-induced cardiomyocyte hypertrophy. *J Clin Invest*, **102**:1311–1320.
- Clark RS, English M, McNeill GP, and Newton RW (1985). Effect of intravenous infusion of insulin in diabetics with acute myocardial infarction. *Br Med J (Clin Res Ed)* **291**, 303-305.
- Clark, J.E., Sarafraz, N., Marber, and M.S. (2007). Potential of p38-MAPK inhibitors in the treatment of ischaemic heart disease. *Pharmacol Ther*, **116**: 192–206.
- Clerk, A. and Sugden, P. (1998). The p38-MAPK inhibitor, SB 203580, inhibits cardiac stress-activated protein kinases/c-jun N-terminal kinases(SAPKs/JNKs). *FEBS Lett*, **426**: 93–96.
- Clerk, A., Aggeli, I.K.S., Stathopoulou, K. and Sugden, P.H. (2006). Peptide growth factors signal differentially through protein kinase C to extracellular signal-regulated kinases in neonatal cardiomyocytes. *Cell Signal*, **18**: 225–235.
- Coghlan, C., and Hoffman, J. (2006). Leonardo da Vinci's flights of the mind must continue: cardiac architecture and the fundamental relation of form and function revisited. *Eur J Cardiothorac Surg*, **29 Suppl 1**: S4-17.

- Comparison of inhibition of glucose-stimulated insulin secretion in rat islets of Langerhans by streptozotocin and methyl and ethyl nitrosoureas and methanesulphonates. Lack of correlation with nitric oxide-releasing or O₆-alkylating ability. *Biochem Pharmacol* **50**, 2015-2020.
- Connelly, K.A., Kelly, D.J., Zhang, Y. , Prior, D.L. , Advani, A. and Cox, A.J. , et al.(2009). Inhibition of protein kinase C-beta by ruboxistaurin preserves cardiac function and reduces extracellular matrix production in diabetic cardiomyopathy. *Circ Heart Fail*, **2**: 129–137.
- Cross, H., Li, M., Petrich, B., Murphy, E., Wang, Y., and Steenbergen, C. (2009). Effect of p38 MAP kinases on contractility and ischemic injury in intact heart. *Acta Physiol Hung*, **96**: 307–323.
- Cuenda, A. and Rousseau, S. (2007). p38 MAP-kinases pathway regulation, function and role in human diseases. *Biochim Biophys Acta*, **1773**:1358–1375.
- Cullingford, T., Markou, T., Fuller, S., Giraldo, A., Pikkarainen, S., Zoumpoulidou, G., Alsafi, A., Ekere, C., Kemp, T., Dennis, J., Game, L., Sugden, P.H., and Clerk, A. 2008. Temporal regulation of expression of immediate early and second phase transcripts by endothelin-1 in cardiomyocytes. *Genome Biol*, **9**: R32-42..
- D'Souza, A., Hussain, M., Howarth, C.F., Woods, N.M., Bidasee, K.A. and Singh, J. (2009). Pathogenesis and pathophysiology of accelerated atherosclerosis in the diabetic heart. *Molec. Cell Biochem*, **331 (1/2)**: 89-116.
- D'Souza, A., Wood, N.M., Boyett, M., Adeghate, E., Howarth, C.F., Bidasee, K.A. and Singh, J. (2011). Left Ventricle Structural Remodelling in the Prediabetic Goto-Kakizaki Rat- Potential role of Transforming Growth Factor β 1. *Exp Phys*, **96.9**:875-888.
- Das, A., Salloum, F.N., Xi, L., Rao, Y.J., and Kukreja, R.C. (2009). ERK phosphorylation mediates sildenafil-induced myocardial protection against ischemia-reperfusion injury in mice. *Am J Physiol Heart CircPhysiol*, **296**: H1236–H1243.
- Das, A., Xi, L., and Kukreja, R.C. (2008).Protein Kinase G-dependent cardioprotective mechanism of phosphodiesterase-5 inhibition involves phosphorylation of ERK and GSK3 β . *J Biol Chem*, **283**: 29572–29585.
- Das, M., Das, S. and Das, D.K. (2007). Caveolin and MAP kinase interaction in angiotensin II preconditioning of the myocardium. *J Cell Mol Med*, **11**: 788–797.
- Davies, E.J., Moxham, T., Rees, K., Singh, S., Coats, A.J., Ebrahim, S., Lough, F., and Taylor, R.S. (2010). Exercise training for systolic heart failure: Cochrane

systematic review and meta-analysis. *Eur J Heart Fail*, **12**:706–715.

- Davis, R.J. (2000). Signal transduction by the JNK group of MAP kinases. *Cell*, **103**: 239–252.
- De Windt, L.J. , Lim, H.W. , Haq, S., Force, T. and Molkentin, J.D.(2000). Calcineurin promotes protein kinase C and c-Jun NH₂-terminal kinase activation in the heart. Cross-talk between cardiac hypertrophic signaling pathways. *J Biol Chem*, **275**: 13571–13579.
- Degens, H., Gilde, A. J., Lindhout, M., Willemsen, P. H., Van Der Vusse, G. J., and Van Bilsen, M. (2003). Functional and metabolic adaptation of the heart to prolonged thyroid hormone treatment. *Am J Physiol Heart Circ Physiol*, **284** (1): H108-115.
- Delaney CA, Dunger A, Di MM, Cunningham JM, Green MH, and Green IC (1995). Comparison of inhibition of glucose-stimulated insulin secretion in rat islets of Langerhans by streptozotocin and methyl and ethyl nitrosoureas and methanesulphonates. *Biochem Pharmacol* (**12**):2015-2020
- Depre, C., Young, M.E., Ying, J. et al. (2000). Streptozotocin-induced changes in cardiac gene expression in the absence of severe contractile dysfunction. *J Mol Cell Cardiol*, **32**:985-996
- Dhalla NS, Pierce GN, Innes IR, and Beamish RE (1985). Pathogenesis of cardiac dysfunction in diabetes mellitus. *Can J Cardiol*, **1**, 263-281.
- Dhanasekaran, D., Kashef, K., Lee, C., Xu, H. and Reddy, E. (2007). Scaffold protein of MAPK-kinase modules. *Oncogene*, **26**: 3185–3202.
- Dhingra, S., Sharma, A.K., Arora, R.C., Slezak, J., and Singal, P.K. (2009). IL-10 attenuates TNF- α -induced NF- κ B pathway activation and cardiomyocyte apoptosis. *Cardiovasc Res*, **82**: 59–66.
- Dhingra, S., Sharma, A.K., Singla, D.K., and Singal, P.K. (2007). p38 and ERK1/2/MAPKs mediate the interplay of TNF- α and IL-10 in regulating oxidative stress and cardiac myocyte apoptosis. *Am J Physiol Heart Circ Physiol*, **293**: H3524–H3531.
- Diaz, R., Goyal, A., Mehta, S.R., Afzal, R., Xavier, D., Pais, P., Chrolavicius, S., Zhu, J., Kazmi, K., Liu, L., Budaj, A., Zubaid, M., Avezum, A., Ruda, M., and Yusuf, S. (2007). Glucose-insulin-potassium therapy in patients with ST-segment elevation myocardial infarction. *JAMA*, **298**:2399–2405.
- Diwan, A. and Dorn, G.W. II. (2007). Decompensation of cardiac hypertrophy: cellular mechanisms and novel therapeutic targets. *Physiology*, **22**:56–64.
- Dorn, G. W., 2nd. (2007). The fuzzy logic of physiological cardiac hypertrophy.

Hypertension, **49**(5): 962-970.

- Dorn, G.W. and Force, T. (2005). Protein kinase cascades in the regulation of cardiac hypertrophy. *J Clin Invest*, **115**: 527–537.
- Dorn, G.W., 2nd and Molkenin, J.D. (2004). Manipulating cardiac contractility in heart failure: data from mice and men. *Circulation*, **109**: 150–158.
- Dougherty, C.J., Kubasiak, L.A., Prentice, H., Andreka, P., Bishopric, N.H., and Webster, K.A. (2002). Activation of c-Jun N-terminal kinase promotes survival of cardiac myocytes after oxidative stress. *Biochem J*, **362**: 561–571.
- Downey, J., Davis, A., and Cohen, M. (2007). Signaling pathways in ischemic preconditioning. *Heart Fail Rev*, **12**: 181–188.
- Easton, R.M., Cho, H., Roovers, K., Shineman, D.W., Mizrahi, M., Forman, M.S., Lee, V.M., Szabolcs, M., de Jong, R., Oltersdorf, T., Ludwig, T., Efstratiadis, A., and Birnbaum, M.J. (2005). Role for Akt3/protein kinase Bgamma in attainment of normal brain size. *Mol Cell Biol*, **25**: 1869–1878.
- Eber, B., Schumacher, M., Langsteger, W., Zweiker, R., Fruhwald, F. M., Pokan, R., et al. (1995). Changes in thyroid hormone parameters after acute myocardial infarction. *Cardiology*, **86** (2): 152-156.
- Eckel, J. and Reinauer, H. (1990). Insulin action on glucose transport in isolated cardiac myocytes: signalling pathways and diabetes-induced alterations. *Biochem Soc Trans*, **18**: 1125-1127
- Eisner DA and Trafford AW (2000). No Role for the Ryanodine Receptor in Regulating Cardiac Contraction? *News Physiol Sci* **15**, 275-279.
- Engel, F.B., Hsieh, P.C., Lee, R.T., and Keating, M.T. (2006). FGF1/p38 MAP kinase inhibitor therapy induces cardiomyocyte mitosis, reduces scarring, and rescues function after myocardial infarction. *Proc Natl Acad Sci USA*, **103**: 15546–15551.
- Engelbrecht, A.M., Niesler, C., Page, C., and Lochner, A. (2004). p38 and JNK have distinct regulatory functions on the development of apoptosis during simulated ischaemia and reperfusion in neonatal cardiomyocytes. *Basic Res Cardiol*, **99**: 338–350.
- Enomoto, A., Murakami, H., Asai, N., Morone, N., Watanabe, T., Kawai, K., Murakumo, Y., Usukura, J., Kaibuchi, K., and Takahashi, M. (2005). Akt/PKB regulates actin organization and cell motility via Girdin/APE. *Dev Cell*, **9**: 389–402.
- Esaki, T., Suzuki, H., Cook, M., Shimoji, K., Cheng, S. Y., Sokoloff, L., et al. (2004). Cardiac glucose utilization in mice with mutated alpha- and beta-

- thyroid hormone receptors. *Am J Physiol Endocrinol Metab*, **287**(6): E1149-1153.
- Fabiato A (1983). Calcium-induced release of calcium from the cardiac sarcoplasmic reticulum. *Am J Physiol*, **245**, C1-14.
- Faerman I, Faccio E, Milei J, Nunez R, Jadzinsky M, Fox D, and Rapaport M (1977). Autonomic neuropathy and painless myocardial infarction in diabetic patients. Histologic evidence of their relationship. *Diabetes***26**, 1147-1158.
- Falcao-Pires, I., Goncalves, N., Moura, C. et al. (2009). Effects of diabetes mellitus, pressure-overload and their association on myocardial structure and function. *Am J Hypertens*, **22**:1190-1198
- Fan, G.C., Chu, G., and Kranias, E.G. (2005). Hsp20 and its cardioprotection. *Trends Cardiovasc Med*, **15**: 138–141.
- Fan, G.C., Yuan, Q., Song, G., Wang, Y., Chen, G., Qian, J., Zhou, X., Lee, Y.J., Ashraf, M., and Kranias, E.G. (2006). Small heat-shock protein Hsp20 attenuates β -agonist-mediated cardiac remodeling through apoptosis signal-regulating kinase 1. *Circ Res*, **99**: 1233–1242.
- Fan, W.J., Genade, S., Genis, A., Huisamen, B., and Lochner, A. (2009). Dexamethasone-induced cardioprotection: a role for the phosphatase MKP-1? *Life Sci*, **84**: 838–846.
- Fang, Z.Y., Prins, J.B. and Marwick, T.H.(2004). Diabetic cardiomyopathy: evidence, mechanisms, and therapeutic implications. *Endocr Rev*, **25**:543-567
- Fedak, P.W., Verma, S., Weisel, R.D. and Li, R.K. (2005). Cardiac remodelling and failure: from molecules to man (Part I). *Cardiovasc Path*, **14**(1): 1-11.
- Fedak, P.W., Verma, S., Weisel, R.D. and Li, R.K. (2005). Cardiac remodelling and failure: from molecules to man (Part II). *Cardiovasc Path*, **14**(2): 49-60.
- Fedak, P.W., Verma, S., Weisel, R.D., Skrtic, M., and Li, R.K. (2005). Cardiac remodelling and failure: from molecules to man (Part III). *Cardiovasc Path*, **14**(3): 109-119.
- Ferrandi, C., Ballerio, R., Gaillard, P., Carboni, S., Vitte, P., Gotteland, J., and Cirillo, R. (2004). Inhibition of c-Jun N-terminal kinase decreases cardiomyocyte apoptosis and infarct size after myocardial ischemia and reperfusion in anaesthetized rats. *Br J Pharmacol*, **142**:953–960.
- Fiedler, B., Feil, R., Hofmann, F., Willenbockel, C., Drexler, H., Smolenski, A., Lohmann, S.M., and Wollert, K.C. (2006). cGMP-dependent protein kinase type I inhibits TAB1-p38 mitogen-activated protein kinase apoptosis signaling

in cardiac myocytes. *J Biol Chem*, **281**:32831–32840.

- Fischer, T.A., Ludwig, S., Flory, E., Gambaryan, S., Singh, K., Finn, P., and Pfeffer, M.A., Kelly, R.A., Pfeffer, J.M. (2001). Activation of cardiac c-JunNH2-terminal kinases and p38-mitogen-activated protein kinases with abrupt changes in hemodynamic load. *Hypertension*, **37**: 1222–1228.
- Flamant, F., and Samarut, J. (2003). Thyroid hormone receptors: lessons from knockout and knock-in mutant mice. *Trends Endocrinol Metab*, **14**(2): 85-90.
- Flesch, M., Margulies, K.B., Mochmann, H.C., Engel, D., Sivasubramanian, N., and Mann, D.L. (2001). Differential regulation of mitogen-activated protein kinases in the failing human heart in response to mechanical unloading. *Circulation*, **104**: 2273–2276.
- Fliegel, L. (2008). Molecular biology of the myocardial Na₂/H₂ exchanger. *J Mol Cell Cardiol*, **44**: 228–237.
- Fliegel, L. (2009). Regulation of the Na₂/H₂ exchanger in the healthy and diseased myocardium. *Expert Opin Ther Targets*, **13**: 55–68.
- Force, T. and Kerkela, R. (2008). Cardiotoxicity of the new cancer therapeutics—mechanisms of and approaches to the problem. *Drug Discov Today*, **17–18**: 778–784.
- Forini, F., Lionetti, V., Ardehali, H., Pucci, A., Cecchetti, F., Ghanefar, M., et al. (2010). Early long-term L-T3 replacement rescues mitochondria and prevents ischemic cardiac remodeling in rats. *J Cell Mol Med*, DOI:10.1111/j.1582-4934.2010.01014.
- Frantz, S., Berh, T., Hu, K., Fraccarollo, D., Strotmann, J., Goldberg, E., Ertl, G., Angermann, C., and Bauersachs, J. (2007). Role of p38 mitogen activated protein kinase in cardiac remodeling. *Br J Pharmacol*, **150**: 130–135.
- Frey, N., and Olson, E.N. (2003). Cardiac hypertrophy: the good, the bad, and the ugly. *Annu Rev Physiol*, **65**: 45–79.
- Friberg, L., Werner, S., Eggertsen, G., and Ahnve, S. (2002). Rapid down-regulation of thyroid hormones in acute myocardial infarction: is it cardioprotective in patients with angina? *Arch Intern Med*, **162**(12): 1388-1394.
- Fryer, L.G., Holness, M.J., Decock, J.B., and Sugden, M.C. (1998). Cardiac protein kinase C expression in two models of cardiac hypertrophy associated with an activated cardiac reninangiotensin system: effects of experimental hyperthyroidism and genetic hypertension (the mRen-2 rat). *J Endocrinol*, **158**:27–33.
- Fryer, R.M., Patel, H.H., Hsu, A.K., and Gross, G.J. (2001). Stress-activated protein kinase phosphorylation during cardioprotection in the ischemic myocardium.

Am J Physiol Heart Circ Physiol, **281**: H1184–H1192.

- Furlow, J. D., and Neff, E. S. (2006). A developmental switch induced by thyroid hormone: *Xenopus laevis* metamorphosis. *Trends Endocrinol Metab*, **17**(2): 40-47.
- Furlow, J. D., Yang, H. Y., Hsu, M., Lim, W., Ermio, D. J., and Chiellini, G., et al. (2004). Induction of larval tissue resorption in *Xenopus laevis* tadpoles by the thyroid hormone receptor agonist GC-1. *J Biol Chem*, **279**(25): 26555-26562.
- Ganda OP, Rossini AA, and Like AA (1976). Studies on streptozotocin diabetes. *Diabetes* **25**, 595-603.
- Garvey, W.T., Hardin, D., and Juhaszova, M. et al. (1993). Effects of diabetes on myocardial glucose transport system in rats: implications for diabetic cardiomyopathy. *Am J Physiol*, **264**:H837-844
- Ge, B., Gram, H., Di Padova, F., Huang, B., New, L., Ulevitch, R.J., and Luo Y, J.H.(2002). MAPKK-independent activation of p38alpha mediated by TAB1-dependent autophosphorylation of p38alpha. *Science*, **295**:1291–1294.
- Gerdes, A. M., and Iervasi, G. (2010). Thyroid replacement therapy and heart failure. *Circulation*, **122**(4): 385-393.
- Gerits, N., Kostenko, S. and Moens, U. (2007). In vivo functions of mitogenactivatedprotein kinases: conclusions from knock-in and knockout mice. *Transgenic Res*, **16**: 281–314.
- Giannuzzi, P., Temporelli, P.L., Corra, U., Gattone, M., Giordano, A., and Tavazzi, L. (1997). Attenuation of unfavorable remodeling by exercise training in postinfarction patients with left ventricular dysfunction: results of the Exercise in Left Ventricular Dysfunction (ELVD) trial. *Circulation*, **96**:1790–1797.
- Gloss, B., Trost, S., Bluhm, W., Swanson, E., Clark, R., and Winkfein, R., et al. (2001). Cardiac ion channel expression and contractile function in mice with deletion of thyroid hormone receptor alpha or beta. *Endocrinology*, **142** (2): 544-550.
- Golden KL, Ren J, O'Connor J, Dean A, DiCarlo SE, and Marsh JD (2001). In vivo regulation of Na/Ca exchanger expression by adrenergic effectors. *Am J Physiol Heart Circ Physiol* **280**, H1376-H1382.
- Goldenberg S, Alex M, and Blumenthal HT (1958). Sequelae of arteriosclerosis of the aorta and coronary arteries; a statistical study in diabetes mellitus. *Diabetes* **7**, 98-108.
- Goldsmith, Z.G, and Dhanasekaran, D.N. (2007) G Protein regulation of

MAPK networks. *Oncogene* **26**: 3122–3142.

- Goldspink, P.H., Montgomery, D.E., Walker, L.A., Urboniene, D., McKinney, R.D., and Geenen, D.L., et al. (2004). Protein kinase Cepsilon overexpression alters myofilament properties and composition during the progression of heart failure. *Circ Res*, **95**: 424–432.
- Gorin, M.A. and Pan, Q. (2009). Protein kinase C epsilon: an oncogene and emerging tumor biomarker. *Mol Cancer*, **8**:9.
- Gorog, D.A., Jabr, R., Tanno, M., Sarafraz, N., Clark, J.E., Fisher, S., Cao, X.B., Bellahcene, M., Dighe, K., Kabir, A.M.N, Quinlan, R.A., Kato, K., Gaestel, M., and Marber, M.S. (2009). MAPKAPK-2 modulates p38-MAPK localization and small heat shock protein phosphorylation but does not mediate the injury associated with p38-MAPK activation during myocardial ischemia. *Cell Stress Chaperones*, **14**: 477–489.
- Gosselin, H., Beliveau, L., Burelle, Y., Clement, R., Lajoie, C., and El-Helou, V. et al. (2006). Disparate regulation of signaling proteins after exercise and myocardial infarction. *Med Sci Sports Exerc*, **38**:455-462.
- Graham, H.K. and Trafford, A.W. (2007). Spatial disruption and enhanced degradation of collagen with transition from compensated ventricular hypertrophy to symptomatic congestive heart failure. *Amer J Physiol Heart Circ Physiol*, **292** (3): 1364-1372.
- Gu, X. and Bishop, S.P. (1994). Increased protein kinase C and isozyme redistribution in pressure-overload cardiac hypertrophy in the rat. *Circ Res*, **75**: 926–931.
- Gudernatsch, J. (1912). Feeding experiments on tadpoles: The influence of specific organs given as food on growth and differentiation. A contribution to the knowledge of organs with internal secretion. *Wilhelm Roux Arch Entwicklungsmech Organismen*, **35**: 457-483.
- Gupta S, Prahash AJ, and Anand IS (2000). Myocyte contractile function is intact in the post-infarct remodeled rat heart despite molecular alterations. *Cardiovasc Res* **48**, 77-88.
- Gysembergh, A., Simkhovich, B., Kloner, R., and Przyklenk, K. (2001). p38MAPK activity is not increased early during sustained coronary artery occlusion in preconditioned versus control rabbit heart. *J Mol Cell Cardiol*, **33**: 681–690.
- Hagiwara, Y., Miyoshi S., Fukuda, K., Nishiyama, N., Ikegami, Y., Tanimoto, K., Murata, M., Takahashi, E., Shimoda, K., Hirano, T., Mitamura, H., and Ogawa, S. (2007). SHP2-mediated signaling cascade through gp130 is essential for LIF-dependent [Ca^L], [Ca²⁺]_i transient, APD increase in cardiomyocytes. *J Mol*

Cell Cardiol, **43**: 710–716.

- Hahn, H.S. , Marreez, Y., Odley, A., Sterbling, A., Yussman, M.G. and Hilty, K.C. , et al. (2003). Protein kinase Calpha negatively regulates systolic and diastolic function in pathological hypertrophy. *Circ Res*, **93**: 1111–1119.
- Hall-Jackson, C., Goedert, M., Hedge, P., and Cohen, P.(1999). Effects of SB203580 on the activity of c-Raf in vitro and in vivo. *Oncogene*, **18**:2047–2054.
- Hambleton, M., Hahn, H., Pleger, S.T., Kuhn, M.C., Klevitsky R. and Carr, A.N. , et al. (2006). Pharmacological- and gene therapy-based inhibition of protein kinase Calpha/beta enhances cardiac contractility and attenuates heart failure. *Circulation*, **114**: 574–582.
- Han, J., Lee, J., Bibbs, L., Ulevitch, R. (1994). A MAP kinase targeted by endotoxin and hyperosmolarity in mammalian cells. *Science*, **265**:808–811.
- Han, J., Lee, J., Tobias, P., and Ulevitch, R. (1993). Endotoxin induces rapid protein tyrosine phosphorylation in 70Z/3 cells expressing CD14. *J Biol Chem*, **268**: 25009–25014.
- Harris, I.S., Zhang, S., Treskov, I., Kovacs, A., Weinheimer, C., and Muslin, A.J. (2004). Raf-1 kinase is required for cardiac hypertrophy and cardiomyocyte survival in response to pressure overload. *Circulation*, **110**: 718–723.
- Hatano, N., Mori, Y., Oh-hora, M., Kosugi, A., Fujikawa, T., Nakai, N., Niwa, H., Miyazaki, J., Hamaoka, T., and Ogata, M. (2003). Essential role for ERK2 mitogen-activated protein kinase in placental development. *Genes Cells*, **8**: 847–856.
- Hattori, Y., Matsuda, N., and Kimura, J., et al. (2000). Diminished function and expression of the cardiac Na⁺ - Ca²⁺ exchanger in diabetic rats: implication in Ca²⁺ overload. *J Physiol*, **527**: 85–94.
- Hausenloy, D., and Yellon, D.(2007). Reperfusion injury salvage kinase signalling: taking a RISK for cardioprotection. *Heart Fail Rev*, **12**: 217–234.
- Hausenloy, D.J., Tsang, A., and Yellon, D.M. (2005). The reperfusion injury salvage kinase pathway: a common target for both ischemic preconditioning and postconditioning. *Trends Cardiovasc Med*, **15**:69–75.
- Hayashi H and Noda N (1997). Cytosolic Ca²⁺ concentration decreases in diabetic rat myocytes. *Cardiovasc Res* **34**, 99-103.
- Hayashi, M. and Lee, J. (2004). Role of the BMK/ERK5 signaling pathway: lessons from knockout mice. *J Mol Med*, **82**: 800–808.
- Hayashi, M., Kim, S., Imanaka-Yoshida, K., Yoshida, T., Abel, E., Eliceiri, B.,

Yang Y, R.J.U, and Lee, J. (2004). Targeted deletion of BMK1/ERK5 in adult mice perturbs vascular integrity and leads to endothelial failure. *J Clin Invest*, **113**: 1138–1148.

Heart disease and stroke statistics: 2008 update. 2008. American Heart Association.

Held PH, Yusuf S, and Furberg CD (1989). Calcium channel blockers in acute myocardial infarction and unstable angina: an overview. *BMJ* **299**, 1187-1192.

Henderson, K. K., Danzi, S., Paul, J. T., Leya, G., Klein, I., and Samarel, A. M. (2009). Physiological replacement of T3 improves left ventricular function in an animal model of myocardial infarction-induced congestive heart failure. *Circ Heart Fail*, **2**(3): 243-252.

Hennemann G (2005). Notes on the history of cellular uptake and deiodination of thyroid hormone. *Thyroid* **15**, 753-756.

Herdrich, B. J., Danzer, E., Davey, M. G., Allukian, M., Englefield, V., Gorman, J. H., 3rd, et al. (2011). Regenerative healing following foetal myocardial infarction. *Eur J Cardiothorac Surg*, **38**(6): 691-698.

Herlitz J, Malmberg K, Karlson BW, Ryden L, and Hjalmarson A (1988). Mortality and morbidity during a five-year follow-up of diabetics with myocardial infarction. *Acta Med Scand* **224**, 31-38.

Hibi, M., Lin, A., Smeal, T., Minden, A., and Karin, M. (1993). Identification of an oncoprotein- and UV-responsive protein kinase that binds and potentiates the c-Jun activation domain. *Genes Dev*, **7**: 2135–2148.

Hidalgo, C., Hudson, B., Bogomolovas, J., Zhu, Y., Anderson, B. and Greaser, M., et al. (2009). PKC phosphorylation of titin's PEVK element: a novel and conserved pathway for modulating myocardial stiffness. *Circ Res*, **105**: 631–638.

Hilfiker-Kleiner, D., Hilfiker, A., Castellazzi, M., and Wollert, K.C. et al. (2006). JunD attenuate phenylephrine-mediated cardiomyocyte hypertrophy by negatively regulating AP-1 transcriptional activity. *Card Res*, **71**(1): 108-117.

Hilfiker-Kleiner, D., Hilfiker, A., Kaminski, K., Schaefer, A., Park, J.K., Michel, K., Quint, A., Yaniv, M., Weitzman, J.B., and Drexler, H. (2005). Lack of JunD promotes pressure overload-induced apoptosis, hypertrophic growth, and angiogenesis in the heart. *Circulation*, **112**: 1470–1477.

Ho, P.D., Fan, J.S., Hayes, N.L., Saada, N., Palade, P.T., Glembotski, C.C., and McDonough, P.M. (2001). Ras reduces L-type calcium channel current in cardiac myocytes: corrective effects of L-channels and SERCA2 on $[Ca^{2+}]_i$ regulation and cell morphology. *Circ Res*, **88**: 63–69

Ho, P.D., Zechner, D., He, H., Dillmann, W., Glembotski, C., and Mc-Donough,

- P.M. (1998). The Raf-MEK-ERK cascade represents a common pathway for alteration of intracellular calcium by Ras and protein kinase C in cardiac myocytes. *J Biol Chem*, **273**: 21730–21735.
- Holland, F. W., 2nd, Brown, P. S., Jr., Weintraub, B. D., and Clark, R. E. (1991). Cardiopulmonary bypass and thyroid function: a "euthyroid sick syndrome". *Ann Thorac Surg*, **52**(1): 46-50.
- Hollander J, Martin J, Belke D, Scott B, Swanson E, Krishnamoorthy V, and Dillmann W. (2004) Overexpression of wild-type heatshock protein 27 and a nonphosphorylatable heat shock protein 27 mutant protects against ischemia/reperfusion injury in a transgenic mouse model. *Circulation* **110**: 3544–3552,
- Hori, M., and Nishida, K. (2009). Oxidative stress and left ventricular remodeling after myocardial infarction. *Cardiovasc Res*, **81**: 457–464.
- Houser SR and Margulies KB (2003). Is depressed myocyte contractility centrally involved in heart failure? *Circ Res* **92**, 350-358.
- Howarth, F.C. and Singh, J. (1999). Altered handling of calcium during the process of excitation contraction coupling in streptozotocin-induced diabetic heart. A mini review. *Int. J. Diabetes* **7**, 52-64.
- Howarth, F.C., Qureshi, M.A. and White, E., (2002). Effects of hyperosmotic shrinkage on ventricular myocyte shortening and intracellular Ca^{2+} in streptozotocin-induced diabetic rats. *Pflügers Arch*. **444**: 446–451.
- Hreniuk, D., Garay, M., Gaarde, W., Monia, B.P., McKay, R.A., and Cioffi, C.L. (2001). Inhibition of c-Jun N-terminal kinase 1, but not c-Jun N-terminal kinase 2, suppresses apoptosis induced by ischemia/reoxygenation in rat cardiac myocytes. *Mol Pharmacol*, **59**: 867–874.
- Huang, L., Wolska, B.M., Montgomery, D.E., Burkart, E.M., Buttrick, P.M. and Solaro, R.J.. (2001). Increased contractility and altered Ca^{2+} transients of mouse heart myocytes conditionally expressing PKC β . *Am J Physiol Cell Physiol*, **280**: C1114–C1120.
- Huang, W.Y., Aramburu, J., Douglas, P.S., and Izumo, S. (2000). Transgenic expression of green fluorescence protein can cause dilated cardiomyopathy. *Nat Med*, **6**: 482–483.
- Huang, X. and Walker, J.W. (2004). Myofilament anchoring of protein kinase C- ϵ in cardiac myocytes. *J Cell Sci*, **117**: 1971–1978.
- Huang, Y., Wright, C.D., Kobayashi, S., Healy, C.L., Elgethun, M., Cypher, A., Liang, Q., and O'Connell, T.D. (2008). GATA4 is a survival factor in adult cardiac myocytes but is not required for β_1 -adrenergic receptor survival

signaling. *Am J Physiol Heart Circ Physiol*, **295**:H699–H707.

- Huang, Y., Wright, C.D., Merkwani, C.L., Baye, N.L., Liang, Q., Simpson, P.C., and O'Connell, T.D. (2007). An α_1 -adrenergic-extracellular signal regulated kinase survival signaling pathway in cardiac myocytes. *Circulation*, **115**: 763–772.
- Huebert, R.C., Li, Q., Adhikari, N., Charles, N.J., Han, X., Ezzat, M.K., Grindle, S., Park, S., Ormaza, S., Fermin, D., Miller, L.W., and Hall, J.L. (2004). Identification and regulation of Sprouty1, a negative inhibitor of the ERK cascade, in the human heart. *Physiol Genomics*. **18**: 284–289.
- Hunter, J., Tanaka, N., Rockman, H., Ross, J. Jr, and Chien, K.R. (1995). Ventricular expression of a MLC-2v-ras fusion gene induces cardiac hypertrophy and selective diastolic dysfunction in transgenic mice. *J Biol Chem*, **270**: 23173–23178.
- Hutchinson, K.R., Stewart, J.A Jr and Lucchesi, P.A. (2010). Extracellular matrix remodelling during the progression of volume overload-induced heart failure. *J Molec. Cell Card*, **48**(3): 564-569.
- Ichiki, T. (2010). Thyroid hormone and atherosclerosis. *Vascul Pharmacol*, **52**(3-4): 151-156.
- Iervasi, G., Pingitore, A., Landi, P., Raciti, M., Ripoli, A., and Scarlattini, M., et al. (2003). Low-T3 syndrome: a strong prognostic predictor of death in patients with heart disease. *Circulation*, **107**(5): 708-713.
- Irukayama-Tomobe, Y., Miyauchi, T., Sakai, S., Kasuya, Y., Ogata, T., Takanashi, M., Iemitsu, M., Sudo, T., Goto, K., and Yamaguchi, I. (2004). Endothelin-1-induced cardiac hypertrophy is inhibited by activation of peroxisome proliferator-activated receptor- α partly via blockade of c-Jun NH₂-terminal kinase pathway. *Circulation*, **109**:904–910.
- Izumiya, Y., Kim, S., Izumi, Y., Yoshida, K., Yoshiyama, M., Matsuzawa, A., Ichijo, H., and Iwao, H. (2003). Apoptosis signal-regulating kinase 1 plays a pivotal role in angiotensin II-induced cardiac hypertrophy and remodeling. *Circ Res*, **93**: 874–883.
- Izumiya, Y., Shiojima, I., Sato, K., Sawyer, D.B., Colucci, W.S., and Walsh, K. (2006). Vascular endothelial growth factor blockade promotes the transition from compensatory cardiac hypertrophy to failure in response to pressure overload. *Hypertension*, **47**:887–893.
- Jalili, T., Takeishi, Y., Song, G, Ball, N.A., Howles, G., and Walsh, R.A. (1999). PKC translocation without changes in α and β protein abundance in cardiac hypertrophy and failure. *Am J Physiol Heart Circ*

Physiol, **277**: H2298–H2304.

- Jaswal, J.S., Gandhi, M., Finegan, B.A., Dyck, J.R.B., and Clanachan, A.S. (2007). Inhibition of p38 MAPK and AMPK restores adenosine-induced cardioprotection in hearts stressed by antecedent ischemia by altering glucose utilization. *Am J Physiol Heart Circ Physiol*, **293**:H1107–H1114.
- Jaswal, J.S., Gandhi, M., Finegan, B.A., Dyck, J.R.B., and Clanachan, A.S. (2007). p38 mitogen-activated protein kinase mediates adenosine-induced alterations in myocardial glucose utilization via 5'-AMP-activated protein kinase. *Am J Physiol Heart Circ Physiol*, **292**: H1978–H1985.
- Jesmin, S., Hattori, Y., Maeda, S., Zaedi, S., Sakuma, I., and Miyauchi, T. (2006). Subdepressor dose of benidipine ameliorates diabetic cardiac remodeling accompanied by normalization of upregulated endothelin system in rats. *Am J Physiol Heart Circ Physiol*, **290**: H2146–H2154.
- Jetton, T.L., Lausier, J., LaRock, K., Trotman, W.E., Larmie, B., Habibovic, A., Peshavaria, M., and Leahy, J.L. (2005). Mechanisms of compensatory beta-cell growth in insulin-resistant rats: roles of Akt kinase. *Diabetes*, **54**:2294–2304.
- Jiang, Y., Chen, C., Li, Z., Guo, W., Gergner, J., Lin, S., and Han, J. (1996). Characterization of the structure and function of a new mitogen-activated protein kinase (p38b). *J Biol Chem*, **271**: 17920–17926.
- Jin, D., Takai, S., and Sugiyama, T. et al. (2009). Long-term angiotensin II blockade may improve not only hyperglycemia but also age-associated cardiac fibrosis. *J Pharmacol Sci*, **109**:275-284
- Jirousek, M.R., Gillig, J.R., Gonzalez, C.M, Heath, W.F., McDonald, J.H. and Neel, D.A. et al. (1996). (S)-13-[(dimethylamino)methyl]-10, 11, 14, 15-tetrahydro-4, 9:16, 21-dimetheno-1 H, 13 H-dibenzo[e, k]pyrrolo[3, 4-h][1, 4, 13]oxadiazacyclohexadecene-1, 3(2 H)-dione (LY333531) and related analogues: isozyme selective inhibitors of protein kinase C beta. *J Med Chem*, **39**: 2664–2671.
- Jopling, C., Sleep, E., Raya, M., Marti, M., Raya, A., and Belmonte, J. C. (2010). Zebrafish heart regeneration occurs by cardiomyocyte dedifferentiation and proliferation. *Nature*, **464**(7288): 606-609.
- Jorgensen AO, Shen AC, Daly P, and MacLennan DH (1982). Localization of Ca²⁺ + Mg²⁺ - ATPase of the sarcoplasmic reticulum in adult rat papillary muscle. *J Cell Biol***93**, 883-892.
- Juntilla, M., Li, S. and Westermarck, J.(2008). Phosphatase-mediated crosstalk between MAPK signaling pathways in the regulation of cell survival. *FASEB J*, **22**: 954–964.

- Kaestner, K.H., Flores-Riveros, J.R., and McLenithan, J.C. et al. (1991). Transcriptional repression of the mouse insulin-responsive glucose transporter (GLUT4) gene by cAMP. *Proc Natl Acad Sci U S A*, **88**:1933-1937
- Kai, H., Muraishi, A., Sugi, Y., Nishi, H., Seki, Y., Kuwahara, F., Kimura, A., Kato, H., and Imaizumi, T. (1998). Expression of proto-oncogenes and gene mutation of sarcomeric proteins in patients with hypertrophic cardiomyopathy. *Circ Res*, **83**: 594–601.
- Kainulainen, H., Breiner, M., and Schurmann, A. et al. (1994). In vivo glucose uptake and glucose transporter proteins GLUT1 and GLUT4 in heart and various types of skeletal muscle from streptozotocin-diabetic rats. *Biochim Biophys Acta*, **1225**:275-282
- Kaiser, R., Bueno, O., Lips, D., Doevendans, P., Jones, F., Kimball, T., and Molkentin, J. (2004). Targeted inhibition of p38 mitogen-activated protein kinase antagonizes cardiac injury and cell death following ischemia-reperfusion in vivo. *J Biol Chem*, **279**: 15524–15530.
- Kaiser, R.A., Liang, Q., Bueno, O., Huang, Y., Lackey, T., Klevitsky, R., Hewett, T.E., and Molkentin, J.D. (2005). Genetic inhibition or activation of JNK1/2 protects the myocardium from ischemia-reperfusion-induced cell death in vivo. *J Biol Chem*, **280**: 32602–32608.
- Kalofoutis, C., Mourouzis, I., Galanopoulos, G., Dimopoulos, A., Perimenis, P., and Spanou, D., et al. (2010). Thyroid hormone can favorably remodel the diabetic myocardium after acute myocardial infarction. *Mol Cell Biochem*, **345**(1-2): 161-169.
- Kamakura, S., Moriguchi, T. and Nishida, E. (1999). Activation of the protein kinase ERK5/BMK1 by receptor tyrosine kinases. Identification and characterization of a signaling pathway to the nucleus. *J Biol Chem*, **274**: 26563–26571.
- Kang N, Alexander G, Park JK, Maasch C, Buchwalow I, Luft FC, and Haller H (1999). Differential expression of protein kinase C isoforms in streptozotocin-induced diabetic rats. *Kidney Int* **56**, 1737-1750.
- Kaptein, E. M., Sanchez, A., Beale, E., and Chan, L. S. (2010). Clinical review: Thyroid hormone therapy for postoperative nonthyroidal illnesses: a systematic review and synthesis. *J Clin Endocrinol Metab*, **95**(10): 4526-4534.
- Kasler, H., Victoria, J., Duramad, O., and Winoto, A. (2000). ERK5 is a novel type of mitogen-activated protein kinase containing a transcriptional activation domain. *Mol Cell Biol*, **20**: 8382–8389.
- Katz, M., Amit, I., and Yarden, Y. (2007). Regulation of MAPKs by growth factors and receptor tyrosine kinases. *Biochim Biophys Acta*, **1773**:1161–1176.

- Kemi, O.J., Ceci, M., Wisloff, U., Grimaldi, S., Gallo, P., Smith, G.L., Condorelli, and G., Ellingsen, O. (2008). Activation or inactivation of cardiac Akt/mTOR signaling diverges physiologically from pathological hypertrophy. *J Cell Physiol*, **214**:316–321.
- Kennedy, R.A., Kemp, T.J., Sugden, P.H., and Clerk, A. (2006). Using U0126 to dissect the role of the extracellular signal-regulated kinase 1/2 (ERK1/2) cascade in the regulation of gene expression by endothelin-1 in cardiac myocytes. *J Mol Cell Cardiol*, **41**: 236–247.
- Kerkela, R., Grazette, L., Yacobi, R., Iliescu, C., Beahm, C., Walters, B., Shevtsov, S., Pesant, S., Clubb, F., Rosenzweig, A., Salomon, R., Van Etten, R.A., Alroy, J., Durand, J., and Force, T. (2006). Cardiotoxicity of the cancer therapeutic agent imatinib mesylate. *Nat Med*, **12**. (8):908-916
- Kim, H., Wang, X., Zhang, J., Suh, G., Benjamin, I., Ryter, S., and Choi, A. (2005). Heat shock protein-70 mediates the cytoprotective effect of carbon monoxide: involvement of p38 beta MAPK and heat shock factor 1. *J Immunol*, **175**: 2622–2629.
- Kim, J., Pedram, A., Razandi, M., and Leven, E. (2006). Estrogen prevents cardiomyocyte apoptosis through inhibition of reactive oxygen species and differential regulation of p38 kinase isoforms. *J Biol Chem*, **281**: 6760–6767.
- Kim, S.J., Abdellatif, M., Koul, S., and Crystal, G.J. (2008). Chronic treatment with insulin-like growth factor I enhances myocyte contraction by upregulation of Akt-SERCA2 signaling pathway. *Am J Physiol Heart Circ Physiol*, **295**:H130–H135.
- Kimura, T., Kanda, T., Kotajima, N., Kuwabara, A., Fukumura, Y., and Kobayashi, I. (2000). Involvement of circulating interleukin-6 and its receptor in the development of euthyroid sick syndrome in patients with acute myocardial infarction. *Eur J Endocrinol*, **143**(2): 179-184.
- King H, Aubert RE, & Herman WH (1998). Global burden of diabetes, 1995-2025: prevalence, numerical estimates, and projections. *Diabetes Care* **21**, 1414-1431.
- King, E. S. (1940). Regeneration in Cardiac Muscle. *Br Heart J*, **2** (3): 155-164.
- Kinugawa, K., Jeong, M. Y., Bristow, M. R., and Long, C. S. (2005). Thyroid hormone induces cardiac myocyte hypertrophy in a thyroid hormone receptor alpha1-specific manner that requires TAK1 and p38 mitogen-activated protein kinase. *Mol Endocrinol*, **19**(6): 1618-1628.
- Kinugawa, K., Jeong, M.Y., Bristow, M.R. and Long, C.S. (2005). Thyroid hormone induces cardiac myocyte hypertrophy in a thyroid hormone receptor

- _1-specific manner that requires TAK1 and p38 mitogenactivatedprotein kinase. *Mol Endocrinol*, **19**: 1618–1628.
- Kinugawa, K., Yonekura, K., Ribeiro, R. C., Eto, Y., Aoyagi, T., and Baxter, J. D., et al. (2001). Regulation of thyroid hormone receptor isoforms in physiological and pathological cardiac hypertrophy. *Circ Res*, **89** (7): 591-598.
- Kitamura, T., Asai, N., Enomoto, A., Maeda, K., Kato, T., Ishida, M., Jiang, P., Watanabe, T., Usukura, J., Kondo, T., Costantini, F., Murohara, T., and Takahashi, M. (2008). Regulation of VEGF-mediated angiogenesis by the Akt/PKB substrate Girdin. *Nat Cell Biol*, **10**:329–337.
- Kumar, P. and Clark, M (2002). Diabetes mellitus and other disorders of metabolism. In: *Clinical Medicine* (5th Edition), Pub:W.B. Saunders, London, pp 1069-112.
- Klauck ,T.M., Faux, M.C., Labudda, K., Langeberg, L.K., Jaken, S., and Scott, J.D. 1996. Coordination of three signaling enzymes by AKAP79, a mammalian scaffold protein. *Science*, **271**:1589–1592
- Klein, G., Schaefer, A., Hilfiker-Kleiner, D., Oppermann, D., Shukla, P., Quint, A., Podewski, E., Hilfiker, A., Schroder, F., Leitges, M., and Drexler, H. (2005). Increased collagen deposition and diastolic dysfunction but preserved myocardial hypertrophy after pressure overload in mice lacking PKC ϵ . *Circ Res*, **96**: 748–755.
- Knight, R.J. and Buxton, D.B. (1996). Stimulation of c-Jun kinase and mitogenactivatedprotein kinase by ischemia and reperfusion in the perfused rat heart. *Biochem Biophys Res Commun*, **218**: 83–88.
- Kobayashi, S., Lackey, T., Huang, Y., Bisping, E., Pu, W.T., and Boxer, L.M. (2006). Transcription factor GATA4 regulates cardiac BCL2 gene expression in vitro and in vivo. *FASEB J* **20**: 800–802.
- Koch, W.J. (2004). Genetic and phenotypic targeting of beta-adrenergic signaling in heart failure. *Mol Cell Biochem*, **263**: 5–9.
- Koide, Y., Tamura, K., Suzuki, A., Kitamura, K., Yokoyama, K., and Hashimoto, T., et al. (2003). Differential induction of protein kinase C isoforms at the cardiac hypertrophy stage and congestive heart failure stage in Dahl salt-sensitive rats. *Hypertens Res*, **26**:421–426.
- Koitabashi, N., Bedja, D., Zaiman, A.L., Pinto, Y.M., Zhang, M., Gabrielson K.L., Takimoto, E., and Kass, D.A. (2009). Avoidance of transient cardiomyopathy in cardiomyocyte-targeted tamoxifen-induced Mer-CreMer gene deletion models. *Circ Res*, **105**: 12–15.
- Kompa, A.R., See, F., Lewis, D.A., Adrahtas, A., Cantwell, D.M., Wang, B.H., and Krum, H. (2008). Long-term but not short-term p38 mitogen-activated protein

kinase inhibition improves cardiac function and reduces cardiac remodeling post-myocardial infarction. *J Pharmacol Exp Ther*, **325**: 741–750.

Kong, L., Andrassy, M., Chang, J.S., Huang, C., Asai, T., Szabolcs, M.J., Homma, S., Liu, R., Zou, Y.S., Leitges, M., Yan, S.D., Ramasamy, R., Schmidt, A.M., and Yan, S.F. (2008). PKC ϵ modulates ischemia-reperfusion injury in the heart. *Am J Physiol Heart Circ Physiol*, **294**: H1862–H1870.

Konhilas, J.P., Maass, A.H., Luckey, S.W., Stauffer, B.L., Olson, E.N., and Leinwand, L.A. (2004). Sex modifies exercise and cardiac adaptation in mice. *Am J Physiol Heart Circ Physiol*, **287**: H2768–H2776.

Konopatskaya, O., Gilio, K., Harper, M.T., Zhao, Y., Cosemans, J.M., and Karim, Z.A., et al. (2009). PKC α regulates platelet granule secretion and thrombus formation in mice. *J Clin Invest*, **119**: 399–407.

Kontaridis, M.I., Yang, W., Bence, K.K., Cullen, D., Wang, B., Bodyak, N., Ke, Q., Hinek, A., Kang, P.M., Liao, R., and Neel, B.G. (2008). Deletion of Ptpn11 (Shp2) in cardiomyocytes causes dilated cardiomyopathy via effects on the extracellular signal-regulated kinase/mitogen-activated protein kinase and RhoA signaling pathways. *Circulation*, **117**: 1423–1435.

Kooij, V., Boontje, N., Zaremba, R., Jaquet, K., dos Remedios, C., and Stienen, G.J., et al. (2010). Protein kinase C alpha and epsilon phosphorylation of troponin and myosin binding protein C reduce Ca²⁺ sensitivity in human myocardium. *Basic Res Cardiol*, **105**: 289–300.

Kovacs, K., Hanto, K., Bogнар, Z., Tapodi, A., Bogнар, E., Kiss, G., Szabo, A., Rappai, G., Kiss, T., Sumegi, B., and Gallyas, F. (2009). Prevalent role of Akt and ERK activation in cardioprotective effect of Ca²⁺ channel- and beta-adrenergic receptor blockers. *Mol Cell Biochem*, **321**: 155–164.

Kress, E., Rezza, A., Nadjar, J., Samarut, J., and Plateroti, M. (2008). The thyroid hormone receptor-alpha (TR alpha) gene encoding TR alpha1 controls deoxyribonucleic acid damage-induced tissue repair. *Mol Endocrinol*, **22**(1): 47–55.

Krishnamurthy, P., Subramanian, V., Singh, M., and Singh, K. (2007). α_1 Integrins modulate α_1 -adrenergic receptor-stimulated cardiac myocyte apoptosis and myocardial remodeling. *Hypertension*, **49**: 865–872.

Kumphune, S., Bassi, R., Jacquet, S., Sicard, P., Clark, J.E., and Verma, S., et al. (2009). A chemical genetic approach reveals p38 alpha MAPK activation by diphosphorylation aggravates myocardial infarction and is prevented by the direct binding of SB203580. *J Biol Chem* **285**(5): 2968–2975.

Kuster, G., Pimentel, D., Adachi, T., Ido, Y., Brenner, D., Cohen, R., Liao, R., Siwik,

- D., and Colucci, W. (2005). Alpha-adrenergic receptor-stimulated hypertrophy in adult rat ventricular myocytes is mediated via thioredoxin-1-sensitive oxidative modification of thiols on Ras. *Circulation*, **111**: 1192–1198.
- Kuwahara, F., Kai, H., Tokuda, K., Kai, M., Takeshita, A., Egashira, K. and Imaizumi, T. (2002). Transforming growth factor- β function blocking prevents myocardial fibrosis and diastolic dysfunction in pressure-overloaded rats *Circulation*. **106**: 130-135
- Kyoi, S., Otani, H., Matsuhisa, S., Akita, Y., Tatsumi, K., Enoki, C., Fujiwara, H., Imamura, H., Kamihata, H., and Iwasaka, T. (2006). Opposing effect of p38 MAP kinase and JNK inhibitors on the development of heart failure in the cardiomyopathic hamster. *Cardiovasc Res*, **69**:888–898.
- Kyriakis, J., and Avruch, J. (1990). pp54 microtubule-associated protein 2 kinase. A novel serine/threonine protein kinase regulated by phosphorylation and stimulated by poly-L-lysine. *J Biol Chem*, **265**:17355–17363.
- Kyriakis, J., Brautigan, D., Ingebritsen, T., and Avruch, J. (1991). pp54 microtubule-associated protein-2 kinase requires both tyrosine and serine/threonine phosphorylation for activity. *J Biol Chem*, **266**:10043–10046.
- Kyriakis, J.M. and Avruch, J. (2001). Mammalian mitogen-activated protein kinase signal transduction pathways activated by stress and inflammation. *Physiol Rev*, **81**: 807–869.
- Laderoute, K.R., and Webster, K.A. (1997). Hypoxia/reoxygenation stimulates jun kinase activity through redox signaling in cardiac myocytes. *Circ Res*, **80**: 336–344.
- Lagadic-Gossmann D, Buckler KJ, Le PK, and Feuvray D (1996). Altered Ca²⁺ handling in ventricular myocytes isolated from diabetic rats. *Am J Physiol* **270**, H1529-H1537.
- Lali, F.V., Hunt, A.E., Turner, S.J., and Foxwell, B.M.J. (2000). The pyridinylimidazole inhibitor Sb203580 blocks phosphoinositide-dependent protein kinase activity, protein kinase B phosphorylation, retinoblastoma hyperphosphorylation in interleukin-2-stimulated T cells independently of p38 mitogen-activated protein kinase. *J Biol Chem*, **275**: 7395–7402.
- Landau, D., Chayat, C., Zucker, N., Golomb, E., Yagil, C., and Yagil, Y. et al. (2008). Early blood pressure-independent cardiac changes in diabetic rats. *J Endocrinol*, **197**:75-83.
- Lawler, S., Fleming, Y., Goedert, M., and Cohen, P. (1998). Synergistic activation of SAPK1/JNK1 by two MAP kinase kinases in vitro. *Curr Biol*, **8**: 1387–

- Leblanc N and Hume JR (1990). Sodium current-induced release of calcium from cardiac sarcoplasmic reticulum. *Science* **248**, 372-376.
- Lechner, C., Zahalaka, M., Giot, J., Moler, N., and Ullrich, A. (1996). ERK6, amitogen-activated protein kinase involved in C2C12 myoblast differentiation. *Proc Natl Acad Sci USA*, **93**: 4355–4359.
- Lee, J., Laydon, J., McDonnell, P., Gallagher, T., Kumar, S., Green, D., McNulty, D., Blumenthal, M., Keys, J., Landvatter, S., Strickler, J., McLaughlin, M., Siemens, I., Fisher, S., Livi, G., White, J., Adams, J., and Young, P. (1994). A protein kinase involved in the regulation of inflammatory cytokine biosynthesis. *Nature*, **372**: 739–746.
- Lee, J.D., Ulevitch, R.J., and Han, J.H. (1995). Primary structure of BMK1: a new mammalian MAP kinase. *Biochem Biophys Res Commun*, **213**:715–724.
- Levi AJ, Ferrier GR (1997) *Biophys J* **72(2)**:A161-Tu-Pos130 (Abstract)
- Li, G., Ali, I.S., and Currie, R.W. (2008). Insulin-induced myocardial protection in isolated ischemic rat hearts requires p38 MAPK phosphorylation of Hsp27. *Am J Physiol Heart Circ Physiol*, **294**: H74–H87.
- Li, J., Miler, E., Ninomiya-Tsuji, J., Russell, R., and Young, L. (2005). AMP-activated protein kinase activates p38 mitogen-activated protein kinase by increasing recruitment of p38 MAPK to TAB1 in the ischemic heart. *Circ Res*, **97**: 872–879.
- Li, M., Georgakopoulos, D., Lu, G., Hester, L., Kass, D., Hasday, J., and Wang, Y. (2005). p38 MAP kinase mediates inflammatory cytokine induction in cardiomyocytes and extracellular matrix remodeling in heart. *Circulation*, **111**: 2494–2502.
- Li, Z., Jiang, Y., Ulevitch, R., and Han, J. (1996). The primary structure of p38 γ : a new member of the p38 group of MAP kinase. *Biochem Biophys Res Commun*, **228**: 334–340.
- Liang, Q., Bueno, O., Wilkins, B.J., Kuan, C., Xia, Y., and Molkentin, J. (2003). c-Jun N-terminal kinases (JNK) antagonize cardiac growth through cross-talk with calcineurin-NFAT signaling. *EMBO J*, **22**: 5079–5089.
- Liang, Q., and Molkentin, J. (2003). Redefining the roles of p38 and JNK signaling in cardiac hypertrophy: dichotomy between cultured myocytes and animal models. *J Mol Cell Cardiol*, **35**: 1385–1394.

- Liang, Q., Wiese, R.J., Bueno, O.F., Dai, Y.S., Markham, B.E., and Molkenin, J.D. (2001). The transcription factor GATA4 is activated by extracellular signal-regulated kinase 1- and 2-mediated phosphorylation of serine 105 in cardiomyocytes. *Mol Cell Biol*, **21**: 7460–7469
- Liao, P., Georgakopoulos, D., Kovacs, A., Zheng, M., Lerner, D., Pu, H., Saffitz, J., Chien, K.R., Xiao, R., Kass, D., and Wang, Y. (2001). The in vivo role of p38 MAP kinases in cardiac remodeling and restrictive cardiomyopathy. *Proc Natl Acad Sci USA*, **98**: 12283–12288.
- Liao, P., Wang, S.Q., Wang, S., Zheng, M., Zheng, M., Zhang, S.J., Cheng, H., Wang, Y., and Xiao, R.P. (2002). p38 Mitogen-activated protein kinase mediates a negative inotropic effect in cardiac myocytes. *Circ Res*, **90**:190–196.
- Liedtke, A.J., DeMaison, L., and Eggleston, A.M. et al. (1988). Changes in substrate metabolism and effects of excess fatty acids in reperfused myocardium. *Circ Res*, **62**:535-542
- Lim, H., New, L., Han, J., and Molkenin, J. (2001). Calcineurin enhances MAPKphosphatase-1 expression and p38 MAPK inactivation in cardiac myocytes. *J Biol Chem*, **276**: 15913–15919.
- Lipp P and Niggli E (1994). Sodium current-induced calcium signals in isolated guinea-pig ventricular myocytes. *J Physiol* **474**, 439-446.
- Lipp P, Laine M, Tovey SC, Burrell KM, Berridge MJ, Li W, and Bootman MD (2000). Functional InsP3 receptors that may modulate excitation-contraction coupling in the heart. *Curr Biol* **10**, 939-942.
- Lips, D., Bueno, O., Wilkins, B.J., Purcell, N., Kaiser, R., Lorenz, J., Voisin, L., Saba-El-Leill, M., Meloche, S., Pouyssegur, J., Pages, G., De Windt, L.J., Doevendans, P., and Molkenin, J. (2004). MEK1-ERK2 signalling pathway protects myocardium from ischemic injury in vivo. *Circulation*, **109**: 1938–1941.
- Litwin SE, Li J, and Bridge JH (1998). Na-Ca exchange and the trigger for sarcoplasmic reticulum Ca release: studies in adult rabbit ventricular myocytes. *Biophys J* **75**, 359-371.
- Liu, J., Mao, W., Ding, B., and Liang, C.S. (2008). ERKs/p53 signal transduction pathway is involved in doxorubicin-induced apoptosis in H9c2 cells and cardiomyocytes. *Am J Physiol Heart Circ Physiol*, **295**: H1956–H1965.
- Liu, J., Sadoshima, J., Zhai, P., Hong, C., Yang, G., Chen, W., Yan, L., Wang, Y., Vatner, S.F., and Vatner, D.E. (2006). Pressure overload induces greater hypertrophy and mortality in female mice with p38_{MAPK} inhibition. *J Mol*

Cell Cardiol, **41**: 680–688.

- Liu, Q. , Chen, X. , Macdonnell, S.M., Kranias, E.G. , Lorenz, J.N., and Leitges, M. , et al. (2009). Protein kinase C{alpha}, but not PKC{beta} or PKC{gamma}, regulates contractility and heart failure susceptibility: implications for ruboxistaurin as a novel therapeutic approach. *Circ Res*, **105**: 194–200.
- Liu, W., Zi, M., Jin, J., Prehar, S., Oceandy, D., Kimura, T.E., Lei, M., Neyses, L., Weston, A.H., Cartwright, E.J., and Wang, X. (2009). Cardiac-specific deletion of Mkk4 reveals its role in pathological hypertrophic remodelling but not in physiological cardiac growth. *Circ Res*, **104**:905–914.
- Liu, Y.H., Wang, D., Rhaleb, N.E., Yang, X.P., Xu, J., Sankey, S.S., Rudolph, A.E., and Carretero, O.A. (2005). Inhibition of p38 mitogen-activated protein kinase protects the heart against cardiac remodeling in mice with heart failure resulting from myocardial infarction. *J Cardiac Failure*, **11**: 74–81.
- Lommi J, Koskinen P, Naveri H, Harkonen M, and Kupari M (1997). Heart failure ketosis. *J Intern Med* 242, 231-238.
- Longnus, S.L., Segalen, C., Giudicelli, J., Sajan, M.P., Farese, R.V., and Van Obberghen, E. (2005). Insulin signalling downstream of protein kinase B is potentiated by 5'AMP-activated protein kinase in rat hearts in vivo. *Diabetologia*, **48**:2591–2601.
- Lorenz, K., Schmitt, J.P., Schmitteckert, E.M., and Lohse, M.J. (2009). A new type of ERK1/2 autophosphorylation causes cardiac hypertrophy. *Nat Med*, **15**: 75–83.
- Lu, G., Kang, Y., Han, J., Herschman, H., Stefani, E., and Wang, Y. (2006). TAB-1 modulates intracellular localization of p38 MAP kinase and downstream signaling. *J Biol Chem*, **281**: 6087–6095.
- Lu, Y., Shioda, N., Han, F., Kamata, A., Shirasaki, Y., Qin, Z., and Fukunaga, K. (2009). DY-9760e inhibits endothelin-1-induced cardiomyocyte hypertrophy through inhibition of CaMKII and ERK activities. *Cardiovasc Ther*, **27**: 17–27.
- Lubbe WF, Podzuweit T, and Opie LH (1992). Potential arrhythmogenic role of cyclic adenosine monophosphate (AMP) and cytosolic calcium overload: implications for prophylactic effects of beta-blockers in myocardial infarction and proarrhythmic effects of phosphodiesterase inhibitors. *J Am Coll Cardiol* **19**, 1622-1633.
- Lymvaivos I, Mourouzis I, Cokkinos DV, Dimopoulos MA, Toumanidis ST, and Pantos C (2011). Thyroid hormone and recovery of cardiac function in patients with acute myocardial infarction: a strong association? *Eur J Endocrinol* **165**,

- Ma, X., Kumar, S., Gao, F., Louden, C., Lopez, B., Christopher, T., Wang, C., Lee, J., Feuerstein, G.Z., and Yue, T.L. (1999). Inhibition of p38 mitogen-activated protein kinase decreases cardiomyocyte apoptosis and improves cardiac function after myocardial ischemia and reperfusion. *Circulation*, **99**: 1685–1691.
- MacDonald MR, Petrie MC, Hawkins NM, Petrie JR, Fisher M, McKelvie R, Aguilar D, Krum H, and McMurray JJ (2008). Diabetes, left ventricular systolic dysfunction, and chronic heart failure. *Eur Heart J* **29**, 1224-1240.
- Mackay, K., and Mochly-Rosen, D. (1999). An inhibitor of p38 mitogen-activated protein kinase protects neonatal cardiac myocytes from ischemia. *J Biol Chem*, **274**: 6272–6279.
- Mackay, K., and Mochly-Rosen, D. (2001). Localization, anchoring, and functions of protein kinase C isozymes in the heart. *J Mol Cell Cardiol*, **33**:1301–7.
- Majumder, P.K., and Sellers, W.R. (2005). Akt-regulated pathways in prostate cancer. *Oncogene*, **24**:7465–7474.
- Malhotra, A. and Sanghi, V. (1997). Regulation of contractile proteins in diabetic heart. *Cardiovasc Res*, **34**:34-40
- Malhotra, R. , D'Souza, K.M. , Staron, M.L. , Birukov, K.G., Bodi, I. , and Akhter, S.A. (2010). G α (q)-mediated activation of GRK2 by mechanical stretch in cardiac myocytes: the role of protein kinase C. *J Biol Chem*, **285**:13748–13760.
- Mammucari, C., Milan, G., Romanello, V., Masiere, E., Rudolf, R., Del Piccolo, P., Burden, S.J., Di Lisi, R., Sandri, C., Zhao, J., Goldberg, A.L., Schiaffino, S. and Sandri, M. (2007). FoxO3 controls autophagy in skeletal muscle in vivo. *Cell Metab*, **6**:458–471.
- Mammucari, C., Schiaffino, S., and Sandri, M. (2008). Downstream of Akt: FoxO3 and mTOR in the regulation of autophagy in skeletal muscle. *Autophagy*, **4**:524–526.
- Mann, D.L., Bogaev, R., and Buckberg, G.D. (2010). Cardiac remodelling and myocardial recovery: lost in translation? *Eur J Heart Fail*, **12**:789–796.
- Mansen, A., Tiselius, C., Sand, P., Fauconnier, J., Westerblad, H., and Rydqvist, B., et al. (2011). Thyroid hormone receptor α can control action potential duration in mouse ventricular myocytes through the KCNE1 ion channel subunit. *Acta Physiol (Oxf)*, **198**(2): 133-142.

- Marais, E., Genade, S., Huisamin, B., Strijdom, J., Moolman, J., and Lochner, A. (2001). Activation of p38 MAPK induced by a multi-cycle ischaemic preconditioning protocol is associated with attenuated p38 MAPK activity during sustained ischaemia and reperfusion. *J Mol Cell Cardiol*, **33**: 769–778.
- Martin, J., Avkiran, M., Quinlan, R.A., Cohen, P., and Marber, M.S. (2001). Antiischemic effects of SB203580 are mediated through the inhibition of p38 mitogen-activated protein kinase: evidence from ectopic expression of an inhibition-resistant kinase. *Circ Res*, **89**: 750–752.
- Martin, J., Hickey, E., Weber, L., Dillmann, W.H., and Mestril, R. (1999). Influence of phosphorylation and oligomerization on the protective role of the small heat shock protein 27 in rat adult cardiomyocytes. *Gene Exp*, **7**: 349–355.
- Martin, J., Mestril, R., Hilal-Dandan, R., Brunton, L., and Dillmann, W. (1997). Small heat shock proteins and protection against ischemic injury in cardiac myocytes. *Circulation*, **96**: 4343–4348.
- Martin, J.H., Connelly, K.A., Boyle, A., Kompa, A., Zhang, Y., and Kelly, D. et al. (2009). Effect of Atorvastatin on Cardiac Remodelling and Mortality in Rats Following Hyperglycemia and Myocardial Infarction. *Int J Cardiol*. **242**: 60-81
- Matsui, T., Li, L., del Monte, F., Fukui, Y., Franke, T.F., Hajjar, R.J., and Rosenzweig, A. (1999). Adenoviral gene transfer of activated phosphatidylinositol 3'-kinase and Akt inhibits apoptosis of hypoxic cardiomyocytes in vitro. *Circulation*, **100**:2373–2379.
- Matsui, T., Nagoshi, T. and Rosenzweig, A. (2003). Akt and PI 3-kinase signaling in cardiomyocyte hypertrophy and survival. *Cell Cycle*, **2**:220–223.
- Matsui, T., Tao, J., del Monte, F., Lee, K.H., Li, L., Picard, M., Force, T.L., Franke, T.F., Hajjar, R.J., and Rosenzweig, A. (2001). Akt activation preserves cardiac function and prevents injury after transient cardiac ischemia in vivo. *Circulation*, **104**:330–335.
- Matsumoto-Ida, M., Takimoto, Y., Aoyama, T., Akao, M., Takeda, T., and Kita, T. (2006). Activation of TGF- β 1-TAK1-p38 MAPK pathway in spared cardiomyocytes is involved in left ventricular remodeling after myocardial infarction in rats. *Am J Physiol Heart Circ Physiol*, **290**:H709–H715.
- Matusaka, H., Kinugawa, S., and Ide, T. et al. (2006). Angiotensin II type 1 receptor blocker attenuates exacerbated left ventricular remodeling and failure in diabetes-associated myocardial infarction. *J Cardiovasc Pharmacol*, **48**:95-102
- Maulik, N., Yoshida, T., Zu, Y.L., Sato, M., Banerjee, A., and Das, D.K. (1998). Ischaemic preconditioning triggers tyrosine kinase signalling: a potential role

- for MAPKAP kinase 2. *Am J Physiol Heart Circ Physiol*, **275**: H1857–H1864.
- Maytin, M. and Colucci, W.S. (2002). Molecular and cellular mechanisms of myocardial remodelling. *J. Nucl Card*, **9** (3):319-327.
- McCaw, B.J., Chow, S.Y., Wong, E.S.M., Tan, K.L., Guo, H., and Guy, G.R. (2005). Identification and characterization of mErk5-T, a novel Erk5/Bmk1splice variant. *Gene*, **345**: 183–190.
- McKay, M.M., and Morrison, D.K. (2007) Integrating signals from RTKs toERK/MAPK. *Oncogene*, **26**: 3113–3121.
- McKelvie, R.S., Teo, K.K., McCartney, N., Humen, D., Montague, T., and Yusuf, S. (1995). Effects of exercise training in patients with congestive heart failure: a critical review. *J Am Coll Cardiol*, **25**:789–796.
- Meischl, C., Buermans, H. P., Hazes, T., Zuidwijk, M. J., Musters, R. J., and Boer, C., et al. (2008). H9c2 cardiomyoblasts produce thyroid hormone. *Am J Physiol Cell Physiol*, **294**(5): C1227-1233.
- Menick, D., Renaud, L., Buchholz, A., Muller, J., Zhou, H., Kappler, C., Kubalak, S., Conway, S., and Xu, L. (2007). Regulation of Ncx1 gene expression in the normal and hypertrophic heart. *Ann NY Acad Sci*, **1099**:195–203.
- Miki, T., Miura, T., Tanno, M., Nishihara, M., Naitoh, K., Sato, T., Takahashi, A., and Shimamoto, K. (2007). Impairment of cardioprotective PI3K-Akt signaling by post-infarct ventricular remodeling is compensated by an ERK-mediated pathway. *Basic Res Cardiol*, **102**:163–170.
- Milano, G., Morel, S., Bonny, C., Samaja, M., von Segesser, L.K., Nicod, P., and Vassalli, G. (2007). A peptide inhibitor of c-Jun NH2-terminal kinase reduces myocardial ischemia-reperfusion injury and infarct size in vivo. *Am J Physiol Heart Circ Physiol*, **292**: H1828–H1835.
- Miller, T.B., Jr. (1983). Altered regulation of cardiac glycogen metabolism in spontaneously diabetic rats. *Am J Physiol*, **245**:E379-383
- Minamino, T., Yujiri, T., Terada, N., Taffet, G., Michael, L., Johnson, G., and Schneider, M. (2002). MEKK1 is essential for cardiac hypertrophy and dysfunction induced by Gq. *Proc Natl Acad Sci USA*, **99**: 3866–3871.
- Miner, E.C. and Miller, W.L. (2006). A look between the cardiomyocytes: the extracellular matrix in heart failure. *Mayo Clin Proc*, **81**(1): 71-76.
- Mischak, H., Goodnight, J.A., Kolch, W., Martiny-Baron, G., Schaehtle, C., and Kazanietz, M.G., et al. (1993). Overexpression of protein kinase C-delta and -epsilon in NIH 3T3 cells induces opposite effects on growth, morphology,

anchorage dependence, and tumorigenicity. *J Biol Chem*, **268**:6090–6096.

- Mischak, H., Pierce, J.H., Goodnight, J., Kazanietz, M.G., Blumberg, P.M., and Mushinski, J.F. (1993). Phorbol ester-induced myeloid differentiation is mediated by protein kinase C-alpha and -delta and not by protein kinase C-beta II, -epsilon, -zeta, and -eta. *J Biol Chem*, **268**:20110–20115.
- Mitchell, S., Ota, A., Foster, W., Zhang, B., Fang, Z., Patel, S., Nelson, S.F., Horvath, S., and Wang, Y. (2006). Distinct gene expression profiles in adult mouse heart following targeted MAP kinase activation. *Physiol Genomics*, **25**: 50–59.
- Miyachi, M., Yazawa, H., Furukawa, M., Tsuboi, K., Ohtake, M., Nishizawa, T., Hashimoto, K., Yokoi, T., Kojima, T., Murate, T., Yokota, M., Murohara, T., Koike, Y., and Nagata, K. (2009). Exercise training alters left ventricular geometry and attenuates heart failure in Dahl salt-sensitive hypertensive rats. *Hypertension*, **53**:701–707.
- Miyamoto, T., Takeishi, Y., Takahashi, H., Shishido, T., Arimoto, T., Tomoike, H., and Kubota, I. (2004). Activation of distinct signal transduction pathways in hypertrophied hearts by pressure and volume overload. *Basic Res Cardiol*, **99**: 328–337.
- Miyata S, Minobe W, Bristow MR, and Leinwand LA (2000). Myosin heavy chain isoform expression in the failing and nonfailing human heart. *Circ Res* **86**, 386-390.
- Mizukami, Y., Yoshioka, K., Morimoto, S., and Yoshida, K.I. (1997). A novel mechanism of JNK1 activation. Nuclear translocation and activation of JNK1 during ischemia and reperfusion. *J Biol Chem*, **272**:16657–16662.
- Mocanu, M.M., Baxter, G.F., Yue, Y., Critz, S.D., and Yellon, D.M. (2000). The p38MAPK inhibitor, SB203580, abrogates ischaemic preconditioning in rat heart but timing of administration is critical. *Basic Res Cardiol*, **95**: 472–478.
- Mochly-Rosen, D., Wu, G., Hahn, H., Osinska, H., Liron, T., and Lorenz, J.N., et al. (2000). Cardioprotective effects of protein kinase C epsilon: analysis by in vivo modulation of PKCepsilon translocation. *Circ Res*, **86**:1173–1179.
- Mohammadi, K., Rouet-Benzineb, P., Laplace, M., and Crozatier, B. (1997). Protein kinase C activity and expression in rabbit left ventricular hypertrophy. *J Mol Cell Cardiol*, **29**:1687–1694
- Molkentin, J.D. (2004). Calcineurin-NFAT signaling regulates the cardiac hypertrophic response in coordination with the MAPKs. *Cardiovasc Res*, **63**:

- Morel, O.E., Buvry, A., Le Corvoisier, P., Tual, L., Favret, F., and Leon-Velarde, F., et al. (2003). Effects of nifedipine-induced pulmonary vasodilatation on cardiac receptors and protein kinase C isoforms in the chronically hypoxic rat. *Pflugers Arch*, **446**:356–364.
- Morimoto, T., Hasegawa, K., Kaburagi, S., Kakita, T., Wada, H., and Yanazume, T. (2000). Phosphorylation of GATA-4 is involved in alpha1-adrenergic agonist-responsive transcription of the endothelin-1 gene in cardiac myocytes. *J Biol Chem*, **275**: 13721–13726.
- Morrissey, R. P., Czer, L., and Shah, P. K. (2010). Chronic heart failure: current evidence, challenges to therapy, and future directions. *Am J Cardiovasc Drugs*, **11**(3): 153-171.
- Mudgett, J., Ding, J., Guh-Siesel, L., Chartrain, N., Yang, L., Gopal, S., and Chen, M. (2000). Essential role for p38_ mitogen-activated protein kinase in placental angiogenesis. *Proc Natl Acad Sci USA*, **97**:10454–10459.
- Muller P (1965). Ouabain effects on cardiac contraction, action potential and cellular potassium. *Circ Res*, **17**:46-56.
- Nadruz, W. Jr, Corat, M.A.F., Marin, T.M., Guimaraes Pereira, G.A., and Franchini, K.G. (2005). Focal adhesion kinase mediates MEF2 and c-Jun activation by stretch: role in the activation of the cardiac hypertrophic genetic program. *Cardiovasc Res*, **68**: 87–97.
- Nadruz, W. Jr, Kobarg, C.B., Kobarg, J., and Franchini, K.G. (2004). c-Jun is regulated by combination of enhanced expression and phosphorylation in acute-overloaded rat heart. *Am J Physiol Heart Circ Physiol* **286**: H760–H767.
- Nagai, H., Noguchi, T., Takeda, K., and Ichijo, H. (2007). Pathophysiological roles of ASK1-MAP kinase signaling pathways. *J Biochem Mol Biol*, **40**: 1–6.
- Nagarkatti, D, and Sha'afi, R. (1998). Role of p38 MAP kinase in myocardial stress. *J Mol Cell Cardiol*, **30**: 1651–1664.
- Naitoh, K., Ichikawa, Y., Miura, T., Nakamura, Y., Miki, T., Ikeda, Y., Kobayashi, H., Nishihara, M., Ohori, K., and Shimamoto, K. (2006). MitoKATP channel activation suppresses gap junction permeability in the ischemic myocardium by an ERK-dependent mechanism. *Cardiovasc Res*, **70**: 374–383.
- Nakamura, K., Uhlik, M., Johnson, N., Hahn, K., and Johnson, G. (2006). PB1 domain-dependent signaling complex is required for extracellular signal-regulated kinase 5 activation. *Mol Cell Biol*, **26**: 2065–2079.

- Nakamura, K., and Johnson, G. (2003). PB1 domains of MEKK2 and MEKK3 interact with the MEK5 PB1 domain for activation of the ERK5 pathway. *J Biol Chem*, **278**: 36989–36992.
- Nakao K, Minobe W, Roden R, Bristow MR, and Leinwand LA (1997). Myosin heavy chain gene expression in human heart failure. *J Clin Invest* **100**, 2362-2370.
- Nakhost, A., Forscher, P., and Sossin, W.S. (1998). Binding of protein kinase C isoforms to actin in *Aplysia*. *J Neurochem*, **71**:1221–31.
- Narula, J., Haider, N., Virmani, R., Di Salvo, T.g., and Kolodgie, F.D., et al. (1996). Apoptosis in myocytes in end-stage heart failure. *N Engl J Med*, **335**(16): 1182-1189.
- Nemoto, S., Sheng, Z., and Lin, A. (1998). Opposing effects of jun kinase and p38 mitogen-activated protein kinases on cardiomyocyte hypertrophy. *Mol Cell Biol*, **18**: 3518–3526.
- Nian, M., Lee, P., Khaper, N. and Liu, P. (2004). Inflammatory cytokines and postmyocardial infarction remodeling. *Circ Res*, **94**: 1543–1553.
- Nicoll, J. B., Gwinn, B. L., Iwig, J. S., Garcia, P. P., Bunn, C. F., and Allison, L. A. (2003). Compartment-specific phosphorylation of rat thyroid hormone receptor alpha1 regulates nuclear localization and retention. *Mol Cell Endocrinol*, **205**(1-2): 65-77.
- Nishida, K., Yamaguchi, O., Hirotani, S., Hikoso, S., Higuchi, Y., Watanabe, T., Takeda, T., Osuka, S., Morita, T., Kondoh, G., Uno, Y., Kashiwase, K., Taniike, M., Nakai, A., Matsumura, Y., Miyazaki, J., Sudo, T., Hongo, K., Kusakari, Y., Kurihara, S., Chien, K.R., Takeda, J., Hori, M., and Otsu, K. (2004). p38 Mitogen-activated protein kinase plays a critical role in cardiomyocyte survival but not in cardiac hypertrophic growth in response to pressure overload. *Mol Cell Biol*, **24**:10611–10620.
- Nishimoto, S. and Nishida, E. (2006). MAPK signalling ERK5 versus ERK1/2. *EMBO* **7**: 782–786.
- Nishizuka, Y. (1992). Intracellular signaling by hydrolysis of phospholipids and activation of protein kinase C. *Science*, **258**:607–614.
- Nishizuka, Y. (1995). Protein kinase C and lipid signaling for sustained cellular responses. *FASEB J*, **9**:484–496.
- Nishizuka, Y. (1984). The role of protein kinase C in cell surface signal transduction and tumour promotion. *Nature*, **308**:693–8

- Noda N, Hayashi H, Miyata H, Suzuki S, Kobayashi A, and Yamazaki N (1992). Cytosolic Ca²⁺ concentration and pH of diabetic rat myocytes during metabolic inhibition. *J Mol Cell Cardiol* **24**, 435-446.
- Noma, T., Lemaire, A., Naga Prasad, S., Barki-Harrington, L., Tilley, D., Chen, J., Le Corvoisier, P., Violin, J., Wei, H., Lefkowitz, R., and Rockman, H. (2007). Beta-arrestin mediated beta(1)-adrenergic receptor transactivation of the EGFR confers cardioprotection. *J Clin Invest*, **117**: 2445–2458.
- Nukatsuka, M., Yoshimura, Y., Nishida, M., and Kawada, J. (1990) Allopurinol protects pancreatic beta cells from the cytotoxic effect of streptozotocin: in vitro study, *J Pharmacobiodyn*, **13**:259–262.
- O'Connor, C.M., Whellan, D.J., Lee, K.L., Keteyian, S.J., Cooper, L.S., Ellis, S.J., Leifer, E.S., Kraus, W.E., Kitzman, D.W., Blumenthal, J.A., Rendall, D.S., Miller, N.H., Fleg, J.L., Schulman, K.A., McKelvie, R.S., Zannad, F., and Pina, I.L. (2009). Efficacy and safety of exercise training in patients with chronic heart failure: HF-ACTION randomized controlled trial. *JAMA*, **301**:1439–1450.
- Odelberg, S. J. (2002). Inducing cellular dedifferentiation: a potential method for enhancing endogenous regeneration in mammals. *Semin Cell Dev Biol*, **13**(5): 335-343.
- Ojamaa, K. (2010). Signaling mechanisms in thyroid hormone-induced cardiac hypertrophy. *Vascul Pharmacol*, **52**(3-4): 113-119.
- Ojamaa, K., Kenessey, A., Shenoy, R., and Klein, I. (2000). Thyroid hormone metabolism and cardiac gene expression after acute myocardial infarction in the rat. *Am J Physiol Endocrinol Metab*, **279**(6): E1319-1324.
- Olivetti, G., Abbi, R., Quaini, F., Kajstura, J., Cheng, W., and Nitahara, J.A. et al. (1997). Apoptosis in the failing human heart. *N. Engl J Med*, **336** (16): 1131-1141.
- Ono, K. and Han, J. (2000). The p38 signal transduction pathway activation and function. *Cell Signal*, **12**: 1–13.
- Otsu, K., Yamashita, N., Nishida, K., Hirotani, S., Yamaguchi, O., Watanabe, T., Hikoso, S., Higuchi, Y., Matsumura, Y., Maruyama, M., Sudo, T., Osada, H., and Hori, M. (2003). Disruption of a single copy of the p38alpha MAP kinase gene leads to cardioprotection against ischemia-reperfusion. *Biochem Biophys Res Commun*, **302**: 56–60.
- Owens, D.M. and Keyse, S.M. (2007) Differential regulation of MAP kinase signalling by dual-specificity protein phosphatases. *Oncogene*, **26**:3203–3213.

- Pages, G., Guerin, S., Grall, D., Bonino, F., Smith, A., Anjuere, F., Auberger, P., and Pouyssegur, J. (1999). Defective thymocyte maturation in p44MAP kinase (Erk1) knockout mice. *Science*, **286**: 1374–1377.
- Pal, B, Singh, K, Rasipe, B, Broadway, K, Chegouchi, M, Meggs, LG and Malhotra, S (2003) Protein kinase C Signalling and expression of the diabetic cardiac phenotype : In atherosclerosis, hypertension and diabetes (Eds: CN Pierce, M Nagano, P Zahradka and NS Dhalla). Klower Press, Boston, pp 407-426.
- Palaniyandi, S.S. , Sun, L. , Ferreira, J.C. and Mochly-Rosen, D. (2009). Protein kinase C in heart failure: a therapeutic target?. *Cardiovasc Res*, **82**: 229–239.
- Pan, J., Singh, U., Takahashi, T., Oka, Y., Palm-Leis, A., Herbelin, B., and Baker, K. (2005). PKC mediates cyclic stretch-induced cardiac hypertrophy through Rho family GTPases and mitogen-activated protein kinases in cardiomyocytes. *J Cell Physiol*, **2002**: 536–553.
- Pandur, P., Maurus, D. and Kuhl, M. (2002). Increasingly complex: new players enter the Wnt signaling network. *Bioessays*, **24**: 60-75
- Pantos C, Mourouzis I, and Cokkinos DV (2010a). Rebuilding the post-infarcted myocardium by activating 'physiologic' hypertrophic signaling pathways: the thyroid hormone paradigm. *Heart Fail Rev* **15**, 143-154.
- Pantos C, Mourouzis I, and Cokkinos DV (2011). New insights into the role of thyroid hormone in cardiac remodeling: time to reconsider? *Heart Fail Rev* **16**, 79-96.
- Pantos C, Mourouzis I, and Cokkinos DV (2012). Thyroid hormone and cardiac repair/regeneration: from Prometheus myth to reality? *Can J Physiol Pharmacol*. **63**: 1-12
- Pantos C, Mourouzis I, Galanopoulos G, Gavra M, Perimenis P, Spanou D, and Cokkinos DV (2010b). Thyroid hormone receptor alpha1 downregulation in postischemic heart failure progression: the potential role of tissue hypothyroidism. *Horm Metab Res* **42**, 718-724.
- Pantos C, Mourouzis I, Saranteas T, Clave G, Ligeret H, Noack-Fraissignes P, Renard PY, Massonneau M, Perimenis P, Spanou D, Kostopanagiotou G, and Cokkinos DV (2009). Thyroid hormone improves postischemic recovery of function while limiting apoptosis: a new therapeutic approach to support hemodynamics in the setting of ischemia-reperfusion? *Basic Res Cardiol* **104**, 69-77.

- Pantos C, Mourouzis I, Xinaris C, Papadopoulou-Daifoti Z, and Cokkinos D (2008). Thyroid hormone and "cardiac metamorphosis": potential therapeutic implications. *Pharmacol Ther* **118**, 277-294.
- Pantos, C. I., Malliopolou, V. A., Mourouzis, I. S., Karamanoli, E. P., Paizis, I. A., and Steimberg, N., et al. (2002). Long-term thyroxine administration protects the heart in a pattern similar to ischemic preconditioning. *Thyroid*, **12** (4): 325-329.
- Pantos, C. I., Malliopolou, V. A., Mourouzis, I. S., Karamanoli, E. P., Tzeis, S. M., and Carageorgiou, H. C., et al. (2001). Long-term thyroxine administration increases heat stress protein-70 mRNA expression and attenuates p38 MAP kinase activity in response to ischaemia. *J Endocrinol*, **170**(1): 207-215.
- Pantos, C., Dritsas, A., Mourouzis, I., Dimopoulos, A., Karatasakis, G., and Athanassopoulos, G., et al. (2007a). Thyroid hormone is a critical determinant of myocardial performance in patients with heart failure: potential therapeutic implications. *Eur J Endocrinol*, **157**(4): 515-520.
- Pantos, C., Malliopolou, V., Mourouzis, I., Karamanoli, E., Moraitis, P., and Tzeis, S., et al. (2003a). Thyroxine pretreatment increases basal myocardial heat-shock protein 27 expression and accelerates translocation and phosphorylation of this protein upon ischaemia. *Eur J Pharmacol*, **478**(1): 53-60.
- Pantos, C., Malliopolou, V., Mourouzis, I., Thempeyioti, A., Paizis, I., and Dimopoulos, A., et al. (2006). Hyperthyroid hearts display a phenotype of cardioprotection against ischemic stress: a possible involvement of heat shock protein 70. *Horm Metab Res*, **38** (5): 308-313.
- Pantos, C., Malliopolou, V., Paizis, I., Moraitis, P., Mourouzis, I., and Tzeis, S., et al. (2003b). Thyroid hormone and cardioprotection: study of p38 MAPK and JNKs during ischaemia and at reperfusion in isolated rat heart. *Mol Cell Biochem*, **242**(1-2): 173-180.
- Pantos, C., Mourouzis, I., and Cokkinos, D. V. (2011a). New insights into the role of thyroid hormone in cardiac remodeling: time to reconsider? *Heart Fail Rev*, **16**(1): 79-96.
- Pantos, C., Mourouzis, I., Dimopoulos, A., Markakis, K., Panagiotou, M., and Xinaris, C., et al. (2007b). Enhanced tolerance of the rat myocardium to ischemia and reperfusion injury early after acute myocardial infarction. *Basic Res Cardiol*, **102**(4): 327-333
- Pantos, C., Mourouzis, I., Galanopoulos, G., Gavra, M., Perimenis, P., and Spanou, D., et al. (2010). Thyroid hormone receptor alpha1 downregulation in postischemic heart failure progression: the potential role of tissue

hypothyroidism. *Horm Metab Res*, **42** (10): 718-724.

- Pantos, C., Mourouzis, I., Malliopoulou, V., Paizis, I., Tzeis, S., and Moraitis, P., et al. (2005a). Dronedarone administration prevents body weight gain and increases tolerance of the heart to ischemic stress: a possible involvement of thyroid hormone receptor alpha1. *Thyroid*, **15**(1): 16-23.
- Pantos, C., Mourouzis, I., Markakis, K., Dimopoulos, A., Xinaris, C., and Kokkinos, A. D., et al. (2007c). Thyroid hormone attenuates cardiac remodeling and improves hemodynamics early after acute myocardial infarction in rats. *Eur J Cardiothorac Surg*, **32**(2): 333-339.
- Pantos, C., Mourouzis, I., Markakis, K., Tsagoulis, N., Panagiotou, M., and Cokkinos, D. V. (2008a). Long-term thyroid hormone administration reshapes left ventricular chamber and improves cardiac function after myocardial infarction in rats. *Basic Res Cardiol*, **103**(4): 308-318.
- Pantos, C., Mourouzis, I., Paizis, I., Malliopoulou, V., Xinaris, C., and Moraitis, P., et al. (2007d). Pharmacological inhibition of TRalpha1 receptor potentiates the thyroxine effect on body weight reduction in rats: potential therapeutic implications in controlling body weight. *Diabetes Obes Metab*, **9**(1): 136-138.
- Pantos, C., Mourouzis, I., Saranteas, T., Brozou, V., Galanopoulos, G., and Kostopanagiotou, G., et al. (2011b). Acute T3 treatment protects the heart against ischemia-reperfusion injury via TRalpha1 receptor. *Mol Cell Biochem*, **353** (1-2): 235-241.
- Pantos, C., Mourouzis, I., Saranteas, T., Clave, G., Ligeret, H., and Noack-Fraissignes, P., et al. (2009a). Thyroid hormone improves postischaemic recovery of function while limiting apoptosis: a new therapeutic approach to support hemodynamics in the setting of ischaemia-reperfusion? *Basic Res Cardiol*, **104** (1): 69-77.
- Pantos, C., Mourouzis, I., Saranteas, T., Paizis, I., Xinaris, C., and Malliopoulou, V., et al. (2005b). Thyroid hormone receptors alpha1 and beta1 are downregulated in the post-infarcted rat heart: consequences on the response to ischaemia-reperfusion. *Basic Res Cardiol*, **100** (5): 422-432.
- Pantos, C., Mourouzis, I., Tsagoulis, N., Markakis, K., Galanopoulos, G., and Roukounakis, N., et al. (2009b). Thyroid hormone at supra-physiological dose optimizes cardiac geometry and improves cardiac function in rats with old myocardial infarction. *J Physiol Pharmacol*, **60**(3): 49-56.
- Pantos, C., Mourouzis, I., Xinaris, C., Papadopoulou-Daifoti, Z., and Cokkinos, D. (2008b). Thyroid hormone and "cardiac metamorphosis": potential therapeutic implications. *Pharmacol Ther*, **118** (2): 277-294.

- Pantos, C., Xinaris, C., Mourouzis, I., Malliopolou, V., Kardami, E., and Cokkinos, D. V. (2007e). Thyroid hormone changes cardiomyocyte shape and geometry via ERK signaling pathway: potential therapeutic implications in reversing cardiac remodeling? *Mol Cell Biochem*, **297** (1-2): 65-72.
- Pantos, C., Xinaris, C., Mourouzis, I., Perimenis, P., Politi, E., and Spanou, D., et al. (2008c). Thyroid hormone receptor alpha 1: a switch to cardiac cell "metamorphosis"? *J Physiol Pharmacol*, **59**(2): 253-269.
- Partamian JO nad Bradley RF (1965). Acute myocardial infarction in 258 cases of diabetes. Immediate mortality and five-year survival. *N Engl J Med* **273**, 455-461.
- Pass, J.M. , Gao J., Jones, W.K., Wead, W.B., Wu, X. and Zhang, J. et al. (2001). Enhanced PKC beta II translocation and PKC beta II-RACK1 interactions in PKC epsilon-induced heart failure: a role for RACK1. *Am J Physiol Heart Circ Physiol*, **281**: H2500–H2510.
- Paul, K., Ball, N.A., Dorn, 2nd G.W., and Walsh, R.A. (1997). Left ventricular stretch stimulates angiotensin II-mediated phosphatidylinositol hydrolysis and protein kinase C epsilon isoform translocation in adult guinea pig hearts. *Circ Res*,**81**: 643–650.
- Pearson, G., Robinson, F., Beers Gibson, T., Xu Be Karandikar, M.,Berman, K., and Cobb, MH. (2001). Mitogen-activated protein (MAP) kinase pathways: regulation and physiological functions. *Endocr Rev*, **22**:153–183.
- Pells and D'alonzo ca (1963). Acute myocardial infarction in a large industrial population: report of a 6-year study of 1,356 cases. *JAMA* **185**, 831-838.
- Peng, X.D., Xu, P.Z., Chen, M.L., Hahn-Windgassen, A., Skeen, J., Jacobs, J.,Sundararajan, D., Chen, W.S., Crawford, S.E., Coleman, K.G., and Hay, N. (2003). Dwarfism, impaired skin development, skeletal muscle atrophy, delayed bone development, and impeded adipogenesis in mice lacking Akt1 and Akt2. *Genes Dev*,**17**:1352–1365.
- Pentassuglia, L., and Sawyer, D.B. (2009).The role of Neuregulin-1_/ErbB signaling in the heart. *Exp Cell Res*, **315**: 627–637.
- Perletti, G.P., Folini, M., Lin, H.C., Mischak, H., Piccinini, F., Tashjian, and Jr A.H. (1996). Over-expression of protein kinase C epsilon is oncogenic in rat colonic epithelial cells. *Oncogene*, **12**:847–854.
- Petrich, B.G., Eloff, B.C., Lerner, D.L., Kovacs, A., Saffitz, J.E., Rosenbaum, D.S., and Wang, Y. (2004). Targeted activation of c-Jun N-terminal kinase in vivo induces restrictive cardiomyopathy and conduction defects. *J Biol Chem*, **279**:

- Petrich, B.G., Gong, X., Lerner, D.L., Wang, X., Brown, J.H., Saffitz, J.E., and Wang, Y. (2002). c-Jun N-terminal kinase activation mediates down-regulation of connexin43 in cardiomyocytes. *Circ Res* **91**: 640–647.
- Petrich, B.G., Molkenin, J.D. and Wang, Y.(2003). Temporal activation of c-JunN-terminal kinase in adult transgenic heart via cre-loxP-mediated DNA recombination. *FASEB J*, **02**–0438fje.
- Pfeffer MA and Braunwald E (1990). Ventricular remodeling after myocardial infarction. Experimental observations and clinical implications. *Circulation* **81**, 1161-1172.
- Phung, T.L., Ziv, K., Dabydeen, D., Eyiah-Mensah, G., Riveros, M., Perruzzi, C., Sun, J., Monahan-Earley, R.A., Shiojima, I., Nagy, J.A., Lin, M.I., Walsh, K., Dvorak, A.M., Briscoe, D.M., Neeman, M., Sessa, W.C., Dvorak, H.F., and Benjamin, L.E. (2006). Pathological angiogenesis induced by sustained Akt signaling and inhibited by rapamycin. *CancerCell*, **10**:159–170.
- Ping, P. , Zhang, J., Qiu, Y., Tang, X.L., Manchikalapudi S. and Cao, X., et al. (1997). Ischemic preconditioning induces selective translocation of protein kinase C isoforms epsilon and eta in the heart of conscious rabbits without subcellular redistribution of total protein kinase C activity. *Circ Res*, **81**: 404–414.
- Ping, P., Zhang, J., Huang, S., Cao, X., Tang, X.L., Li, R.C.X., Zheng, Y.T., Qiu, Y., Clerk, A., Sugden, P., Han, J., and Bolli, R. (1999). PKC-dependent activation of p46/p54 JNKs during ischemic preconditioning in conscious rabbits. *Am J Physiol Heart Circ Physiol*, **277**: H1771–H1785.
- Ping, P., Zhang, J., Pierce, Jr W.M., and Bolli, R. (2001). Functional proteomic analysis of protein kinase C epsilon signaling complexes in the normal heart and during cardioprotection. *Circ Res*, **88**:59–62.
- Pingitore, A., Chen, Y., Gerdes, A. M., and Iervasi, G. (2011). Acute myocardial infarction and thyroid function: New pathophysiological and therapeutic perspectives. *Ann Med*.
- Pingitore, A., Iervasi, G., Barison, A., Prontera, C., Pratali, L., and Emdin, M., et al. (2006). Early activation of an altered thyroid hormone profile in asymptomatic or mildly symptomatic idiopathic left ventricular dysfunction. *J Card Fail*, **12**(7): 520-526.
- Porrello, E. R., Mahmoud, A. I., Simpson, E., Hill, J. A., Richardson, J. A., and Olson, E. N., et al. (2011). Transient regenerative potential of the neonatal

mouse heart. *Science*, **331**(6020): 1078-1080.

- Prabhu S. 2004. Cytokine-induced modulation of cardiac function. *CircRes*, **95**: 1140–1153.
- Prekeris, R., Hernandez, R.M., Mayhew, M.W., White, M.K., and Terrian, D.M. (1998). Molecular analysis of the interactions between protein kinase C-epsilon and filamentous actin. *J Biol Chem*, **273**:26790–26798.
- Prekeris, R., Mayhew, M.W., Cooper, J.B., and Terrian, D.M. (1996). Identification and localization of an actin-binding motif that is unique to the epsilon isoform of protein kinase C and participates in the regulation of synaptic function. *J Cell Biol*, **132**:77–90.
- Purcell, N., Wilkins, B.J., York, A., Saba-El-Leil, M., Meloche, S., Robbins, J., and Molkenkin, J. (2007). Genetic inhibition of cardiac ERK1/2 promotes stress-induced apoptosis and heart failure but has no effect on hypertrophy in vivo. *Proc Natl Acad Sci USA*, **104**: 14074–14079.
- Racken, N. K, Woodall, A .J, Howarth, F.C., & Singh, J. (2004). Voltage dependence of contraction in streptozotocin-induced diabetic myocytes. *Molec Cell Biochem*. **261** (1), 235-243.
- Rajabi, M., Kassiotis, C., Razeghi, P., and Taegtmeyer, H. 2007. Return to the fetal gene program protects the stressed heart: a strong hypothesis. *Heart Fail Rev*, **12**(3-4): 331-343.
- Raman, M., Chen, W., and Cobb, M.H.(2007). Differential regulation and properties of MAPKs. *Oncogene*, **26**: 3100–3112.
- Ramos, J.W. (2008). The regulation of extracellular signal-regulated kinase(ERK) in mammalian cells. *Int J Biochem Cell Biol*, **40**: 2707–2719.
- Ranasinghe, A. M., Quinn, D. W., Pagano, D., Edwards, N., Farouqi, M., and Graham, T. R., et al. (2006). Glucose-insulin-potassium and tri-iodothyronine individually improve hemodynamic performance and are associated with reduced troponin I release after on-pump coronary artery bypass grafting. *Circulation*, **114**(1 Suppl): I 245-250.
- Rathmell, J.C., Elstrom, R.L., Cinalli, R.M., and Thompson, C.B. (2003). Activated Akt promotes increased resting T cell size, CD28-independent T cell growth, and development of autoimmunity and lymphoma. *Eur J Immunol*, **33**:2223–2232.
- Regan, C., Li, W., Boucher, D., Spatz, S., Su, M. and, Kuida, K. (2002). Erk5 null mice display multiple extraembryonic vascular and embryonic cardiovascular defects. *Proc Natl Acad Sci USA*, **99**: 9248–9253.

- Reiser PJ, Portman MA, Ning XH, and Schomisch MC (2001). Human cardiac myosin heavy chain isoforms in fetal and failing adult atria and ventricles. *Am J Physiol Heart Circ Physiol* **280**, H1814-H1820.
- Remondino, A., Kwon, S.H., Communal, C., Pimentel, D.R., Sawyer, D.B., Singh, K., and Colucci, WS. (2003). Adrenergic receptor-stimulated apoptosis in cardiac myocytes is mediated by reactive oxygen species/c-Jun NH2-terminal kinase-dependent activation of the mitochondrial pathway. *Circ Res*, **92**: 136–138.
- Reyland, M.E., Anderson, S.M., Matassa, A.A, Barzen, K.A., and Quissell, D.O. (1999). Protein kinase C delta is essential for etoposide-induced apoptosis in salivary gland acinar cells. *J Biol Chem*, **274**:19115–19123.
- Riad, A., Jager, S., Sobirey, M., Escher, F., Yaulema-Riss, A., Westermann, D., Karatas, A., Heimesaat, M.M., Bereswill, S., Dragun, D., Pauschinger, M., Schultheiss, H.P., and Tschöpe, C. (2008). Toll-like receptor-4 modulates survival by induction of left ventricular remodeling after myocardial infarction in mice. *J Immunol* **180**: 6954–6961.
- Ricci, R., Eriksson, U., Oudit, G., Eferl, R., Akhmedov, A., Sumara, I., Sumara, G., Kassiri, Z., David, J., Bakiri, L., Sasse, B., Idarraga, M., Rath, M., Kurz, D., Theussl, H., Perriard, J., Backx, P., Penninger, J., and Wagner, E. (2005). Distinct functions of junD in cardiac hypertrophy and heart failure. *Genes Dev*, **19**: 208–213.
- Rincón, M. and Davis, R. (2009). Regulation of the immune response by stress activated protein kinases. *Immunol Rev*, **228**: 212–224.
- Robledo, M. (1956). Myocardial regeneration in young rats. *Am J Pathol*, **32**(6): 1215-1239.
- Rodrigues, B., Cam, M.C., and McNeill, J.H. (1998). Metabolic disturbances in diabetic cardiomyopathy. *Mol Cell Biochem*, **180**:53-57
- Roger, V. L. (2010). The heart failure epidemic. *Int J Environ Res Public Health*, **7**(4): 1807-1830.
- Rouet-Benzineb, P., Mohammadi, K., Perennec, J., Poyard, M., Bouanani Nel, H., and Crozatier, B. (1996). Protein kinase C isoform expression in normal and failing rabbit hearts. *Circ Res*, **79**:153–161.
- Roussel, É., Gaudreau, M., Plante, É., Drolet, M.C., Breault, C., Couet, J., and Arsénault, M. (2008). Early responses of the left ventricle to pressure overload in Wistar rats. *Life Sci*, **82**: 265–272.
- Roux, P. and Blenis, J. (2004). ERK and p38 MAPK-activated protein kinases: a family of protein kinases with diverse biological functions. *Microbiol Mol Biol*

Rev, **68**: 320–344.

- Ruan, H., Mitchell, S., Vainoriene, M., Lou, Q., Xie, L.H., Ren, S., Goldhaber, J.I., and Wang, Y. (2007). Gi₁-mediated cardiac electrophysiological remodeling and arrhythmia in hypertrophic cardiomyopathy. *Circulation* **116**: 596–605.
- Russell, B., Curtis, M.W., Koshman, Y.E., and Samarel, A.M. (2010). Mechanical stress-induced sarcomere assembly for cardiac muscle growth in length and width. *J Mol Cell Cardiol*, **48**:817–823.
- Saba-El-Leill, M., Vella, F., Vernay, B., Voisin, L., Chen, L., Labrecque, N., Ang, S., and Meloche, S. (2003). An essential function of the mitogen-activated protein kinase Erk2 in mouse trophoblast development. *EMBO J*, **4**: 964–986.
- Sabbah, H.N. (2000). Apoptotic cell death in heart failure. *Cardiovasc Res*, **45**(3): 704-712.
- Sadoshima, J., Montagne, O., Wang, Q., Yang, G., Warden, J., Lui, J., Takagi, G., Karoor, V., Hong, C., Johnson, G., Vatner, D., and Vatner, S. (2002). The MEKK1-JNK pathway plays a protective role in pressure overload but does not mediate cardiac hypertrophy. *J Clin Invest*, **110**:271–279.
- Salazar, N.C., Chen, J., and Rockman, H.A. (2007). Cardiac GPCRs: GPCR signalling in healthy and failing hearts. *Biochim Biophys Acta*, **1768**:1006–1018.
- Salvador, J.M., Mittelstadt, P.R., Guszczynski, T., Copeland, T.D., Yamaguchi, H., Appella, E., and Fornace, A.J.J. (2005). Alternative p38 activation pathway mediated by T cell receptor-proximal tyrosine kinases. *Nat Immunol* **6**: 390–395.
- Salvetella, G., Hirsch, E., Notte, A., Tarone, G. and Lembo, G. (2004). Adaptive and metadaptive hypertrophic pathways points of convergence and divergence. *Card. Res*, **63**(3): 373-380.
- Sanada, S., Kitakaze, M., Papst, P., Hatanaka, K., Asanuma, H., Aki, T., Shinozaki, Y., Ogita, H., Node, K., Takashima, S., Asakura, M., Yamada, T., Fukushima, T., Ogai, A., Kuzuya, T., Mori, H., Terada, N., Yoshida, K., and Hori, M. (2001). Role of phasic dynamism of p38 mitogen activated protein kinase activation in ischemic preconditioning of the canine heart. *Circ Res*, **88**: 175–180.
- Sanchez Alvarado, A. (2000). Regeneration in the metazoans: why does it happen? *Bioessays*, **22**(6): 578-590.
- Sandri, M. (2008). Signaling in muscle atrophy and hypertrophy. *Physiology*

(Bethesda),**23**:160–170.

- Sato, Y., Buchholz, D. R., Paul, B. D., and Shi, Y. B. (2007). A role of unliganded thyroid hormone receptor in postembryonic development in *Xenopus laevis*. *Mech Dev*, **124**(6): 476-488.
- Satoh, M., Matter, C.M., Ogita, H., Takeshita, K., Wang, C.Y., Dorn, G.W. II, and Liao, J.K. (2007). Inhibition of apoptosis-regulated signaling kinase-1 and prevention of congestive heart failure by estrogen. *Circulation*, **115**: 3197–3204.
- Saurin, A., Martin, J., Heads, R., Mockridge, J., Foley, C., Wright, M., Wang, Y., and Marber, M.S. (2000). The role of differential activation of p38-mitogen-activated protein kinase in preconditioned ventricular myocytes. *FASEB J*, **14**: 2237–2246.
- Schnabel, K., Wu, C. C., Kurth, T., and Weidinger, G. (2011). Regeneration of cryoinjury induced necrotic heart lesions in zebrafish is associated with epicardial activation and cardiomyocyte proliferation. *PLoS One*, **6**(4): e18503.
- Schneider, S., Chen, W., Hou, J., Steenbergen, C., and Murphy, E. (2001). Inhibition of p38 MAPK alpha/beta reduces ischemic injury and does not block protective effects of preconditioning. *Am J Physiol Heart Circ Physiol*, **280**: H499–H508.
- Schwartz, H., Carter, J., Abdudurehman, M., Russ, M., Buerke, U., Schlitt, A., Muller-Werdan, U., Prondzinsky, R., and Werdan, K. (2007). Myocardial ischemia/reperfusion causes VDAC phosphorylation which is reduced by cardioprotection with a p38 MAP kinase inhibitor. *Proteomics*, **7**: 4579–4588.
- See, F., Thomas, W., Way, K., Tzanidis, A., Kompa, A., Lewis, D., Itescu, S., and Krum, H. (2004). p38 Mitogen-activated protein kinase inhibition improves cardiac function and attenuates left ventricular remodeling following myocardial infarction in the rat. *J Am Coll Cardiol*, **44**:1679–1689.
- Sehgal, S., and Drazner, M. H. (2007). Left ventricular geometry: does shape matter? *Am Heart J*, **153**(2): 153-155.
- Seko, Y., Takahashi, N., Tobe, K., Kadowaki, T. and Yazaki, Y. (1997). Hypoxia and hypoxia/reoxygenation activate p65PAK, p38 mitogen-activated protein kinase (MAPK), stress-activated protein kinase (SAPK) in cultured rat cardiac myocytes. *Biochem Biophys Res Commun*, **239**: 840–844.
- Sellers DJ and Chess-Williams R (2001). The effect of streptozotocin-induced diabetes on cardiac beta-adrenoceptor subtypes in the rat. *J Auton Pharmacol* **21**, 15-21.
- Selvetella, G., Hirsch, E., Notte, A., Tarone, G. and Lembo, G. (2004). Adaptive and maladaptive hypertrophic pathways: points of convergence and divergence.

Cardiovasc Res, **63**: 373–380.

- Sena, S., Hu, P., Zhang, D., Wang, X., Wayment, B., and Olsen, C. et al. (2009). Impaired insulin signaling accelerates cardiac mitochondrial dysfunction after myocardial infarction. *J Mol Cell Cardiol*, **46**:910-918.
- Shaffer, S.W. (1991). Cardiomyopathy associated with non-insulin-dependent diabetes. *Mol. Cell Biochem.* **107**, 1-20.
- Shah, A.M. and Solomon, S.D. (2010). A unified view of ventricular remodeling. *Eur J Heart Fail*, **12**:779–781.
- Shao, C-H, Rozanski, G.J., Nagi, R., Stockdale, F.E., Patel, K.P., Wang, M., Singh, J., Mayhan, M.G. and Bidasee, K.R. (2010). Carbonylation of myosin heavy chains in rat hearts during diabetes. *Biochemical Pharmacol* , **80**: 205-217
- Shao, Z., Bhattacharya, K., Hsieh, E., Park, L., Walters, B., Germann, U., Wang, Y.M., Kyriakis, J., Mohanlal, R., Kuida K, Namchuk M, Salituro F, Yao Ym Hou Wm Chen X, Aronovitz M, Tschlis PN, Bhattacharya S, Force T, and Kilter H. (2006). c-Jun N-terminal kinases mediate reactivation of Akt and cardiomyocyte survival after hypoxic injury in vitro and in vivo. *Circ Res*, **98**: 111–118.
- Sherwood, D.E. (2008). Electromyographic control of movement time in a rapid aiming movement. *Perc Mot Skills*, **16**(8): 946-954.
- Shi, Y. B., Fu, L., Hsia, S. C., Tomita, A., and Buchholz, D. (2001). Thyroid hormone regulation of apoptotic tissue remodeling during anuran metamorphosis. *Cell Res*, **11**(4): 245-252.
- Shimizu, N., Yoshiyama, M., Omura, T., Hanatani, A., Kim, S., Takeuchi, K., Iwao, H., and Yoshikawa, J. (1998). Activation of mitogen-activated protein kinases and activator protein-1 in myocardial infarction in rats. *Cardiovasc Res* **38**: 116–124.
- Shimojo, N., Jesmin, S., Zaedi, S., Maeda, S., Soma, M., Aonuma, K., Yamaguchi, I., and Miyauchi, T. (2006). Eicosapentaenoic acid prevents endothelin-1-induced cardiomyocyte hypertrophy in vitro through the suppression of TGF-beta1 and phosphorylated JNK. *Am J Physiol Heart Circ Physiol*, **291**: H835–H845.
- Shiojima, I. and Walsh, K. (2006). Regulation of cardiac growth and coronary angiogenesis by the Akt/PKB signaling pathway. *Genes Dev*, **20**:3347–3365.
- Shiojima, I., Walsh, K. 2002. Role of Akt signaling in vascular homeostasis and angiogenesis. *Circ Res*, **90**:1243–1250.

- Shiojima, I., Yefremashvili, M., Luo, Z., Kureishi, Y., Takahashi, A., Tao, J., Rosenzweig, A., Kahn, C.R., Abel, E.D., and Walsh, K. (2002). Akt signaling mediates postnatal heart growth in response to insulin and nutritional status. *J Biol Chem*, **277**:37670–37677.
- Shiomi, T., Tsutsui, H., and Ikeuchi, M. et al. (2003). Streptozotocin-induced hyperglycemia exacerbates left ventricular remodeling and failure after experimental myocardial infarction. *J Am Coll Cardiol*, **42**:165-172
- Simonis, G. , Briem, S.K. , Schoen, S.P. , Bock, M. , Marquetant R. and Strasser, R.H. (2007). Protein kinase C in the human heart: differential regulation of the isoforms in aortic stenosis or dilated cardiomyopathy. *Mol Cell Biochem*, **305**: 103–111.
- Simonis, G., Briem, S.K., Schoen, S.P., Bock, M., Marquetant, R., and Strasser, R.H. (2007). Protein kinase C in the human heart: differential regulation of the isoforms in aortic stenosis or dilated cardiomyopathy. *Mol Cell Biochem*, **305**:103–111.
- Singh, J., Chonkar, A., Bracken, N.K., Adeghate, E. , Latt, Z. and Hussain, M. (2006). Effect of streptozotocin-Induced Type 1 diabetes mellitus on contraction, calcium transient and cation contents in the isolated rat heart. *Annals N.Y. Acad. Sci.* **1084**: 503-519.
- Sipido KR, Carmeliet E, and Pappano A (1995). Na⁺ current and Ca²⁺ release from the sarcoplasmic reticulum during action potentials in guinea-pig ventricular myocytes. *J Physiol* **489** (Pt 1), 1-17.
- Sirlak, M., Yazicioglu, L., Inan, M. B., Eryilmaz, S., Taso, R., and Aral, A., et al. (2004). Oral thyroid hormone pretreatment in left ventricular dysfunction. *Eur J Cardiothorac Surg*, **26**(4): 720-725.
- Siwik, D.A., Kuster, G.M., Brahmabhatt, J.V., Zaidi, Z., Malik, J., Ooi, H., and Ghorayeb, G. (2008). EMMPRIN mediates α -adrenergic receptor-stimulated matrix metalloproteinase activity in cardiac myocytes. *J Mol Cell Cardiol*, **44**: 210–217.
- Skvara, H. , Dawid, M. , Kleyn, E. , Wolff, B., Meingassner, J.G. and Knight, H. , et al. (2008). The PKC inhibitor AEB071 may be a therapeutic option for psoriasis. *J Clin Invest*, **118**: 3151–3159.
- Slack, J. M., Lin, G., and Chen, Y. (2008). The *Xenopus* tadpole: a new model for regeneration research. *Cell Mol Life Sci*, **65** (1): 54-63.
- Sniderman, A, Michel, C and Racine, N. (2002). Heart disease in patients with diabetes mellitus. *J. Clin. Epidemiol.* **45** (12): 1357-1359.

- Soler NG, Bennett MA, Pentecost BL, Fitzgerald MG, & Malins JM (1975). Myocardial infarction in diabetics. *Q J Med* **44**, 125-132.
- Somanath, P.R., Razorenova, O.V., Chen, J., and Byzova, T.V. (2006). Akt1 in endothelial cell and angiogenesis. *Cell Cycle*, **5**:512–518.
- Song, Z., Ji ,X., Li, X., Wang, S. and Wang, S. (2008). Inhibition of the activity of poly (ADP-ribose) polymerase reduces heart ischaemia/reperfusioninjury via suppressing JNK-mediated AIF translocation. *J Cell Mol Med*, **12**: 1220–1228.
- Sopontammarak, S., Aliharoob, A., Ocampo, C., Arcilla, R., Gupta, M., and Gupta, M. (2005). Mitogen-activated protein kinases (p38 and c-JunNH2-terminal kinase) are differentially regulated during cardiacvolume and pressure overload hypertrophy. *Cell Biochem Biophys*, **43**: 61–76.
- Spinale, F.G. (2007). Myocardial matrix remodelling and the matrix metalloproteinases influence on cardiac form and function. *Physiol Rev*, **87** (4): 1285-1342.
- Steenbergen C. (2002). The role of p38 mitogen-activated protein kinase in myocardial, ischemia/reperfusion, injury: relationship to ischemic preconditioning. *Basic Res Cardiol*, **97**: 276–285.
- Stock, A., and Sies, H. (2000). Thyroid hormone receptors bind to an element in the connexin43 promoter. *Biol Chem*, **381**(9-10): 973-979.
- Strandness, E., and Bernstein, D. (1997). Developmental and afterload stress regulation of heat shock proteins in the ovine myocardium. *Pediatr Res*, **41** (1): 51-56.
- Su, H.F., Samsamshariat, A., Fu, J., Shan, Y.X., Chen, Y.H., Piomelli, D., and Wang, P.H. (2006). Oleyethanolamide activates Ras-Erk pathway and improves myocardial function in doxorubicin-induced heart failure. *Endocrinology*, **147**: 827–834.
- Sucher, R., Gehwolf, P., Kaier, T., Hermann, M., Maglione, M., Oberhuber, R., Ratschiller, T., Kuznetsov, A.V., Bösch, F., Kozlov, A.V., Ashraf, M.I., Schneeberger S, Brandacher G, Öllinger R, Margreiter R, and Troppmair J. (2009). Intracellular signaling pathways control mitochondrial events associated with the development of ischemia/reperfusion-associated damage. *Transplant Int*, **22**: 922–930.
- Sumandea, M.P. , Pyle, W.G. , Kobayashi, T. , de Tombe, P.P. and Solaro, R.J. . (2003). Identification of a functionally critical protein kinase C phosphorylation residue of cardiac troponin T. *J Biol Chem*, **278**: 35135–35144.

- Sung Il Kim, Hey Jin Kim, Dong Cheol Han and Hi Bahl Lee (2000). Effect of lovastatin on small GTP binding proteins and on TGF- β Kidney International.58, S88–S92; doi:10.1046/j.1523-1755.2000.07714.x
- Sussman, M.A. , Hamm-Alvarez, S.F. , Vilalta, P.M. , Welch, S. and Kedes, L. (1997). Involvement of phosphorylation in doxorubicin-mediated myofibril degeneration. An immunofluorescence microscopy analysis. *Circ Res*, **80**: 52–61.
- Swynghedauw, B. (1999). Molecular mechanisms of myocardial remodeling. *Physiol Rev*, **79** (1): 215-262.
- Szokodi, I., Kerkela, R., Kubin, A.M., Sarman, B., Pikkarainen, S., Konyi, A., Horvath, I.G., Papp, L., Toth, M., Skoumal, R. and Ruskoaho, H.(2008). Functionally opposing roles of extracellular signal-regulated kinase 1/2 and p38 mitogen-activated protein kinase in the regulation of cardiac contractility. *Circulation* **118**: 1651–1658.
- Tachibana, H., Perrino, C., Takaoka, H., Davis, R.J., Naga Prasad, S.V., and Rockman, H A. (2006). JNK1 is required to preserve cardiac function in the early response to pressure overload. *Biochem Biophys Res Commun*, **343**: 1060–1066.
- Taegtmeyer, H., Sen, S., and Vela, D. (2010). Return to the fetal gene program: a suggested metabolic link to gene expression in the heart. *Ann N Y Acad Sci*, **1188**: 191-198.
- Takahashi, E., Fukuda, K., Miyoshi, S., Murata, M., Kato, T., Ita, M., Tanabe, T., and Ogawa, S. (2004). Leukemia inhibitory factor activates cardiac L-type Ca²⁺ channels via phosphorylation of serine 1829 in the rabbit Cav1.2 subunit. *Circ Res*, **94**: 1242–1248.
- Takeda, N., Nakamura, I., and Hatanaka, T. et al. (1988). Myocardial mechanical and myosin isoenzyme alterations in streptozotocin-diabetic rats. *Jpn Heart J*, **29**:455-463
- Takeishi, Y., Bhagwat, A., Ball, N.A., Kirkpatrick, D.L., Periasamy, M., and Walsh, R.A. (1999). Effect of angiotensin-converting enzyme inhibition on protein kinase C and SR proteins in heart failure. *Am J Physiol*, **276**:H53–62.
- Takeishi, Y., Ping, P., Bolli, R., Kirkpatrick, D.L., Hoit, B.D., and Walsh, R.A. (2000). Transgenic overexpression of constitutively active protein kinase C epsilon causes concentric cardiac hypertrophy. *Circ Res*, **86**:1218–1223.
- Takemura, G. and Fujiwara, H.(2007). Doxorubicin-induced cardiomyopathy: from the cardiotoxic mechanisms to management. *Prog Cardiovasc Dis* 49: 330–352.

- Tamura, K., Sudo, T., Senftleben, U., Dadak, A., Johnson, R., and Karin, M. (2000). Requirement for p38alpha in erythropoietin expression: a role of stress kinases in erythropoiesis. *Cell*, **102**: 221–231.
- Tang, Y.D., Kuzman, J.A., Said, S., Anderson, B.E., Wang, X., and Gerdes, A.M. (2005). Low thyroid function leads to cardiac atrophy with chamber dilatation, impaired myocardial blood flow, loss of arterioles, and severe systolic dysfunction. *Circulation*, **112**:3122-3130.
- Taniike, M., Yamaguchi, O., Tsujimoto, I., Hikoso, S., Takeda, T., Nakai, A., Omiya, S., Mizote, I., Nakano, Y., Higuchi, Y., Matsumura, Y., Nishida, K., Ichijo, H., Hori, M., and Otsu, K. (2008). Apoptosis signal-regulating kinase 1/p38 signaling pathway negatively regulates physiological hypertrophy. *Circulation*, **117**: 545–552.
- Taniyama, Y., and Walsh, K. (2002). Elevated myocardial Akt signaling ameliorates doxorubicin-induced congestive heart failure and promotes heart growth. *J Mol Cell Cardiol*, **34**:1241–1247.
- Tanno, M., Bassi, R., Gorog, D.A., Saurin, A.T., Jiang, J., Heads, R.J., Martin, J.L., Davis, R.J., and Flavell, R.A. (2003). Diverse mechanisms of myocardial p38 mitogen-activated protein kinase activation: evidence for MKK-independent activation by a TAB1-associated mechanism contributing to injury during myocardial ischemia. *Circ Res*, **93**:254–261.
- Tavi, P., Sjogren, M., Lunde, P. K., Zhang, S. J., Abbate, F., and Vennstrom, B., et al. (2005). Impaired Ca²⁺ handling and contraction in cardiomyocytes from mice with a dominant negative thyroid hormone receptor alpha1. *J Mol Cell Cardiol*, **38**(4): 655-663.
- Tenhunen, O., Rysa, J., Ilves, M., Soini, Y., Ruskoaho, H., and Leskinen, H. (2006). Identification of cell cycle regulatory and inflammatory genes as predominant targets of p38 mitogen-activated protein kinase in the heart. *Circ Res*, **99**: 485–493.
- Teos, L.Y., Zhao, A., Alvin, Z., Laurence, G.G., Li, C., and Haddad, G.E. (2008). Basal and IGF-I-dependent regulation of potassium channels by MAP kinases and PI3-kinase during eccentric cardiac hypertrophy. *Am J Physiol Heart Circ Physiol*, **295**: H1834–H1845.
- The PKC-DRS Study Group. (2007). Effect of ruboxistaurin in patients with diabetic macular edema: thirty-month results of the randomized PKC-DMES clinical trial. *Arch Ophthalmol*, **125**: 318–324.
- Thornton, T., and Rincón, M. (2008). Non-classical p38 map kinase functions: cell cycle checkpoints and survival. *Int J Biol Sci*, **5**: 44–52.

- Thornton, T.M., Pedraza-Alva, G., Deng, B., Wood, C.D., Aronshtam, A., Clements, J.L., Sabio, G., Davis, R.J., Matthews, D.E., Doble, B., and Rincon, M. (2008). Phosphorylation by p38 MAPK as an alternative pathway for GSK3 β inactivation. *Science*, **320**: 667–670.
- Tjälve, H., Wilander, E., and Johansson, E. B. (1976) Distribution of labelled streptozotocin in mice: uptake and retention in pancreatic islets, *J Endocrinol*, **69**:455–456.
- Tongers, J., Losordo, D. W., and Landmesser, U. (2011). Stem and progenitor cell-based therapy in ischaemic heart disease: promise, uncertainties, and challenges. *Eur Heart J*, **32**(10): 1197-1206.
- Toth, A., Nickson, P., Mandl, A., Bannister, M.L., Toth, K., Erhardt, P.(2007). Endoplasmic reticulum stress as a novel therapeutic target in heart diseases. *Cardiovasc Hematol Disord Drug Targets*, **7**: 205–218.
- Toth, M.J., Ward, K., van der Velden, J., Miller, M.S., Vanburen, P., Lewinter, M.M., and Ades, P.A. (2011). Chronic heart failure reduces Akt phosphorylation in human skeletal muscle: relationship to muscle size and function. *J Appl Physiol*, **110**: 892–900.
- Tran, T.H., Andreka, P., Rodrigues, C.O., Webster, K.A., and Bishopric, N.H. (2007). Jun kinase delays caspase-9 activation by interaction with the apoptosome. *J Biol Chem*, **282**: 20340–20350.
- Uetani, T., Nakayama, H., Okayama, H., Okura, T., Higaki, J., Inoue, H., and Higashiyama, S. (2009). Insufficiency of Pro-heparin-binding epidermal growth factor-like growth factor shedding enhances hypoxic cell death in H9c2 cardiomyoblasts via the activation of caspase-3 and c-Jun N-terminal kinase. *J Biol Chem*, **284**: 12399–12409.
- Ueyama, T., Kawashima, S., Sakoda, T., Rikitake, Y., Ishida, T., Kawai, M., Yamashita, T., Ishido, S., Hotta, H., and Yokoyama, M.(2000). Requirement of activation of the extracellular signal-regulated kinase cascade in myocardial cell hypertrophy. *J Mol Cell Cardiol*, **32**:947–960.
- Ursitti, J.A., Petrich, B.G., Lee, P.C., Resneck, W.G., Ye, X., Yang, J., Randall, W.R., and Bloch, R.J. (2007). Role of an alternatively spliced form of α II-spectrin in localization of connexin 43 in cardiomyocytes and regulation by stress-activated protein kinase. *J Mol Cell Cardiol*, **42**: 572–581.
- Vahebi, S., Ota, A., Li, M., Warren, C.M., de Tombe, P.P., Wang, Y., and Solaro, R.J. (2007). p38-MAPK induced dephosphorylation of β -tropomyosin is associated with depression of myocardial sarcomeric tension and ATPase activity. *Circ Res*, **100**: 408–415.

- Van der Heide, S. M., Joosten, B. J., Dragt, B. S., Everts, M. E., and Klaren, P. H. (2007). A physiological role for glucuronidated thyroid hormones: preferential uptake by H9c2(2-1) myotubes. *Mol Cell Endocrinol*, **264** (1-2): 109-117.
- Van der Putten, H. H., Joosten, B. J., Klaren, P. H., and Everts, M. E. (2002). Uptake of tri-iodothyronine and thyroxine in myoblasts and myotubes of the embryonic heart cell line H9c2(2-1). *J Endocrinol*, **175**(3): 587-596.
- Van Heerebeek, L., Haundani, N., Handoko, M.L., Falcao-Pires, I., Musters, R.J., and Kupreishvili, K. et al. (2008). Diastolic stiffness of the failing diabetic heart: Importance of fibrosis, advanced glycation end products and myocyte resting tension. *Circulation*, **117**(1): 43-51.
- Vander A, Sherman J and Luccano D. (2007). In: *Human Physiology; The Mechanism of Body Function*. 7th Edition .Pub: WCB McGraw Hill, New York,pp 120-150.
- Vavra JJ, et al (1959/1960) Streptozotocin, a new antibacterial antibiotic, *Antibiot*, **7**: 230-235
- Venero, C., Guadano-Ferraz, A. ,and Herrero, AI. et al. (2005). Anxiety, memory impairment, and locomotor dysfunction caused by a mutant thyroid hormone receptor alpha1 can be ameliorated by T3 treatment. *Genes Dev*, **19**:2152-2163
- Ventura-Clapier, R., De Sousa, E. and Veksler, V. (2002). Metabolic myopathy in heart failure. *News Physiol Sci*, **17**:191–196.
- Ventura-Clapier, R., Mettauer, B., and Bigard, X. (2007). Beneficial effects of endurance training on cardiac and skeletal muscle energy metabolism in heart failure. *Cardiovasc Res*, **73**:10–18.
- Vincent, F., Duquesnes, N., Christov, C., Damy, T., Samuel, J.L., and Crozatier, B. (2006). Dual level of interactions between calcineurin and PKC-epsilon in cardiomyocyte stretch. *Cardiovasc Res*, **71**:97–107.
- Walker, C.A. and Spinale, F.G. (1999). The structure and function of the cardiac myocyte: a review of the fundamental concepts. *J. Thor Card Surg*, **118** (2):375-382.
- Walsh, K.B., Sweet, J.K., Parks, G.E. and Long, K.J. (2001). Modulation of outward potassium currents in aligned cultures of neonatal rat ventricular myocytes during phorbol ester-induced hypertrophy. *J Mol Cell Cardiol*,**33**: 1233–1247.
- Wang, G.S. , Kuyumcu-Martinez, M.N. , Sarma, S. , Mathur, N. , Wehrens, X.H. and Cooper, T.A. (2009). PKC inhibition ameliorates the cardiac phenotype in a mouse model of myotonic dystrophy type 1. *J Clin Invest*, **119**: 3797–3806.
- Wang, J., Paradis,P., Aries, A., Komati, H., Lefebvre C. and Wang H. et al.

- (2005). Convergence of protein kinase C and JAK-STAT signaling on transcription factor GATA-4. *Mol Cell Biol*, **25**: 9829–9844.
- Wang, J., Wang, H., Chen, J., Wang, X., Sun, K., Wang, Y., Wang, J., Yang, X., Song, X., Xin, Y., Liu, Z., and Hui, R. (2008). GADD45B inhibits MKK7-induced cardiac hypertrophy and the polymorphisms of GADD45B associated with inter-ventricular septum hypertrophy. *Biochem Biophys Res Commun*, **372**: 623–628.
- Wang, X. and Tournier, C. (2006). Regulation of cellular functions by the ERK5 signalling pathway. *Cell Signal*, **18**: 753–760.
- Wang, Y., Huang, S., Sah, V., Ross, J. Jr, Brown, J.H., Han, J., and Chien, K.R. (1998). Cardiac muscle cell hypertrophy and apoptosis induced by distinct members of the p38 mitogen-activated protein kinase family. *J Biol Chem* **273**: 2161–2168.
- Wang, Y., Su, B., Sah, V., Brown, J.H., Han, J., and Chien, K.R. (1998). Cardiac hypertrophy induced by mitogen-activated protein kinase kinase 7, a specific activator for c-Jun NH2-terminal kinase in ventricular muscle cells. *J Biol Chem*, **273**: 5423–5426.
- Wang, H., Grant, J.E., Doede, C.M., Sadayappan, S., Robbins J., and Walker, J.W. (2006). PKC-betaII sensitizes cardiac myofilaments to Ca²⁺ by phosphorylating troponin I on threonine-144. *J Mol Cell Cardiol*, **41**: 823–833.
- Watanabe, K.I., Ma, M., Hirabayashi, K.I., Gurusamy, N., Veeraveedu, P.T., Prakash, P., Zhang, S., Muslin, A.J., Kodama, M., and Aizawa, Y. (2007). Swimming stress in DN 14–3–3 mice triggers maladaptive cardiac remodeling: role of p38 MAPK. *Am J Physiol Heart Circ Physiol*, **292**: H1269–H1277
- Watanabe, T., Ono, Y., Taniyama, Y., Hazama, K., Igarashi, K., and Ogita, K., et al. (1992). Cell division arrest induced by phorbol ester in CHO cells overexpressing protein kinase C-delta subspecies. *Proc Natl Acad Sci USA*, **89**: 10159–10163
- Weinbrenner, C., Liu, G.S., Cohen, M.V., and Downey, J.M. (1997). Phosphorylation of tyrosine 182 of p38 mitogen-activated protein kinase correlates with the protection of preconditioning in the rabbit heart. *J Mol Cell Cardiol*, **29**: 2383–2391.
- Whellan, D.J., O'Connor, C.M., Lee, K.L., Keteyian, S.J., Cooper, L.S., Ellis, S.J., Leifer, E.S., Kraus, W.E., Kitzman, D.W., Blumenthal, J.A., Rendall, D.S., Houston-Miller, N., Fleg, J.L., Schulman, K.A., and Pina, I.L. (2007). Heart failure and a controlled trial investigating outcomes of exercise training (HF-ACTION): design and rationale. *Am Heart J*, **153**: 201–211.

- White, P., Burton, K. A., Fowden, A. L., and Dauncey, M. J. (2001). Developmental expression analysis of thyroid hormone receptor isoforms reveals new insights into their essential functions in cardiac and skeletal muscles. *Faseb J*, **15**(8): 1367-1376.
- Wikstrom, L., Johansson, C., Salto, C., Barlow, C., Campos Barros, A., and Baas, F., et al. (1998). Abnormal heart rate and body temperature in mice lacking thyroid hormone receptor alpha 1. *Embo J*, **17**(2): 455-461.
- Wilhelm FL , Podzuweit, T and Opie LH. (1992). Potential arrhythmogenic role of cyclic adenosine monophosphate (AMP) and cytosolic calcium overload: Implications for prophylactic effects of beta-blockers in myocardial infarction and proarrhythmic effects of phosphodiesterase inhibitors *J. Amer. College Cardiol.***19** (7): 1922 -1633.
- Wisler, J., MS, DeWire, S., Whalen, E., Violin, J., Drake, M., Ahn, S., Shenoy, S., and Lefkowitz, R. (2007). A unique mechanism of β -blocker action: carvedilol stimulates β -arrestin signaling. *Proc Natl Acad Sci USA*, **104**: 47-58.
- Witman, N., Murtuza, B., Davis, B., Arner, A., and Morrison, J. I. (2011). Recapitulation of developmental cardiogenesis governs the morphological and functional regeneration of adult newt hearts following injury. *Dev Biol*, **354** (1): 67-76.
- World Health Organisation (2011)
<http://www.who.int/mediacentre/factsheets/fs312/en/> (Accessed January 27th 2012)
- Wright, C.D., Chen, Q., Baye, N.L., Huang, Y., Healy, C.L., Kasinathan, S., and O'Connell, T.D. (2008). Nuclear α 1-adrenergic receptors signal activated ERK localization to caveolae in adult cardiac myocytes. *Circ Res*, **103**: 992–1000.
- Wu, L. and Derynck, R. (2009). Essential role of TGF- β signalling in glucose-induced cell hypertrophy. *Dev Cell*, **17**(1): 35-48.
- Xiang, P., Deng, H., Li, K., Huang, G, Chen, Y., Tu, L., Ng, P., Pong, N., Zhao, H, Zhang, L., and Sung, R. (2009). Dexrazoxane protects against doxorubicin-induced cardiomyopathy: upregulation of Akt and Erk phosphorylation in a rat model. *Cancer Chemother Pharmacol*, **63**: 343–349.
- Xiao, L., Pimental, D.R., Amin, J.K., Singh, K., Sawyer, D.B., and Colucci, W.S. (2001). MEK1/2-ERK1/2 mediates β 1-adrenergic receptor-stimulated hypertrophy in adult rat ventricular myocytes. *J Mol Cell Cardiol*, **33**: 779–787.
- Xiao, L., Pimentel, D.R., Wang, J., Singh, K., Colucci, W.S., and Sawyer, D.B.

- (2002). Role of reactive oxygen species and NAD(P)H oxidase in alpha1-adrenoceptor signaling in adult rat cardiac myocytes. *Am J Physiol Cell Physiol*, **282**: C926–C934.
- Xie, P., Guo, S., Fan, Y., Zhang, H., Gu, D., and Li, H. (2009). Atrogin-1/MAFbx enhances simulated ischemia/reperfusion-induced apoptosis in cardiomyocytes through degradation of MAPK phosphatase-1 and sustained JNK activation. *J Biol Chem*, **284**: 5488–5496.
- Xu, C., Bailly-Maitre, B. and Reed, J.C. (2005). Endoplasmic reticulum stress: cell life and death decisions. *J Clin Invest*, **115**: 2656–2664.
- Xu, L., Kappler, C., Mani, S., Shepherd, N., Renaud, L., Snider, P., Conway, S., and Menick, D. (2009). Chronic administration of KB-R7943 induces up-regulation of cardiac NCX1. *J Biol Chem*, **284**: 27265–27272.
- Yada, H., Murata, M., Shimoda, K., Yuasa, S., Kawaguchi, H., Ieda, M., Adachi, T., Murata, M., Ogawa, S., and Fukuda, K. (2007). Dominant negative suppression of Rad leads to QT prolongation and causes ventricular arrhythmias via modulation of L-type Ca₂₊ channels in the heart. *Circ Res*, **101**: 69–77.
- Yamaguchi, O., Watanabe, T., Nishida, K., Kashiwase, K., Higuchi, Y., Takeda, T., Hikoso, S., Hirotsu, S., Asahi, M., Taniike, M., Nakai, A., Tsujimoto, I., Matsumura, Y., Miyazaki, J., Chien, K.R., Matsuzawa, A., Sadamitsu, C., Ichijo, H., Baccarini, M., and Hori, M. (2004). Cardiac-specific disruption of the c-raf-1 gene induces cardiac dysfunction and apoptosis. *J Clin Invest*, **114**: 937–943.
- Yamamoto, H., Uchigata, Y., and Okamoto, H. (1981) Streptozotocin and alloxan induce DNA strand breaks and poly (ADP-ribose) synthetase in pancreatic islets, *Nature*, **294**: 284–286
- Yamamoto, M., Yang, G., Hong, C., Liu, J., Holle, E., Yu, X., Wagner, T., Vatner, S., and Sadoshima, J. (2003). Inhibition of endogenous thioredoxin in the heart increases oxidative stress and cardiac hypertrophy. *J Clin Invest*, **112**: 1395–1406.
- Yan, C., Luo, H., Lee, J.D., Abe, J., and Berk, B.C. (2001). Molecular cloning of mouse ERK5/BMK1 splice variants and characterization of ERK5 functional domains. *J Biol Chem*, **276**: 10870–10878.
- Yan, W., Wang, P., Zhao, C.X., Tang, J., Xiao, X., and Wang, D.W. (2012). Decore gene delivery inhibits cardiac fibrosis in spontaneously hypertensive rats by modulation of transforming growth factor- β /Smad and p38 mitogen-activated protein kinase signaling pathways. *Human Gene Therapy*.
- Yang, L., Doshi, D., Morrow, J., Katchman, A., Chen, X. and Marx, S.O. (2009).

Protein kinase C isoforms differentially phosphorylate Ca(v)1.2 alpha(1c). *Biochemistry*, **48**: 6674–6683.

- Yang, L., Zou, X., Liang, Q., Chen, H., Feng, J., Yan, L., Wang, Z., Zhou, D., Li, S., Yao, S., and Zheng, Z. (2007). Sodium tanshinone IIA sulfonate depresses angiotensin II-induced cardiomyocyte hypertrophy through MEK/ERK pathway. *Exp Mol Med*, **39**: 65–73.
- Yang, T., Xiong, Q., Enslen, H., R.J.D. and Chow, C. (2002). Phosphorylation of NFATc4 by p38 mitogen-activated protein kinases. *Mol Cell Biol*, **22**: 3892–3904.
- Yao, Y., Li, W., Wu, J., Germann, U., Su, M., Kuida, K., and Bouche, R D. (2003). Extracellular signal-regulated kinase 2 is necessary for mesoderm differentiation. *Proc Natl Acad Sci USA*, **100**: 12759–12764.
- Yin, T., Sandhu, G., Wolfgang, C.D, Burrier, A., Webb, R.L., Rigel, D.F., Hai, T., and Whelan, J. (1997). Tissue-specific pattern of stress kinase activation in ischemic/reperfused heart and kidney. *J Biol Chem*, **272**: 19943–19950.
- Yoon, S. and Seger, R. (2006). The extracellular signal-regulated kinase: multiple substrates regulate diverse cellular functions. *Growth Factors*, **21**: 21–44.
- You Fang, Z. and Marwick, T.H. (2003). Mechanisms of exercise training in patients with heart failure. *Am Heart J*, **145**: 904–911.
- Yue, T.L., Gu, J.L., Wang, C., Reith, A.D., Lee, J.C., Mirabile, R.C., Kreutz, R., Wang, Y., Maleeff, B., Parsons, A.A., and Ohlstein, E.H. (2000). Extracellular signal-regulated kinase plays an essential role in hypertrophic agonists, endothelin-1 and phenylephrine-induced cardiomyocyte hypertrophy. *J Biol Chem*, **275**: 37895–37901.
- Yue, T.L., Wang, C., Gu, J.L., Ma, X.L., Kumar, S., Lee, J.C., Feuerstein, G.Z., Thomas, H., Maleeff, B., and Ohlstein, E.H. (2000). Inhibition of extracellular signal-regulated kinase enhances ischemia/reoxygenation-induced apoptosis in cultured cardiac myocytes and exaggerates reperfusion injury in isolated perfused heart. *Circ Res*, **86**: 692–699.
- Zarubin, T. and Han, J. (2005). Activation and signaling of the p38 MAP kinase pathway. *Cell Res*, **15**: 11–18.
- Zechner, D., Thuerauf, D.J., Hanford, D.S., McDonough, P.M., and Glembotski, C.C. (1997). A role for the p38 mitogen-activated protein kinase pathway in myocardial cell growth, sarcomeric organization, and cardiac-specific gene expression. *J Cell Biol*, **139**: 115–127.

- Zeidan, A., Javadov, S., Chakrabarti, S. and Karmazyn, M. (2008). Leptin-induced cardiomyocyte hypertrophy involves selective caveolae and RhoA/ROCK-dependent p38 MAPK translocation to nuclei. *Cardiovasc Res*, **77**: 64–72.
- Zhai, P., Gao, S., Holle, E., Yu, X., Yatani, A., Wagner, T., and Sadoshima, J. (2007). Glycogen synthase kinase-3 β reduces cardiac growth and pressure overload-induced cardiac hypertrophy by inhibition of extracellular signal-regulated kinases. *J Biol Chem*, **282**: 33181–33191.
- Zhang, H.X., Zang, Y.M., Huo, J.H., Liang, S.J., Zhang, H.F., Wang, Y.M., Fan, Q., Guo, W.Y., Wang, H.C., and Gao, F. (2006). Physiologically tolerable insulin reduces myocardial injury and improves cardiac functional recovery in myocardial ischemic/reperfused dogs. *J Cardiovasc Pharmacol*, **48**: 306–313.
- Zhang, J., Li, X.X., Bian, H.J., Liu, X.B., Ji, X.P., and Zhang, Y. (2009). Inhibition of the activity of Rho-kinase reduces cardiomyocyte apoptosis in heart ischemia/reperfusion via suppressing JNK-mediated AIF translocation. *Clin Chim Acta*, **401**: 76–80.
- Zhang, S., Weinheimer, C., Courtois, M., Kovacs, A., Zhang, C., Cheng, A., Wang, Y., and Muslin, A. (2003). The role of the Grb2-p38 MAPK signaling pathway in cardiac hypertrophy and fibrosis. *J Clin Invest*, **111**: 833–841.
- Zheng, M., Dilly, K., Dos Santos Cruz, J., Li, M., Gu, Y., Ursitti, J.A., Chen, J., Ross, J., Jr, Chien, K.R., Lederer, J.W., and Wang, Y. (2004). Sarcoplasmic reticulum calcium defect in Ras-induced hypertrophic cardiomyopathy heart. *Am J Physiol Heart Circ Physiol*, **286**: H424–H433.

Appendix

PRESENTATION AND PUBLICATIONS